

***In vitro* functional studies of the tumour vascular target
PCDH7 and identification of novel tumour vascular targets
in colorectal cancer**

by

Aleksandra Korzystka



A thesis submitted to The University of Birmingham for the degree of
DOCTOR OF PHILOSOPHY

Institute of Cardiovascular Sciences
College of Medical and Dental Sciences
The University of Birmingham
August 2018

UNIVERSITY OF
BIRMINGHAM

University of Birmingham Research Archive

e-theses repository

This unpublished thesis/dissertation is copyright of the author and/or third parties. The intellectual property rights of the author or third parties in respect of this work are as defined by The Copyright Designs and Patents Act 1988 or as modified by any successor legislation.

Any use made of information contained in this thesis/dissertation must be in accordance with that legislation and must be properly acknowledged. Further distribution or reproduction in any format is prohibited without the permission of the copyright holder.

ABSTRACT

Protocadherin 7 (PCDH7) is a member of PCDHs belonging to the cadherin superfamily. It was recently identified as potential tumour endothelial marker (TEM). Although it is expressed in many solid tumours, its function in endothelial cells and its binding partner(s) on endothelial cell surface are unknown. Thus a major aim of this thesis was to determine the role of its extracellular domain (ECD) in endothelial cells and to potentially identify novel ligand(s) of its ECD on endothelial cell surface. Recombinant human Fc fused hPCDH7 ECD significantly inhibited endothelial network formation, cell proliferation and chemotaxis *in vitro*. This was mediated by the first five N-terminal cadherin repeats of the ECD. However, no ligands of the ECD were identified. A second part of this thesis involved the identification of novel TEMs from colorectal cancer. Apelin (APLN), endothelial cell-specific molecule-1 (ESM-1), matrix metalloproteinase-12 (MMP12) and epiregulin (EREG) identified as potential candidates will be further validated. Additionally, the angiogenic potential of protein C receptor (PROCR), chromosome 1 open reading frame 54 (C1ORF54) and stabilin 1 (STAB1) which were enriched in tumour endothelium was investigated, with a role for PROCR in endothelial network formation identified. The findings of this thesis enhance our understanding of the molecular signature of tumour endothelial cells and lay the foundation for the potential development of novel anti-cancer therapies.

**Dla mojego ukochanego Dziadka,
który zawsze we mnie wierzył**

Acknowledgements

I would like to thank my primary supervisor Professor Roy Bicknell and Dr Laurens van der Flier for the opportunity to participate in the Marie Skłodowska-Curie PhD program and to work in their labs.

I would like to thank my co-supervisor Dr Victoria Heath, for the advice, willingness to help, constructive scientific feedback, and patience, especially during the past year.

I would also like to thank members of SomantiX, Dr Ruben Postel, Sander Mertens and Dr Ingrid de Vries. Many thanks for being such great teachers, colleagues and friends. I would also like to thank members of Interna Technologies for making me feel part of the group. I had a wonderful time with you all in Utrecht, even during endless boring discussions about soccer 😊

I would like to express my special thanks to Marta Coric and Marco Mambretti, whom I have started my PhD journey with. I am happy we had each other. I will miss you.

I would also like to thank all my old and new friends from Poland, the Netherlands, United Kingdom and other parts of Europe. I am very grateful to have you around. Special thanks go to Dorota, Alessia, Ewelina, Agnieszka, Yurena and Krzysiek. I could not wish for better friends!

Justyna, I am very proud of you! I am happy we met. You were an important part of my life in Birmingham and became my true friend 😊

Finally, my deepest gratitude goes to my whole family, especially my beloved parents and brother, wonderful grandmas, and my late grandpa. Your love, faith and invaluable support gave me the strength to finalize my PhD. Also, I would like to thank my boyfriend. Your encouragement and ability to motivate me during the past months were invaluable.

Podziękowania

Chciałabym serdecznie podziękować mojemu promotorowi Profesorowi Royowi Bicknell i Dr Laurensowi van der Flier za możliwość uczestnictwa w programie i za możliwość pracy w ich laboratoriach.

Chciałabym również podziękować Dr Victorii Heath za jej pomoc, konstruktywne komentarze i naukowe rady oraz okazaną cierpliwość, zwłaszcza w ostatnim roku.

Serdecznie podziękowania również dla wszystkich z SomantiX: Dr Rubena Postela, Sandera Mertensa i Dr Ingrid de Vries. Dziękuję Wam za bycie świetnymi nauczycielami. Dodatkowe podziękowania dla Interny Technologies. Czas w Utrechcie był wspaniałą przygodą, nawet podczas nieskończonych dyskusji o piłce nożnej.

Specjalne podziękowania dla Marty Coric i Marco Mambretti, z którymi rozpoczęłam i skończyłam swoją doktorancką przygodę. Jestem szczęśliwa, że się poznaliśmy i dziękuję za Wasze wsparcie.

Chciałabym również podziękować wszystkim starym i nowym przyjaciołom z Polski, Holandii, Anglii i innych części Europy, którzy niezmiennie mnie wspierali. Cieszę się, że jesteście! Specjalne podziękowania dla Doroty, Alessii, Eweliny, Agnieszki, Yureny i Krzycha. Za wszystko 😊

Justyna, jestem z Ciebie dumna! Wiedziałam, że dasz radę 😊 Cieszę się, że się poznałyśmy. Jedno piwo wystarczyło by między nami zaiskrzyło!

Na końcu chciałabym podziękować całej mojej rodzinie, szczególnie moim cudownym Rodzicom i Bratu oraz ukochanym Babciom i Śp. Dziadkowi. Wasza miłość, wiara we mnie i wsparcie dały mi siłę do skończenia doktoratu. Dziękuję również mojemu Chłopakowi. Twoja umiejętność rozbawiania i motywowania mnie do pracy w ciągu ostatnich miesięcy była nieoceniona.

CONTENTS

CHAPTER 1: INTRODUCTION	1
1.1 Angiogenesis	2
1.2 Discovery of tumour endothelial markers and their clinical potential	6
1.3 Targeting the tumour vasculature	10
1.3.1 Anti-angiogenic agents (AAs)	10
1.3.2 Vascular disrupting agents (VDAs)	12
1.3.2.1 Small-molecule VDAs	12
1.3.2.2 Utilizing TEMs as ligand-based and antibody VDAs	14
1.3.3 Vascular targeted therapy (VTT)	15
1.4 Identification of new tumour endothelial markers in non-small cell lung carcinoma (NSCLC)	16
1.5 Cadherin superfamily	17
1.5.1 Protocadherin subfamily	20
1.5.2 Protocadherin 7 (PCDH7)	23
1.6 <i>In vitro</i> angiogenesis assays	28
1.6.1 2D HUVEC/HDF <i>in vitro</i> co-culture assay	30
1.6.2 3D HUVEC/HDF <i>in vitro</i> co-culture assay	30
1.6.3 Spheroid assay	31
1.6.4 Scratch assay	31
1.6.5 Transmigration assay	32
1.6.6 Proliferation assay	32
1.7 Hypotheses and aims	33
CHAPTER 2: MATERIALS AND METHODS	35
2.1 Reagents	36
2.1.1 Buffers	36
2.1.2 Primary antibodies	37
2.1.3 Secondary antibodies	38
2.1.4 Recombinant proteins	39
2.2 Molecular biology	39

2.2.1	DNA vectors	39
2.2.2	DNA inserts	40
2.2.3	Cloning Primers	40
2.2.4	DNA amplification	42
2.2.5	DNA agarose electrophoresis	43
2.2.6	DNA gel extraction	43
2.2.7	Restriction enzyme digest	43
2.2.8	TOPO cloning	44
2.2.9	Gibson cloning	44
2.2.10	Bacterial transformation	45
2.2.11	Plasmid DNA isolation	45
2.2.12	DNA sequencing	46
2.2.13	Genomic DNA isolation	46
2.2.14	RNA isolation	46
2.2.15	cDNA synthesis	47
2.2.16	Quantitative PCR (qPCR)	47
	2.2.16.1 Primer design and validation	47
	2.2.16.2 qPCR	49
2.3	Biochemistry	50
2.3.1	Protein lysis	50
2.3.2	BCA protein concentration assay	50
2.3.3	SDS-PAGE electrophoresis	51
2.3.4	Western blot	51
2.4	Immunoprecipitation (IP)	52
2.5	Mass spectrophotometry (MS)	53
2.6	Cell culture	53
2.6.1	Cell culture	53
2.6.2	Transfection with plasmid DNA	54
2.6.3	Production of lentiviruses	55
2.6.4	Lentiviral transduction of HUVEC	55
2.6.5	Short hairpin RNA (shRNA)	56
2.6.6	CellTiter 96 Non-Radioactive Cell Proliferation Assay (MTT)	57

2.6.7	Scratch assay	57
2.6.8	Transwell migration assay	58
2.6.9	Spheroid assay	59
2.6.10	3D HUVEC/HDF co-culture angiogenesis assay in fibrin matrix	60
2.6.11	2D HUVEC/HDF co-culture angiogenesis assay	61
2.6.12	Cell adhesion assay	62
2.7	Recombinant protein production	62
2.7.1	Small scale production of Fc fused and His tagged recombinant proteins	62
2.7.2	Large scale production of Fc fused recombinant proteins	63
2.7.3	Purification of Fc fused recombinant proteins	64
2.8	Flow cytometry	64
2.9	Immunofluorescence (IF) staining of cells	65
2.10	Statistical analysis	66

CHAPTER 3: *IN VITRO* FUNCTIONAL STUDIES OF Fc FUSED PCDH7 EXTRACELLULAR DOMAIN **67**

3.1	Introduction	68
3.2	Anti-human PCDH7 antibody recognizes an overexpressed full length PCDH7	69
3.3	PCDH7 is expressed in HUVEC	70
3.4	Generation and production of the recombinant hPCDH7 C7-Fc fusion protein	71
3.4.1	Recombinant hPCDH7 C7-Fc fusion protein is successfully generated	71
3.4.2	Recombinant hPCDH7 C7-Fc fusion protein is successfully produced on a small scale but the production yield is low	75
3.4.3	Recombinant hPCDH7 C7-Fc fusion protein is successfully produced on a large scale	75
3.5	Recombinant hPCDH7 C7-Fc fusion protein inhibits endothelial network formation in <i>in vitro</i> 3D HUVEC/HDF co-culture angiogenesis assay in a concentration dependent manner	80

3.6	Recombinant hPCDH7 C7-Fc fusion protein inhibits endothelial cell proliferation in a MTT assay	84
3.7	Recombinant hPCDH7 C7-Fc fusion protein non-significantly affects endothelial cell migration in a scratch assay	86
3.8	Generation and production of truncated hPCDH7 ECD-Fc fusion proteins	89
3.8.1	Truncated hPCDH7 C7-Fc fusion proteins are successfully generated	89
3.8.2	Truncated hPCDH7 C7-Fc fusion proteins are successfully produced on a small scale	92
3.8.3	Truncated hPCDH7 C7-Fc fusion proteins are successfully produced on a large scale	92
3.9	Truncated hPCDH7 C5-Fc and hPCDH7 C7-Fc significantly inhibit endothelial cell proliferation in a MTT assay	93
3.10	Truncated hPCDH7 C5-Fc and hPCDH7 C7-Fc significantly inhibit endothelial network formation in 3D HUVEC/HDF co-culture angiogenesis assay	97
3.11	Truncated hPCDH7 C5-Fc and hPCDH7 C7-Fc significantly inhibit endothelial network formation in 2D HUVEC/HDF co-culture angiogenesis assay	98
3.12	Truncated hPCDH7 C5-Fc and hPCDH7 C7-Fc significantly inhibit endothelial transmigration in a transwell assay	104
3.13	Truncated hPCDH7 ECD-Fc fusion proteins do not affect endothelial cell sprouting in a spheroid assay	104
3.14	Discussion	108

CHAPTER 4: FURTHER INVESTIGATIONS OF INTERACTIONS OF HUMAN PCDH7 EXTRACELLULAR DOMAIN

4.1	Introduction	114
4.2	Recombinant hPCDH7 C5-Fc and hPCDH7 C7-Fc fusion proteins do not bind to HUVEC as assessed by flow cytometry	115
4.3	Recombinant hPCDH7 C5-Fc and hPCDH7 C7-Fc fusion proteins do not increase adherence of HUVEC	116

4.4	Homophilic interactions of hPCDH7 extracellular domain could not be detected by immunoprecipitation of hPCDH7 FL from HEK293T-hPCDH7 FL-FLAG cells	121
4.5	Mass spectrometry analysis of hPCDH7 C7-Fc pull down from HUVEC lysate revealed two potential binding partners	127
4.6	EFEMP1 is expressed in HUVEC and its expression level is not affected upon treatment with the hPCDH7 C5-Fc and hPCDH7 C7-Fc fusion proteins	130
4.7	Human PCDH7 C7-Fc pull down from HUVEC lysate resulted in nonspecific interactions of EFEMP1 and hPCDH7 ECD	131
4.8	The interaction between hPCDH7 ECD-Fc fusion proteins and EFEMP1-HA recombinant protein was nonspecific	135
4.9	PCDH7 is expressed in the 2D HUVEC/PC but not in the 2D HUVEC/HDF <i>in vitro</i> endothelial network	137
4.10	Discussion	145

CHAPTER 5: THE IDENTIFICATION OF POTENTIAL COLORECTAL CANCER TUMOUR VASCULATURE MARKERS AND INVESTIGATION OF GENE FUNCTION IN THE ENDOTHELIAL CELLS

5.1	Introduction	152
5.2	SomantiX B.V. successfully performed a transcriptomic analysis of colorectal (CRC) tumour vs. healthy colon endothelial cells	153
5.3	Analysis of the microarray data enables selection of potential CRC vascular markers	156
5.4	Analysis of endothelial expression and qPCR primer validation for selected genes	158
5.5	Study of selected targets expression in TEC and NEC samples provided by SomantiX revealed several genes enriched in TECs	162
5.6	Anti-human C1ORF54 and PROCR antibodies recognize their targets	170
5.7	Validation of shRNA-mediated knockdown was successful for <i>PROCR</i> but not for <i>C1orf54</i> and <i>STAB1</i>	171

5.8	Determining the role of <i>STAB1</i> and <i>PROCR</i> knockdown on endothelial network formation in 3D HUVEC/HDF co-culture assay	177
5.9	Discussion	181
CHAPTER 6: GENERAL DISCUSSION		185
6.1	General discussion	186
APPENDIX		192
REFERENCES		205
LIST OF ABSTRACTS AND DETAILS OF MEETINGS WHERE WORK CONTAINED IN THIS THESIS WAS PRESENTED		223

LIST OF FIGURES

CHAPTER 1: INTRODUCTION

Figure 1.1 Sprouting angiogenesis	4
Figure 1.2 Classification of cadherin superfamily	18
Figure 1.3 Structure and organization of protocadherin 7 (PCDH7) isoform A	24
Figure 1.4 <i>In vitro</i> angiogenesis assays	29

CHAPTER 3: IN VITRO FUNCTIONAL STUDIES OF Fc FUSED PCDH7

EXTRACELLULAR DOMAIN

Figure 3.1 PCDH7 FL is recognized by anti-human PCDH7 antibody	72
Figure 3.2 PCDH7 is expressed in HUVEC	73
Figure 3.3 The hPCDH7 C7-Fc fusion protein was successfully generated and secreted to the medium	74
Figure 3.4 Small scale production of the hPCDH7 C7-Fc fusion protein	77
Figure 3.5 Optimal duration of a large scale production of the hPCDH7 C7-Fc fusion protein was 20 days	78
Figure 3.6 The hPCDH7 C7-Fc fusion protein was successfully produced on a large scale	79
Figure 3.7A The hPCDH7 C7-Fc fusion protein significantly inhibits an endothelial network formation in a 3D HUVEC/HDF co-culture angiogenesis assay in a concentration dependent manner	82
Figure 3.7B The hPCDH7 C7-Fc fusion protein significantly inhibits an endothelial network formation in a 3D HUVEC/HDF co-culture angiogenesis assay in a concentration dependent manner	83
Figure 3.8 The hPCDH7 C7-Fc fusion protein significantly reduces HUVEC proliferation in a MTT assay	85
Figure 3.9A The hPCDH7 C7-Fc non-significantly reduces HUVEC migration in a scratch assay	87
Figure 3.9B The hPCDH7 C7-Fc non-significantly reduces HUVEC migration in a scratch assay	88

Figure 3.10 Schematic representation of the truncated hPCDH7 ECD-Fc fusion proteins	90
Figure 3.11 The truncated hPCDH7 ECD-Fc fusion proteins were expressed and secreted to the medium	91
Figure 3.12 The truncated hPCDH7 ECD-Fc fusion proteins were successfully produced on a small scale	94
Figure 3.13 The truncated hPCDH7 ECD-Fc fusion proteins were successfully produced on a large scale	95
Figure 3.14 The hPCDH7 C5-Fc and hPCDH7 C7-Fc fusion proteins significantly reduce HUVEC proliferation in a MTT assay	96
Figure 3.15A The hPCDH7 C5-Fc and hPCDH7 C7-Fc fusion proteins comparably inhibit an endothelial network formation in a 3D HUVEC/HDF co-culture angiogenesis assay	100
Figure 3.15B The hPCDH7 C5-Fc and hPCDH7 C7-Fc fusion proteins comparably inhibit an endothelial network formation in a 3D HUVEC/HDF co-culture angiogenesis assay	101
Figure 3.16A The hPCDH7 C5-Fc and hPCDH7 C7-Fc fusion proteins comparably inhibit an endothelial network formation in a 2D HUVEC/HDF co-culture angiogenesis assay	102
Figure 3.16B The hPCDH7 C5-Fc and hPCDH7 C7-Fc fusion proteins comparably inhibit endothelial network formation in a 2D HUVEC/HDF co-culture angiogenesis assay	103
Figure 3.17 The hPCDH7 C5-Fc and hPCDH7 C7-Fc fusion proteins reduce endothelial cell transmigration towards a serum in a transwell assay	106
Figure 3.18 The hPCDH7 C5-Fc and hPCDH7 C7-Fc fusion proteins do not affect HUVEC sprouting in a spheroid assay	107
Figure 3.19 The mPCDH7 C7-Fc and mPCDH7 C7-His fusion proteins were successfully expressed but their small scale production yield was extremely low	112

CHAPTER 4: FURTHER INVESTIGATIONS OF INTERACTIONS OF HUMAN PCDH7 EXTRACELLULAR DOMAIN

Figure 4.1 No binding of hPCDH7 C5-Fc and hPCDH7 C7-Fc to HUVEC is detected using a flow cytometry	118
Figure 4.2 No binding of hPCDH7 C5-Fc and hPCDH7 C7-Fc to HEK293-hPCDH7 FL cells is detected using the flow cytometry	119
Figure 4.3 The hPCDH7 C5-Fc and hPCDH7 C7-Fc do not enhance the adherence of HUVEC in an adhesion assay	120
Figure 4.4 The hPCDH7 FL-FLAG is expressed in HEK293T cells	123
Figure 4.5 The hPCDH7 C7-Fc immunoprecipitation on HEK293T-hPCDH7 FL-FLAG cells for mass spectrometry analysis	124
Figure 4.6 The hPCDH7 C5-Fc and hPCDH7 C7-Fc fusion proteins did not immunoprecipitate hPCDH7 FL-FLAG from HEK293T-hPCDH7 FL-FLAG cells	126
Figure 4.7 The hPCDH7 C7-Fc immunoprecipitation on HUVEC for mass spectrometry analysis	128
Figure 4.8 Anti-human EFEMP1 antibody recognizes a recombinant EFEMP1-HA protein	132
Figure 4.9 EFEMP1 is expressed in HUVEC and its expression does not change upon treatment with hPCDH7 ECD-Fc fusion proteins	133
Figure 4.10 Pulldown of EFEMP1 from HUVEC lysate is nonspecific	134
Figure 4.11 The interaction between hPCDH7 ECD-Fc fusion proteins and EFEMP1 is nonspecific	136
Figure 4.12 Anti-human PCDH7 antibody recognizes hPCDH7 FL localised at cell-cell contacts of PCDH7 positive cells	140
Figure 4.13 Staining with anti-human CD31 antibody enables visualisation of endothelial cell membranes within the network	141
Figure 4.14 PCDH7 is not detected in the 2D HUVEC/HDF co-culture network	142
Figure 4.15 PCDH7 is detected in the 2D HUVEC/PC co-culture network	143
Figure 4.16 PCDH7 is expressed in PC but not in HDF	144
Figure 4.17 The expression of VE-cadherin does not change upon treatment with the hPCDH7 ECD-Fc fusion proteins	150

CHAPTER 5: THE IDENTIFICATION OF POTENTIAL COLORECTAL CANCER TUMOUR VASCULATURE MARKERS AND INVESTIGATION OF GENE FUNCTION IN THE ENDOTHELIAL CELLS

Figure 5.1 Representative example of flow cytometry cell sorting analysis conducted by SomantiX	154
Figure 5.2 Most selected potential markers are expressed in HUVEC and gene specific qPCR primers selectively amplify correctly-sized DNA fragments	160
Figure 5.3 <i>EREG</i> and <i>MMP12</i> specific qPCR primer sets amplify only <i>EREG</i> and <i>MMP12</i> cDNA fragments from MFC7 cells and do not give a background on –RT	161
Figure 5.4 <i>ANGT2</i> and <i>EpCAM</i> qPCR primer validation	164
Figure 5.5 The mRNA expression of <i>ANGPT2</i> , <i>CD45</i> and <i>EpCAM</i> markers confirmed a successful separation of different cell fractions for transcriptomic analysis	165
Figure 5.6 qPCR analysis of candidate TEMs	166
Figure 5.7 Validation of anti-human PROCR and anti-human C1ORF54 antibodies	173
Figure 5.8 ShRNA-mediated knockdown of <i>PROCR</i> , <i>C1orf54</i> and <i>STAB1</i> results in a reduction of mRNA expression	174
Figure 5.9 PROCR is successfully knocked down by using specific shRNAs	175
Figure 5.10 Despite a successful knockdown of <i>C1orf54</i> on mRNA level, C1ORF54 protein is undetectable in HUVEC	176
Figure 5.11 shRNA-mediated <i>PROCR</i> knockdown in HUVEC results in a decrease of the endothelial network formation	177
Figure 5.12 The level of shRNA-mediated <i>STAB1</i> knockdown in HUVEC does not correlate with the impairment of the endothelial network formation	180

APPENDIX

Figure A.1 Example of qPCR primer design using the Primer-BLAST tool	193
Figure A.2 3D HUVEC/HDF co-culture <i>in vitro</i> angiogenesis assay involves different steps of angiogenic process	194
Figure A.3 Human dermal fibroblasts form a scaffold in the fibrin matrix in 3D HUVEC/HDF co-culture assay	195

Figure A.4 3D HUVEC/HDF co-culture assay depends on the VEGF/bFGF signalling pathway and MMP-mediated ECM degradation	196
Figure A.5 2D HUVEC/HDF co-culture assay depends on the VEGF signalling pathway but it does not require MMP-mediated ECM degradation	197
Figure A.6 Human pericytes support HUVEC network formation in both 3D and 2D co-culture assays	198
Figure A.7 Amino acid sequences of the hPCDH7 FL-FLAG and the hPCDH7 ECD-Fc fusion proteins	199
Figure A.8 Amino acid sequences of the mPCDH7 ECD(C7)-Fc and the mPCDH7 ECD(C7)-His fusion proteins	200
Figure A.9 Melting curves of gene specific qPCR primers	201
Figure A.10 Melting curves of <i>EREG</i> and <i>MMP12</i> specific qPCR primers	202
Figure A.11 Melting curves of <i>ANGPT2</i> and <i>EpCAM</i> specific qPCR primers	203
Figure A.12 Yield and purity of normal and tumour endothelial and epithelial samples provided by SomantiX used for qPCR reaction	204

LIST OF TABLES

CHAPTER 1: INTRODUCTION

Table 1.1 Selected TEMs and techniques that led to their discovery	9
Table 1.2 Examples of antibody-based AAs either approved or in clinical trials	11
Table 1.3 Examples of small-molecule VDAs in clinical trials	13
Table 1.4 Reported functions of few selected non-clustered δ -PCDHs	22

CHAPTER 2: MATERIALS AND METHODS

Table 2.1 Commonly used buffers and their composition	36
Table 2.2 Primary antibodies and their working concentration for various applications	37
Table 2.3 Secondary antibodies and their working concentration for various applications	38
Table 2.4 Recombinant proteins, their size and working concentration	39
Table 2.5 Commercial vectors used for cloning	39
Table 2.6 DNA inserts used as templates for cloning	40
Table 2.7 Oligonucleotides used for cloning, their sequence and DNA template used for PCR reaction	41
Table 2.8 List of generated plasmid DNA constructs with information about vector backbone and primers used for cloning	44
Table 2.9 Quantitative PCR (qPCR) primers with their indicated product length	48
Table 2.10 SDS-PAGE gels composition	51
Table 2.11 List of cell types and their culture conditions	54
Table 2.12 Amounts of HEK293T cells and reagents quantities used for transfection	55
Table 2.13 List of shRNAs constructs used in knockdown experiments	56

CHAPTER 4: FURTHER INVESTIGATIONS OF INTERACTIONS OF HUMAN PCDH7 EXTRACELLULAR DOMAIN

Table 4.1 Potential extracellular ligands of the hPCDH7 ECD identified by mass spectrometry	129
--	-----

CHAPTER 5: THE IDENTIFICATION OF POTENTIAL COLORECTAL CANCER (CRC) TUMOUR VASCULATURE MARKERS AND INVESTIGATION OF GENE FUNCTION IN THE ENDOTHELIAL CELLS

Table 5.1 Antibodies and appropriate fluorescent labels used for the detection and sorting of different cell types 155

Table 5.2 Examples of well-known angiogenesis-associated genes and TEMs upregulated in CRC endothelial cells based on the transcriptomic analysis performed by SomantiX B.V. 156

Table 5.3 List of potential CRC vascular markers based on the microarray data analysis 157

ABBREVIATIONS

2D – Two dimensional

3D – Three dimensional

aa – Amino acid

AA – Anti-angiogenic agent

ANG-2 – Angiopoietin-2

AP – Alkaline phosphatase

APLN – Apelin

APP – Aminopeptidase P

APS – Ammonium persulfate

BCA – Bicinchoninic acid

BCIP/NBT – 5-bromo-4-chloro-3-indolyl phosphate/nitro blue tetrazolium

bFGF – Basic fibroblasts growth factor

BGUS – β -glucuronidase

bp – Base pairs (DNA)

BSA – Bovine serum albumin

C1ORF54 – Chromosome 1 open reading frame 54

Ca₂Cl – Calcium chloride

CAFs – Cancer associated fibroblasts

CaM – Calmodulin

CD31 – Cluster of differentiation 31 (PECAM)

CD45 – Cluster of differentiation 45 (PTPRC)

cDMEM – Complete Dulbecco's modified Eagle Medium

cDNA – Complementary DNA

cGMP – Cyclic guanosine monophosphate

CLEC14A – C-type lectin-like domain containing 14A

CM1-3 – Cnn motif 1-3

COS-7 – African green monkey fibroblast

Cx43 – Connexin 43

DAPI – 4', 6-diamidino-2-phenylindole

DCHS1 – Dachshous cadherin related 1

DII4 – Delta-like 4
DMEM – Dulbecco's modified Eagle Medium
DPBS – Dulbecco's phosphate-buffered saline
DTSSP – 3,3'-Dithiobis(sulfosuccinimidylpropionate)
E. coli – *Escherichia coli*
EBM-2 – Endothelial growth basal medium 2
ECD – Extracellular domain
ECM – Extracellular matrix
ECSCR – Endothelial cell surface expressed chemotaxis and apoptosis regulator
ED-B – Extradomain B
EDTA – Ethylene-diamine-tetra-acetic acid
EFEMP1 – EGF-containing fibulin-like extracellular matrix protein
eGFP – Enhanced green fluorescent protein
EGFR – Epidermal growth factor receptor
ELTD1 – EGF, latrophilin and seven transmembrane domain-containing protein 1
EMT – Epithelial mesenchymal transition
ENG – Endoglin
EpCAM – Epithelial cell adhesion molecule
EREG – Epregrulin
ERK – Extracellular signal regulated kinase
ESM-1 – Endothelial cell-specific molecule-1
FAM174B – Family with sequence similarity 174
FBS – Fetal bovine serum
FC – Flow cytometry
Fc – Fragment crystallisable
FITC – Fluorescein isothiocyanate
FL – Full length
FW – Forward primer
gDNA – Genomic deoxyribonucleic acid
GFP – Green fluorescent protein
HBEC – Human bronchial epithelial cells
HDF – Human dermal fibroblast

HEK293T – Human embryonic kidney 293 cells expressing SV40 large T antigen
HEPES – 4-(2-hydroxyethyl)-1-piperazineethanesulfonic acid
hFc – Human fragment crystallisable
His – Polyhistidine tag
HPRT1 – Hypoxanthine phosphoribosyltransferase
HRP – Horse radish peroxidase
HUVEC – Human umbilical vein endothelial cells
HYAL2 – Hyaluronoglucosamidase 2
ICD – Intracellular domain
IF – Immunofluorescence
IFN α – Interferon-alpha
IL-12 – Interleukin-12
IP – Immunoprecipitation
IRES – Internal ribosomal entry site
kDa – Kilo Dalton
KH₂PO₄ – Potassium hydrogen phosphate
KRAS – K-ras
LAMA4 – Laminin subunit alpha-4
LB broth – Luria-Bertani broth
logFC – Log2 fold change
LSGS – Low serum growth supplement
MAPK – Mitogen activated protein kinase
MCAM – Melanoma cell adhesion molecule
MCF7 – Human breast adenocarcinoma
MDA231 – Human breast adenocarcinoma
MDA-MB-231 – triple-negative metastatic breast adenocarcinoma
mg – Milligram
miliQ water – Ultrapure water
min. – Minute
mMMRN2 – Mouse multimerin-2
MMP-2/-9/-12 – Matrix metalloproteinase-2/-9/-12
MMPs – Matrix metalloproteinases

mRNA – Messenger ribonucleic acid
MS – Mass spectrometry
MTT – 3-(4,5-Dimethyl-2-thiazolyl)-2,5-diphenyl-2H-tetrazolium bromide
N – Number of experimental repeats
n – Number of sample replicates
Na₂PO₄ – Disodium hydrogen phosphate dehydrate
NaCl – Sodium chloride
NaOH – Sodium hydroxide
NEC – Normal endothelial cells
NEpiC – Normal epithelial cells
NFPC – NF(neural fold)-protocadherin
NF- κ β – Nuclear factor kappa-light-chain-enhancer of activated B cells
Ni-NTA – Nickel nitrilotriacetic acid
nm – Nanometre
Notch - Neurogenic locus notch homolog protein 1
NP-40 – Nonyl phenoxyethoxyethanol 40
PAPC – Paraxial protocadherin
PBS – Phosphate buffered saline
PC – Pericyte
PCDH – Protocadherin
PCR – Polymerase chain reaction
PDGF – Platelet-derived growth factor
PDGFR α – Platelet-derived growth factor receptor α
PDIA1 – Protein disulphide isomerase
PE – Phycoerythrin
PEI – Polyethylenimine
PFA – Paraformaldehyde
pH – Per hydrogen
PMSF – Phenylmethanesulfonyl fluoride
PP1 α – Protein phosphatase 1 α
PP2A – Protein phosphatase 2A
PROCR – Protein C receptor

PVDF – Polyvinylidene difluoride
qPCR – Quantitative polymerase chain reaction
RhoJ – Ras homolog family member J
RIPA – Radioimmunoprecipitation assay
RNA-Seq – RNA sequencing
ROBO4 – Roundabout guidance receptor 4
RT – Room temperature
RV – Reverse primer
s - second
SAGE – Serial analysis of gene expression
SD – Standard deviation
SDS – Sodium dodecyl sulphate
SELE – E-selectin
SET – SET nuclear proto-oncogene
shRNA – Short hairpin ribonucleic acid
SILAC – Stable isotope labelling with amino acids in cell culture
siRNA – Short interference ribonucleic acid
SPARC – Secreted protein acidic and rich in cysteine
STAB1 – Stabilin 1
STAT1 – Signal transducer and activator of transcription 1
TAE – Tris-acetate-EDTA
TAMs – Tumour associated macrophages
TBE – Tris-borate-EDTA
TEC – Tumour endothelial cells
TEM – Tumour endothelial marker
TEM1/TEM7/TEM8 – Tumour endothelial marker 1,7 and 8
TEMED – Tetramethylethylenediamine
TEpiC – Tumour epithelial cells
TM – Transmembrane domain
TNF α – Tumour necrosis factor α
Tris – Trisaminomethane
VDA – Vascular disrupting agent

VEGF– Vascular endothelial growth factor

VEGFR – Vascular endothelial growth factor receptor

VEGFR-2/VEGFR-1 – Vascular endothelial growth factor receptor-2 and -1

VTT – Vascular targeted therapy

VWF – Willebrand factor

WB – Western blot

xg – Times gravity - unit of relative centrifugal force (RCF)

SYNOPSIS

Work presented in this thesis was part of the VAMPIRE project funded by Marie Skłodowska-Curie European Industrial Doctorate (EID) actions as a collaboration between the University of Birmingham in the United Kingdom and SomantiX B.V., a biotechnology company in Utrecht, The Netherlands.

The major interest of the project was focused on tumour vascular targeting that could ultimately lead to the development of novel therapies for cancer patients. The different subprojects were divided between five PhD students enrolled in this program. The work presented in this thesis was completed over 36 months (3 years) with time shared equally between the company and the university.

The first 18 months of the studies were carried out at SomantiX B.V. and were focused on screening for novel tumour endothelial markers in colorectal cancer. Although generated at the beginning of PhD, data from this period are presented and discussed in the final results chapter, Chapter 5.

The second half of the studies was spent at the University of Birmingham. This part of the project was focused on determining the role of the extracellular domain of tumour vascular target PCDH7 in endothelial cells and to potentially identify its ligand(s) on endothelial cell surface. Data from this period of the project are summarized and discussed in first two results chapters, Chapter 3 and Chapter 4.

CHAPTER 1: INTRODUCTION

CHAPTER 1: INTRODUCTION

1.1 Angiogenesis

Blood vessels facilitate tissue growth, organ functions, gas and metabolic products exchange, transport of nutrients and signalling molecules. During early embryonic development the first primitive vascular system is formed *de novo* from endothelial precursor cells (Potente *et al.*, 2011). However, subsequent growth and remodelling of the vasculature occurs via angiogenesis, the formation of new blood vessels from pre-existing ones (Potente *et al.*, 2011). The most extensively studied mechanism and the most prevalent in adults is sprouting angiogenesis that will be introduced below. Other modes of angiogenesis include intussusception where existing vessels split into two increasing vascular density (Mentzer *et al.*, 2014).

Sprouting angiogenesis is tightly coordinated and regulated and involves many signalling molecules (Potente *et al.*, 2011; Ribatti *et al.*, 2012). The following gives a brief overview of this process highlighting the major angiogenic factors. Sprouting is triggered by elevated concentrations of secreted pro-angiogenic factors (Figure 1.1A). A key player initiating an angiogenic cascade is vascular endothelial growth factor A (VEGF-A, in the results chapters referred to as VEGF). By binding to VEGFR-2 receptor on the surface of endothelial cells, VEGF-A actively modulates their proliferation, differentiation and chemotactic responses. Mural cells stabilizing the vessel detach as a response to the release of angiopoietin-2 (ANG-2) by endothelial cells. The basement membrane surrounding the vessel is locally degraded by matrix metalloproteinases (MMPs). Through degrading extracellular

matrix (ECM) and cleaving its components, MMPs not only enable the outgrowth of endothelial cells but also generate more pro- and anti-angiogenic stimuli hence partially regulating the sprouting. The concentration gradient of VEGF-A and Dll4/Notch signalling facilitates the specification of endothelial cells into migratory tip and stalk cells which together form the sprout. Upon the stimulation with VEGF, endothelial cells dynamically compete for a tip position by expressing Dll4, a ligand for Notch receptor. The cell with the highest Dll4 expression activates Notch signalling on its neighbours that in turn downregulate the expression of VEGFR-2 reducing cells' responsiveness to VEGF-A. The tip cell which highly expresses VEGFR-2 receptor starts forming filopodia and moves from the vessel wall penetrating ECM towards pro-angiogenic chemotactic stimuli (Figure 1.1B). In contrast, the highly proliferative stalk cells behind the tip cell extend the newly emerging sprout (Figure 1.1C). They are also able to form a lumen and produce basement membrane to stabilize the growing sprout. Upon a contact between two sprouts or a sprout and existing vessel, a new capillary is formed through anastomosis (fusion) (Figure 1.1D). The lumen can be generated either during the sprouting or after a new vessel is formed. Subsequently EC proliferation is reduced and vessel is stabilized thus enabling blood flow. The recruitment of pericytes stimulates vessel maturation, promotes its quiescence and deposition of new basement membrane and ECM. It is the correct balance between microenvironmental pro- and anti-angiogenic stimuli that ensures the stability and quiescence of the blood vessels. It is normally the case that in an adult organism an antiangiogenic environment and vessel quiescence predominate (Potente,

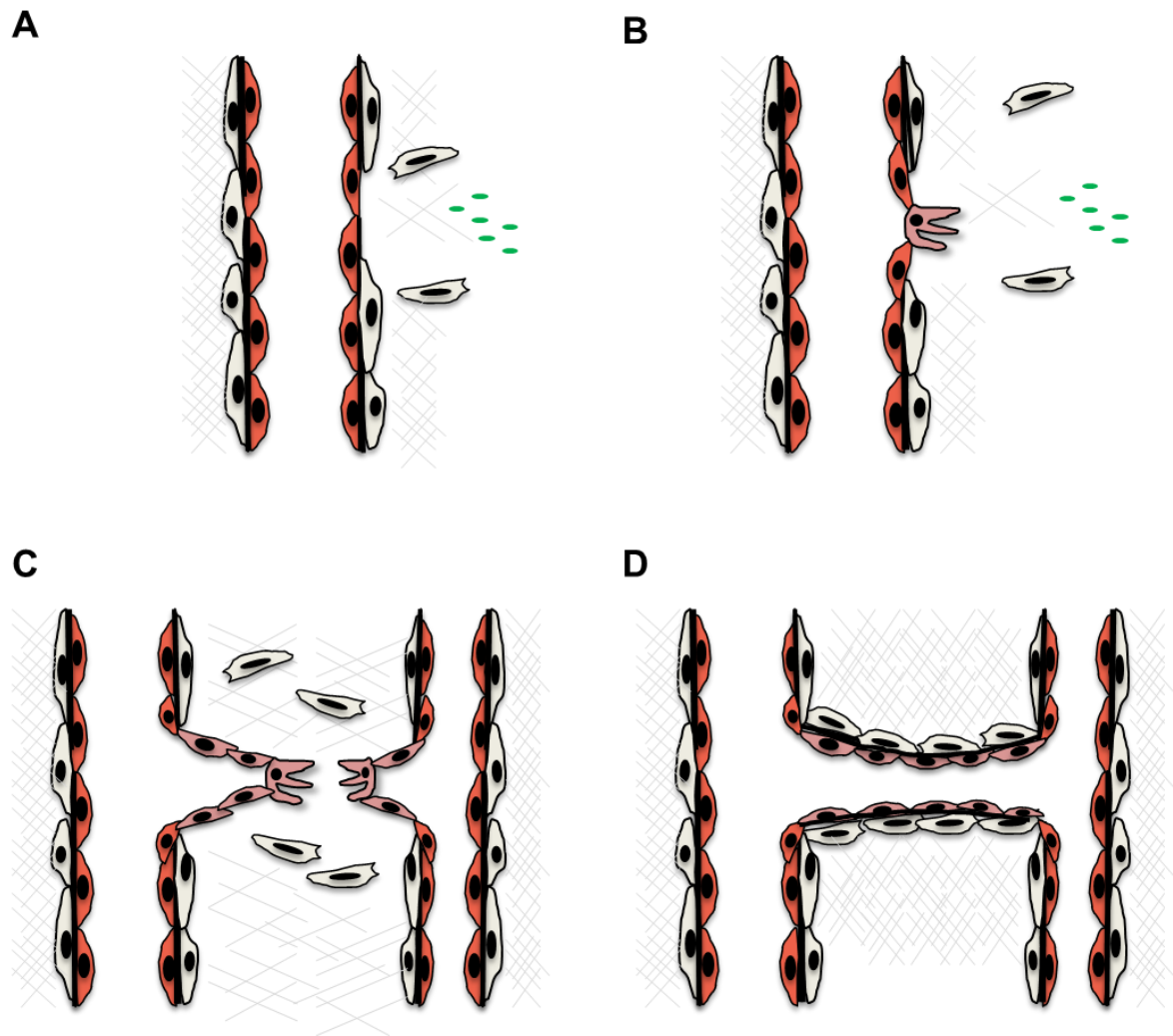


Figure 1.1 Sprouting angiogenesis. A) Upon increased pro-angiogenic stimuli such as VEGF-A (green ovals) angiogenic sprouting is triggered. Pericytes (white coloured cells) detach from the vessel and basement membrane (black tick line) and extracellular matrix (grey mesh) is degraded by proteolytic enzymes MMPs thus enabling migration of endothelial cells (red coloured cells) out of the vessel wall and through the basement membrane. B) Differentiated tip cell forms protrusions and migrates towards a chemotactic gradient. C) Newly emerging sprout is elongated due to proliferation of stalk cells behind the tip. Lumen is formed by the stalk cells. D) New vessel is generated due to anastomosis of two sprouts (or a sprouts and an established capillary) enabling a blood flow. Vessel is stabilized by the recruitment of pericytes and the deposition of new extracellular matrix.

et al., 2011). In healthy individuals angiogenesis occurs exclusively during specific events such as wound healing and tissue repair or menstrual cycle and pregnancy (Chung *et al.*, 2011). However, angiogenesis is a feature of a number of pathologies in adults, for example in cancer as will be discussed below.

Neovascularisation is generally accepted to be one of the hallmarks of cancer progression (Hanahan *et al.*, 2000). To grow, tumour demands a constant supply of nutrients and oxygen. The existing vasculature becomes insufficient to provide enough of these after tumour reaches 1-2 mm in diameter (Chung *et al.*, 2011). As a result of oxygen and nutrient deprivation, the tumour microenvironment becomes hypoxic triggering expression of pro-angiogenic factors. The shift in favour of pro-angiogenic stimuli is known as the 'angiogenic switch' and leads to the dynamic and uncontrolled formation of new vessels (Hanahan *et al.*, 1996; Bergers *et al.*, 2003). Depending on the tumour type, grade, its location, the 'angiogenic switch' occurs at different stages of tumour growth (Bergers *et al.*, 2003; De Palma *et al.*, 2017) and is modulated by many different factors including the major players, hypoxia and VEGF-A. The contribution of myeloid cells such tumour associated macrophages (TAMs) and cancer-associated fibroblasts (CAFs) to tumour vascularization and progression has been also shown. They fuel tumour growth and progression through secretion of various pro-angiogenic factors including VEGF-A, PDGF and MMP9 (Tao *et al.*, 2017; Rivera *et al.*, 2015).

Due to excessive and continuous pro-angiogenic stimuli, tumour vessels fail to reach quiescence. This ultimately leads to the formation of a tumour vasculature that is

phenotypically and morphologically distinct from its normal counterpart. These tumour blood vessels are disorganized, irregular and tortuous (reviewed by Nagy *et al.*, 2009) often with defective pericyte coverage (Bielenberg *et al.*, 2016). This extensively branched network is leaky and haemorrhagic with many blind ends causing poor and chaotic blood flow, interstitial hypertension and vascular compression (Weis *et al.*, 2005).

Notably, the tumour vascular network is heterogeneous thus not exclusively originated from capillary sprouting. Other mechanisms involving cancer cells functioning as endothelial-like cells (known as vascular mimicry), cancer stem cells differentiated into endothelial-like cells or endothelial precursor cells incorporated into the vessel wall are significant contributors to tumour angiogenesis (Lyden *et al.*, 2001; Carmeliet *et al.*, 2011). Moreover, effective utilization of existing vasculature by a tumour mass (known as vessel co-option) can bypass the requirement for new vessel sprouting (Carmeliet *et al.*, 2011).

1.2 Discovery of tumour endothelial markers and their clinical potential

As well as the phenotypic and morphological differences between the normal and tumour vasculature, tumour vessels have a distinct protein expression pattern. There are numerous examples of proteins abundant on tumour vasculature with little or weak expression on normal vessels; such proteins are known as tumour endothelial markers (TEMs) (St. Croix, 2000). A number of methods have been used to discover novel TEMs including a phage display, transcriptomic and proteomic profiling and

bioinformatics. These methods will be briefly described below. Examples of TEMs and techniques that led to their discovery are presented in Table 1.1.

The first markers were identified using immunohistochemical staining. For example, aiming to explore a biological function of extradomain-B (ED-B) of fibronectin, Carnemolla *et al.* (1989) generated a monoclonal antibody towards this splice variant of fibronectin. After staining of various normal and tumour tissues, they observed that ED-B is present on vessels or stroma in many neoplastic tissues while being undetectable in normal tissues except in the ovary. Another technique, phage display analysis has been performed *in vivo*. In this method a phage-displayed peptide library was intravenously administered into mice. After a period of incubation, mice tissues were excised, the endothelial cells isolated and phage peptides bound to these cells were further analysed for their protein targets (Trepel *et al.*, 2002). As an example, phage display led to the identification of peptides specific to aminopeptidase P (APP) on the breast cancer vasculature (Essler *et al.*, 2002).

Major advancements to the identification of novel TEMs was brought with the use of genome-wide transcriptome profiling methods such as microarrays, serial analysis of gene expression (SAGE) or RNA sequencing (RNA-Seq). These techniques enable a high throughput comparative study of gene expression based on RNA extracted from tumour and normal endothelial cells isolated from clinical samples. This allows the identification of differentially expressed genes. As reviewed by Clarke *et al.* (2006), microarrays consist of millions of short oligonucleotides probes from predetermined gene sets from genomic DNA. RNA extracted from cells is transcribed

into cDNA that is subsequently labelled with a fluorescent moiety. The labelled cDNA hybridizes to complementary oligonucleotides on the microarray. The strength of the fluorescence signal enables the quantitative analysis of expressed genes. In contrast, SAGE and RNA-Seq can identify gene transcripts and quantify their abundance without the need of having predetermined complementary oligonucleotides. Although their methodology differs, they both rely on short nucleotide sequence that are tagged, aligned and subsequently sequenced and analysed (Yamamoto *et al.*, 2001; Wang *et al.*, 2009). Microarrays were applied for example by Ghilardi *et al.* (2008) to search for novel markers in ovarian carcinoma. SAGE was used by St. Croix (2000) to identify several novel TEMs on colon tumour endothelium including TEM8. A combined microarray and RNA-Seq methodology was used by Zhuang *et al.* (2015) to identify novel TEMs in NSCLC as will be described later in this chapter.

Other methods include bioinformatics data mining (Huminiacki *et al.*, 2002; Huminiacki *et al.*, 2000) and cDNA libraries screening (Herbert *et al.*, 2008) that applied mathematical algorithms to predict transcriptional profiling of endothelium based on available datasets. These methods revealed ROBO4 (Huminiacki *et al.*, 2002) and ECSCR (Herbert *et al.*, 2008) as TEMs.

Additionally, proteomic analysis of tumour endothelium isolated from lung tumour-bearing rodents using silica beads played its part in the recognition of annexin A1 (Oh *et al.* 2004).

Table 1.1 Selected TEMs and techniques that led to their discovery.

Technique	TEM	Tumour type	Reference
Immunohistochemical staining	ED-B Endosialin Endoglin (CD105)	Various solid tumours	Carnemolla <i>et al.</i> 1989 Rettig <i>et al.</i> 1992 Burrows <i>et al.</i> 1995
<i>In vivo</i> phage display	Aminopeptidase P	Breast cancer	Essler <i>et al.</i> 2002
SAGE	TEM7 TEM8	Various solid tumours	St. Croix 2000
Bioinformatics	ROBO4, ECSCR ELTD1	Various tumour types	Huminiecki <i>et al.</i> 2000; Huminiecki <i>et al.</i> 2002 Herbert <i>et al.</i> 2008 Masiero <i>et al.</i> 2013
Transcriptomic profilig	TEM7 TEM8 CLEC14a	Various solid tumours Hepatocellular carcinoma	St. Croix 2000 Mura <i>et al.</i> 2012
Proteomic profiling	Annexin A1	Lung tumour, solid tumours	Oh <i>et al.</i> 2004

The uniqueness of tumour vessel biology raises a hope for the development of novel treatment alternatives for cancer patients by developing therapies targeted to tumour vessels as will be described later in this chapter.

In addition to therapeutic potential, TEMs can be used as diagnostic or prognostic markers. For example, ⁸⁹Zr labelled L2mAb (anti-TEM8 mIgG) antibody and TRC105 (anti-endoglin) antibody were successfully applied as immuno-PET imaging agents in lung and colon cancer mouse xenografts (Kuo *et al.*, 2014) and murine breast cancer-bearing mice (Hong *et al.*, 2012), respectively. Another marker TEM7 was proposed to be a prognostic marker in ovarian cancer (Czekierdowski *et al.*, 2018). Moreover, it was recently shown that high expression of the TEMs, MCAM and LAMA4, in renal cell carcinoma correlates with poor patient survival (Wragg *et al.* 2016).

1.3 Targeting the tumour vasculature

1.3.1 Anti-angiogenic agents (AAs)

The therapeutic potential of inhibiting the formation of the tumour vasculature in the treatment of cancer has been long proposed (Folkman, 1971). Blocking the VEGF signalling pathway has been considered the most promising route since its significant role in promoting both physiological and pathological neovascularization was elucidated (reviewed by Hoeben *et al.* 2004). This approach relies on the inhibition of growth of new blood vessels by anti-angiogenic agents (AAs): small molecules and antibodies (reviewed by Siemann *et al.*, 2017). One of the first to be clinically approved was bevacizumab (Avastin®). Bevacizumab is a humanized monoclonal antibody against VEGF-A, approved initially for the treatment of metastatic colorectal cancer in 2004. This and few other examples of antibody-based AAs that are either approved for treatment or currently in clinical trials are listed in Table 1.2. In contrast, chemically synthesized small molecule inhibitors such as Sunitinib or Sorafenib inhibit VEGF receptor (VEGFR) signalling (reviewed by Siemann *et al.*, 2017)

Table 1.2 Examples of antibody-based AAs either approved or in clinical trials.

AAs (brand name)	Company	Type and target	Indication/ clinical trials
Bevacizumab (Avastin)	Genentech	Humanized IgG1 against VEGF-A	NSCLC, glioblastoma, metastatic RCC and cervical carcinoma, epithelial ovarian cancer
Ramucirumab (Cyramza)	ImClone Systems	Fully human IgG1 against VEGFR-2	Stomach carcinoma and EAC, metastatic CRC, metastatic NSCLC
Ziv-aflibercept (Zaltrap)	Regeneron Pharmaceuticals	Recombinant fusion protein (VEGF-binding fragment of VEGFR-1/2 fused to Fc fragment of human IgG1) against VEGF-A, VEGF-B and PLGF	Metastatic CRC
Olaratumab (Lartruvo)	Eli Lilly	Fully human IgG1 against PDGFR α	Soft tissue sarcoma
IMC-18F1	ImClone Systems	Fully human IgG1 against VEGFR-2 against VEGFR-1	Phase II – colon, rectal and breast cancer

References: www.cancer.gov and www.clinicaltrials.gov (accessed 24 July 2018) and Kong *et al.* (2017); NSCLC – non small cell lung carcinoma; RCC – renal cell cancer; EAC – esophageal cancer; CRC – colorectal cancer

Despite very promising pre-clinical data in murine models, anti-angiogenic therapy has encountered several major challenges (reviewed by Shojaei, 2012). Firstly, tumours can adapt to anti-angiogenic agents causing drug resistance. The blockade of angiogenesis can be circumvented by secreting alternative pro-angiogenic factors such as basic fibroblast growth factor (bFGF) sustaining the tumour growth (Casanovas *et al.*, 2005). Secondly, the infiltration of drug from the bloodstream to the tumour mass is often limited. Another hurdle is the lack of validated biomarkers that would help to determine the tumour responsiveness to the therapy. Some groups

also suggest an accelerated tumour invasiveness and metastasis caused by anti-angiogenic treatment (Rapisarda *et al.*, 2009).

1.3.2 Vascular disrupting agents (VDAs)

The distinct features of tumour vasculature provide opportunities for treating tumours by preferentially targeting their existing vascular network. The advantages of this approach include an increased specificity and selectivity towards tumour vessels leading to an extensive tumour necrosis due to vascular loss (Siemann *et al.*, 2004; Thorpe, 2004). Thus, vascular targeting should minimize side effects by not disrupting normal tissue adjacent to the tumour. Moreover, drugs circulating in the bloodstream easily recognize targets on tumour vasculature thus omitting the problem of a poor drug infiltration into the tumour mass. This selective destruction of established vessels can be mediated via vascular disrupting agents (VDAs) generally distinguished into two groups: small-molecule agents and ligand-based biologics (Thorpe, 2004).

1.3.2.1 Small-molecule VDAs

Most of the small-molecules VDAs are tubulin inhibitors or flavonoids (Siemann *et al.*, 2017). These small-molecules target the characteristic features of tumour vessels such as their higher proliferation rate, permeability and increased tubulin dependence rather than a specific molecular target on the endothelial surface (Thorpe, 2004). A major obstacle of using small molecule VDAs is that they often show

cardiovascular toxicity (Subbiah *et al.*, 2011; Hollebecque *et al.*, 2012) indicating that they are not selective enough towards tumour vessels. There are many examples of compounds for which clinical trials were either suspended or terminated such as for ZD6129 developed by AstraZeneca (www.clinicaltrials.gov; accessed 24 July 2018). However, selective activation in tumour might reduce the cardiovascular side effects. This mode of action has been reported for ICT01-2588 (Gill *et al.*, 2014) that is currently being developed. Examples of small molecule VDAs that are currently in clinical trials are presented in Table 1.3.

Table 1.3 Examples of small-molecule VDAs in clinical trials.

Small-molecule VDA	Company	Type	Indication/ Clinical trials
Plinabulin NPI 2358	BeyondSpring Pharmaceuticals	microtubule destabilising drug	Phase III - NSCLC
Fosbretabulin (CA4P)	National Cancer Institute (NCI)	microtubule destabilising drug	Phase II - recurrent fallopian tube, ovarian, primary peritoneal carcinoma Phase II – neurocrine tumour
Oxi4503	Oxigene	microtubule destabilising drug	Phase I/II - acute myelogenous leukemia
BNC-105	Bionomics	microtubule destabilising drug	Phase I/II – RCC Phase I - chronic lymphocytic leukemia
EPC-2407	Epicept	microtubule destabilising drug	Phase I/II - solid tumour, anaplastic thyroid cancer
Vadimezan (ASA404)	Novartis	cytokine-inducing compound	Phase I - NSCLC

References: www.clinicaltrials.gov (accessed 24 July 2018); Mita *et al.* 2013); NSCLC – non small cell lung carcinoma; RCC – renal cell cancer;

1.3.2.2 Utilizing TEMs as ligand-based and antibody VDAs

Ligand-based VDAs target the tumour vessels by binding selectively to TEMs on the tumour endothelial surface (Thorpe, 2004). As mentioned before, such accessibility of potential targets directly from the bloodstream might circumvent drug delivery problems. Several approaches have been developed. They are based on antibody derivatives or peptides conjugated with bioactive molecules such as cytokines (tumour necrosis factor α - TNF α , interleukin-12 - IL-12), cytotoxic agents (paclitaxel), radionuclides (Iodine-131), toxins (ricin, gelonin) or drugs (Schliemann *et al.*, 2007). While ligand specifically delivers a conjugate to the tumour vasculature, the bioactive moiety destroys it.

Although ligand-based VDAs are much less advanced in clinical development than other anti-vascular therapies there are several candidates currently undergoing clinical trials such as conjugates of L19 antibody directed against ED-B. A study combining the use of L19-IL-12 and L19-TNF α is now in Phase III for malignant melanoma and L19-IL12 is independently in Phase I/II for metastatic melanoma (www.clinicaltrials.gov, accessed 24 July 2018). Pre-clinical work has also been promising. Recently published work by Guo *et al.* (2018) has shown that anti-TEM1 antibody 75Fc conjugated with saporin toxin is effective against human sarcoma in mice.

Moreover, unconjugated antibodies directed against TEMs have been shown to effectively reduce tumour growth *in vivo*, for example as was discovered with the anti-

TEM8 antibody in colon tumour models (Chaudhary *et al.*, 2013), anti-ELTD1 antibody in glioma model (Ziegler *et al.*, 2017) or anti-CLEC14a in Lewis lung carcinoma (Noy *et al.*, 2015).

1.3.3 Vascular targeted therapy (VTT)

The major drawback of VDAs-based treatment is the remaining presence of living tumour cells around the rim of the necrotic tumour (Siemann, 2004; Tozer *et al.*, 2005). It is believed that these peripheral tumour cells take advantage of adjacent normal blood vessels resulting in regions insensitive to VDAs (Siemann, 2004). Since surviving cancer cells will likely allow tumour regrowth, successful use of VDAs as a monotherapy is doubtful (Siemann, 2011). Therefore, combined therapies of VDAs with AAs, radiotherapy or chemotherapy have been extensively investigated. The major advantage of such a combined vascular targeted therapy (VTT) approach is that the limitations of both AAs and VDAs are minimized by making use of their distinct mechanisms of action to both prevent forming new blood vessels (AAs) and destroy established vessels (VDAs) (Siemann *et al.* 2017). For example the combination of Pazopanib (AA) and anti-endoglin antibody (TRC105 or carotuximab) is now in Phase III of clinical trials for advanced angiosarcoma (www.clinicaltrials.gov, accessed 24 July 2018).

Alternative VTT approach involves tumour vascular normalisation. As reviewed by Viallard *et al.* (2017), restoring tumour vessels to normal-like state improves blood flow. This in turn enhances the effectiveness of drugs. Therapeutic effect was

observed for combined therapy of bevacizumab and chemotherapy. Bevacizumab monotherapy did not yield long term therapeutic benefits (Mayer, 2004) but it increased survival when administered with chemotherapy (Hurwitz *et al.*, 2004). Jain (2005) proposed that this was achieved due to vessel normalisation mediated by bevacizumab. Similarly, tumour vessel normalisation was observed when targeting a TEM, CD160, using CL1-R2 antibody in melanoma-bearing mice thus increasing the accessibility of the tumour to chemotherapeutics (Chabot *et al.*, 2011).

Since the expression pattern of TEMs differs between various tumours it is unlikely that one VTT would be universally successful against all solid tumours. Hence, ideally vascular targeting approach should be individually adjusted to the tumour type. Although very promising, this approach requires a target to be a true TEM to avoid severe off-target side effects in normal tissue.

1.4 Identification of new tumour endothelial markers in non-small cell lung carcinoma (NSCLC)

In our laboratory, transcriptomic profiling using microarray together with RNA-seq methodology was used to identify TEMs from non-small cell lung carcinoma (NSCLC) tumour endothelial cells (TECs). A detailed experimental methodology and results are presented in the doctoral thesis: Validation and identification of tumour endothelial markers and their uses in cancer vaccine (2012) and subsequent publication (Zhuang *et al.*, 2015).

Among several genes identified by Zhuang *et al.*, protocadherin 7 (PCDH7) a member of δ 1-protocadherin group of cadherin superfamily, was highly overexpressed in tumour compared to normal lung endothelial cells according to qPCR analysis. These data were further supported by the immunohistochemical analysis. Indeed, PCDH7 showed evident vascular staining on lung tumour while being absent in healthy lung tissue sections. The expression of PCDH7 was also detected in placenta, a vascularized organ of active angiogenesis. In the light of this finding, PCDH7 was considered as a promising target for further studies on its functional role in the endothelial cells and the tumour vasculature.

1.5 Cadherin superfamily

The cadherins are type I transmembrane glycoproteins representing a large group of cell adhesion superfamily proteins. The defining feature for all cadherin superfamily members is the presence of multiple ~110 amino acid long cadherin repeats within their extracellular domain (Hulpiau *et al.*, 2016). Moreover, extracellular domains bind several Ca^{2+} ions rigidifying their structure and this is crucial for their function (Shapiro *et al.*, 2009). Based on their amino acid sequence and properties, the cadherin superfamily can be divided into subgroups, these are classical cadherins, desmosomal cadherins and protocadherins as shown in Figure 1.2 (Chidgey *et al.*, 2016; Gumbiner, 2016; Jontes, 2016; Mah *et al.*, 2016).

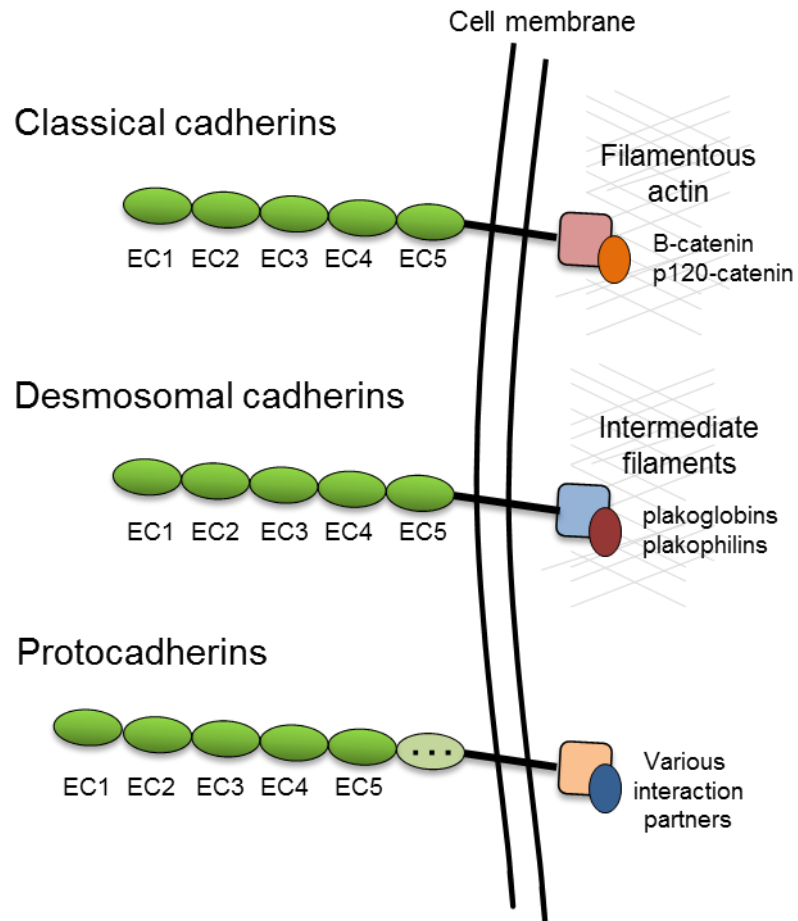


Figure 1.2 Classification of cadherin superfamily. Schematic structure and interactions of A) classical cadherin, B) desmosomal cadherins and C) protocadherins. Both classical and desmosomal cadherins contain five cadherin repeats (EC) in their extracellular domain (ECD) while they differ in their intracellular interactions. Protocadherins contain various numbers of EC in their ECD and differ in their intracellular partners.

The extracellular domains of both classical and desmosomal cadherins contain five conserved EC repeats (EC1-EC5). They mediate strong, calcium-dependent and mainly *trans*-homophilic cell-cell junctions through their N-terminal, membrane-distal EC1 repeat. Their biological function varies depending on their intracellular interacting proteins (Saito *et al.*, 2012).

As reviewed by Gumbiner (2016), cytoplasmic domain of classical cadherins interacts with armadillo repeats of different proteins such as β -catenin or p120-catenin. This enables the formation of adherens junction by connecting classical cadherins with filamentous actin. Since actin is one of the most abundant components of eukaryotic cells' cytoskeleton, its complexes with cadherins play significant roles in regulating cell morphology, structural support, motility, migration and cell division. An endothelial example of a classical cadherin family member is vascular endothelial (VE)-cadherin. It is essential for angiogenesis and regulates endothelial junctional integrity and permeability (Vestweber, 2008). Additionally to its adhesive properties, VE-cadherin plays a significant role in cell signalling by interacting with various extracellular and intracellular partners such as VEGFR-2 (Vestweber, 2008).

In contrast, the desmosomal cadherins (desmogleins and desmocollins) form desmosome complexes by indirect interaction with intermediate filaments through plakoglobins and plakophilins (Saito *et al.*, 2012). They are expressed mainly in epithelial and myocardial tissues (Saito *et al.*, 2012) which are susceptible to excessive stretching. In these cell types they play a crucial role in maintaining tissue integrity and protecting cells from a mechanical stress (Brooke *et al.*, 2012).

Protocadherins (PCDHs) constitute the largest cadherin subfamily. Their classification, cellular distribution and functions will be further expanded below.

1.5.1 Protocadherin subfamily

Depending on their genomic organization, protocadherins are classified either into a clustered or non-clustered group. They are structurally similar to the classical cadherins but there are several features distinguishing PCDHs from other cadherin subfamilies. A common characteristic of all PCDHs includes the lack of catenin binding sequences in their variable cytoplasmic domains (Lefebvre, 2017). Moreover, with few exceptions, their extracellular domains are encoded by a single exon (Kim *et al.*, 2011).

Members of clustered group, protocadherins α , β and γ , are encoded by three tandem gene clusters containing multiple large exons located on chromosome 5 (Redies *et al.*, 2005). This compacted genomic organization enables the expression of 58 various clustered protocadherin isoforms by alternative promoters, alternative splicing and epigenetic modifications (Hayashi *et al.*, 2015; Lefebvre, 2017). The extracellular domains of all clustered PCDHs contain six EC repeats (EC1-EC6) from which EC1-EC4 are involved in highly specific *trans*-homophilic interactions (Lefebvre, 2017) from which EC2-EC3 are likely responsible for their specificity (Schreiner *et al.*, 2010). Notably, the strength of PCDHs' homophilic interactions is generally weaker than that of classical cadherins (Redies *et al.*, 2005). Therefore, a greater number of clustered PCDHs in the cell membrane might be necessary to

stabilize those interactions and trigger intracellular signalling (Rubinstein *et al.*, 2015).

Clustered protocadherins are widely expressed in the vertebrate nervous system (CNS) therefore their function has been studied primarily from this perspective (Weiner *et al.*, 2013; Hayashi *et al.*, 2015). They are reported in neural circuit formation. Members of α -PCDHs are implicated in the coalescence of axons in olfactory sensory neurons. Another group, γ -PCDHs, emerged as important in neurite 'self-avoidance' suggesting their importance in neuronal development and survival. The knowledge about the function of β -PCDHs is limited, however two members of this group, β -PCDH16 and β -PCDH22, have been found in post-synaptic compartments of retinal and cerebellar neurons (Junghans *et al.*, 2008). Aberrant DNA methylation of clustered PCDHs genes are implicated in several types of nervous system cancers such as astrocytoma or neuroblastoma as well as human paediatric kidney cancer, prostate cancer and breast cancer (Mah *et al.*, 2016).

On the contrary to the clustered PCDHs, non-clustered protocadherins genes are scattered in the genome. Two major subgroups δ 1 and δ 2 have been identified consisting of seven or six EC repeats, respectively (Kim *et al.*, 2011), and containing N-linked glycosylation sites with the number depending on the group (Vester-Christensen *et al.*, 2013). Their cytoplasmic domains have low to moderate homology. They share conserved motifs CM1 and CM2 although interacting partners to these motifs have not been determined (Kim *et al.*, 2011). Furthermore, δ 1-PCDHs interact with protein phosphatase-1 α (PP1 α) through their additional conserved CM3

(RRVTF) motif (Kim *et al.*, 2011). Similarly to clustered PCDHs, δ -PCDHs are prevalent in CNS thus being studied mostly in the context of its development and patterning (Vanhalst *et al.*, 2005). However, a few members were found also in other tissues during mouse embryonic development (Kim *et al.*, 2011). Moreover, dysregulated expression of δ -PCDHs is implied in many diseases. Nevertheless, their function is still poorly understood. The reported functions of selected δ -PCDHs are presented in Table 1.4. As PCDH7 is further discussed below, it is not included in this table.

Table 1.4 Reported functions of few selected non-clustered δ -PCDHs.

Group	PCDH	Selected functions
$\delta 1$	PCDH1	<ul style="list-style-type: none"> Localized in adherens junctions in epithelial cells in asthma where it mediates cell adhesion (Faura Tellez <i>et al.</i>, 2016) Expressed in mouse lung endothelial cells (Favre <i>et al.</i>, 2003) Its expression is silenced in breast cancer (Vasilatos <i>et al.</i>, 2013)
	PCDH11	<ul style="list-style-type: none"> Its binding to β-catenin may regulate Wnt signaling and prostate cancer tumorigenesis (Chen <i>et al.</i>, 2002)
$\delta 2$	PCDH8	<ul style="list-style-type: none"> Its <i>Xenopus</i> orthologue PAPC is involved in gastrulation by downregulating C-cadherin mediated adhesion (X. Chen <i>et al.</i>, 2006) PAPC is involved in Wnt signalling (Kraft <i>et al.</i>, 2012) Interacts directly with N-cadherin promoting its internalization (Yasuda <i>et al.</i>, 2007) Its expression is silenced in many types of tumours including RCC, bladder cancer, gastric cancer and breast cancer (Jontes, 2016)
	PCDH17	<ul style="list-style-type: none"> Mediates weak cell adhesion in cell aggregation assay and regulates presynaptic vesicle assembly (Hoshina <i>et al.</i>, 2013) Its expression is silenced in many types of tumours (Jontes, 2016)
	PCDH19	<ul style="list-style-type: none"> Exhibits homophilic adhesion when in complex with N-cadherin (Emond <i>et al.</i>, 2011); Involved in regulation of neuronal progenitor cells differentiation (Homan <i>et al.</i>, 2018) Involved in PCDH19-related epilepsy (Lyons <i>et al.</i>, 2017)

1.5.2 Protocadherin 7 (PCDH7)

Human PCDH7 was first identified in brain and heart by Yoshida *et al.* (1998) and thus originally named BH-protocadherin. As mentioned before, it belongs to $\delta 1$ -PCDHs group containing 7 EC repeats and includes several isoforms with a conserved extracellular domain. A detailed depiction of the structure of the most abundant PCDH7 isoform A is presented in Figure 1.3. Similarly to other $\delta 1$ -PCDHs members it interacts intracellularly with PP1 α (Yoshida *et al.*, 1999). PCDH7 is primarily expressed in the nervous system. It has been shown to be involved in axon initiation and elongation in retinal ganglion cells (Piper *et al.*, 2008) and in the early *Xenopus* development (Bradley *et al.*, 1998).

Dysregulated expression of PCDH7 has been reported in epilepsy (Poduri, 2015) and in many types of solid tumours where its function has been investigated and elucidated mainly in this context as comprehensively reviewed below.

Li *et al.* (2013) have reported that PCDH7 participates in the development of bone metastases in breast cancer. *In vitro* data showed that PCDH7 expression was significantly higher in the bone metastatic breast cancer cell line (MDA-MB-231) compared to normal and non-bone metastatic breast cancer cells. Furthermore, *in vitro* siRNA-mediated PCDH7 knockdown in MDA-MB-231 cells resulted in impaired cell proliferation, migration, and invasion. The opposite enhancing effects on the cell proliferation and invasion were observed when MDA-MB-231 stably overexpressed PCDH7. Similarly, *in vivo* experiments using immuno-deficient mice

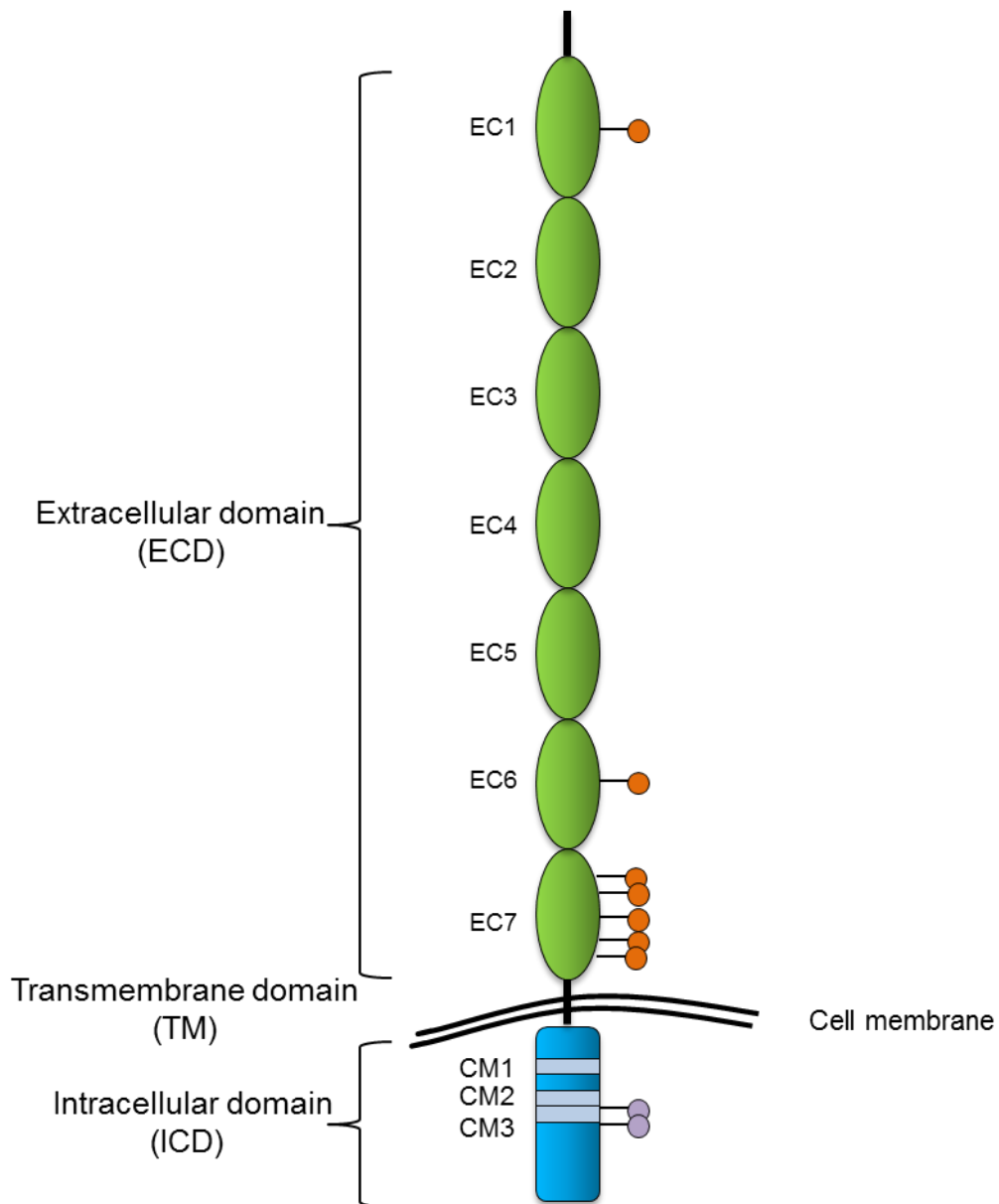


Figure 1.3 Structure and organization of protocadherin 7 (PCDH7) isoform A. PCDH7a consists of an extracellular domain (ECD) with 7 EC that is conserved among all PCDH7 isoforms, a short transmembrane domain (TM) and an intracellular domain (ICD). The ECD is subjected to N-linked glycosylation (orange coloured circles) and contains several Ca^{2+} binding sites. The ICD has three regions CM1, CM2 and CM3 conserved within $\delta 1$ PCDHs group and two phosphorylation sites (purple coloured circles). Isoform A is the most abundant of all PCDH7 isoforms that slightly differ only in their ICD sequences.

implanted with MDA-MB-231-PCDH7 cells showed a higher volume of metastatic lesions in the bones than mice implanted with control cells. However, the molecular mechanism by which PCDH7 participates in this process was not determined.

Zhou *et al.* (2017) have studied the expression of PCDH7 in available NSCLC gene microarray datasets and found a significant correlation between high PCDH7 expression and poor clinical outcome. This mRNA analysis was consistent with immunohistochemical staining of NSCLC tissue arrays. Next, Zhou *et al.* (2017) investigated a role of PCDH7 in NSCLC. Their data suggested oncogenic activity of PCDH7 in mutant *KRAS* or *EGFR* human bronchial epithelial cells (HBEC) since it augmented MAPK signalling in these cells. Moreover, CRISPR/Cas9 inactivation of PCDH7 in *KRAS* mutant NSCLC cells resulted in inhibited tumorigenesis *in vivo*. Analysis of tumour lysates revealed decreased phosphorylation of the ERK MAP kinase. Moreover, co-immunoprecipitation experiments revealed that PCDH7 interacts with the SET oncoprotein (known also as phosphatase 2A inhibitor) and protein phosphatase 2 (PP2A). Based on their findings, Zhou *et al.* (2017) proposed a mechanism through which PCDH7 promotes tumorigenesis of NSCLC. In this model, the PCDH7 intracellular interaction with SET mediates PP2A inhibition thus blocking dephosphorylation of ERK. Together with impaired *KRAS* or *EGFR*-induced cell proliferation, PCDH7 potentiates MAPK signalling leading to enhanced tumorigenesis. However, the extracellular interactions of PCDH7 were not investigated in this study.

A distinct role of PCDH7 was discovered in brain metastasis. According to a comprehensive study conducted by Chen *et al.* (2016) PCDH7 participates in the formation of heterocellular gap junctions between brain metastatic cancer cells and astrocytes. This connection involves direct interactions between PCDH7 and Cx43, one of the major gap-junction protein in astrocytes. The exchange of cGMP through these assembled channels between these two cell types ultimately elevates IFN α and TNF α expression by the astrocytes, leading to the activation of the STAT1 and NF- κ B signalling pathways in cancer cells. This supports their outgrowth and chemoresistance. Moreover, Chen *et al.* (2016) showed that PCDH7 or Cx43 shRNA-mediated knockdown in breast or lung cancer cells decreased the occurrence of metastatic lesions in immunocompetent and xenograft mice models. They have proposed that PCDH7 localized in close proximity to Cx43 stabilizes the connection of brain metastatic cells and astrocytes by homophilic interactions and facilitates molecular exchange. Another study on the brain metastatic cells conducted by Ren *et al.* (2018) gave further insight on the mechanism by which PCDH7 promotes tumorigenesis. The PCDH7 strengthened gap-junctions facilitated increased influx of Ca²⁺ ions to cancer cells. This, in turn increased downstream activation of CaM-dependent kinase and nuclear transcription factors that stimulate proliferation of cells.

In contrast to tumorigenic activity described above, PCDH7 is implicated as a tumour suppressor in gastric cancer. Immunohistochemical data presented by Chen *et al.* (2017) indicated that PCDH7 is present in normal gastric mucosa while its expression was downregulated in gastric cancer specimens with the lowest expression in gastric

cancer with lymph node metastasis. They found a correlation between low presence of PCDH7 with a poor patient survival rate. The same study showed that levels of PCDH7 did not affect gastric cancer cell proliferation. However, they observed enhanced cancer cell migration and invasion upon *in vitro* siRNA-mediated PCDH7 knockdown. This was observed together with a decrease in the expression of E-cadherin associated with the epithelial mesenchymal transition (EMT), a crucial step of tumorigenesis (Carrizo, 2017). The exact molecular mechanisms involved were not investigated. A similar correlation between the low expression of PCDH7 and poor overall survival were reported for patients with non-invasive bladder cancer (Lin *et al.*, 2016) or colorectal cancer (Bujko *et al.*, 2015).

Based on studies to date, PCDH7 appears to have distinctive functions depending on the tumour type. On the one hand it seems to play a significant role in the metastasis by supporting tumour colonization in secondary tissues (Li *et al.*, 2013; Chen *et al.*, 2016) but on other its expression might play its part in preventing EMT in primary gastric tumour (Chen *et al.*, 2017). Additionally, PCDH7 strengthens cell-cell interactions and participates in downstream signalling pathways (Chen *et al.*, 2016; Zhou *et al.*, 2017; Ren *et al.*, 2018). However, the published data focuses mostly on the PCDH7 intracellular but not its extracellular interactions. PCDH7 was previously shown to mediate weak cell-cell adhesion in mouse fibroblasts using cell aggregation assay (Yoshida, 2003) however this has not been investigated in detail. Contradictory results reporting a lack of adhesive properties of the PCHD7 extracellular domain using a bead aggregation assay were presented by Blevins *et al.* (2011). To date

there are no published data on a potential role of PCDH7 in endothelial cells or in the tumour vasculature.

1.6 *In vitro* angiogenesis assays

Basic research on endothelial cell biology and angiogenic pathways is usually conducted using numerous *in vitro* assays which model various aspects of angiogenesis. Similarly, to develop effective anti-vascular compounds towards the targets on tumour vasculature such as TEMs, it is beneficial to have a comprehensive knowledge of the function of target antigen and whether it functions to regulate angiogenesis. A deep understanding of mechanism of action of potential targets is advantageous when selecting, characterising and validating the most suitable target proteins. Moreover, *in vitro* studies are conducted before proceeding to the *in vivo* setting.

In recent decades, multiple advancements have been made to establish suitable *in vitro* models that mimic the angiogenic process occurring *in vivo*. Due to the large number of different methods that have been developed, only selected ones used in the research presented in this thesis will be discussed below (Figure 1.4). They feature most commonly used endothelial cell type - human umbilical vein endothelial cells (HUVEC). Network formation assays involve co-culturing of HUVEC with stromal cells such as human dermal fibroblasts (HDF) which support endothelial cell growth and promote tube formation (Lafleur *et al.*, 2002).

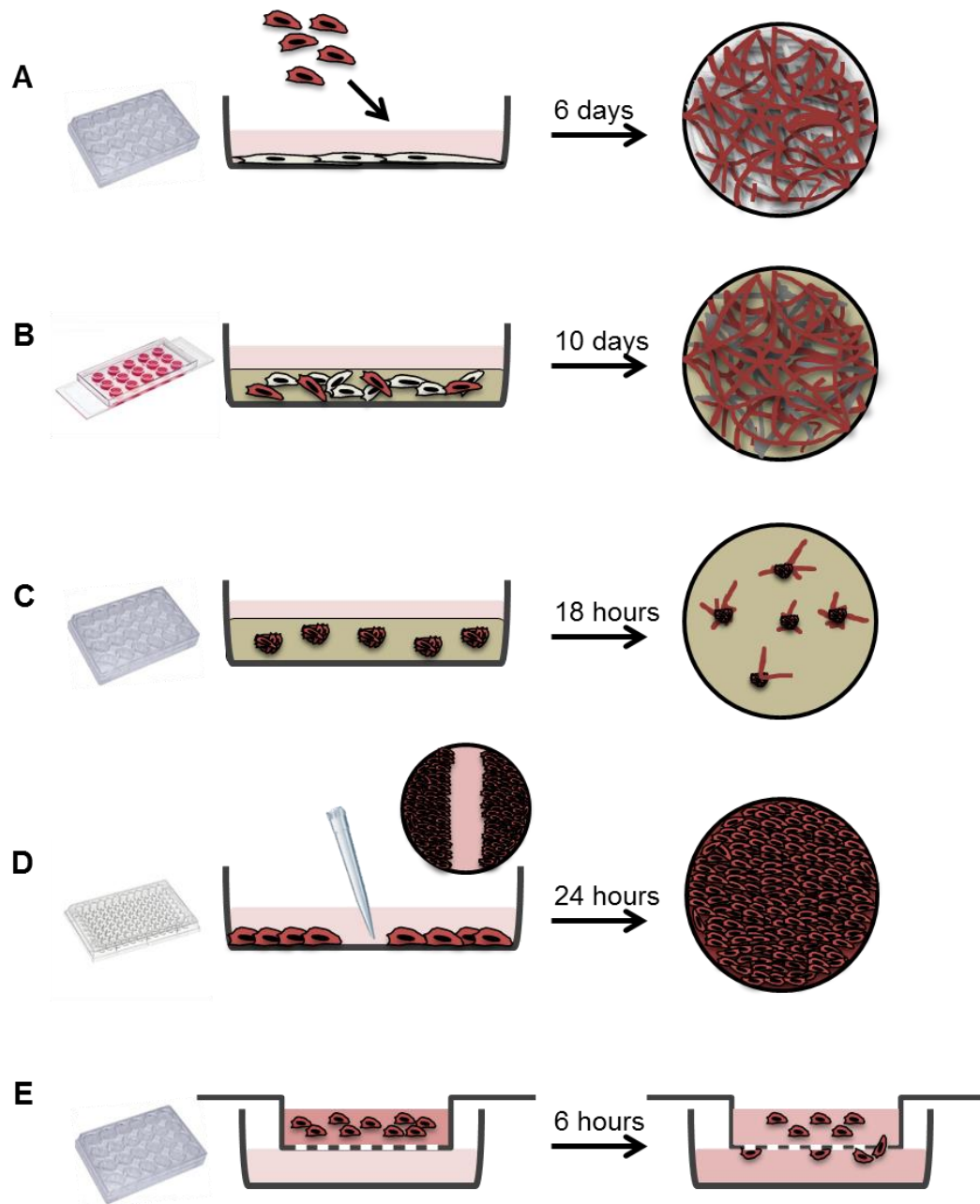


Figure 1.4 *In vitro* angiogenesis assays. A) 2D co-culture assay. HUVEC are seeded on top of a monolayer of HDF and form a network of tubules. B) 3D HUVEC/HDF co-culture assay. A mix of HUVEC and HDF is suspended in a 3D fibrin matrix. Endothelial cells form a 3D network with HDF as a neuronal-like scaffold. C) 3D spheroid assay. Endothelial spheroids are embedded in a 3D collagen matrix and allowed to sprout out into the matrix. D) Scratch assay. A confluent monolayer of HUVEC is scratched to generate a region without cells. Endothelial cells mass migrate to close the wound. E) Transmigration assay. Endothelial cells are seeded on top of a porous filter in the upper chamber and allowed to migrate towards a chemoattractant present in the lower chamber.

1.6.1 2D HUVEC/HDF *in vitro* co-culture assay

In a 2D HUVEC/HDF co-culture assay, the endothelial network formation relies on an endogenous extracellular matrix (ECM) secreted and dynamically remodelled by the fibroblasts. HUVEC are seeded on top of a monolayer of HDF (Figure 1.4A) on which they actively migrate and sprout (Mavria *et al.*, 2006) ultimately forming tubes with lumen (Bishop *et al.*, 1999) and subsequently undergoing senescence (Abraham *et al.* 2009). Network formation is VEGF-dependent (Hetheridge *et al.*, 2011) but not MMP-dependent (Figure A.5). The endothelial network can be fixed and visualised using immunohistochemical methods. Alternatively, the formation of the network can be observed in real time when endothelial cells are for example lentivirally transduced with a fluorescence marker.

1.6.2 3D HUVEC/HDF *in vitro* co-culture assay

In contrast, in a 3D HUVEC-HDF co-culture HUVEC and HDF cell mix is suspended in external 3D matrices such as collagen type I or fibrin (Figure 1.4B). The endothelial cells invade into 3D structure therefore making it closer to *in vivo* microenvironment (Sun *et al.*, 2004). They actively migrate, proliferate and sprout. The network forms multiple branches, anastomoses, matures with the formation of lumen reported (Lafleur *et al.*, 2002) and ultimately undergoes senescence. The network formation is VEGF and bFGF-dependent and MMP-dependent (Lafleur *et al.*, 2002; Sun *et al.*, 2004). Similarly to 2D co-culture, the formation of

the endothelial network can be observed in real time. Alternatively, the mature network can be fixed and stained with lectin.

1.6.3 Spheroid assay

Endothelial cell sprouting involves the degradation and invasion of cells into the extracellular matrix (Potente *et al.*, 2011). The process can be successfully studied using a three-dimensional model in which endothelial cells sprout from cell spheroids embedded in an exogenous matrix, most frequently fibrin or collagen type I (Figure 1.4C). The spheroid-based *in vitro* assay is short (48 hours in total) thus allowing rapid collection of data. Cells can be fluorescently labelled for better visualisation and imaged using either widefield or confocal microscopy. The formation of lumen in this assay has been also reported (Auerbach *et al.*, 2003).

1.6.4 Scratch assay

A scratch assay enables monitoring of the haptotactic cell migration (Eccles *et al.*, 2009) in a two-dimensional setting. It is a simple method in which a confluent cell monolayer is scratched to generate an area without cells (Figure 1.4D). Measuring of the wound closure over time gives an indication of the cell migration rate. This assay is suitable for a qualitative assessment of the cell migratory response.

1.6.5 Transmigration assay

A transmigration (or modified Boyden chamber) assay enables measuring the cell migration rate towards specific chemoattractant (Albini *et al.*, 2004). In this method, cells are placed on top of porous upper filter and allowed to migrate across the membrane in a direction of chemoattractant (such as FBS, VEGF or bFGF) present in a lower chamber (Figure 1.4E). The number of migrated cells gives an indication about the cell migration in given conditions. The short duration of 6 hours excludes the potential cell proliferation co-effect (Staton *et al.*, 2006). However, maintaining of chemoattractant gradient over time is difficult due to continuous diffusion of molecules between upper and lower compartments (Eccles *et al.*, 2009).

1.6.6 Proliferation assay

The number of actively dividing cells gives an indication of the cell proliferation rate. Common methods involve measuring cellular metabolic activity using various chemical reagents such as tetrazolium salt MTT that is converted by mitochondria to formazan crystals. These assays enable for example high-throughput screening of cytotoxic agents and their impact on the cell growth. It is relatively safe and easy to perform (Staton *et al.*, 2006). However, interferences of MTT reagents with cellular components or chemicals have been reported. For example, difference in numbers of mitochondria between small and large cell results in a different amount of formazan that is produced (Van Tonder *et al.*, 2015). Similarly, serum in culture medium might

additionally reduce MTT (Talorete *et al.*, 2006). Therefore, experimental conditions for this assay need to be carefully determined. Proliferation assays are not limited to endothelial cells therefore per se they are not considered as *in vitro* angiogenesis assay, however endothelial proliferation is a feature of angiogenesis.

1.7 Hypotheses and aims

Hypothesis 1 (Chapter 3):

PCDH7 has a role in angiogenesis and the extracellular domain of PCDH7 or its ligand(s) could serve as potential anti-vascular targets in the future.

To test this hypothesis we aimed to determine how the extracellular domain of PCDH7 fused to the Fc portion of immunoglobulin affected the behaviour of endothelial cells in a range of assays modelling different aspects of angiogenesis.

Hypothesis 2 (Chapter 4):

The extracellular domain of PCDH7 exerts its function by interacting with endothelial cell surface protein(s).

To test this hypothesis we sought to identify ligand(s) of PCDH7 ECD on endothelial cell surface using immunoprecipitation and to determine the nature of interactions between the PCDH7 ECD and its binding partner(s).

Hypothesis 3 (Chapter 5):

There exist novel TEM(s) in colorectal cancer which can be revealed with transcriptome profiling.

To test this hypothesis we aimed to identify potential TEM candidates by comparing and analysing the gene expression signature of tumour and normal endothelial cells isolated from CRC patients by applying various online tools and experimental techniques.

CHAPTER 2: MATERIALS AND METHODS

CHAPTER 2: MATHERIALS AND METHODS

2.1 Reagents

2.1.1 Buffers

Table 2.1 Commonly used buffers and their composition.

Buffer	Components
PBS	5 tablets (Sigma, cat no. P4417) in 1 L of miliQ water
PBS-T	PBS, 0.1% (v/v) Tween 20
TAE	40 mM Tris, 20 mM acetic acid, 1 mM EDTA
TBE	89 mM Tris, 89 mM boric acid, 2 mM EDTA
Stacking gel buffer	125 mM Tris-HCl pH 6.8, 0.1% (w/v) SDS
Resolving gel buffer	375 mM Tris-HCl pH 8.8, 0.1% (w/v) SDS
SDS-PAGE running buffer	25 mM Tris, 250 mM glycine, pH 8.3, 0.1% (w/v) SDS.
Western blot transfer buffer	25 mM Tris, 187.2 mM glycine, 20% methanol
Western blot stripping buffer	200 mM glycine pH 2.5, 1% (w/v) SDS
RIPA buffer	50 mM Tris pH8, 150 mM NaCl, 1% (v/v) NP-40, 0.5% (w/v) Sodium deoxycholate, 0.1% (w/v) SDS
4x Laemmli sample buffer	200 mM Tris-HCl pH 6.8, 50 mM EDTA, 40% (v/v) glycerol, 5% (v/v) β -mercaptoethanol, 8% (w/v) SDS, 0.03% (w/v) bromophenol blue
Flow cytometry buffer	10 mM HEPES, 140 mM NaCl, 2.5 mM CaCl ₂
IP lysis buffer	10 mM HEPES, 140 mM NaCl, 2.5 mM CaCl ₂ , 1% (v/v) NP-40, protease inhibitor tablet (Thermo Scientific, cat no. 88666)
IP wash buffer	100 mM Tris pH7.5, 200 mM NaCl, 0.5% (v/v) NP40
IF blocking buffer	PBS, 10% (w/v) BSA, 0.1% (v/v) FBS, 0.01% (v/v) Tween-20, 0.01% (w/v) sodium azide

2.1.2 Primary antibodies

Table 2.2 Primary antibodies and their working concentration for various applications. WB – Western blot; IF – immunofluorescence; FC - flow cytometry.

Antibody	Provider	Cat no.	Application and working dilution
Goat polyclonal anti-human EPCR	R&D Systems	AF2245	WB (0.25 µg/ml)
Rabbit polyclonal anti-human STAB1	Millipore	AB6021	WB (1:1000)
Mouse monoclonal anti-human ESM-1	Abcam	ab56914	WB (1 µg/ml)
Rabbit polyclonal anti-human C1ORF54	Sigma Aldrich	HPA026518	WB (1:200)
Rabbit polyclonal anti-human PCDH7	Atlas Antibodies	HPA011866	WB (0.8 µg/ml) FC (10 µg/ml) IF (1 µg/ml)
Mouse polyclonal anti-human EFEMP-1	Abnova	H00002202-B01P	WB (2.5 µg/ml and 0.25 µg/ml)
Mouse monoclonal anti-human CD31 (clone WM59)	BD Pharmingen	550389	IF (0.3 µg/ml)
Goat anti-human Fc – HRP conjugate	Sigma Aldrich	A0170	WB (1:4000)
Mouse monoclonal anti-V5-HRP conjugate	Thermo Scientific	R96125	WB (1:5000)
Mouse monoclonal anti- FLAG M2 tag	Sigma Aldrich	F3165	WB (0.5 µg/ml)
Mouse monoclonal anti-His tag	R&D Systems	MAB050	WB (0.5 µg/ml)
Mouse monoclonal anti-HA tag (clone 12CA5)	Cancer Research UK		WB (0.025 µg/ml)
Rabbit polyclonal anti-human β-tubulin	Cell Signalling	2144S	WB (1:1000)
Mouse polyclonal anti-human β-actin	SomantiX B.V., Utrecht, NL		WB 1:2000
Rabbit polyclonal anti-human GAPDH	SomantiX B.V., Utrecht NL		WB 1:2000

2.1.3 Secondary antibodies

Table 2.3 Secondary antibodies and their working concentration for various applications. WB – Western blot; IF – immunofluorescence; FC - flow cytometry.

Antibody	Provider	Cat no.	Application and working dilution
Goat anti-rabbit IgG-HRP	Santa Cruz Biotech.	sc-2030,	WB (0.2 µg/ml)
Goat anti- mouse IgG-HRP	Santa Cruz Biotech	sc-2005	WB (0.2 µg/ml)
Goat anti-mouse IgG-HRP	DAKO	P0447	WB (1:5000)
Goat anti-rabbit IgG-HRP	Sigma Aldrich	A0545	WB (1:5000)
Goat anti-rabbit IgG (H+L) Alexa Fluor 647	Thermo Scientific	A-21244	IF (2 µg/ml)
Goat anti-mouse IgG (H+L) Alexa Fluor 647	Thermo Scientific	A-21235	IF (2 µg/ml)
Goat anti-mouse IgG (H+L) Alexa Fluor 488	Thermo Scientific	A-11001	IF (2 µg/ml)
Goat anti-rabbit IgG (H+L) Alexa Fluor 633	Thermo Scientific	A-21070	FC (4 µg/ml)
Goat anti-human IgG (H+L) Alexa Fluor 633	Thermo Scientific	A-21091	FC (4 µg/ml)
Goat anti-mouse IgG (H+L) Alexa Fluor 633	Thermo Scientific	A-21052	FC (4 µg/ml)

2.1.4 Recombinant proteins

Table 2.4 Recombinant proteins, their size and working concentration.

Protein	Abbreviation	Provider	Cat no.	Size (kDa)	Working conc. ($\mu\text{g/ml}$)	
Recombinant human EFEMP1-HA	EFEMP1-HA	R&D Systems	8416-FB-050	52-71	500	
Purified human IgG-Fc fragment	hFc	Bethyl Laboratories	P80-104	~27	38.5	1.54 μM
Human PCDH7 ECD FL (cadherin 1-7)-Fc	hPCDH7 C7-Fc	Aleksandra Korzystka	NA	130	69.3	
Human PCDH7 ECD (cadherin 1-5)-Fc	hPCDH7 C5-Fc	Aleksandra Korzystka	NA	115	115.5	
Human PCDH7 ECD (cadherin 1-3)-Fc	hPCDH7 C3-Fc	Aleksandra Korzystka	NA	75	177	
Human PCDH7 ECD (cadherin 1)-Fc	hPCDH7 C1-Fc	Aleksandra Korzystka	NA	45	200	
Mouse MMRN2-Fc	mMMRN2-Fc	Marco Mambretti	NA	~50	3.2	

2.2 Molecular biology

2.2.1 DNA vectors

Table 2.5 Commercial vectors used for cloning.

Plasmid DNA	Type	Provider	Cat no.
pcDNA3.1 (+)	Mammalian expression vector	Invitrogen	V79020
pSecTag/FRT/V5-His	Mammalian expression vector	Invitrogen	K602501
pIG-Fc	Mammalian expression vector	Bicknell group	NA

pWPI	Lentiviral expression vector	Bicknell group	NA
pPGK-GFP		SomantiX BV	
pMD.G	Lentiviral packaging vector		
pMDLg/pRRE			
pRRL.SIN-18			
pRSV-Rev			

2.2.2 DNA inserts

Table 2.6 DNA inserts used as templates for cloning.

Template DNA	Type	Provider	Cat no.
gBlock DNA fragment hPCDH7 ECD_1-1248 bp	Codon optimized DNA fragment	IDT Technologies	NA
gBlock DNA fragment hPCDH7 ECD_1249-2640 bp	Codon optimized DNA fragment	IDT Technologies	
gBlock DNA fragment hPCDH7 TM+ICD	Codon optimized DNA fragment	IDT Technologies	
gBlock DNA fragment mPCDH7 ECD_1-984bp	Codon optimized DNA fragment	IDT Technologies	
gBlock DNA fragment mPCDH7 ECD_984-2637 bp	Codon optimized DNA fragment	IDT Technologies	
PROCR cDNA clone ID 4907433	Image clone	Dharmacon	MHS6278- 202832725
ESM-1 cDNA clone ID 3882426	Image clone	Dharmacon	MHS6278- 202756641
C1ORF54 cDNA clone ID 4617936	Image clone	Dharmacon	MHS6278- 202840823

2.2.3 Cloning Primers

Oligonucleotides for cloning were ordered from Biologio (NL) or Eurogentec and reconstituted in nuclease free water at the concentration of 100 μ M. Sequences are displayed in Table 2.7. For cloning purposes 10 μ M working concentration of primers was used.

Table 2.7 Oligonucleotides used for cloning, their sequence and DNA template used for PCR reaction.

Primer no.	Primer name	Primer sequences (5'-3')	DNA template
1	FW hPCDH7 ECD_1-1248bp to fuse with hPCDH7 ECD_1249-2640 and hFc into pWPXL	CGAGACTAGCCTCGAGGTTTAAA CGAGAAGATGCTTAGGATGC	gBlock DNA fragment hPCDH7 ECD_1-1248 bp
2	RV hPCDH7 ECD_1-1248bp to fuse with hPCDH7 ECD_1249-2640 and hFc into pWPXL	CTAATTTCTATTGATGGCACATTA TCGTTC	
3	FW hPCDH7 ECD_1249-2640 to fuse with hPCDH7 ECD_1-1248bp and hFc into pWPXL	TGTGCCATCAATAGAAATTAGAA AAATTGGGCG	gBlock DNA fragment hPCDH7 ECD_1249-2640 bp
4	RV hPCDH7 ECD_1249-2640 to fuse with hPCDH7 ECD_1-1248bp and hFc into pWPXL	ATGAAGAACCCCGCTGCTTAGAG ATCTC	
5	FW hFc to fuse with hPCDH7 ECD into pWPXL	TAAGCAGCGGGTTCTTCATCGA GTGAG	pIG-Fc
6	RV hFc to fuse with hPCDH7 ECD into pWPXL	ATTATCATATGACTAGTCCCGGG TTACTATTTACCCGGAGAC	
7	FW PCHD7 ECD to fuse with PCDH7 TM+ICD into pWPI	CTAGCCTCGAGGTTTGAGAAGAT GCTTAGG	pWPXL-hPCDH7 ECD-Fc (or pWPI-hPCDH7 FL for primer 7 when paired with primer 12)
8	RV PCHD7 ECD to fuse with PCDH7 TM+ICD into pWPI	CAATACTGAGCCGCTGCTTAGAG ATCTCGT	
9	FW PCDH7 TM+ICD to fuse with PCDH7 ECD into pWPI	TAAGCAGCGGCTCAGTATTGTCA TTGGCGT	gBlock DNA fragment hPCDH7 TM+ICD
10	RV PCDH7 TM+ICD to fuse with PCDH7 ECD into pWPI	TTCCTGCAGCCCGTAGTTTTTCAG CCAAAC	
11	RV FLAG sequence to add to C-term end of hPCDH7 FL	CTACTTGTCATCGTCATCCTTGTA ATCGCCAAACACAGT	pWPI-hPCDH7 FL
12	RV hPCDH7 FL FLAG into pWPI	CCTGCAGCCCGTAGTTTCTACTT GTCATCGTCATCC	PCR product amplified using primers 7&11
13	FW hPCDH7-Fc into pSec	GCCGCAAAGCAGCTGCTGCGGT ACC	pWPXL-hPCDH7 ECD-Fc
14	RV hPCDH7-Fc into pSec	CTATTTACCCGGAGACAGGGAGA	
15	FW PCDH7 ECD into pIG-Fc	CCGCCAGTGTTGCTGGAATTGGA GAAGATGCTTAGGATG	pWPXL-hPCDH7 ECD-Fc
16	RV PCDH7 ECD C1 into pIG-Fc	CTCGATGAAGAACCGCGGCCGC CAAACGTAGGCGTATTGTC	pWPXL-hPCDH7 ECD-Fc
17	RV PCDH7 ECD C3 into pIG-Fc	CTCGATGAAGAACCGCGGCCGC CTATTGATGGCACATTATC	

18	RV PCDH7 ECD C5 into pIG-Fc	CTCGATGAAGAACCGCGGCCGC CAAATTTGGGATCGTTAT	
19	FW mPCDH7 ECD_1-984bp to fuse with mPCDH7_984-2637 bp into pIG-Fc	CCGCCAGTGTGCTGGAATTCGA GAAGATGCTGCGCATG	gBlock DNA fragment mPCDH7 ECD_1-984bp
20	RV mPCDH7 ECD_1-984bp to fuse with mPCDH7_984-2637 bp into pIG-Fc	CTGCAAATAGGTGTCCCAGGTG CTGA	
21	FW mPCDH7 ECD_984-end bp to fuse with mPCDH7 ECD_1-984 bp into pIG-Fc	GGACACCTATTTTGCAGCTGAGA GCG	gBlock DNA fragment mPCDH7 ECD_984-2637 bp
22	RV mPCDH7 ECD_984-end bp to fuse with mPCDH7 ECD_1-984 bp into pIG-Fc	CTCGATGAAGAACCGCGGCCGC CTCTCTGCTTTGAGATTTTCG	
23	FW mPCDH7 ECD into pSec-His	CACTGGTGACGCGGCCAGCGA TACAAGCAGCTCCTGAGATATC	pIG-mPCDH7 ECD-Fc
24	RV mPCDH7 ECD into pSec-His	TAGGGATAGGCTTACCTTCGGAT ACTCTCTGCTTTGAGATTTTCG	
25	FW PROCR into pcDNA3.1	TTGGTACCGAGCTCGACCATGTT GACAACATTGCT	PROCR cDNA clone ID 4907433
26	RV PROCR into pcDNA3.1	TAGACTCGAGCGGCCTTAACATC GCCGTCCAC	
27	FW ESM-1 into pSec	TGGAGCAATAATTATGCGGTG	ESM-1 cDNA clone ID 3882426
28	RV ESM-1 into pSec	GCGTGGATTTAACCATTTTCC	
29	FW C1ORF54 into pSec	CAAGAATATGAGGATGAAGAAAG AC	C1ORF54 cDNA clone ID 4617936
30	RV C1ORF54 into pSec	CATGAAATACATCCCCACCTG	

2.2.4 DNA amplification

DNA amplification was performed using Phusion Flash HF PCR Master Mix (ThermoScientific, cat no. F-548S) or Phusion High-Fidelity DNA Polymerase (Biolabs, cat no. M0530L), according to the manufacturer's protocol. Primers are listed in Table 2.7. The PCR products were further subjected to agarose gel electrophoresis and purified.

2.2.5 DNA agarose electrophoresis

DNA samples were mixed with 6x DNA loading buffer (Thermo Scientific, cat no. R0611) and separated on 0.7-1% agarose gels (Bioline, cat no. BIO-41026) mixed with SYBR safe DNA gel stain (Thermo Scientific, cat no. S33102), in TBE or TAE buffer. GeneRuler 1 kb DNA ladder (Thermo Scientific, cat no. SM0311) or GeneRuler 100 bp DNA ladder (Thermo Scientific, cat no. SM0241) was loaded as a marker. Gels were ran at 100 V for 30 minutes and visualised using a UV transilluminator or the GeneSnap imaging system (SynGene).

2.2.6 DNA gel extraction

DNA fragments of desired size were excised from 1% agarose gels using a scalpel and purified using QIAquick PCR purification kit (Qiagen, cat no. 28104), according to the manufacturer's protocol.

2.2.7 Restriction enzyme digest

All restriction enzymes were from NEB and used according to the manufacturer's instructions for 1 h at 37°C unless different conditions were stated.

2.2.8 TOPO cloning

Plasmids based on pSecTag/FRT/V5-His vector were cloned using TOPO TA Expression Kit (Thermo Scientific, cat no. K6025-01), according to the manufacturer's protocol. Generated constructs are listed in Table 2.8.

2.2.9 Gibson cloning

Plasmid DNA constructs were generated using the Gibson cloning approach using Gibson Assembly Master Mix (Biolabs, cat no. E2611S) or In-Fusion HD Cloning Kit (Clontech Laboratories, cat no. 11614), according to the manufacturer's protocols. All designed cloning primers included homologous, overlapping ends of at least 15 bp on each PCR product used for DNA fusion with linearized vector. Gibson reaction mixes were then transformed into bacterial competent cells. Generated constructs are listed in Table 2.8.

Table 2.8 List of generated plasmid DNA constructs with information about vector backbone and primers used for cloning.

Construct	Vector	Primers no.
pWPXL-hPCDH7 ECD-Fc	Gibson cloning of three fragments into PmeI/SmaI cut pWPXL	1 & 2 3 & 4 5 & 6
pWPI-hPCDH7 FL	Gibson cloning of two fragments into NotI cut pWPI	7 & 8 9 & 10
pWPI-hPCDH7 FL FLAG	Gibson cloning of one fragment into NotI cut pWPI	7 & 12
pSec-hPCDH7 C7-Fc	TOPO cloning of one fragments into pSecTag/FRT/V5-His	13 & 14
pIG-hPCDH7 C1-Fc	Gibson cloning of one fragment into EcoRI/NotI cut pIG-Fc	15 & 16

pIG-hPCDH7 C3-Fc	Gibson cloning of one fragment into EcorRI/NotI cut pIG-Fc	15 & 17
pIG-hPCDH7 C5-Fc	Gibson cloning of one fragment into EcorRI/NotI cut pIG-Fc	15 & 18
pIG-mPCDH7 C7-Fc	Gibson cloning of two fragments into EcoRI/NotI cut pIG-Fc	19 & 20 21 & 22
pSec-mPCDH7 C7-His	Gibson cloning of one fragments into BamHI/SfiI cut pSec	23 & 24
pcDNA3.1-PROCR	TOPO cloning of PROCR cDNA into BamHI/NotI cut pcDNA3.1	25 & 26
pSec-ESM-1/V5-His	TOPO cloning of ESM-1 cDNA into pSecTag/FRT/V5-His	27 & 28
pSec-C1ORF54/V5-His	TOPO cloning of C1ORF54 cDNA into pSecTag/FRT/V5-His	29 & 30

2.2.10 Bacterial transformation

A vial of α -select silver efficiency (Bioline, cat no. BIO-85026) or Subcloning Efficiency DH5 α *E. coli* competent cells (Thermo Scientific, cat no. 18265017) was thawed on ice. Plasmid DNA was added to a maximum of 10% of total bacterial volume. The transformation mix was incubated for 30 min. on ice and then heat-shocked for 45 seconds at 42°C followed by another 2 min. on ice. LB broth (Sigma, cat no. L3522) without antibiotic was added to the mix and bacteria were incubated at 37°C for 1 h with shaking. Finally, the transformation mix was spread on LB agar (Sigma, cat no. L3147) plates containing appropriate antibiotics (Ampicillin 100 μ g/ml or Kanamycin 50 μ g/ml) and incubated overnight at 37°C.

2.2.11 Plasmid DNA isolation

A single bacterial colony was picked from LB agar plate and inoculated into 3-5 ml of LB medium with antibiotics. Mini-cultures were incubated overnight at 37°C with

shaking for mini prep DNA isolation using Qiaprep Spin Miniprep Kit (Qiagen, cat no. 27104). Alternatively, mini cultures were incubated for 8 h and later inoculated into 100-200 ml of LB broth for overnight incubation and used for maxi prep DNA isolation using NucleoBond Xtra Midi Kit (Macherey-Nagel, cat no. 740410). The concentration of DNA was measured using a NanoDrop 1000 spectrophotometer.

2.2.12 DNA sequencing

DNA sequencing was performed by the Functional Genomics Service (University of Birmingham). Around 350 ng of DNA and 3.2 pmol of specific primer were used in a total volume of 10 μ l for each reaction.

2.2.13 Genomic DNA isolation

Genomic DNA was isolated from HEK293T cells using PureLink Genomic DNA kit (Invitrogen, cat no. K182001), according to the manufacturer's protocol.

2.2.14 RNA isolation

RNA from cells was isolated using RNeasy Mini Kit (Qiagen, cat no. 74104) with on-column DNase treatment (Qiagen, cat no. 79254), prior to further use.

2.2.15 cDNA synthesis

Synthesis of cDNA was performed using iScript cDNA Synthesis Kit (BIO-RAD, cat no. 170-8890), according to the manufacturer's protocol. Additionally, a control without reverse transcriptase (-RT control) was also prepared. The cDNA samples from colorectal tumour and healthy tissues were provided by SomantiX. Due to a very limited amount of RNA available and its low quality (see Figure A.12 for details), 100 ng of RNA was used for 50 µl of cDNA synthesis reaction. For every qPCR reaction, 1.5 µl of cDNA was used (corresponding to 2.5 ng of RNA). In contrast, 200 ng of HUVEC or MCF7 RNA was used for 20 µl of cDNA synthesis reaction. For every qPCR reaction, 1 µl of HUVEC or MCF7 cDNA/-RT was used (corresponding to 10 ng of RNA).

2.2.16 Quantitative PCR (qPCR)

2.2.16.1 Primer design and validation

Specific primers for the selected target genes and control *HPRT1* and *BGUS* 'housekeeping' genes were designed using the Primer-BLAST designing tool on the NCBI website (see Figure A.1 for an example of primer design using the Primer-BLAST). Ideally, primers were designed to recognise fragments spanning exon boundaries in all existing gene isoforms. The product length was a maximum of 150 bp. Primers were synthesized by Biolegio, NL. The validation of primers was performed on HUVEC or MCF7 cDNA, control – reverse transcriptase (-RT) and

human genomic DNA (gDNA) as described in the section 5.4 in Chapter 5. Validated primers are listed in Table 2.9 and were used for qPCR.

Table 2.9 Quantitative PCR (qPCR) primers with their indicated product length.

Gene	Forward primer (5'-3') Reverse primer (5'-3')	PCR product length (bp)
<i>PROCR</i>	GAGTGGTCACCTTCACCCTG GCTTGTTTGGCTCCCTTTTCG	140
<i>APLN</i>	CTCTGGCTCTCCTTGACCG GGCCATTTCCTTGACCCTC	119
<i>HYAL2</i>	CAAGTAGCCTAGCTGGAGAGG AGCTCAGGAAGTGTGTGGGAG	101
<i>GPR126</i>	CTCGGCGCAGTAATGTCAAC GGCACATCCCCACACTGAG	137
<i>FAM174B</i>	GTCTTCAGGTTCGGGAAAGAG TAGTGGCGCCATTTCCACTC	87
<i>C1orf54</i>	CAGATCTGAACGATGCCGTGT CTCTTGCCAGACTCCCATCC	141
<i>DCHS1</i>	CTGAAACACGGTTGGTGCTG GGCGATTGTCATTGGTGTCG	102
<i>STAB1</i>	GCCAGCTACTGCAACCAAAC CATTGCCCTGGATCCCATCA	139
<i>ANGPTL2</i>	GTGCGACCAGAGACACGAC ATGTTCCCAAACCCTTGCTTGTA	111
<i>EDNRB</i>	CTGGCCATTTGGAGCTGAGA AGCAACAGCTCGATATCTGTCA	115
<i>ESM-1</i>	CTTGCTACCGCACAGTCTCA GCCGTAGGGACAGTCTTTGC	125
<i>EREG</i>	TGCACAGCTTTAGTTCAGACAG TGCACTGTCCATGCAAACAA	103
<i>MMP12</i>	CAAAGGCCGTAATGTTCCCC GGGTCTCCATACAGGGACTGA	100
<i>ANGPT2</i>	TGCCACGGTGAATAATTTCAG TTCTTCTTTAGCAACAGT	124
<i>EpCAM</i>	AGCGAGTGAGAACCTACTGG AACGCGTTGTGATCTCCTTCT	111
<i>CD45</i>	ATTTGTGACAGGGCAAAGCC GGGTGAGAATGCAGTGGTGT	115
<i>HPRT1</i>	CCTGGCGTCGTGATTAGTGAT AGACGTTTCAGTCCTGTCCATAA	131
<i>BGUS</i>	GAAAATACGTGGTTGGAGAGT CCGAGTGAAGATCCCCTTTTAA	101

2.2.16.2 qPCR

The experiments were performed using iTaq Universal SYBR Green Supermix (BIO-RAD, cat no. 172-5121), according to the manufacturer's protocol on CFX96 RT-System C1000 Thermal Cycler (BIO-RAD). The qPCR reaction components and set up are shown below.

qPCR reaction mix:

<u>Component</u>	<u>Volume (µl)</u>
iTaq Universal SYBR Green Supermix	10
FW and RV primers (10 µM)	0.5 each
cDNA	1-1.5
miliQ water	7.5-8
Total volume	20

qPCR reaction set up:

Denaturation	95°C	30s	1x
Denaturation	95°C	5s	} 35x
Annealing/Extension	60°C	30s	
Hold	4°C		

The melting curve characteristic was checked for each product. In each experiment, the reaction was performed in duplicate or triplicate for every sample. The maximum cycle number for every reaction was 35. The gene expression was normalized to the expression of 'housekeeping genes' and presented as a relative gene expression. It was calculated based on following equation:

$$\text{Relative gene expression} = E^{Cq(\text{reference gene}) - Cq(\text{sample gene})}$$

E – The efficiency of the reaction. Here assumed as 2, meaning that the template was doubled in each reaction cycle

C_q – Quantification cycle. The cycle at which the fluorescence of the amplicon exceeded the background fluorescence enabling the detection.

2.3 Biochemistry

2.3.1 Protein lysis

Mammalian cells were lysed with RIPA buffer. Lysates were kept on ice for 30 min. and centrifuged for 40 min. at 4°C at 16 600 xg to remove cell debris. Lysate supernatant was used immediately or stored at -20°C.

2.3.2 BCA protein concentration assay

The total protein concentration in samples was measured colorimetrically using BCA Protein Assay Kit (Thermo Scientific, cat no. 23225), according to the manufacturer's protocol. Briefly, a small volume of samples of unknown concentration were pipetted into 96-well plates. The mix of reagents provided in the kit was added and the plate was incubated at 37°C until sufficient signal developed. The absorbance was measured at 562 nm. BSA standards in a concentration range from 0.1 to 2 µg/ml were used to calculate the concentration of proteins in the samples.

2.3.3 SDS-PAGE electrophoresis

The protein samples in RIPA buffer were mixed with 4x Laemmli buffer in the presence of 10% β -mercaptoethanol (Sigma, cat no. M6250), boiled for 5 min. at 95°C and separated on casted 8% or 10% polyacrylamide gels. The composition of gels is listed in Table 2.10. The PageRuler Plus Prestained Protein Ladder (Thermo Scientific, cat no. 26619) was used as a marker of proteins in a range of 10-250 kDa. Gels were either stained with InstantBlue Coomassie stain (Expedeon, cat no. ISB1L) or further subjected to Western blot.

Table 2.10 SDS-PAGE gels composition.

Gel	Composition
8%	375 mM Tris pH 8.8 0.15% (v/v) SDS (Fisher BioReagents, cat no. BP1311-1) 8% (v/v) Protogel 30% (National Diagnostics, cat no. EC-890) 0.1% (w/v) APS (Sigma, cat no. A3678) 0.001% (v/v) TEMED (Sigma, cat no. T9281)
10%	375 mM Tris pH 8.8 0.15% (v/v) SDS 10% (v/v) Protogel 0.1% (w/v) APS 0.001% (v/v) TEMED
Stacking gel	128 mM Tris pH 6.8 0.1% (v/v) SDS 5% (v/v) Protogel 0.1% (w/v) APS 0.001% (v/v) TEMED

2.3.4 Western blot

SDS-PAGE was performed according to a standard protocol. Proteins were transferred to Immobilon-P PVDF membrane (Millipore, cat no. IPVH00010) for 1 h,

100 V at 4°C, blocked with 5% (w/v) BSA in PBS-T buffer and incubated overnight at 4°C with primary antibody diluted in PBS-T/2.5% (w/v) BSA. The membrane was then washed three times with PBS-T buffer, for 5 min. each. The membrane was incubated with secondary antibody conjugated to horseradish peroxidase (HRP) diluted in PBS-T/2.5% (w/v) BSA for 1 h at RT and washed again three times with PBS-T buffer. The signal was generated using Pierce ECL Western blotting Substrate (Thermo Scientific, cat no. 32106) and the membrane was exposed on CL-XPosure Film (Thermo Scientific, cat no. 34088). Antibodies and their working concentrations are listed in Table 2.2 and Table 2.3.

2.4 Immunoprecipitation (IP)

HUVEC or HEK293T-hPCDH7 FL FLAG cells were washed with PBS and detached from culture dishes using non-enzymatic cell dissociation solution (Sigma, cat no. C5914). Next, cells were spun down and washed twice with flow cytometry buffer. The cell pellet was lysed in IP lysis buffer for 30 min. on ice and centrifuged at 16 600 xg for 40 min. In meantime, 20 µl of Protein A Sepharose was washed with PBS and incubated with 0.5 µl of 1.54 µM recombinant proteins for 1 h at 4°C. Next, 1 ml of PBS was added to the beads and spun down at 16 600 xg for 30 s to remove unbound proteins. This washing step was repeated three times. The cell lysate was first pre-cleared on Protein A Sepharose for 1 h at 4°C. Next, the cell lysate was added to Eppendorf tubes with coated beads with or without the addition of DTSSP crosslinker (Thermo Scientific, cat no. 21578) to a final concentration of 2.5 µM. After 4 h of incubation at 4°C, 1 M Tris pH 7.5 was added to all samples to a final

concentration of 50 μ M to stop the crosslinking reaction. The beads were then spun down and the cell lysate was discarded. The beads were then washed with 1 ml of IP wash buffer and spun down at 16 600 xg for 30 s. This was repeated three times. Finally, the bead pellets were resuspended in reducing 4x Laemmli loading buffer, separated by SDS-PAGE and subjected to a mass spectrometry or Western blot.

2.5 Mass spectrophotometry (MS)

Samples containing proteins were excised from SDS-PAGE gel and stored in sterile miliQ water. Samples were further processed at the genomic facility at the University of Birmingham. Results of the mass spectrometry analysis were received as lists of peptide hits in Excel files.

2.6 Cell culture

2.6.1 Cell culture

Mammalian cells were cultured under sterile conditions and maintained at 37°C, 5% CO₂. Cells were passaged twice a week. In order to passage cells, they were washed with sterile PBS and trypsinized (Gibco, cat no. 12563). Next, cells were collected, spun down at 210 xg in a complete DMEM (cDMEM) medium and finally, resuspended in a fresh culture medium. The list of cell types and their culture conditions is shown in Table 2.11. Cells were tested for mycoplasma infection every two months using EZ-PCR Mycoplasma Detection Kit (Biological Industries, cat no. 20-700-20).

Table 2.11 List of cell types and their culture conditions. pn – passage number at which cells were used in the experiments.

Cell type	Provider	Medium
HUVEC pn 2-5 (Human umbilical vein endothelial cells) – pooled donors (information about number of donors not available)	TCS Cellworks, cat no. ZHC-2102	Complete EBM-2 – EBM-2 containing pro-angiogenic factors (VEGF, bFGF, EGF) (EBM-2 Bulletkit, Lonza, cat no. CC-3162)
HDF pn 3-4 (Human dermal fibroblasts)	Gibco, cat no. C-013-5C	M106 + LSGS supplements (Gibco, cat no. M106500 and S00310)
PC pn 2-4 (Pericytes)	PromoCell, cat no. C-12980	Pericyte growth medium kit (Promocell, cat no. C-28040)
HEK293T (Human embryonic kidney cells)	'In house' resources of Prof. Bicknell lab – provided in frozen vials	Complete DMEM (cDMEM) – DMEM High Glucose (Sigma, cat no. D5796) + 10% FBS (Gibco, cat no. 10270106)
HEK293FT (Human embryonic kidney cells) – optimized for generating high-titer lentivirus	'In house' resources of SomantiX B.V. – provider in frozen vials	
COS-7 cells (Afrikan green monkey kidney fibroblast-like cells)		
MCF7 cells (human breast carcinoma cells)		

2.6.2 Transfection with plasmid DNA

Transfection of cells was carried out according to a standard protocol used at SomantiX B.V. It was not specifically optimized for the experiments presented in this thesis. HEK293T cells were seeded on plates, dishes or flasks at the amount listed in Table 2.12, one day before the transfection. Plasmid DNA was vigorously mixed with PEI (Sigma, cat no. 408727) in the ratio 1:3 in OptiMEM I medium (Thermo Scientific, cat no. 31985-070), incubated 10 min. at RT and added to

the cells. After overnight incubation, medium was replaced and cells were cultured for another 48 h.

Table 2.12 Amounts of HEK293T cells and reagents quantities used for transfection.

Plate (flask) size	Amount of seeded cells	Volume of culture medium (ml)	Volume of Opti-Mem I (ml)	Amount of DNA (μg)	Volume of PEI (μl)
6-well	3×10^5	2	0.1	1	3
6 cm (T25)	1×10^6	3	0.3	3	9
10 cm (T75)	3×10^6	10	1	9	27
15 cm	6×10^6	20	2	18	54

2.6.3 Production of lentiviruses

HEK293FT cells were seeded in T25 or T75 flasks at the confluency around 50% one day before transfection. Cells were co-transfected with 6.5 μg of the expression plasmid (encoding the protein of interest or shRNA) and the lentiviral packaging mix: 0.55 μg of pMD.G, 0.55 μg of pMDLg/pRRE, 0.55 μg of pRRL.SIN-18 and 1.1 μg of pRSV.Rev, using 1 mg/ml PEI in the ratio 1:3. After overnight incubation, medium was replaced with 3 ml or 5 ml of cDMEM medium for T25 or T75 flask, respectively. The supernatant with lentivirus was collected for two following days. The harvests were mixed, filtered through 0.45 μm syringe filters, aliquot and stored at -80°C for further use.

2.6.4 Lentiviral transduction of HUVEC

Transduction was carried out according to a standard protocol for lentiviral overexpression of proteins and sRNA-mediated gene knockdown used routinely

at SomantiX B.V. It was not specifically optimized for experiments presented in this thesis. HUVEC pn 3 were seeded on T25 or T75 flask at the amount of 2.5 or 7.5 x 10⁵ cells/flask, accordingly. The next day, cells were transduced with 1.5 ml (T25 flasks) or 3 ml (T75 flask) of appropriate lentivirus(es) in the presence of Polybrene (Sigma, cat no. 107689) at a final concentration of 1 µg/ml, overnight. The medium was replaced and cells were cultured for another 48 h. HUVEC were transduced immediately prior to each experiment.

2.6.5 Short hairpin RNA (shRNA)

Short hairpin RNA constructs for *PROCR*, *ESM-1*, *C1orf54* and *STAB1* genes were purchased from Sigma-Aldrich as MISSION shRNA Bacterial Glycerol Stocks, five shRNA constructs per gene. Plasmids were based on pLKO.1 vector (Sigma Aldrich) with a puromycin resistance gene and shRNA driven by U6 promoter. Scrambled shRNA in pLKO.1 vector (Sigma) was used as a control. Each plasmid was purified, the lentivirus was produced and shRNAs were validated for the highest knockdown efficiency using qPCR. Table 2.13 shows an overview of the shRNA constructs that gave the best knockdown.

Table 2.13 List of shRNAs constructs used in knockdown experiments.

Gene	Catalogue numbers		shRNA number and sequence
<i>PROCR</i>	SHCLNG-NM_006404	trcn0000300564	sh1 - TGGCCTCCAAAGACTTCATATC
		trcn0000377417	sh2 - GAATCACCTGAGGCGTTCAAA
<i>ESM-1</i>	SHCLNG-NM_007036	trcn0000062814	sh1 - CTTCCAATATTCAGTAACCAA
		trcn0000372146	sh2 - AGACCGCAGTGAGTCAAATTA

<i>C1orf54</i>	SHCLNG-NM_024579	trcn0000263665	sh1 - TATTATCAGGTGGTCTATTAT
		trcn0000369988	sh2 - ACTTATCCTGGGACAAGAATA
<i>STAB1</i>	SHCLNG-NM_015136	trcn0000162622	sh1 - CCTGGAATATAAGGAGCTCAA
		trcn0000163231	sh2 - GTCCCTGTCAATGAAGGCTTT
		trcn0000161067	sh3 - GCAGACGTTCAACATCTACAA

2.6.6 CellTiter 96 Non-Radioactive Cell Proliferation Assay (MTT)

Cell proliferation was measured using CellTiter 96 Non-Radioactive Cell Proliferation Assay (MTT) (Promega, cat no. G4000). First, cells were seeded on 96-well plate at the amount of 5×10^3 cells/well, in 100 μ l of a complete EBM-2 containing recombinant proteins at the concentration of 1.54 μ M. As a control, medium without cells was used. After 24 h and 48 h, medium was changed into a fresh medium without phenol red and 15 μ l of the dye solution was added to each well. The plate was incubated at 37°C for 3-4 h and 100 μ l of the solubilisation solution was then added to each well. The plate was stored at 4°C overnight. The absorbance was measured at 570 nm using a Versa Max microplate reader (Molecular Devices, USA).

2.6.7 Scratch assay

HUVEC pn 3 were seeded on an IncuCyte 96-well ImageLock plate (Essen Bioscience, cat no. 4379) at the amount of 6×10^3 cells/well in a complete EBM-2 medium. The cell monolayer was scratched with a Wound Maker (Essen Bioscience, cat no. 4493), washed with PBS and incubated in a complete EBM-2 medium containing recombinant proteins at the concentration of 1.54 μ M for 24 h in IncuCyte

ZOOM Live-Cell analysis system. Cell migration was recorded every 6 h using an IncuCyte ZOOM microscope and software. The wound area was measured manually using ImageJ and was calculated as a percentage of a wound area measured at the given time point to the initial wound area for each sample.

2.6.8 Transwell migration assay

FluoroBlok™ Tissue Culture (TC)-treated Inserts with 8.0 µm High Density PET Membrane (Corning, cat no. 351152) were placed in empty 24-well plate and coated with 0.1% (w/v) gelatin for 30 min. at 37°C. HUVEC pn 3 were starved in serum-free M199 medium containing growth factors (including VEGF and bFGF) for 1 h and trypsinized. Cells were seeded onto inserts at the amount of 3×10^4 cells/well, in 300 µl of serum-free M199 medium with appropriate recombinant proteins at the concentration of 1.54 µM. Inserts with cells were placed into wells filled with 700 µl of a complete M199 medium (with serum) and cells were allowed to migrate for 5 h at 37°C. Inserts were washed with PBS and fixed with 4% PFA. Membranes were cut out using a scalpel and mounted on the microscope glass slide using DAPI mounting medium (Duolink, cat no. 82040-0005), transmigrated cells facing the glass. Only migrated cells were imaged using Olympus 1X2-UCB fluorescent microscope under 10x magnification. The total migrated cells were counted as the number of stained cell nuclei from 16 fields of view from one insert.

2.6.9 Spheroid assay

GFP transduced HUVEC were trypsinized and counted. A complete EBM-2 medium containing cells at the amount of 1.25×10^4 cells/ml was mixed with methyl cellulose (Sigma, cat no. M0512) in the ratio 4:1. HUVEC mix was pipetted into Nunc 60-well microplate (Thermo Scientific, cat no. 439225) in a volume of 20 μ l/well. The plate was inverted to create a hanging drop of HUVEC spheroids and incubated overnight at 37°C, 5% CO₂. The next day, spheroids were collected using a P1000 pipette and spun down in 15 ml tube at 210 xg for 5 min., the supernatant was aspirated. Two collagen mixtures were prepared and kept on ice. Collagen I mix contained 1.37 ml of type I collagen, rat tail (Millipore, cat no. 08-115), 250 μ l of 10x DMEM and 880 μ l of sterile milliQ water. Collagen II mix contained 1.5 ml of a complete EBM-2 medium and 1 ml of methyl cellulose. 10 μ l of 5 M NaOH was added to collagen I mix and both collagen I and collagen II were mixed in the ratio 1:1. Spheroids were resuspended in a volume of 200 μ l collagen mixture and transferred to 24-well plate. The plate was incubated at 37°C for 10 min. to allow polymerization of the collagen matrix. Finally, 100 μ l of a complete EBM-2 medium was added to the well and the plate was incubated for another 18 h followed by fixation with 4% PFA. Samples were imaged under a Zeiss LSM780 confocal microscope. The number of sprouts was calculated manually using ImageJ.

2.6.10 3D HUVEC/HDF co-culture angiogenesis assay in fibrin matrix

The protocol of the assay was adapted from Liu *et al.* (2008) and Lafleur *et al.* (2002). The fibrin solution was prepared as follows: 2.5 mg of fibrinogen (Sigma Aldrich, cat no. F3879) was dissolved in 1 ml DPBS (Life Technologies, cat no. 14080055) at 37°C. The solution was then sterile filtered through 0.45 µm filter and aprotinin (Sigma Aldrich, cat. no A6106, 4 U/ml) was added to a final concentration of 0.15 U/ml. Transduced HUVEC and HDF were trypsinized and counted: 10^6 of knockdown HUVEC and 0.5×10^6 of HDF were combined, pelleted and resuspended in 1 ml of sterile fibrin solution. Thrombin stock (Sigma Aldrich, cat no. T9326, 50 U/ml) was freshly diluted 1:10 in DPBS and 1.25 µl of thrombin was added to a well of µ-Plate Angiogenesis 96-well plate (IBIDI, cat no. 89646) or µ-Slide Angiogenesis (IBIDI, cat no. 81506). 9.5 µl of cell suspension was added to every well. The plate was left 45 min. at 37°C to allow polymerization of the fibrin matrix. At the end, 50-70 µl of a complete EBM-2 medium was added to every well. Medium was changed every second day. Cells were co-cultured for 10 days. Next, cells were fixed with 4% PFA for 20 min. at RT followed by an extensive washing with PBS. Images of the network were taken using an Olympus 1X2-UCB fluorescent microscope at 2x magnification. A single image represented a whole well. Images were saved as 8 bit type, converted to binary images and analysed using a free ImageJ binary tree angiogenesis analyser plug-in created by Gilles Carpentier. Two values were calculated: the total network branching length and the number of nodes (junctions). The branching length refers to sum of length of all connected tubes in

the analysed area excluding isolated tubes. A node (junction) refers to a point where at least three separated tubes connect.

2.6.11 2D HUVEC/HDF co-culture angiogenesis assay

HDF were seeded on 24-well plate at the amount of 3×10^4 cells/well and cultured for 5 days. HUVEC were trypsinized and seeded on top of HDF monolayer at the amount of 1.5×10^4 cells/well and co-cultured for another 6 days in a complete EBM-2 medium. Medium was changed every second day. Cells were fixed with 4% PFA for 20 min. at RT followed by an extensive washing with PBS. HUVEC were visualised by staining for CD31 endothelial marker. First, cells were incubated with 0.1% Triton X-100 for 4 min., washed three times with PBS and blocked with 1% (w/v) BSA in PBS for 1 h. Next, cells were incubated with anti-human CD31 primary antibody in 1% (w/v) BSA for 1 h at RT. After three washes with PBS, cells were incubated with anti-IgG conjugated to alkaline phosphatase diluted 1:500 in 1% (w/v) BSA for 1 h at 37°C. Finally, cells were washed twice with PBS, once with milliQ water and incubated with the chromogenic substrate BCIP/NBT (Sigma, cat no. B5655) dissolved in milliQ water, for 25 min. The reaction was stopped by a final wash with milliQ water. Cells were allowed to dry before the imaging. Images of the network were taken using a Leica 10447157 microscope 1x zoom with XLi digital imaging camera. Images were saved as RGB type and analyzed using a free ImageJ phase contrast angiogenesis analyzer plug-in created by Gilles Carpentier. Two values were calculated: the total network branching length and the number of nodes (junctions).

2.6.12 Cell adhesion assay

Nunc MaxiSorp flat-bottom 96-well ELISA plate (Thermo Scientific, cat no. 44-2404-21) was coated with 100 μ l/well of 0.154 μ M hPCDH7 C5-Fc, hPCDH7 C7-Fc, mMMRN2-Fc, hFc or BSA proteins, overnight at 37°C. Next, plate was washed with PBS and blocked with 3% BSA in PBS for 1 h. HUVEC were detached from culture dishes using non-enzymatic cell dissociation solution (Sigma, cat no. C5914) and seeded on the protein coated plate at the amount of 5×10^4 cells/well in a complete EBM-2 medium. HUVEC were let to attach for 4 h at 37°C, 5% CO₂. Next, cells were washed five times with PBS to remove unattached cells, fixed with 4% PFA followed by washes with PBS and miliQ water. Finally, the remaining cells were stained with a crystal violet solution (Sigma, cat no. C-3886). The excess staining solution was removed by washing three times with PBS and two times with miliQ water. The absorbance was measured at 590 nm using Versa Max microplate reader. Images were taken before and after washing off cells.

2.7 Recombinant protein production

2.7.1 Small scale production of Fc fused and His tagged recombinant proteins

HEK293T cells were seeded on 6-well plate one day before the transfection. Cells were transiently transfected with plasmid encoding hPCDH7 C1, C3, C5 or C7-Fc recombinant protein, using PEI in the ratio 1:3 in OptiMEM I, overnight. Alternatively, cells were transfected with plasmid encoding mPCDH7 ECD(C7)-Fc or mPCDH7 ECD(C7)-His recombinant proteins. The next day, medium was replaced with 3 ml of

fresh OptiMEM I and cells were cultured for another 72 h. The day of supernatant harvest was determined by the phenol red pH indicator in OptimMEM I medium. Change in colour from pink to yellow indicated increasing acidity of the culture conditions and the need for medium replacement. Next, 20 µl of Protein A Sepharose (Sigma, cat no. P9424) or Ni-NTA agarose (Qiagen, cat no. 30210) were washed three times with PBS. One millilitre of supernatant containing Fc fused protein was added to Protein A Sepharose. His tagged protein supernatant was added to Ni-NTA agarose. After 1 h of incubation at 4°C, the supernatant was discarded. The beads were washed three times with 1 ml of PBS. Finally, the beads were spun down for 30 s at 16 000 xg, resuspended in 20 µl of Lammeli buffer and subjected to SDS-PAGE electrophoresis. To compare protein yields, BSA protein standards were run alongside. Proteins on gel were visualised using an InstantBlue Coomassie stain.

2.7.2 Large scale production of Fc fused recombinant proteins

HEK293T cells were seeded on 15 cm dishes one day before the transfection. Cells were transiently transfected with plasmid encoding hPCDH7 C1, C3, C5 or C7-Fc recombinant protein, using PEI in the ratio 1:3 in OptiMEM I, overnight. The next day, medium was replaced with 25 ml of fresh OptiMEM I. Supernatant with secreted protein was collected every 4-5 days for 20 days. The day of supernatant harvest was determined by the phenol red pH indicator in the OptimMEM I. Change in medium colour from pink to yellow indicated increasing acidity of the culture conditions and the need for medium replacement. To inhibit proteases, PMSF

(Sigma, cat no. P7626) and 1 mM EDTA (cat no. 15575020) was added to every harvest.

2.7.3 Purification of Fc fused recombinant proteins

The collected media containing secreted proteins were mixed and filtered using 0.22 µm vacuum filters (Corning, cat no. 431096) before applying to HiTrap Protein A purification column (GE Healthcare, cat no. 17-0403-01) connected to Gilson Miniplus2 peristaltic pump. First, column was washed with 30 ml of 20% ethanol and miliQ water. Next, column was equilibrated with 30 ml of 20 mM Na₂PO₄ pH 7.0. Supernatant was loaded and run at 1 ml per minute and the column was washed with 30 ml of 20 mM Na₂PO₄ pH 7.0 before proceeding with the protein elution. Bound proteins were eluted using 100 mM sodium citrate pH 3.0 and immediately neutralised with 1M Tris pH 9.0 (ratio 2.5:1). The protein was concentrated using an Amicon® Ultra 15 mL centrifuge filter with 10, 50 or 100 kDa cut off depending on the protein (Millipore, cat no. UFC901008, UFC905008, UFC910008), according to the manufacturer's protocol. Finally, proteins were dialyzed to PBS using Slide-A-Lyzer™ Dialysis Cassettes (Thermo Scientific, cat no. 66005) and kept at 4°C for further use.

2.8 Flow cytometry

HUVEC, HEK293T and HEK293T-hPCDH7 FL cells were detached from culture dishes using non-enzymatic cell dissociation solution (Sigma, cat no. C5914), washed with PBS, spun down and resuspend in a flow cytometry buffer. Since

the extracellular domain of PCDH7 contains multiple Ca^{2+} binding sites that might be necessary for its function, calcium ions were added to flow cytometry buffer. The exact buffer composition is listed in Table 2.1. Cells were incubated with 0.5 μl of 15.4 μM hFc control or hPCDH7 ECD-Fc recombinant proteins in the volume of 50 μl for 1 h on ice. As a positive control of binding to HUVEC, mMMRN-Fc was used. Next, 500 μl of flow cytometry buffer was added and cells were spun down at 210 xg to remove the primary binder protein. After washing, cells were resuspend in 50 μl of secondary anti-human AlexaFluor 633 fluorescent antibody diluted 1:100 in flow cytometry buffer and incubated for 1 h on ice. Finally, 500 μl of flow cytometry buffer was added and the fluorescence was analysed using Cyan B flow cytometer.

2.9 Immunofluorescence (IF) staining of cells

Glass coverslips were washed with 1 M HCl for 10 min. at RT, washed with miliQ water and stored in 70% ethanol. Cells were cultured on 0.1% (w/v) gelatin coated coverslips in 24-well plates. Next, cells were briefly washed with PBS and fixed with 4% PFA for 10 min. at RT followed by washing with PBS, neutralization with 50 mM NH_4Cl for 10 min. and washing with PBS. Cells were permeabilised with 0.1% Triton X-100 for 4 min., washed again and blocked with IF blocking buffer for 1 h at RT. Next, cells were incubated with primary antibody for 1 h followed by washing with PBS and incubation with AlexaFluor fluorescent secondary antibody for 1 h. Finally, cells were washed three times with PBS, twice with miliQ water and mounted on microscope glass slides using ProLong Gold Antifade mountant solution with DAPI (Thermo Scientific, cat no. P36935). Slides were left overnight at RT in the dark.

Finally, slides were sealed with nail varnish around the edges and stored at -20°C. Images were taken using a Leica DM6000 fluorescent microscope with 40x magnification.

2.10 Statistical analysis

Statistical analysis was performed using GraphPad Prism 7 software using 1-way ANOVA Tukey's multiple comparisons test, 2-way ANOVA Tukey's multiple comparisons test or t-test, depending on the experiment. ANOVA is the most commonly used test to determine the difference between the means of two or more experimental data sets. It is done in place of multiple t-tests performed concurrently decreasing the chance of statistical errors. One-way ANOVA was used to test the difference between groups with one variable (for example when treating cells with several proteins at the same concentration). Two-way ANOVA was used to test the difference between groups with two variables (for example when treating cells with a range of concentrations of several proteins). In contrast, t-test is used when only two samples are compared.

**CHAPTER 3: *IN VITRO* FUNCTIONAL STUDIES OF
Fc FUSED PCDH7 EXTRACELLULAR DOMAIN**

CHAPTER 3: *IN VITRO* FUNCTIONAL STUDIES OF Fc FUSED PCDH7 EXTRACELLULAR DOMAIN

3.1 Introduction

The single transmembrane glycoprotein PCDH7 is a member of $\delta 1$ -protocadherin subgroup of the cadherin superfamily. Although it is expressed primarily in the nervous system, PCDH7 is also prevalent in many solid tumours. It plays a significant oncogenic role in bone metastasis of breast cancer, tumourigenesis of NSCLC and brain metastasis (Chen *et al.* 2016; Li *et al.* 2013; Zhou *et al.*, 2017). A distinct role as a tumour suppressor has been reported in gastric cancer, non-invasive bladder cancer or colorectal cancer (Bujko *et al.*, 2015; Chen *et al.*, 2017; Lin *et al.*, 2016). Despite these opposite effects in both promoting and inhibiting tumourigenesis, in all cases PCDH7 seems to be involved in strengthening cell-cell interactions and downstream signalling. Zhuang *et al.* (2015) identified that PCDH7 is highly overexpressed in NSCLC tumour endothelial cells when compared to normal lung endothelial cells. This was further confirmed by immunohistochemical staining. To date there is no further literature regarding PCDH7 expression on tumour vasculature. Since an ultimate goal of this project is the development of novel anti-vascular agents which would potentially target PCDH7 or its ligand(s) on tumour vasculature, we wanted to determine if and how PCDH7 regulates endothelial network formation *in vitro*. We have focused on a soluble recombinant version of human PCDH7 extracellular domain (hPCDH7 ECD) that is conserved among PCDH7 isoforms fused to human Fc (hFc) fragment. The presence of Fc enables

protein purification and serves as a control in all *in vitro* assays. For the purpose of this chapter, a full length of hPCDH7 ECD containing seven cadherin repeats will be termed hPCDH7 C7.

PCDH7 was found in lung microvascular cells (Zhuang *et al.*, 2015). However, due to difficulties in isolating lung microvascular cells and a high cost of commercially available cells we decided to use HUVEC isolated from large blood vessels. This cell type is one of the most commonly used models to study angiogenesis. We have also considered using immortal microvascular cell lines however they do not form endothelial network *in vitro*. If data are promising, they can be further confirmed and expanded using more relevant model for lung tumour vasculature.

3.2 Anti-human PCDH7 antibody recognizes an overexpressed full length PCDH7

First, a commercial anti-human PCDH7 antibody was validated to ensure we could reliably detect PCDH7 by Western blot. In order to validate the antibody, a codon optimized hPCDH7 full length construct of the most abundant isoform A (hPCDH7 FL) gene fragments were cloned into pWPI lentiviral vector as described in the Materials and Methods and the sequence of the insert was verified. HEK293T cells were transfected with pWPI-PCDH7 FL plasmid with untransfected cells used as a control. After 48 h, the cell lysates were harvested. Equal amounts of protein were separated by SDS-PAGE and transferred to PDVF. The membrane was cut at around 90 kDa. Part of the membrane above 90 kDa was blotted with anti-human

PCDH7 antibody while part of the membrane below 90 kDa was blotted with anti-human tubulin antibody.

The band of around 130 kDa corresponding to hPCDH7 FL (see Figure A.7 for the amino acid sequence) was observed only in pWPI-hPCDH7 FL transfected cells while being absent in the control (Figure 3.1). Antibody showed a background staining at around 250 kDa. These data indicate that anti-human PCDH7 antibody shows reactivity towards its target when overexpressed in HEK293T cells but it has a nonspecific binding.

3.3 PCDH7 is expressed in HUVEC

Next, the expression of PCDH7 in HUVEC was investigated. Thus, the cell lysates of HUVEC passages from 2 to 7 were collected. Equal amounts of protein were separated by SDS-PAGE and transferred to PDVF. The membrane was cut at around 60 kDa. Part of the membrane above 60 kDa was blotted with anti-human PCDH7 antibody while part of the membrane below 60 kDa was blotted with anti-human tubulin antibody. PCDH7 was successfully detected with anti-human PCDH7 antibody in all passages (Figure 3.2) with two background bands at around 80 kDa and 100 kDa. It was observed that PCDH7 expression across HUVEC passages was variable but this was also observed for 80 kDa background band. This may suggest a presence of an unglycosylated form of PCDH7 or a background binding. This was not further studied. Notably, PCDH7 expression was only observed when very high concentrations of HUVEC protein lysate (from $2-3 \times 10^6$ cells) were loaded on gel.

Therefore, these data suggest that although PCDH7 is present in HUVEC, its basal expression is very low.

3.4 Generation and production of the recombinant hPCDH7 C7-Fc fusion protein

3.4.1 Recombinant hPCDH7 C7-Fc fusion protein is successfully generated

To produce the recombinant hPCDH7 C7-Fc fusion protein, codon optimized hPCDH7 ECD and human Fc (hFc) sequences were cloned into the pSecTOPO vector as described in the Materials and Methods and the sequence of the insert was verified. HEK293T cells were transfected with pSec-hPCDH7 C7-Fc plasmid with untransfected cells used as a control, followed by the change of culture medium to OptiMem I. After 48 h, the culture media were harvested and separated by SDS-PAGE and transferred to PDVF membrane. The expression of the hPCDH7 C7-Fc fusion protein was successfully verified by Western blot using both anti-human PCDH7 and anti-human Fc antibodies giving a band of the expected size (Figure 3.3). These results confirmed that 25 kDa hFc fragment was successfully fused to 110 kDa hPCDH7 C7 fragment to give hPCDH7 C7-Fc fusion protein with the size of around 130 kDa (see Figure A.7 for the amino acid sequence). Moreover, these data confirmed the hPCDH7 C7-Fc fusion protein was secreted to OptiMEM I.

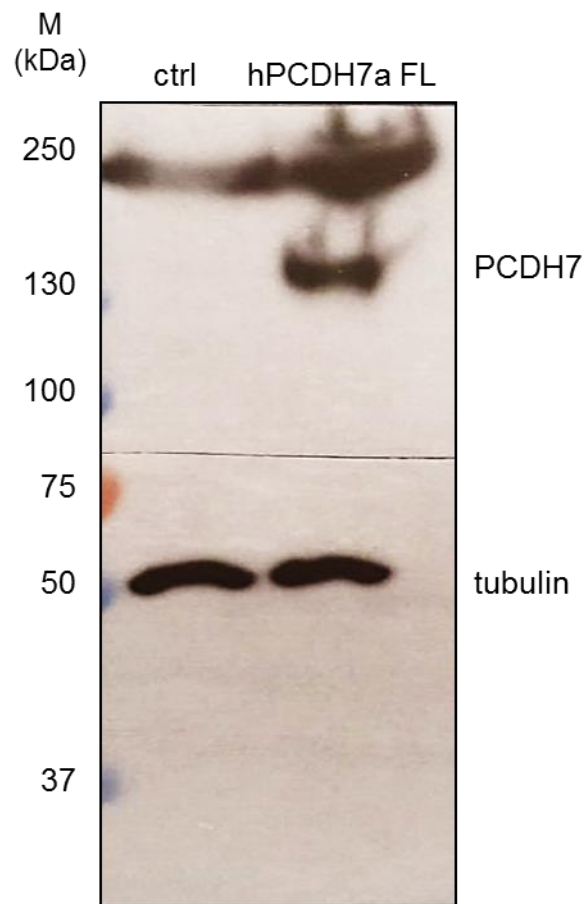


Figure 3.1 PCDH7 FL is recognized by anti-human PCDH7 antibody. HEK293T cells were transiently transfected with pWPI-hPCDH7 FL plasmid with untransfected cells used as a control. The cell lysates were collected 48 h later. Western blot analysis of the cell lysates with anti-human PCDH7 antibody and tubulin as a loading control. The membrane was cut at around 90 kDa with the upper part blotted with anti-human PCDH7 antibody and the lower part blotted with anti-human tubulin antibody.

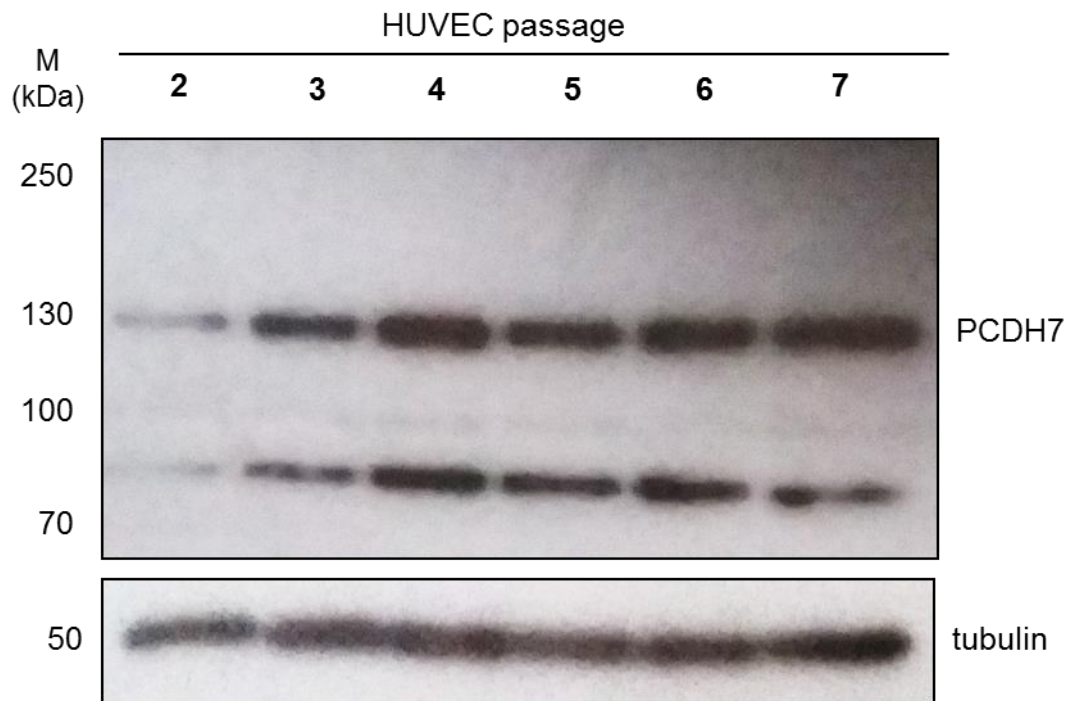


Figure 3.2 PCDH7 is expressed in HUVEC. The cell lysates were harvested from HUVEC passages from 2 to 7. Western blot analysis of the cell lysates with anti-human PCDH7 antibody and tubulin as a loading control. The membrane was cut at around 60 kDa. Part of the membrane above 60 kDa was blotted with anti-human PCDH7 antibody while part of the membrane below 60 kDa was blotted with anti-human tubulin antibody. The experiment was performed once.

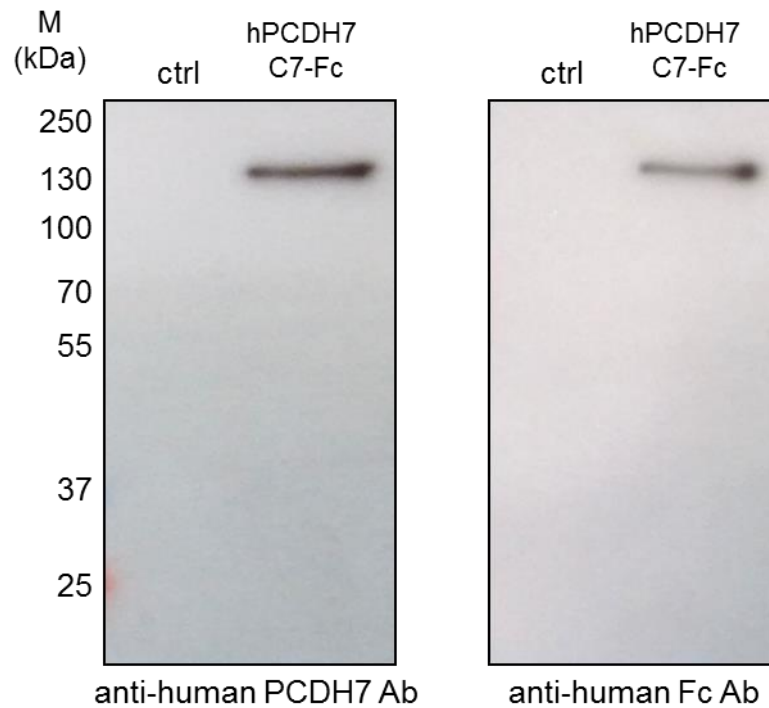


Figure 3.3 The hPCDH7 C7-Fc fusion protein was successfully generated and secreted to the medium. HEK293T cells were transiently transfected with pSec-hPCDH7 C7-Fc. Untransfected cells were used as a control. Culture media were harvested 48 h later. The expression of the hPCDH7 C7-Fc fusion protein was verified on Western blot using both anti-human PCDH7 and anti-human Fc antibodies. The verification of the hPCDH7 C7-Fc fusion protein expression and secretion was performed once.

3.4.2 Recombinant hPCDH7 C7-Fc fusion protein is successfully produced on a small scale but the production yield is low

To estimate the hPCDH7 C7-Fc fusion protein production yield, a pilot small scale production was performed as described in the Materials and Methods. HEK293T cells were transfected with pSec-hPCDH7 C7-Fc plasmid with untransfected cells used as a control, followed by a change of culture medium to OptiMem I. After 72 h, protein from one millilitre of culture supernatant was purified using Protein A Sepharose. The purified protein was checked on a Coomassie blue stained SDS-PAGE gel (Figure 3.4) with BSA standards loaded to estimate yield of the protein. The estimated yield of hPCDH7 C7-Fc was less than 1 mg of a stable purified protein per litre of harvested culture supernatant when extrapolated (Figure 3.4). These results indicate that to produce a larger amount of hPCDH7 C7-Fc protein, a large scale-up production was required.

3.4.3 Recombinant hPCDH7 C7-Fc fusion protein is successfully produced on a large scale

Multiple dishes of HEK293T cells were transiently transfected with pSec-hPCDH7 C7-Fc plasmid as described in the Materials and Methods. The supernatant with secreted protein was harvested every 4-5 days for a total of 20 days and stored at 4°C until used. The period of 20 days as an optimal duration of protein production was determined during a first large scale production (Figure 3.5). To reduce protein degradation during the storage, PMSF protease inhibitor and 1 mM EDTA was

added. Subsequently, the hPCDH7 C7-Fc protein was purified on HiTrap Protein A column, concentrated, dialysed to PBS and stored at 4°C. The purity and stability of the protein was checked on a Coomassie blue stained SDS-PAGE gel. As shown in Figure 3.6, the hPCDH7 C7-Fc of the size around 130 kDa was successfully purified and the protein was stable in PBS with minor impurities. The large scale production yield was around 1.5 mg of the purified protein per litre of harvested supernatant. The production of hPCDH7 C7-Fc protein was performed on a regular basis. The protein stability and its concentration were checked for every batch produced. This hPCDH7 C7-Fc fusion protein was then used in different *in vitro* assays as presented below.

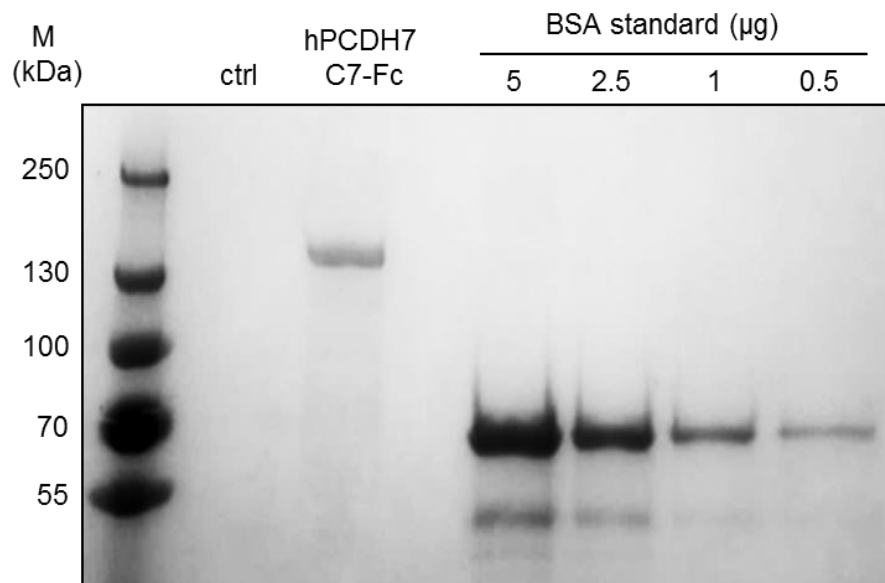


Figure 3.4 Small scale production of the hPCDH7 C7-Fc fusion protein. HEK293T cells were seeded on 6-well plate and transiently transfected with pSec-hPCDH7 C7-Fc with untransfected cells used as a control, followed by a change of medium to OptiMem I. Culture media were harvested after 72 h. The hPCDH7 C7-Fc protein was purified from 1 ml of supernatant using Protein A Sepharose, separated by SDS-PAGE and stained with Coomassie blue. BSA standards of 0.5-5 µg were used to estimate the protein production yield. Small scale hPCDH7 C7-Fc production was performed once.

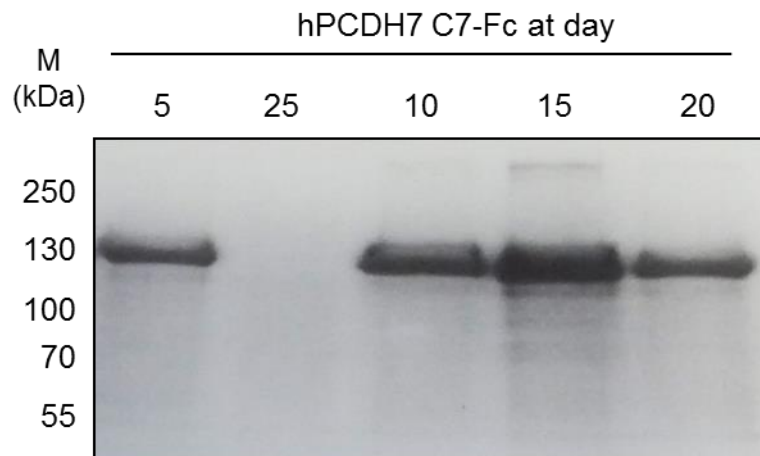


Figure 3.5 Optimal duration of a large scale production of the hPCDH7 C7-Fc fusion protein was 20 days. HEK293T cells were seeded on multiple 15 cm dishes and transiently transfected with pSec-hPCDH7 C7-Fc. Supernatant was harvested every 5 days for 25 days. To determine an optimal duration of protein production, the hPCDH7 C7-Fc protein was purified from 1 ml of each harvest using Protein A Sepharose, separated by SDS-PAGE and stained with Coomassie blue. Protein harvests were further used for large scale purification. A mixed positioning of the samples (25 days after 5 days instead of at the end of the gel) is due to a mistake during loading the samples on gel. The experiment was performed once.

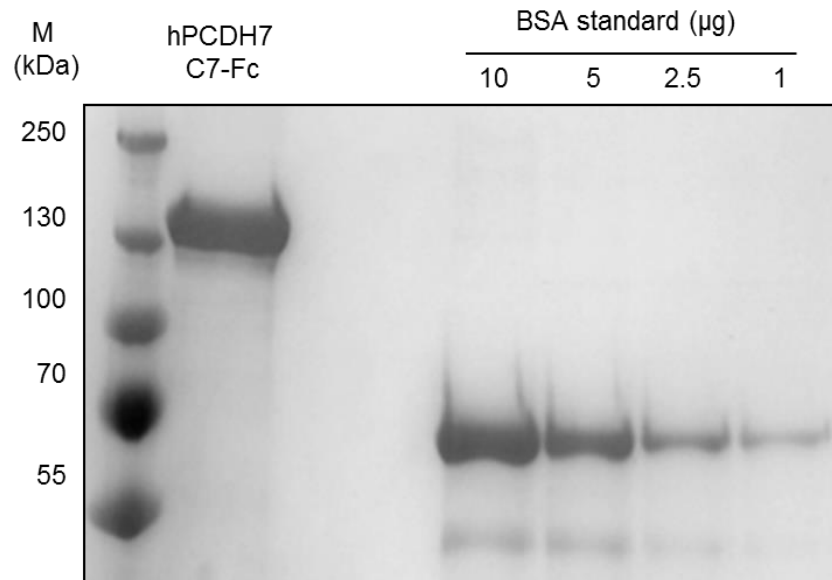


Figure 3.6 The hPCDH7 C7-Fc fusion protein was successfully produced on a large scale. Multiple 15 cm dishes of HEK293T cells were transiently transfected with pSec-hPCDH7 C7-Fc. Supernatant was harvested every 4-5 days for 20 days. The hPCDH7 C7-Fc protein was purified on HiTrap Protein A column, concentrated and dialysed to PBS. Purified protein sample was separated by SDS-PAGE and stained with Coomassie blue. BSA standards of 1-10 μg were used to estimate the hPCDH7 C7-Fc concentration in a sample however an exact protein concentration was determined independently using BCA assay. A representative concentrated protein sample from a single batch. The protein stability and concentration were checked for every batch produced.

3.5 Recombinant hPCDH7 C7-Fc fusion protein inhibits endothelial network formation in *in vitro* 3D HUVEC/HDF co-culture angiogenesis assay in a concentration dependent manner

To determine if hPCDH7 C7-Fc fusion protein modulates endothelial network formation, this was first studied using a 3D HUVEC/HDF co-culture assay in a fibrin matrix. The protocol was adapted from Lafleur *et al.* (2002) and Liu *et al.* (2008) with several modifications including GFP transduction of HUVEC enabling an excellent visualisation of the endothelial cell network formed. The assay gives an insight into the endothelial cell sprouting and tube fusion that can be followed on a daily basis (Figure A.2). An independent mCherry transduction of HDF revealed that HDF form a dense scaffold in the fibrin matrix (Figure A.3). The assay's dependence on the VEGF/bFGF signalling pathway and MMP-mediated ECM degradation was reported in the literature (Lafleur *et al.*, 2002). We have independently demonstrated that Avastin (VEGF inhibitor) and GM6001 (general MMP inhibitor) blocked HUVEC network formation in our setting (Figure A.4) thus validating the assay.

To study a potential effect of the hPCDH7 C7-Fc, HUVEC were transduced with lentivirus encoding GFP protein, mixed with fibroblasts and embedded in the fibrin matrix according to the protocol described in the Materials and Methods. Since a functional concentration of the hPCDH7 C7-Fc had to be determined, a concentration range of 50, 100 and 200 µg/ml hPCDH7 C7-Fc and control hFc diluted in a complete EBM-2 culture medium was used. As an additional control, the mock (PBS treated) sample was compared. The culture medium with proteins

was replaced every second day and the network formation was observed at day 10 of the co-culture. To ensure similar culture conditions, protein solutions of desired concentrations were diluted such that the same volume of PBS was added to all samples. This step avoided the dilution of the culture medium with an increasing volume of the recombinant protein thus ensuring the availability of the same amount of growth factors and nutrients in all samples.

Images were taken using a fluorescent microscope and included a full view of a well. Figure 3.7A shows representative images for all conditions from one experiment. The total network branching length and the number of nodes within the network was determined using ImageJ angiogenesis analyser plug in as described in the Materials and Methods. Statistical analysis of data from three independent experiments is presented in Figure 3.7B.

As expected, human Fc control did not influence the network formation independently of hFc concentration when compared to the mock control (Figure 3.7A and 3.7B). In contrast, a decrease in the network density could be observed for hPCDH7 C7-Fc treated cells. Indeed, a concentration dependent inhibitory effect in the total network branching length and the number of nodes within the network was measured for hPCDH7 C7-Fc treated cells with a statistically significant reduction for the highest concentration 200 µg/ml (Figure 3.7B).

Therefore, 200 µg/ml of the hPCDH7 C7-Fc was chosen and used for further studies presented later in this chapter. Concentrations higher than 200 µg/ml were not tested

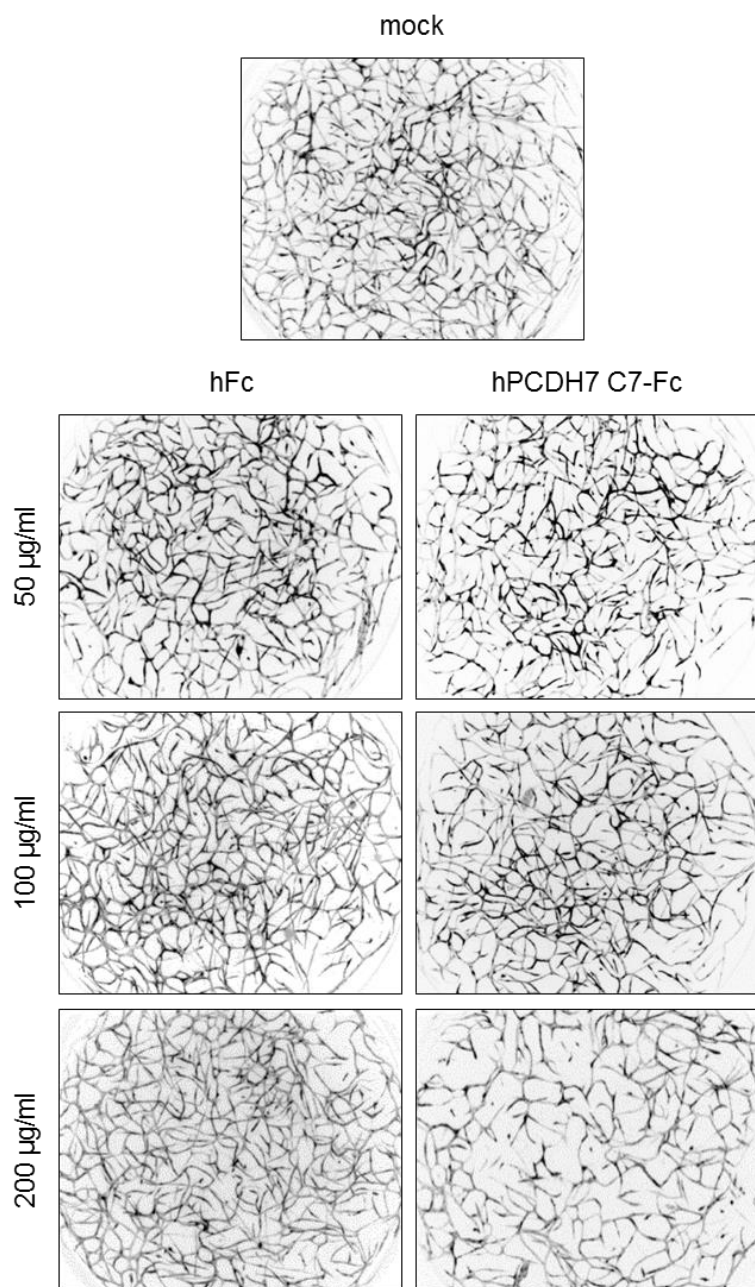


Figure 3.7A The hPCDH7 C7-Fc fusion protein significantly inhibits an endothelial network formation in a 3D HUVEC/HDF co-culture angiogenesis assay in a concentration dependent manner. GFP transduced HUVEC were used in a 3D HUVEC/HDF co-culture assay. The experiment was performed three times (N=3) in triplicates (n=3). Cells were treated with an increasing concentration from 0 to 200 µg/ml of hFc control and hPCDH7 C7-Fc recombinant proteins diluted in a complete EBM-2 medium. The network formation was observed at day 10 via visualisation of GFP. Images were taken using a fluorescence microscope (2x magnification) and inverted into a white background for a better visualisation of the network. Single image represents a whole well. Representative images from one of three experiments.

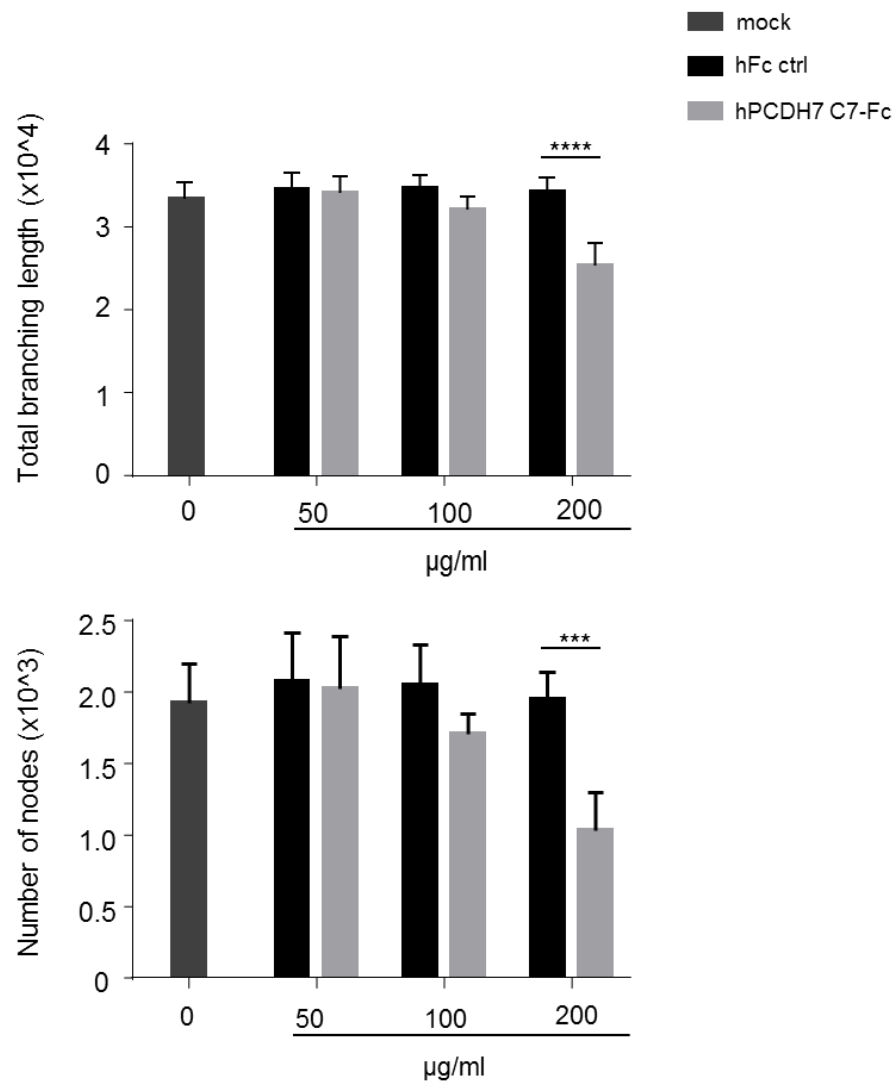


Figure 3.7B The hPCDH7 C7-Fc fusion protein significantly inhibits an endothelial network formation in a 3D HUVEC/HDF co-culture angiogenesis assay in a concentration dependent manner. The total network branching length and the number of nodes were determined using ImageJ angiogenesis analyser plug in. 2-way ANOVA Tukey's multiple comparisons test, *** $p < 0.001$, **** $p < 0.0001$. Error bars represent SD. N=3; n=3.

due to a low availability of the protein. Since hFc is almost five times smaller than hPCDH7 C7-Fc (25 kDa versus 130 kDa), using the same concentration in micrograms per millilitre did not correspond to the same molarity. To ensure the same amount of protein molecules in the samples, the molar concentration of 1.54 μ M equivalent to 200 μ g/ml hPCDH7 C7-Fc was used.

3.6 Recombinant hPCDH7 C7-Fc fusion protein inhibits endothelial cell proliferation in a MTT assay

Next, the effect of the hPCDH7 C7-Fc on HUVEC proliferation was investigated using a MTT assay as described in the Materials and Methods. MTT assay measures a cellular metabolic activity that should be directly proportional to the number of living cells thus giving an indication of cell proliferation rate. The same numbers of HUVEC were seeded on 96-well plate. Cells were treated with 1.54 μ M hFc or hPCDH7 C7-Fc diluted in a complete EBM-2 medium. The assay was performed at 24 h and 48 h after setting up the culture. Mock (PBS treated) cells were used as an additional control.

As expected, human Fc did not affect HUVEC cell proliferation when compared to mock treated cells (Figure 3.8). In contrast, the hPCDH7 C7-Fc treated cells showed a small but statistically significant reduction in the cell proliferation of around 10% after 48 h in culture. These results suggest that the hPCDH7 C7-Fc negatively regulates cell proliferation.

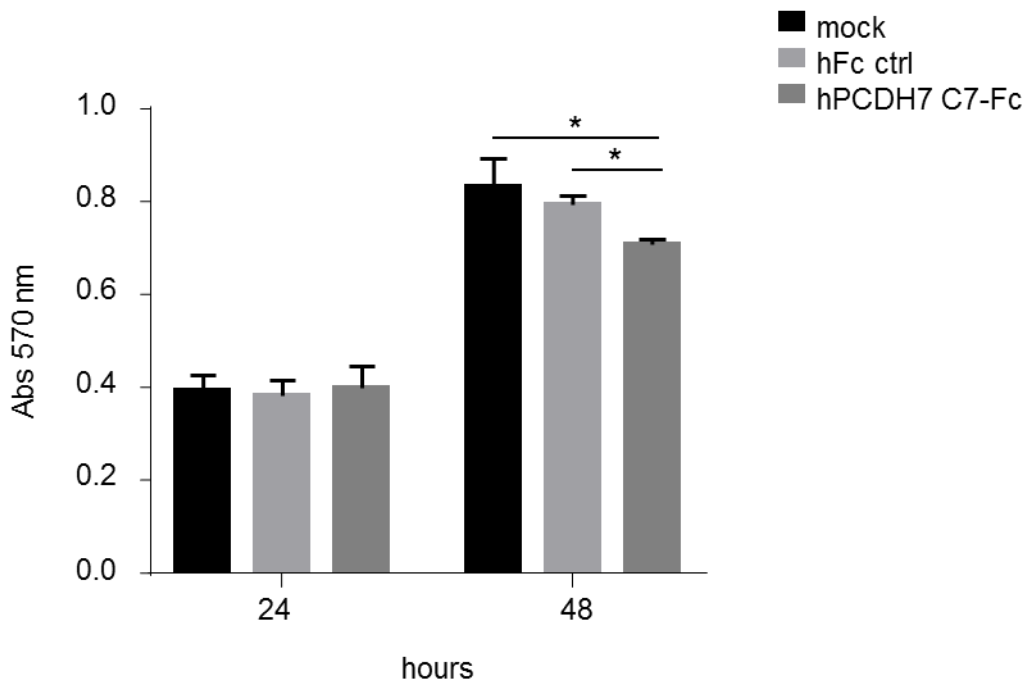


Figure 3.8 The hPCDH7 C7-Fc fusion protein significantly reduces HUVEC proliferation in a MTT assay. HUVEC were seeded on 96-well plate and incubated with hPCDH7 C7-Fc and hFc control to a final concentration of 1.54 μ M diluted in a complete EBM-2 medium. PBS treated (mock) samples were used as an additional control. The proliferation of HUVEC was measured at 24 h and 48 h. 2-way ANOVA Tukey's multiple comparisons test, * p <0.05; Error bars represent SD. The experiment was performed three times (N=3) in triplicates (n=3).

3.7 Recombinant hPCDH7 C7-Fc fusion protein non-significantly affects endothelial cells migration in a scratch assay

The migration of HUVEC upon the treatment with hPCDH7 C7-Fc and control hFc was studied on a scratch assay using an IncuCyte system, as described in the Materials and Methods. Mock cells were used as an extra control. HUVEC were seeded on ImageLock 96-well plate in a complete EBM-2 medium. Cell proliferation was considered as a potential co-factor in this assay. However, we have observed that HUVEC doubling time is around 30 h (personal observations). Since the assay is completed within 24 h we have assumed that proliferation will not affect our results. Thus, cells were not treated to inhibit proliferation in our setting. Scratches were made on a confluent cell monolayer. HUVEC were treated with 1.54 μ M hPCDH7 C7-Fc or hFc control diluted in a complete EBM-2. To ensure reliable results, scratches with similar initial wound area only were analysed with three technical replicates per experiment. The migration of cells within a wound was recorded for 24 h using an IncuCyte software. Wound surface areas were quantified manually using ImageJ. Results were presented as a percentage of the wound area measured at the given time point to the initial wound area for each sample.

Figure 3.9A shows representative images of the cells migration captured every 6 h. Quantified data revealed that there was no difference between the migration of cells between control hFc and mock cells. A small but non-significant reduction in HUVEC migration was measured upon the treatment with the hPCDH7 C7-Fc (Figure 3.9B).

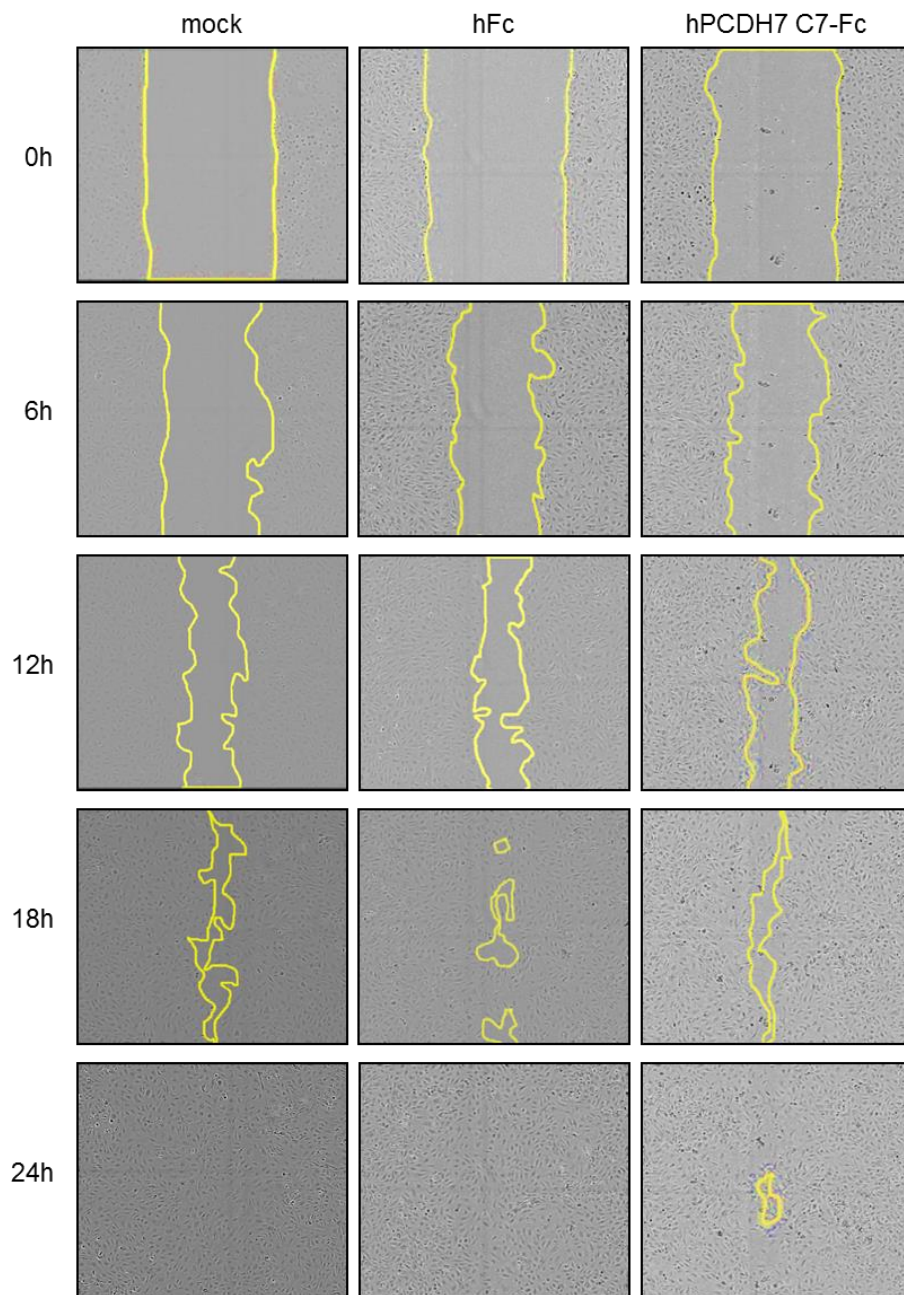


Figure 3.9A The hPCDH7 C7-Fc non-significantly reduces HUVEC migration in a scratch assay. HUVEC were seeded on ImageLock 96-well plate. Scratches were made on confluent cell monolayers using a WoundMaker.. Cells were treated with a complete EBM-2 medium containing hFc or hPCDH7 C7-Fc protein to a final concentration of 1.54 μM . PBS treated (mock) samples were used as an additional control. The plate was placed into IncuCyte incubator and the cell migration was monitored every 6 h using IncuCyte ZOOM software. The experiment was performed three times (N=3) in triplicates (n=3). Representative images from one of three experiments.

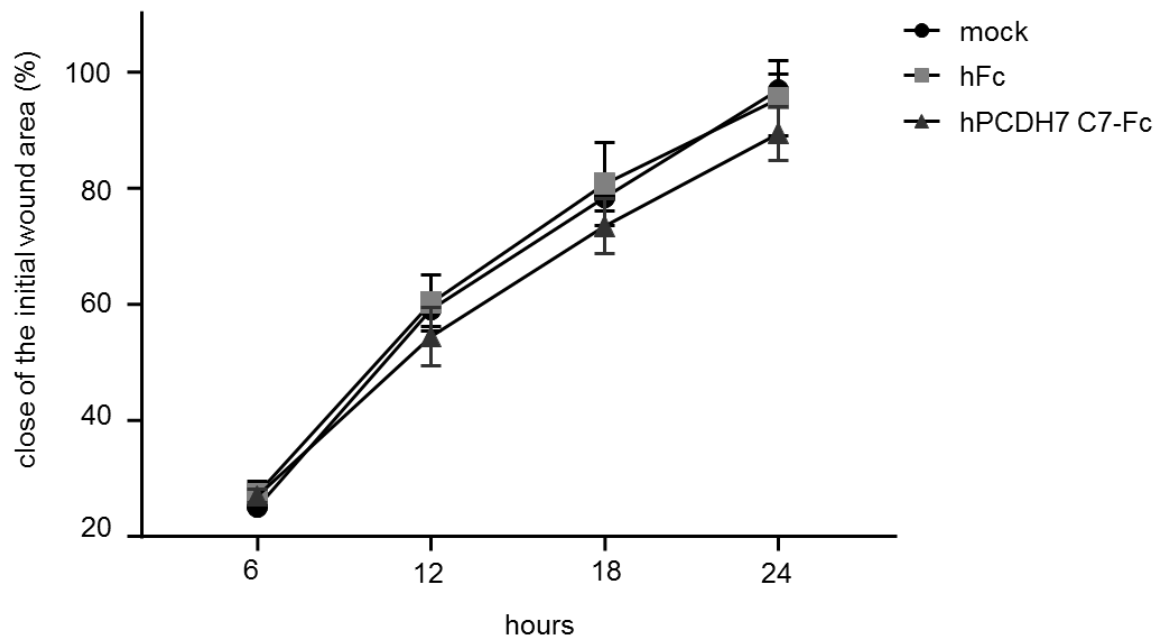


Figure 3.9B The hPCDH7 C7-Fc non-significantly reduces HUVEC migration in a scratch assay. The wound area was measured manually using ImageJ and was calculated as a percentage of the wound area measured at the given time point to the initial wound area for each sample. 2-way ANOVA Tukey's multiple comparisons test. Error bars represent SD, N=3, n=3.

These data suggest that hPCDH7 C7-Fc might slightly affect the endothelial cells but its activity is too low to give a statistically significant difference.

3.8 Generation and production of truncated hPCDH7 ECD-Fc fusion proteins

3.8.1 Truncated hPCDH7 C7-Fc fusion proteins are successfully generated

The next step was to determine which region of hPCDH7 extracellular domain mediates this inhibitory function. Thus, several truncated forms of hPCDH7 C7-Fc were generated as described in the Materials and Methods. The hPCDH7 ECD containing N-terminal DNA fragment of one (C1), three (C3) and five (C5) cadherin repeats were cloned into pIG-Fc vector and their sequence verified. A schematic representation of the truncated proteins is shown in Figure 3.10 and amino acid sequences of the proteins are listed in Figure A.7. HEK293T cells were transfected with the plasmids: pIG-hPCDH7 C1-Fc, pIG-hPCDH7 C3-Fc and pIG-hPCDH7 C5-Fc with untransfected cells used as a control, followed by a change of culture medium to OptiMem I. The culture media from the different transfections were collected 48 h later, separated by SDS-PAGE and transferred to PDVF membrane. The expression of the proteins was verified with both anti-human PCDH7 and anti-human Fc antibodies (Figure 3.11A). Western blotting showed the bands of predicted sizes 45, 75 and 115 kDa for hPCDH7 C1-Fc, hPCDH7 C3-Fc and hPCDH7 C5-Fc, respectively. Moreover, hPCDH7 C3-Fc consistently appeared as a doublet upon a very short exposure time (Figure 3.11B) suggesting that there were two forms of

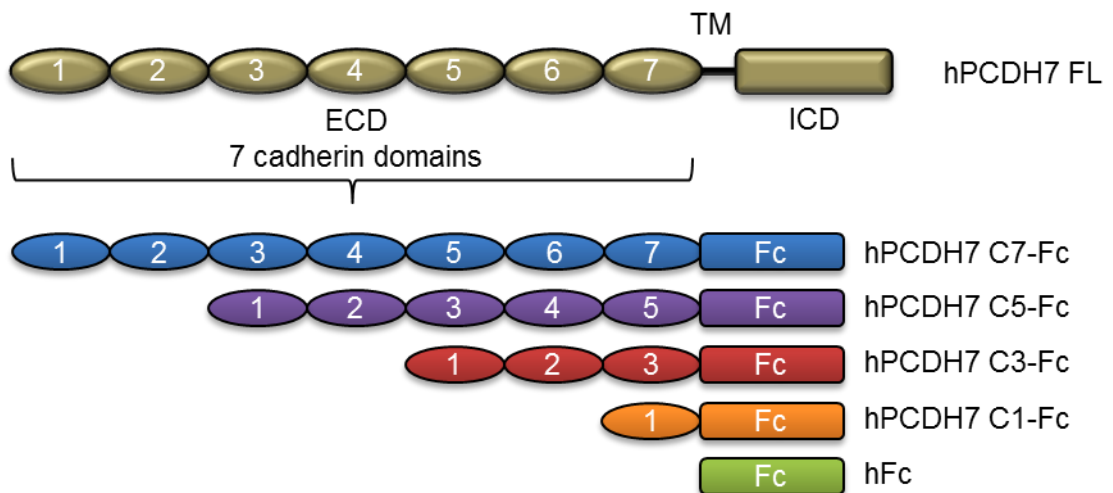


Figure 3.10 Schematic representation of the truncated hPCDH7 ECD-Fc fusion proteins. DNA fragments encoding the extracellular domain containing seven (C7, full length), five (C5), three (C3) or one (C1) N-terminal cadherin repeats of the hPCDH7 ECD were fused to human Fc (hFc). The amino acid sequences can be found in Figure A.7. ECD – extracellular domain; TM – transmembrane domain; ICD – intracellular domain.

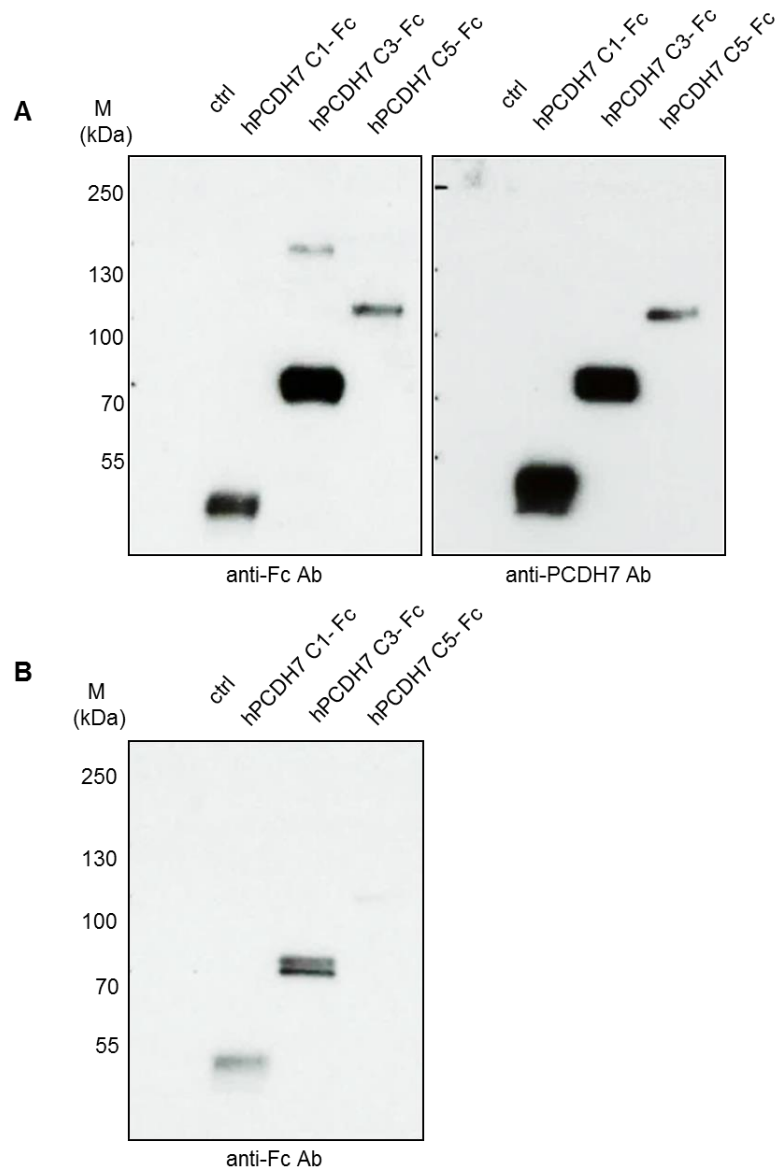


Figure 3.11 The truncated hPCDH7 ECD-Fc fusion proteins were expressed and secreted to the medium. HEK293T cells were transiently transfected with pIG-hPCDH7 C1-Fc, pIG-hPCDH7 C3-Fc or pIG-hPCDH7 C5-Fc. Untransfected cells were used as a control. Culture media were harvested 48 h later. A) The expression of the fusion proteins was verified on Western Blot using both anti-human PCDH7 and anti-human Fc antibodies. B) The anti-Fc stained blot after a very short exposure time revealing two bands of hPCDH7 C3-Fc. The verification of the truncated hPCDH7-ECD fusion proteins was performed once.

the protein, one slightly truncated. These results confirmed that hFc fragment was successfully fused to hPCDH7 C1, C3 and C5 fragments and that the fusion proteins were secreted to the culture medium.

3.8.2 Truncated hPCDH7 C7-Fc fusion proteins are successfully produced on a small scale

To estimate the truncated fusion proteins production yield, a small scale experiment was set up similarly to that described earlier in this chapter. Purified proteins were checked on a Coomassie blue stained SDS-PAGE gel. The estimated production yield was around 10 mg for hPCDH7 C1-Fc and hPCDH7 C3-Fc and 2 mg for hPCDH7 C5-Fc purified protein per litre of harvested culture supernatant (Figure 3.12). These results suggest that the shorter fusion proteins are more efficiently secreted to the culture medium than a full length hPCDH7 C7-Fc, thus allowing bigger protein yields.

3.8.3 Truncated hPCDH7 C7-Fc fusion proteins are successfully produced on a large scale

The hPCDH7 C1, C3 and C5-Fc fusion proteins were produced similarly to hPCDH7 C7-Fc described earlier in this chapter. Again, the purity and stability of the proteins were verified on a Coomassie blue stained SDS-PAGE gel (Figure 3.13). The production yield of hPCDH7 C1-Fc and hPCDH7 C3-Fc was around five times greater than that of hPCDH7 C5-Fc and was around 5 mg of protein per litre of

harvested media. In contrast, the yield of hPCDH7 C5-Fc was similar to that measured before for hPCDH7 C7-Fc, around 1.5 mg per litre. As observed on Western blot, hPCDH7 C3-Fc protein contained two distinctive bands of similar size, confirming the presence of two hPCDH7 C3-Fc isoforms. Additional protein bands that were difficult to remove most probably resulted from protein degradation. These different truncated forms of hPCDH7 ECD-Fc were further used in various *in vitro* proliferation, migration and angiogenesis assays.

3.9 Truncated hPCDH7 C5-Fc and hPCDH7 C7-Fc significantly inhibit endothelial cell proliferation in a MTT assay

To determine which regions of hPCDH7 ECD were involved in modulating the proliferation of HUVEC, a MTT assay was set up similarly to that described earlier in this chapter. Cells were treated with 1.54 μ M hPCDH7 C1, C3 and C5-Fc proteins and hPCDH7 C7-Fc for a direct comparison. As a control, 1.54 μ M hFc was used. Mock cells were not tested as it was shown earlier there was no difference between hFc and PBS treated samples.

The data showed that two smaller recombinant proteins hPCDH7 C1-Fc and hPCDH7 C3-Fc did not show any inhibitory effect on HUVEC proliferation when compared to hFc control (Figure 3.14). In contrast, hPCDH7 C5-Fc significantly reduced cell proliferation with an effect similar to hPCDH7 C7-Fc, around 25% for both proteins. The discrepancies in the percentage of the inhibitory effect for

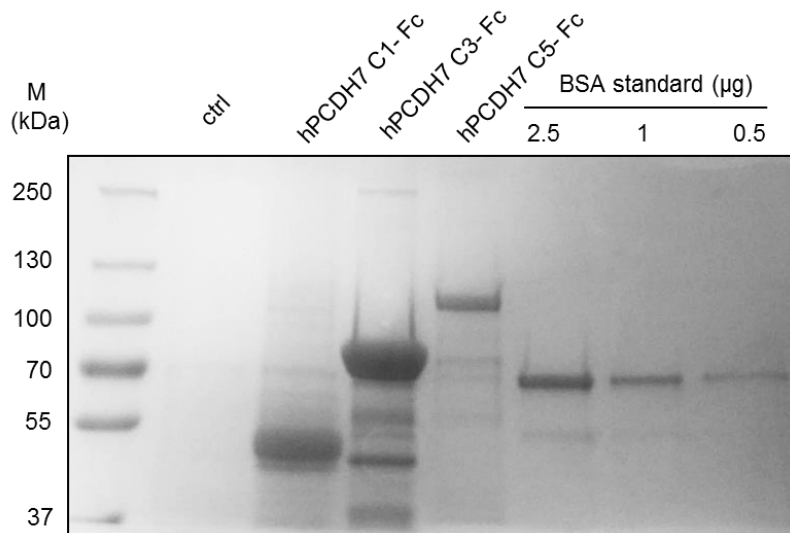


Figure 3.12 The truncated hPCDH7 ECD-Fc fusion proteins were successfully produced on a small scale. HEK293T cells were seeded on 6-well plate and transiently transfected with pIG-hPCDH7 C1-Fc, pIG-hPCDH7 C3-Fc or pIG-hPCDH7 C5-Fc and untransfected cells were used as a control, followed by a change of the culture medium to OptiMem I. Culture media were harvested after 72 h. The proteins were purified from 1 ml of supernatant using Protein A Sepharose, separated by SDS-PAGE and stained with Coomassie blue. BSA standards of 0.5-2.5 µg were used to estimate the proteins production yields. A small scale production of the truncated hPCDH7 ECD-Fc proteins was performed once.

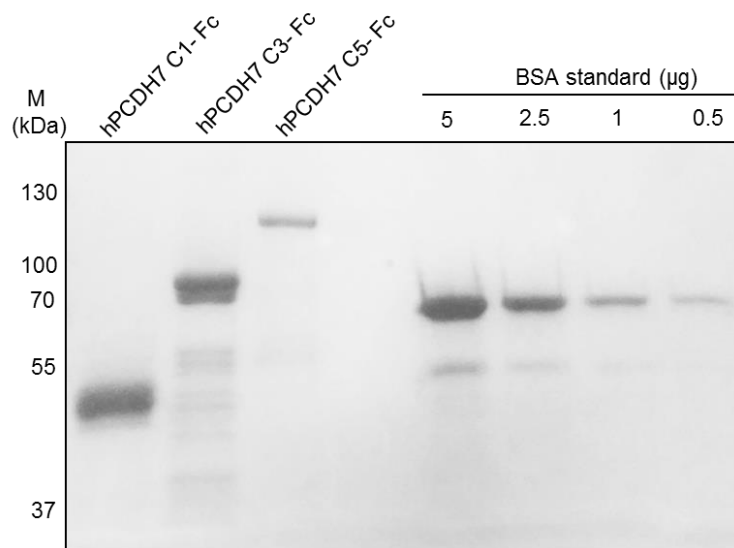


Figure 3.13 The truncated hPCDH7 ECD-Fc fusion proteins were successfully produced on a large scale. Multiple 15 cm dishes of HEK293T cells were transiently transfected with pIG-hPCDH7 C1-Fc, pIG-hPCDH7 C3-Fc or pIG-hPCDH7 C5-Fc. Supernatant was harvested every 4-5 days for 20 days. Proteins were purified on HiTrap Protein A column, concentrated and dialysed to PBS. Purified protein samples were separated by SDS-PAGE and stained with Coomassie blue. BSA standards of 0.5-5 µg were used to estimate protein concentration in samples however exact protein concentrations were determined independently using a BCA assay. Representative concentrated protein samples from single large scale production batches. The protein stability and concentration were checked for every batch produced.

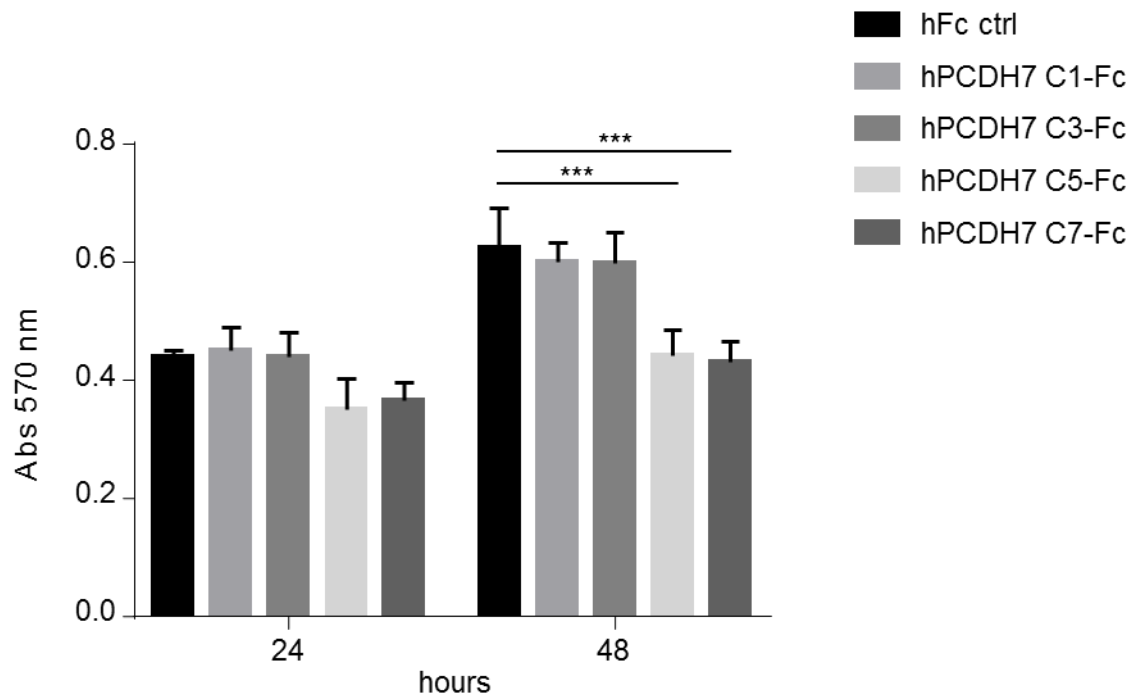


Figure 3.14 The hPCDH7 C5-Fc and hPCDH7 C7-Fc fusion proteins significantly reduce HUVEC proliferation in a MTT assay. HUVEC were seeded on 96-well plate and incubated with hFc control, hPCDH7 C1-Fc, hPCDH7 C3-Fc, hPCDH7 C5-Fc and hPCDH7 C7-Fc to a final concentration of 1.54 μ M diluted in a complete EBM-2 medium. The proliferation of HUVEC was measured at 24 h and 48 h at the 570 nm absorbance. 2-way ANOVA Tukey's multiple comparisons test, *** $p < 0.001$. Error bars represent SD. The experiment was performed three times (N=3) in triplicates (n=3).

hPCDH7 C7-Fc presented earlier (10%) and in this subsection (25%) might result from batch to batch differences between either or both of recombinant proteins and HUVEC isolates. Despite this, the decrease in the proliferation was again observed and it was mediated by both the C5 and full length (C7) hPCDH7-Fc.

3.10 Truncated hPCDH7 C5-Fc and hPCDH7 C7-Fc significantly inhibit endothelial network formation in 3D HUVEC/HDF co-culture angiogenesis assay

To determine which region of the ECD of PCDH7 mediated inhibition of tube formation, a 3D HUVEC/HDF co-culture assay was set up, conducted and analysed as described earlier in this chapter. Co-cultured cells were treated with 1.54 μM control hFc, hPCDH7 C1-Fc, hPCDH7 C3-Fc, hPCDH7 C5-Fc and hPCDH7 C7-Fc diluted in a complete EBM-2 medium. The assay was conducted for 10 days with media changed every second day. Representative images for all conditions from one experiment are shown in Figure 3.15A. A significant and comparable decrease in the number of nodes within the network was observed upon the treatment with hPCDH7 C5-Fc and hPCDH7 C7-Fc proteins when compared to the control (Figure 3.15B). Additionally, there was a small but statistically non-significant reduction in the number of nodes for the two shorter fragments. This suggests they might slightly affect the endothelial cells but their activity is too low to give a statistically significant difference. A similar pattern was observed for the total branching length of the network. Both hPCDH7 C5-Fc and hPCDH7 C7-Fc significantly reduced

the branching of the network while the effect was not detected for hPCDH7 C1-Fc and hPCDH7 C3-Fc.

The results presented here are consistent with the data shown earlier in this chapter for the concentration range of hPCDH7 C7-Fc. Although the effect of 1.54 μ M hPCDH7 C7-Fc is smaller, the trend is similar. The discrepancies might be again caused by variable factors such as a different batch of protein or a different batch of HUVEC. Despite this, it is clear that hPCDH7 C5-Fc and hPCDH7 C7-Fc have a similar inhibitory effect on the endothelial network formation.

3.11 Truncated hPCDH7 C5-Fc and hPCDH7 C7-Fc significantly inhibit endothelial network formation in 2D HUVEC/HDF co-culture angiogenesis assay

A 2D HUVEC/HDF co-culture assay set up differs from 3D co-culture due to the lack of externally added extracellular matrix. Similarly to 3D co-culture assay, we have validated the assay and independently demonstrated that the network formation is dependent on the VEGF signalling pathway however it does not seem to require MMP-mediated ECM degradation (Figure A.5).

To study the effect of truncated hPCDH7 ECD-Fc fusion proteins, HUVEC were plated on top of a confluent monolayer of fibroblast as described in the Materials and Methods and cultured for 6 days. Co-cultured cells were treated with 1.54 μ M control hFc, hPCDH7 C1-Fc, hPCDH7 C3-Fc, hPCDH7 C5-Fc and hPCDH7 C7-Fc diluted in

a complete EBM-2 medium. Media were changed every second day. Next, the co-culture was fixed and the endothelial cells were stained with anti-human CD31 antibody with an AP-conjugated secondary antibody. The images of stained network were taken using a light microscope and contained a full view of the sample. The calculations were performed using ImageJ angiogenesis analyser plug in for the phase contrast images as described in the Materials and Methods.

Representative images for all conditions from one experiment are shown in Figure 3.16A. As expected, the CD31 staining of the endothelial network revealed a dense, interconnected network with long tubes for hFc control. No effect was observed for hPCDH7 C1-Fc and hPCDH7 C3-Fc for which the network was visually indistinguishable to the control. In contrast, a dramatic reduction in the network formation was observed for hPCDH7 C5-Fc and hPCDH7-Fc when compared to hFc control. Tubes in the middle of the well were short and sparse. Slightly longer tubes but a barely interconnected network was observed around the edges of the well. This might be due uneven seeding of cells. These visual observations were confirmed by the statistical analysis from three independent experiments (Figure 3.16B). The total network branching length was about 60% lower for hPCDH7 C5-Fc and hPCDH7 C7-Fc when compared to hFc. A greater inhibitory effect of around 80% was calculated for the number of nodes within the network. These results correspond to those obtained for the 3D co-culture, though inhibition by both hPCDH7 C5-Fc and hPCDH7 C7-Fc is more profound in the 2D assay.

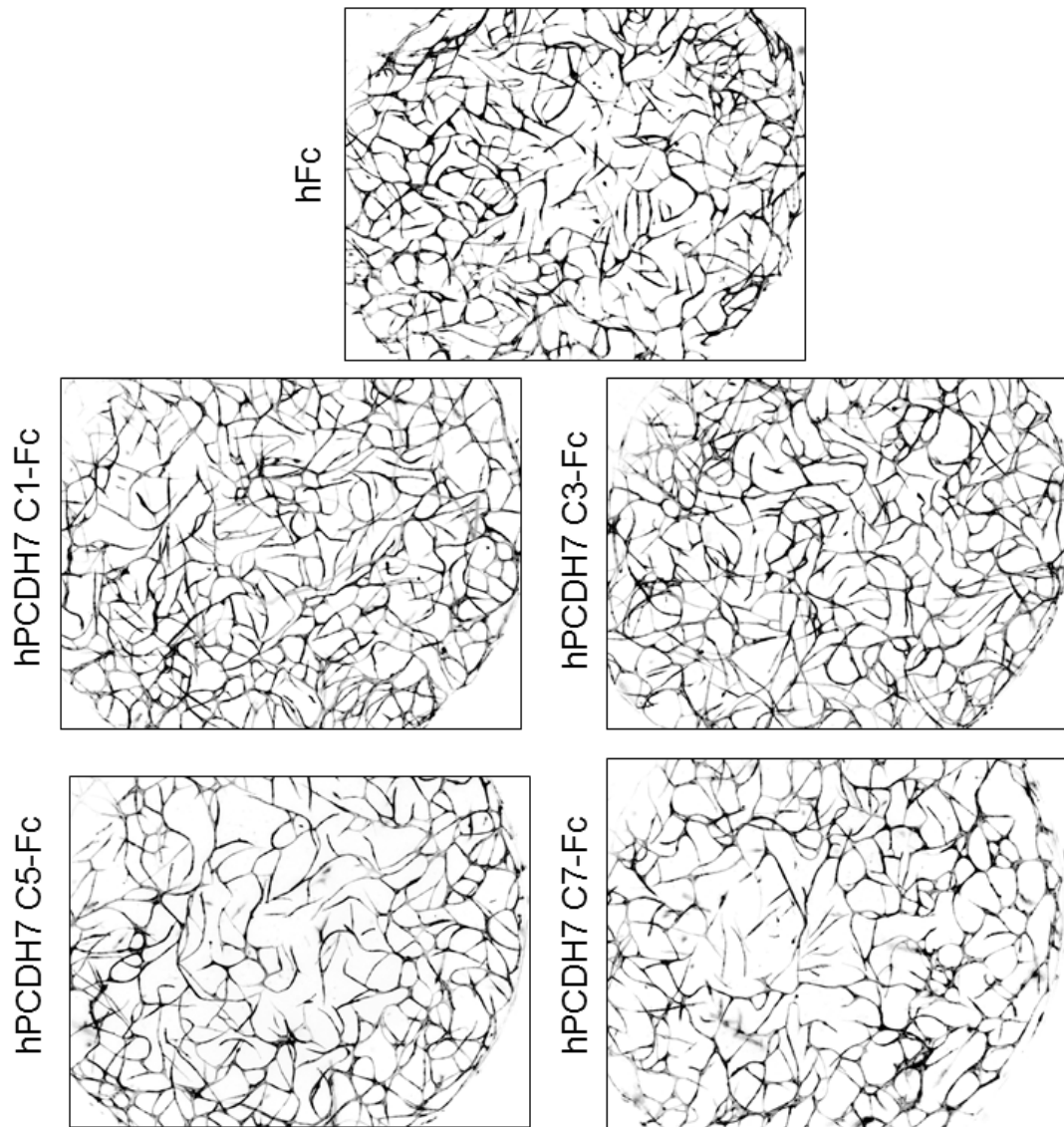


Figure 3.15A The hPCDH7 C5-Fc and hPCDH7 C7-Fc fusion proteins comparably inhibit an endothelial network formation in a 3D HUVEC/HDF co-culture angiogenesis assay. GFP transduced HUVEC were used in a 3D HUVEC/HDF co-culture assay. The experiment was performed three times (N=3) in triplicates (n=3). Cells were treated with hFc, hPCDH7 C1-Fc, hPCDH7 C3-Fc, hPCDH7 C5-Fc or hPCDH7 C7-Fc to a final concentration of 1.54 μ M diluted in a complete EBM-2 medium. The network formation was observed at day 10 via visualisation of GFP. Images were taken using a fluorescence microscope (2x magnification) and inverted into a white background for a better visualisation of the network. Each image represents a whole well. These are representative images from one of three experiments.

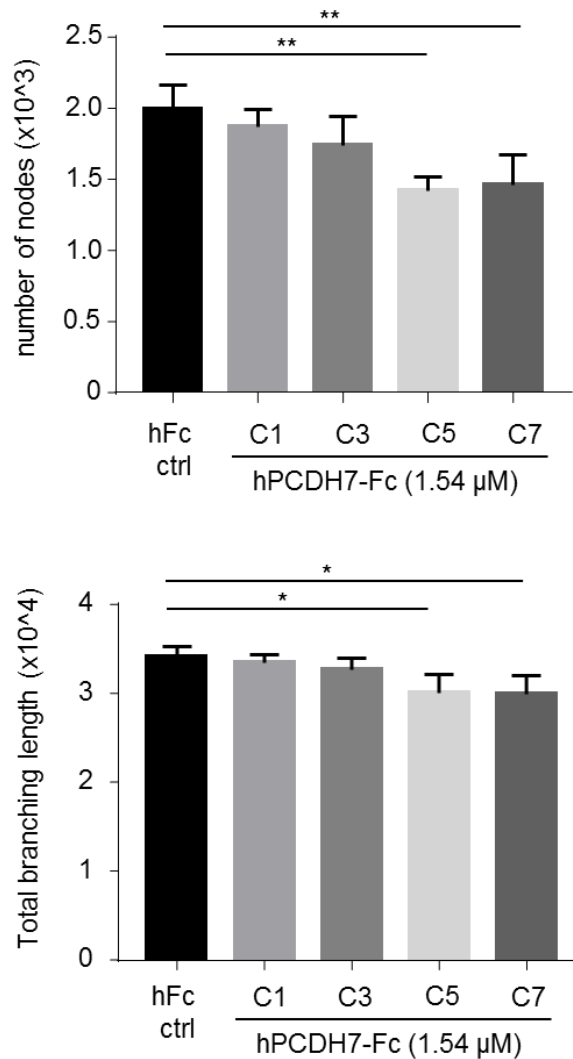


Figure 3.15B The hPCDH7 C5-Fc and hPCDH7 C7-Fc fusion proteins comparably inhibit an endothelial network formation in a 3D HUVEC/HDF co-culture angiogenesis assay. The total network branching length and the number of nodes were determined using ImageJ angiogenesis analyser plug in. 1-way ANOVA Tukey's multiple comparisons test, * $p < 0.05$, ** $p < 0.01$. Error bars represent SD. $N=3$, $n=3$.

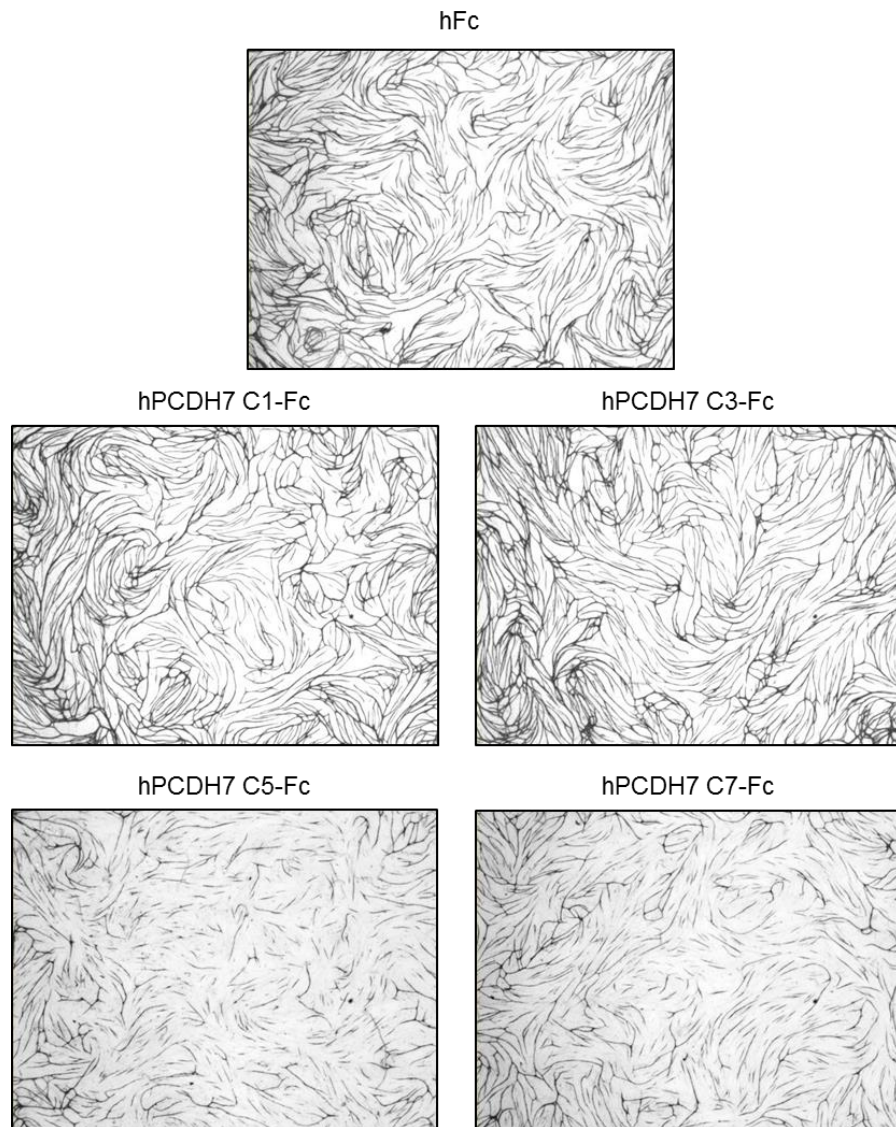


Figure 3.16A The hPCDH7 C5-Fc and hPCDH7 C7-Fc fusion proteins comparably inhibit an endothelial network formation in a 2D HUVEC/HDF co-culture angiogenesis assay. HUVEC were used in a 2D co-culture assay. The experiment was performed three times (N=3) in triplicates (n=3). Cells were treated with hFc, hPCDH7 C1-Fc, hPCDH7 C3-Fc, hPCDH7 C5-Fc or hPCDH7 C7-Fc to a final concentration of 1.54 μ M diluted in a complete EBM-2 medium. Cells were fixed at day 6 and the endothelial cells were stained with anti-human CD31 primary antibody and an AP-conjugated secondary antibody. The signal was developed using BCIP/NBT substrate. Images were taken using a light microscope. Each image represents a whole well. Representative images from one of three experiments.

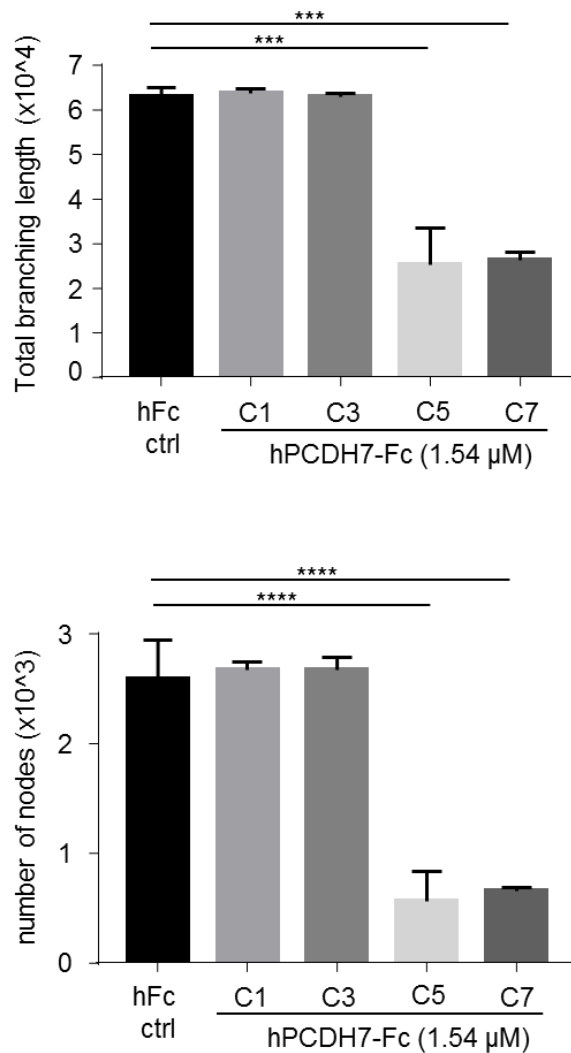


Figure 3.16B The hPCDH7 C5-Fc and hPCDH7 C7-Fc fusion proteins comparably inhibit an endothelial network formation in a 2D HUVEC/HDF co-culture angiogenesis assay. The total network branching length and the number of nodes were determined using ImageJ angiogenesis analyser plug in; 1-way ANOVA Tukey's multiple comparisons test. *** $p < 0.001$, **** $p < 0.0001$. Error bars represent SD. N=3, n=3.

3.12 Truncated hPCDH7 C5-Fc and hPCDH7 C7-Fc significantly inhibit endothelial transmigration in a transwell assay

Functional hPCDH7 C5-Fc and hPCDH7-Fc fusion proteins were further studied for their effect on the endothelial cell transmigration across a porous membrane from serum free medium towards a complete medium with fetal bovine serum (FBS) as a chemoattractant. A transwell assay was performed according to the protocol described in the Materials and Methods.

Serum starved HUVEC were seeded onto FluorBlock cell culture inserts in a serum free M199 medium containing 1.54 μ M hPCDH7 C5-Fc, hPCDH7-C7-Fc and hFc control and placed into wells filled with M199 medium containing FBS. After 6 h of incubation, cells were fixed and membranes were mounted in DAPI onto the microscope slides. DAPI stained nuclei of the migrated cells were imaged under a fluorescent microscope and counted as described in the Materials and Methods. The results showed that both hPCDH7 C5-Fc and hPCDH7 C7-Fc significantly reduced HUVEC transmigration towards a serum containing medium by around 25% when compared to hFc control (Figure 3.17).

3.13 Truncated hPCDH7 ECD-Fc fusion proteins do not affect endothelial cell sprouting in a spheroid assay

To investigate whether both hPCDH7 C5-Fc and hPCDH7 C7-Fc fusion proteins affected the sprouting of HUVEC, a spheroid assay was performed as described in

the Materials and Methods. Spheroids were generated with GFP transduced HUVEC and embedded in a collagen I matrix. Spheroids were incubated with active 1.54 μ M hPCDH7 C5-Fc, hPCDH7 C7-Fc and hFc control diluted in a complete EBM-2 medium. After 18 h of incubation samples were fixed and imaged under a fluorescence confocal microscope. The number of sprouts were counted manually using ImageJ.

As shown in Figure 3.18A there was no obvious difference in sprouting between control and hPCDH7 C5-Fc and hPCDH7 C7-Fc. These visual observations were supported by statistical analysis of the average number of sprouts from three independent experiments (Figure 3.18B). To avoid biased analysis, sprouts were also counted blindly by another researcher with similar results. These results suggest that neither hPCDH7 C5-Fc nor hPCDH7 C7-Fc influence endothelial cell sprouting.

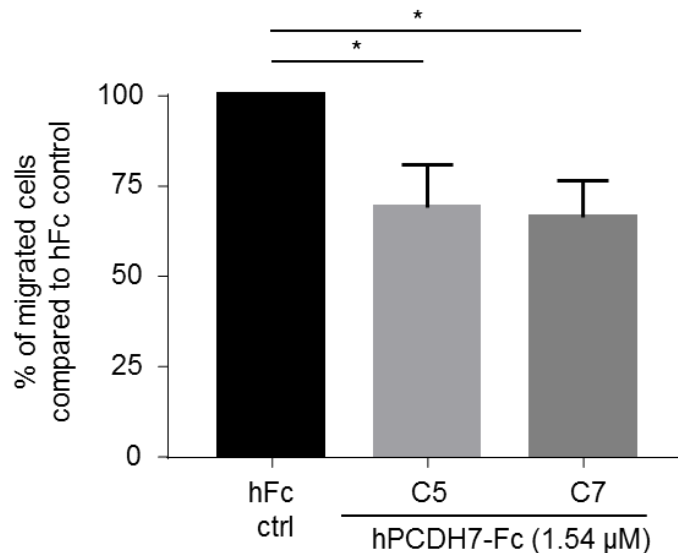


Figure 3.17 The hPCDH7 C5-Fc and hPCDH7 C7-Fc fusion proteins reduce endothelial cell transmigration towards a serum in a transwell assay. HUVEC were starved for one hour in a serum-free M199 medium containing growth factors. Next, cells were seeded onto FluorBlock cell culture inserts in serum-free medium containing 1.54 μ M hFc, hPCDH7 C5-Fc or hPCDH7 C7-Fc. The inserts with cells were placed into wells filled with M199 medium with growth factors and serum and incubated for 6 h. Cells were fixed, membranes cut out from the inserts and embedded on the microscope slides in DAPI mounting medium. The nuclei of the migrated cells were imaged under a fluorescence microscope (10x magnification). For each sample, a total number of cell nuclei was calculated manually from 16 fields of view. Calculations were normalized to the hFc control (100%); 1-way ANOVA Tukey's multiple comparisons test, * $p < 0.05$, Error bars represent SD. The experiment was performed three times (N=3; n=1).

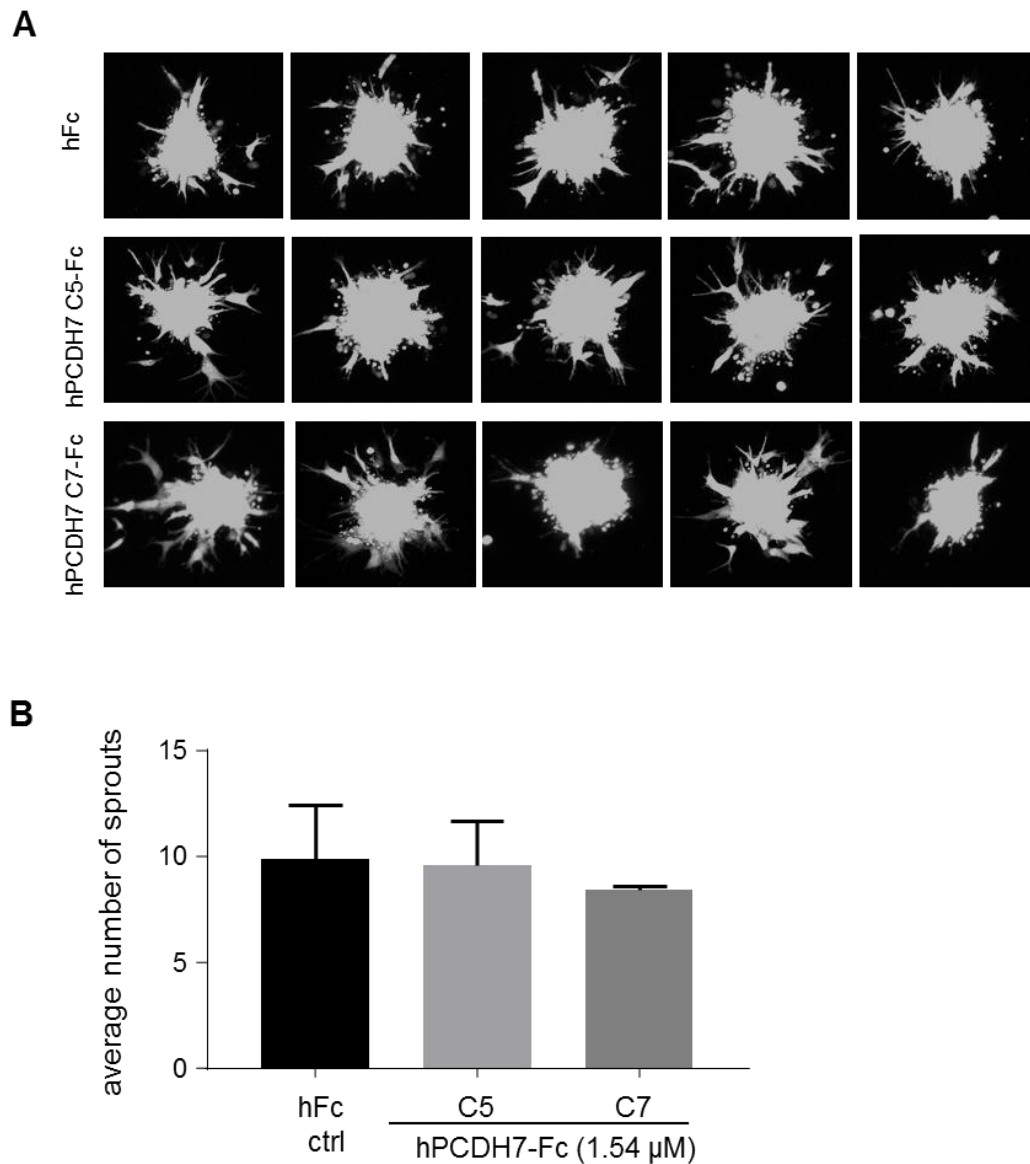


Figure 3.18 The hPCDH7 C5-Fc and hPCDH7 C7-Fc fusion proteins do not affect HUVEC sprouting in a spheroid assay. HUVEC-GFP spheroids embedded in collagen I matrix were incubated with medium containing hFc, hPCDH7 C5-Fc and hPCDH7 C7-Fc to a final concentration of 1.54 μM diluted in a complete EBM-2 medium. After 18 h of incubation samples were fixed and imaged under a fluorescence confocal microscope, five spheroids per sample. A) Representative images of the spheroids from one of three experiments. B) Statistical analysis of the average number of sprouts counted manually using ImageJ. 1-way ANOVA Tukey's multiple comparisons test. Error bars represent SD. The experiment was performed three times (N=3; n=5).

3.14 Discussion

The extracellular domain of hPCDH7 fused to Fc and produced as a soluble recombinant protein showed biological activity inhibiting endothelial cell proliferation, network formation and chemotaxis. In contrast, it non-significantly reduced the migration of cells in the scratch assay and did not affect sprouting of the endothelial cells. This is the first report of the blocking effect of the hPCDH7 extracellular domain on the endothelial network formation *in vitro* and supports our hypothesis that PCDH7 plays a role in angiogenesis.

The hPCDH7 C7-Fc inhibited HUVEC proliferation. Özlü *et al.* (2015) has shown that PCDH7 is expressed on the cell surface of cancer cells during mitosis while being retained in the cytoplasm during interphase. For this reason, it would be interesting to investigate whether soluble hPCDH7 ECD-Fc affects the cell cycle using for example flow cytometry with PI staining of the genomic DNA. It is also possible that the hPCDH7 ECD-Fc ligand is present in the serum of cell culture medium and the soluble PCDH7 is neutralizing it thus preventing from positively regulating cell proliferation. The MTT assay measures cells' metabolic activity. This should be proportional to the number of cells, but the possibility remains that the hPCDH7 ECD-Fc may disrupt the metabolic activity of cells, rather than cell proliferation. Also, potential difference in the number of mitochondria between cells might result in different amount of formazan that is produced negatively affecting the results and giving false positive data. The MTT assay was chosen due to its requirements for small numbers of cells. Therefore, to confirm these results it would be necessary to

repeat the experiment by simply counting of cells or using other assays measuring DNA synthesis rate as the most accurate method of proliferation analysis. These alternative approaches were not used due to the large number of cells and large amounts of recombinant proteins that would have been required. As well as inhibiting proliferation, hPCDH7 C7-Fc reduced the chemotactic transmigration of cells. Since this assay is too short to involve HUVEC proliferation, hPCDH7 C7-Fc may be functioning to affect HUVEC in a different way than it does for proliferation. It is not clear whether it does this via inhibition of the same or different ligands.

The soluble extracellular domain of PCDH7 inhibited endothelial network formation in both 2D and 3D tube formation assays. A slightly lower inhibitory effect was observed in the 3D HUVEC/HDF co-culture in fibrin matrix assay when compared to the 2D HUVEC/HDF co-culture assay. In the 2D assay, the endothelial cells adhere to the monolayer of fibroblasts and are directly exposed to the protein in the medium, while in the 3D assay the recombinant protein must penetrate the fibrin matrix to exert an effect. It could be simply that the increased accessibility of the hPCDH7 C7-Fc in the 2D assay to the cells resulted in more efficient inhibitory activity. Another possibility is that hPCDH7 C7-Fc ligand(s) required for its function are expressed at higher levels in the 2D assay compared with the 3D assay setting thus inducing stronger inhibitory effect.

The reduced network formation caused by the hPCDH7 C7-Fc might be partially explained by its ability to reduce cell proliferation and motility rather than the endothelial sprouting. This hypothesis could be tested by monitoring cell

proliferation during the assay by measuring, for example, endothelial cell nuclei. Transduction of HUVEC was attempted with lentivirus encoding both GFP to visualise endothelial cell cytoplasm and nuclear localized mCherry to visualise exclusively endothelial nuclei. Unfortunately, there were difficulties with an efficient transduction probably caused by problems with viral packaging due to the large size of the expression plasmid.

By expressing and testing the properties of PCDH7 extracellular domain truncation mutants, we have deduced that the entire PCDH7 extracellular domain is not necessary for its activity. The data generated in this chapter indicate that the inhibitory activity of the hPCDH7 ECD is located within the first five N-terminal cadherin repeats. Since activity is lost after deletion of domains 4 and 5, it would be useful to test the function of a fragment containing the first four cadherin repeats. Finer mapping could also be achieved by constructing and testing the inhibitory activity of a series of N-terminal truncations as well as the first five cadherin repeats individually. Another approach involves generating EC domain swapping chimeric constructs. This was successfully applied in functional mapping of ECD's EC repeats of clustered γ -PCDHs (Schreiner *et al.*, 2010). Once the region of activity is more finely mapped the importance of individual residues could be tested using site-directed mutagenesis.

The recombinant extracellular domain of PCDH7 exhibited a promising anti-angiogenic potential *in vitro*. If data are further confirmed in different models, it would be important to validate whether hPCDH7 ECD functions to modulate *in vivo*

angiogenesis. This could be tested using assays such as sponge assay or aortic ring assay in mice using a mouse version of PCDH7 ECD (mPCDH7 ECD). The Fc fused and His tagged constructs of mPCDH7 ECD were successfully expressed (Figure 3.19A and 3.19B); see Figure A.8 for the amino acid sequence. Unfortunately, the production yield for both proteins was extremely low (Figure 3.19C), making it difficult to produce sufficient amount of proteins for *in vivo* work.

As part of this project, we have also attempted to investigate the function of endogenous PCDH7 in endothelial cells. Initial studies considered its shRNA-mediated knockdown in HUVEC. However, due to its low expression and thus difficulties with validation of the knockdown this approach to determine PCDH7 function was not pursued.

Due to unknown binding partners for the extracellular domain of PCDH7 in HUVEC and the nature of its interactions, it is difficult to speculate on its exact function. However, given a low endogenous expression of PCDH7 in HUVEC, it is unlikely that it interacts with itself but rather exhibits heterophilic interactions with proteins involved in regulating cell proliferation. Therefore, identification of ligands was the next step towards revealing the function of the extracellular domain of PCDH7 which will be further explored in Chapter 4. Successful mapping the regions of PCDH7 ECD which mediate its anti-angiogenic activity and identification of its ligands creates an opportunity for generating vascular specific PCDH7 ECD-based small proteins or peptides able to modulate angiogenesis in a range of pathologies.

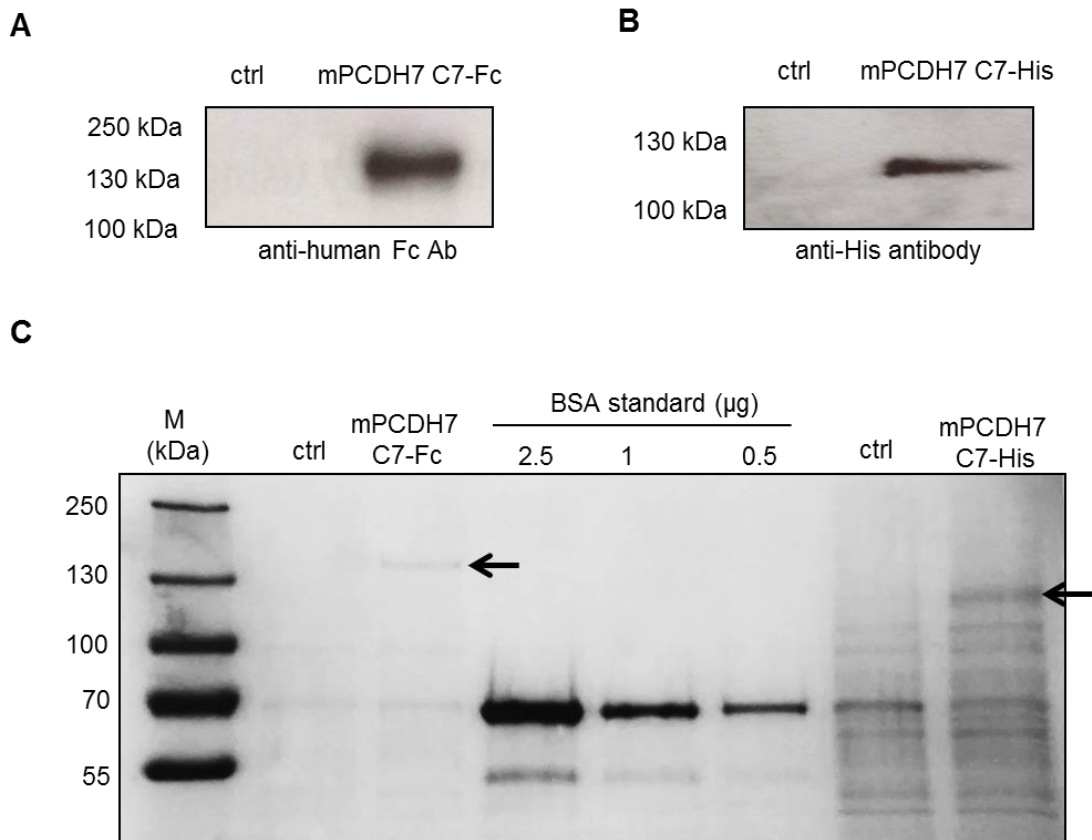


Figure 3.19 The mPCDH7 C7-Fc and mPCDH7 C7-His fusion proteins were successfully expressed but their small scale production yield was extremely low. HEK293T cells were seeded on 6-well plate and transiently transfected with pIG-mPCDH7 C7-Fc or pSec-mPCDH7 C7-His with untransfected cells as a control, followed by a change of the culture medium to OptiMem I. Culture media were harvested after 72 h. A) The expression of the mPCDH7 C7-Fc fusion protein was verified on Western blot using anti-human Fc antibody. B) The expression of the mPCDH7 C7-His fusion protein was verified on Western blot using anti-His antibody. The verification of the proteins was performed once. C) The proteins were purified from 1 ml of supernatant using Protein A Sepharose or Ni-NTA Agarose for the mPCDH7 C7-Fc and the mPCDH7 C7-His, respectively. The purified proteins were separated by SDS-PAGE and stained with a Coomassie blue. BSA standards of 0.5-2.5 μ g were used to estimate the proteins production yield. Both fusion proteins were indicated by black arrows. A small scale production was performed twice with a similar outcome.

**CHAPTER 4: FURTHER INVESTIGATIONS OF
INTERACTIONS OF HUMAN PCDH7
EXTRACELLULAR DOMAIN**

CHAPTER 4: FURTHER INVESTIGATIONS OF INTERACTIONS OF HUMAN PCDH7 EXTRACELLULAR DOMAIN

4.1 Introduction

Most research on PCDH7 has yielded information about its intracellular interactions while insight into the function of its extracellular domain is very limited. PCDH7 was shown to bind intracellularly with PP1 α (Yoshida *et al.*, 1999) and the PP2A inhibitor (Zhou *et al.*, 2017). Also, PCDH7 depletion downregulated E-cadherin expression in gastric cancer although the mechanism was not determined (Chen *et al.*, 2017). Özlü *et al.* (2015) demonstrated that PCDH7 is enriched on the plasma membrane of mitotic cancer cells. A complex of PCDH7 and Cx43 is proposed to form heterocellular gap junctions formation between brain metastatic cancer cells and astrocytes (Chen *et al.*, 2016). Adhesive properties of PCDH7 studied using cell aggregation assay have been reported (Yoshida, 2003), however another study showed that the extracellular domain of PCDH7 did not possess homophilic adhesion in a standard bead aggregation assay typically used to test cadherins (Blevins *et al.*, 2011).

Due to a promising inhibitory effect observed for the hPCDH7 C7-Fc on endothelial proliferation and network formation we aimed to determine the nature of the interactions between the hPCDH7 ECD and HUVEC surface proteins. We have sought to identify the binding partners for the hPCDH7 ECD. Due to the low

endogenous expression of PCDH7 in a cultured monolayer of HUVEC, we have also investigated whether PCDH7 can be detected in endothelial tubules *in vitro*.

4.2 Recombinant hPCDH7 C5-Fc and hPCDH7 C7-Fc fusion proteins do not bind to HUVEC as assessed by flow cytometry

First, flow cytometry was used to determine whether hPCDH7 extracellular domain binds to proteins on the cell surface of HUVEC. Endogenous expression of PCDH7 in HUVEC is low such that it was expected that this approach would likely reveal heterophilic, rather than homophilic interactions. To enhance the strength of potential homophilic interactions and increase the chance of their detection, HEK293T cells overexpressing a full length human PCDH7 isoform A (HEK293T-hPCDH7 FL) were also used in this experiment.

Flow cytometry binding experiments were performed as described in the Materials and Methods. Human Fc protein was used as a negative control in all experiments together with non-active hPCDH7 C1-Fc. Mouse CRT4 (anti-human CLEC14a) antibody was used as a positive control of binding to HUVEC (Noy *et al.*, 2015). In contrast, a positive control for a protein binding to HEK293T-hPCDH7 FL cells was the use of anti-human PCDH7 antibody. As expected, CRT4 antibody bound to HUVEC when compared to control (Figure 4.1A and 4.1E). In contrast, no binding was observed for hPCDH7 C1-Fc, hPCDH7 C5-Fc and hPCDH7 C7-Fc proteins when compared to hFc control (Figure 4.1B-E).

Next, binding experiments using HEK293T-hPCDH7 FL cells showed the expected binding of anti-human PCDH7 antibody (Figure 4.2A and 4.2E) thus confirming the presence of PCDH7 FL on the cell surface. Similarly to HUVEC, no binding was detected for hPCDH7 C1-Fc, hPCDH7 C5-Fc and hPCDH7 C7-Fc proteins (Figure 4.2B-E).

These data suggest that there are either no homophilic interactions between hPCDH7 ECD or any homophilic interactions are too weak to be observed by this methodology. Similarly, heterophilic interactions between the hPCDH7 ECD-Fc and the HUVEC surface proteins, if they occurred, were too weak to be detected by flow cytometry analysis.

4.3 Recombinant hPCDH7 C5-Fc and hPCDH7 C7-Fc fusion proteins do not increase adherence of HUVEC

Next, the adhesive properties of the hPCDH7 ECD-Fc fusion proteins were investigated. A 96-well nunc multi sorb plate was coated overnight with active hPCDH7 C5-Fc, hPCDH7 C7-Fc and negative controls hFc and non-active hPCDH7 C1-Fc. Fc tagged recombinant mouse multimerin-2 (mMMRN2-Fc) protein was used as a positive control for a protein which adheres to HUVEC (Khan *et al.*, 2017). It was kindly produced and provided by Marco Mambretti. Wells coated with either BSA or PBS were used as mock controls. After coating, plate was blocked with BSA. To ensure intact cell surface proteins, HUVEC were disassociated from the culture plate with a non-enzymatic solution. Cells were resuspended in PBS and seeded onto

the protein coated plate and allowed to attach for four hours. Unattached cells were extensively washed away with PBS and any remaining adhered cells were fixed and stained with a crystal violet. The absorbance was measured at 590 nm and microscope images were additionally taken using a phase contrast microscope.

As expected, mMMRN2-Fc coating significantly increased HUVEC adherence (Figure 4.3). The two controls hFc and hPCDH7 C1-Fc did not enhance cell adhesion when compared to both PBS and BSA mock controls. Moreover, no adhesion was observed and measured for hPCDH7 C5-Fc and hPCDH7 C7-Fc when compared to control samples suggesting they do not have adhesive properties in this assay.

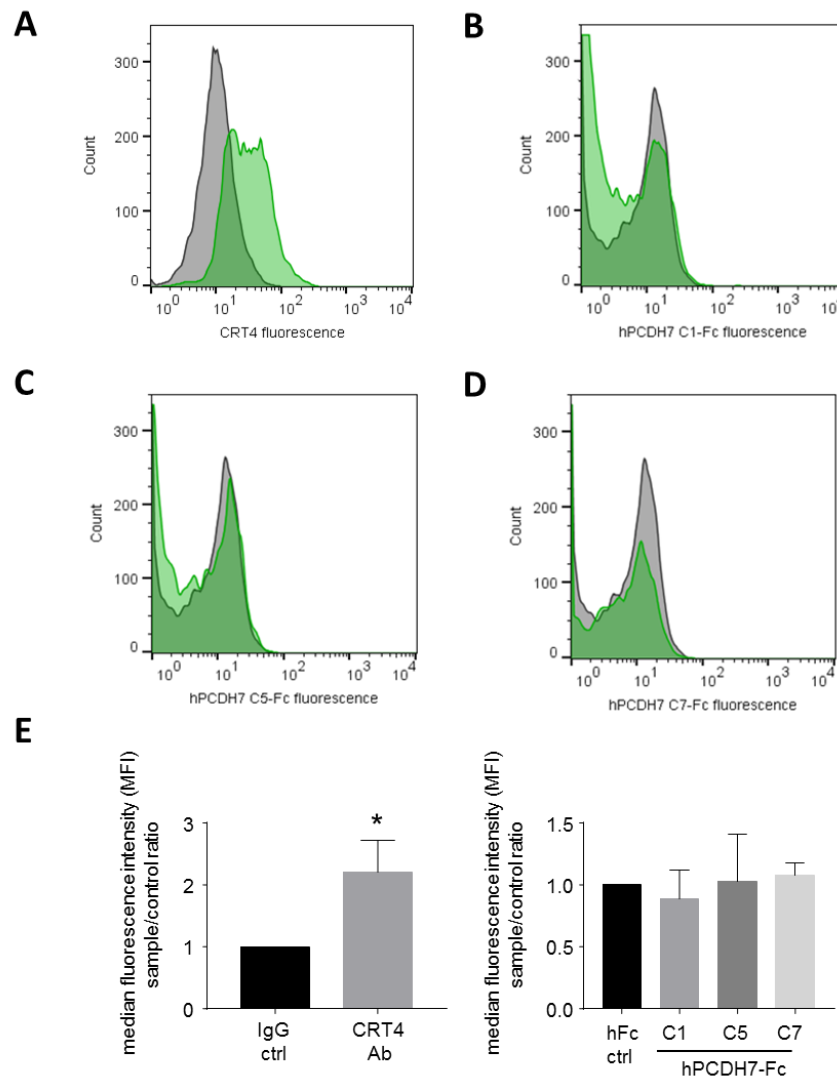


Figure 4.1 No binding of hPCDH7 C5-Fc and hPCDH7 C7-Fc to HUVEC is detected using a flow cytometry. Flow cytometry of HUVEC stained with A) mouse CRT4 antibody (green) compared to mouse IgG control (grey), B) hPCDH7 C1-Fc (green) C) hPCDH7 C5-Fc (green) and D) hPCDH7 C7-Fc (green), all compared to hFc control staining (grey). Anti-human IgG AlexaFluor 633 secondary antibody was used to detect hFc fragments of antibodies and recombinant proteins. The plot was gated on live cells by forward (FCS) and side (SCC) scatter. Representative figures from one of three experiments. E) The statistical analysis of median fluorescence intensity (MFI) calculated as a ratio sample/control. T-test was used to compare anti-human CLEC14A (CRT4) Ab with IgG control. One-way ANOVA was used to compare recombinant proteins with hFc control. Experiment was repeated three times (N=3; n=1). Error bars represent SD.

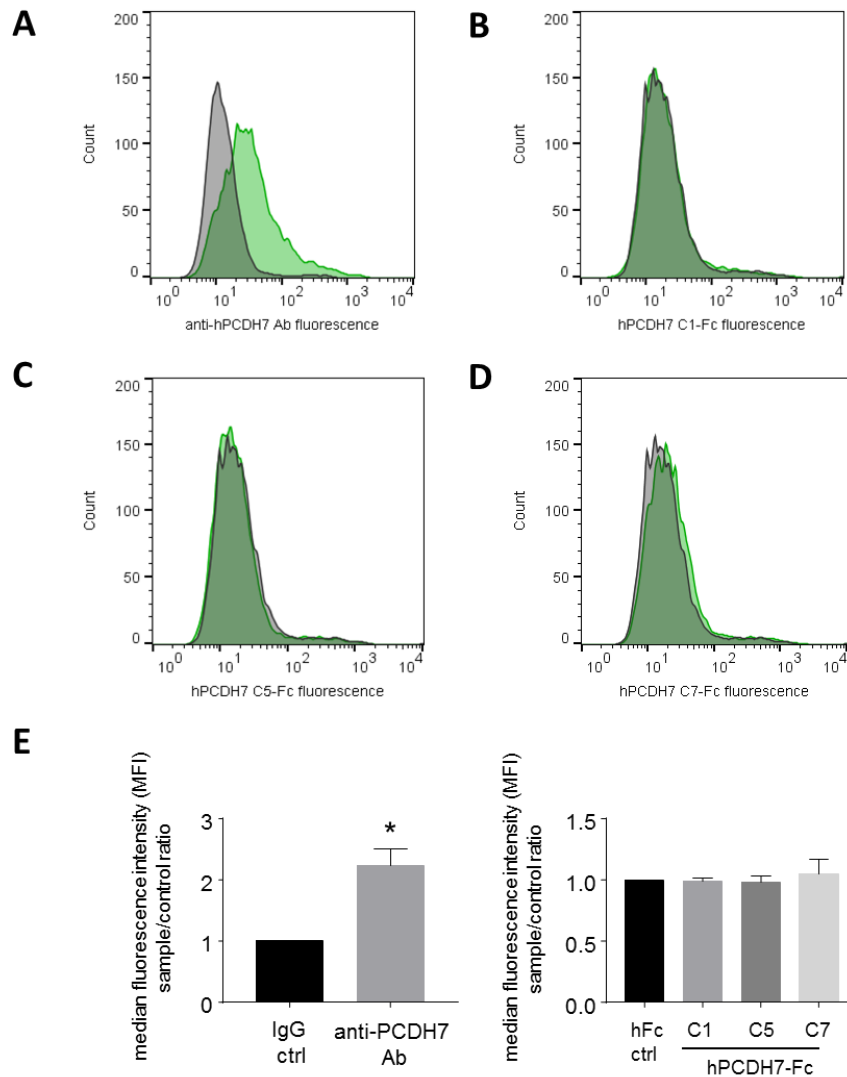


Figure 4.2 No binding of hPCDH7 C5-Fc and hPCDH7 C7-Fc to HEK293-hPCDH7 FL cells is detected using the flow cytometry. Flow cytometry of HEK293-hPCDH7 FL cells stained with A) rabbit anti-PCDH7 antibody (green) compared to rabbit IgG control (grey), B) hPCDH7 C1-Fc (green), C) hPCDH7 C5-Fc (green), D) hPCDH7 C7-Fc (green), all compared to hFc control staining (grey). Anti-rabbit and anti-human IgG AlexaFluor 633 secondary antibodies were used to detect hFc fragments of antibodies and recombinant proteins. The plot was gated on live cells by forward (FCS) and side (SCC) scatter. Representative figures from one of three experiments. E) The statistical analysis of median fluorescence intensity (MFI) calculated as a ratio sample/control. T-test was used to compare anti-human PCDH7 Ab with IgG control while 1-way ANOVA was used to compare recombinant proteins with hFc control. Experiment was repeated three times (N=3; n=1). Error bars represent SD.

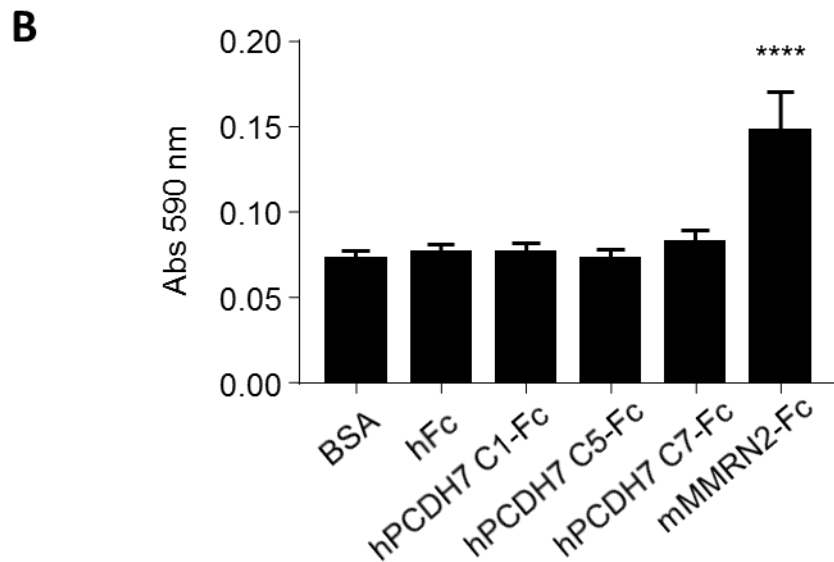
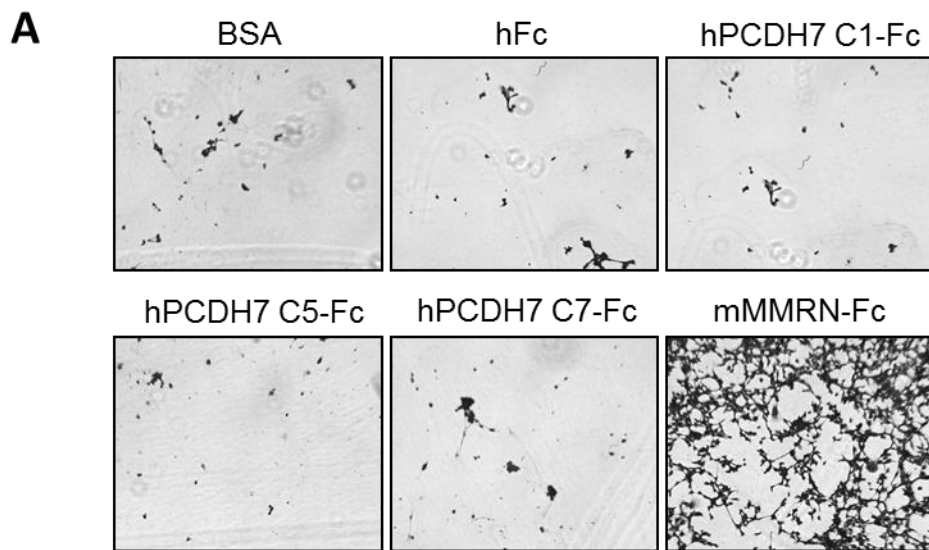


Figure 4.3 The hPCDH7 C5-Fc and hPCDH7 C7-Fc do not enhance the adherence of HUVEC in an adhesion assay. HUVEC resuspended in PBS were seeded onto 96-well nunc multi sorb plate coated with the hPCDH7 ECD-Fc fusion proteins and blocked with BSA. BSA or only PBS coated wells were used as negative control and the mMMRN2-Fc was used as a positive control. Cells were incubated for 4 h and non-adhered cells were washed away with PBS. The remaining cells were fixed and stained with a crystal violet. After extensive washing with PBS and miliQ water, the absorbance was measured at 590 nm. A) Representative images of adhered cells stained with a crystal violet from one of three experiments. B) The statistical analysis of the absorbance at 590 nm measured for adhered cells; 1-way ANOVA Tukey test; **** $p < 0.0001$. Experiment was repeated three times (N=3) in triplicates (n=3). Error bars represent SD.

4.4 Homophilic interactions of hPCDH7 extracellular domain could not be detected by immunoprecipitation of hPCDH7 FL from HEK293T-hPCDH7 FL-FLAG cells

The potential homophilic interactions between PCDH7 extracellular domains were also investigated using immunoprecipitation (IP). The hPCDH7 C7-Fc was used to attempt to pull down hPCDH7 FL-FLAG from HEK293T cells stably expressing FLAG tagged full length human PCDH7 isoform A. These samples were further analysed using mass spectrometry (MS) and Western blotting. The FLAG sequence was introduced to distinguish between hPCDH7 FL and hPCDH7 C7-Fc that are of a similar size.

First, HEK293T-hPCDH7 FL-FLAG cells were generated. A full length PCDH7 isoform A tagged with FLAG sequence was cloned into pWPI lentiviral vector as described in the Materials and Methods, the sequence of the insert was verified and hPCDH7 FL-FLAG lentivirus was produced. Next, HEK293T cells were transduced with lentivirus with untransduced cells used as a control. Cell lysates were collected 48 h post transduction. Equal amounts of protein were separated by SDS-PAGE, transferred to PDVF membrane and blotted with both anti-human PCDH7 and anti-FLAG antibodies. The staining with both antibodies revealed the band of around 130 kDa corresponding to the hPCDH7 FL-FLAG protein (see Figure A.7 for the amino acid sequence) and this band was observed only in hPCDH7 FL-FLAG transduced cells while being absent in the control cells (Figure 4.4). These data confirm that hPCDH7 FL was successfully tagged with the FLAG sequence,

the protein was expressed in HEK293T cells and that these cells could be used in IP experiments.

The immunoprecipitation was performed as described in the Materials and Methods. Initially, HEK293T-hPCDH7 FL-FLAG cells were harvested and lysed with IP lysis buffer. The cell lysate was pre-cleared with protein A beads in order to reduce nonspecific binding of the lysate to protein A. This was then loaded on hFc and hPCDH7 C7-Fc protein coated protein A beads. Since homophilic interactions between protocadherins are weaker than those of classical cadherins, a DTSSP reagent was added to capture potentially transient interactions. DTSSP chemically crosslinks proteins via its reactive sulfo-NHS ester groups. They interact with primary amines of proteins to generate stable but reversible disulphide bonds. Finally, the hFc and hPCDH7 C7-Fc beads after IP were resuspended in SDS-PAGE sample buffer. The β -mercaptoethanol present in sample buffer cleaved disulphide bonds generated by the DTSSP crosslinker thus allowing separation of crosslinked products on a SDS-PAGE gel (Figure 4.5). Since this experiment was focused on potential homophilic interactions between 130 kDa-sized proteins, only parts of gels above 100 kDa were analysed using a mass spectrometry at the genomic facility at the University of Birmingham.

The transmembrane (TM) and intracellular (ICD) domain sequences of PCDH7 as well as FLAG sequence were added to the pool of peptide probes thus allowing detection of PCDH7 FL. The MS analysis resulted in the list of around 800 peptides for both samples. The peptide hits corresponding to TM, ICD and FLAG sequences

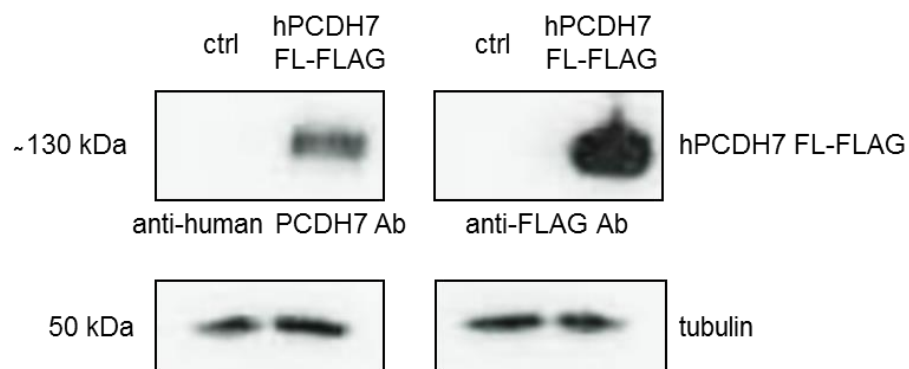


Figure 4.4 The hPCDH7 FL-FLAG is expressed in HEK293T cells. HEK293T cells were transduced with lentivirus expressing the hPCDH7 FL-FLAG. Untransduced cells were used as a control. Protein lysates were collected 48 h post transduction. Western blot analysis of cell lysates with both anti-human PCDH7 and anti-FLAG antibodies with tubulin as a loading control.

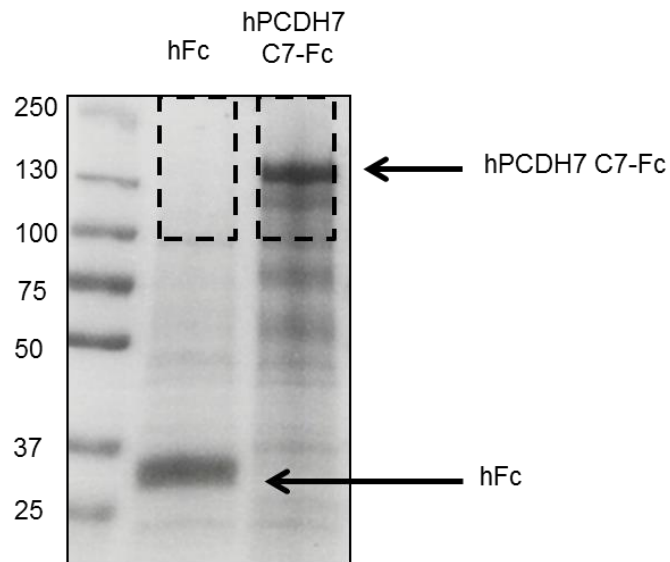


Figure 4.5 The hPCDH7 C7-Fc immunoprecipitation on HEK293T-hPCDH7 FL-FLAG cells for mass spectrometry analysis. The hPCDH7 C7-Fc fusion protein was used to test if the hPCDH7 FL-FLAG could be immunoprecipitated from HEK293T-hPCDH7 FL-FLAG cells. Multiple dishes of freshly cultured HEK293T-hPCDH7 FL-FLAG cells were lysed in IP lysis buffer. The cell lysate was incubated with Protein A beads coated with hFc control or hPCDH7 C7-Fc protein, with the DTSSP crosslinker. Proteins bound on beads were further separated by SDS-PAGE. Black dashed boxes indicate the gel fragments of hFc and hPCFH7 C7-Fc samples that were sent for MS analysis. Block arrows indicate bands of hFc and the hPCDH7 C7-Fc proteins used for IP. MS analysis was performed once from a single immunoprecipitation experiment using pooled cells from ten 15 cm dishes per sample.

were not found in hPCDH7 C7-Fc sample. Due to the high cost of MS analysis, the experiment was not repeated.

Together with MS analysis, the pulldown samples were investigated by Western blotting for the presence of hPCDH7 FL-FLAG using anti-FLAG antibody. Coating of beads with Fc tagged fusion proteins was confirmed using anti-human Fc antibody. The IP experiment was performed as described above and repeated several times with similar results. The IP was performed for both functional hPCDH7 C5-Fc and hPCDH7 C7-Fc fusion proteins with the DTSSP crosslinker. Moreover, non-functional hPCDH7 C1-Fc was used as an additional control. Representative data are presented in Figure 4.6. Staining with anti-human Fc antibody confirmed a strong signal of all Fc fused recombinant proteins bound to protein A beads (Figure 4.6A). Next, membrane was incubated with anti-FLAG antibody. The staining resulted in a blank blot even after a long exposure (Figure 4.6B). The presence of hPCDH7 FL-FLAG protein in the cell lysate used for the IP was confirmed (Figure 4.6C).

Overall, no homophilic interactions between the extracellular domains of hPCDH7 could be detected using this methodology. It was hypothesized that the hPCDH7 ECD interacts with other ligands on HUVEC surface and this idea was further examined.

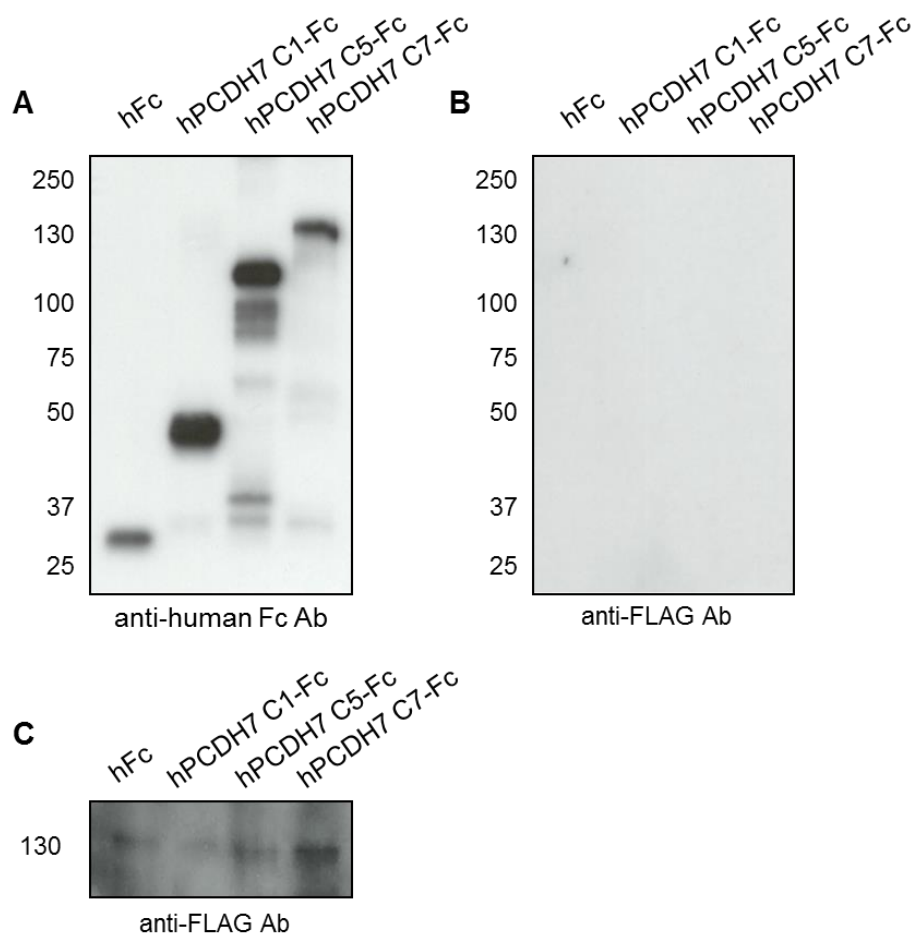


Figure 4.6 The hPCDH7 C5-Fc and hPCDH7 C7-Fc fusion proteins do not immunoprecipitate hPCDH7 FL-FLAG from HEK293T-hPCDH7 FL-FLAG cells. Multiple dishes of freshly cultured HEK293T-hPCDH7 FL-FLAG cells were lysed in IP lysis buffer. The cell lysate was incubated with Protein A beads coated with the hPCDH7 C5-Fc, hPCDH7 C7-Fc protein and control hFc or non-functional hPCDH7 C1-Fc, with the DTSSP crosslinker. Western blot analysis of beads post IP with A) anti-human Fc and B) anti-FLAG antibodies. C) Western blot analysis of HEK293T-hPCDH7 FL-FLAG lysates used for IP with anti-FLAG antibody. The experiment was performed three times with similar results.

4.5 Mass spectrometry analysis of hPCDH7 C7-Fc pull down from HUVEC lysate revealed two potential binding partners

To identify potential binding partners of the extracellular domain of PCDH7, the hPCDH7 C7-Fc fusion protein and hFc control were used to pull down candidate proteins from HUVEC lysate in the presence of the DTSSP crosslinker. The immunoprecipitation was performed similarly to that described earlier with HEK293T-hPCDH7 FL-FLAG cells. HUVEC lysate was pre-cleared with protein A beads and then added to hFc and hPCDH7 C7-Fc coated protein A beads. Finally, the IP samples were boiled in SDS-PAGE reducing buffer and separated by SDS-PAGE (Figure 4.7). Entire gel lanes for both samples were sent for a mass spectrometry analysis at the genomic facility.

The MS analysis of both control hFc and hPCDH7 C7-Fc samples resulted in the list of around 900 detected peptide hits. First, hits with at least three unique peptides were compared. Peptides present exclusively in hPCDH7 C7-Fc sample were further examined. From this pool, all intracellular proteins were excluded leaving only membrane or extracellular protein candidates. The selection resulted in two potential ligands presented in Table 4.1.

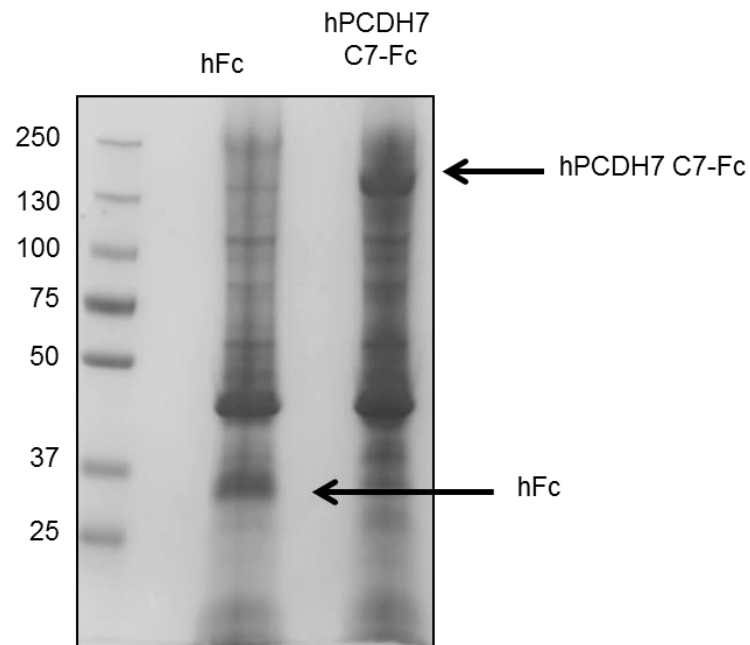


Figure 4.7 The hPCDH7 C7-Fc immunoprecipitation on HUVEC for mass spectrometry analysis. The hPCDH7 C7-Fc fusion protein was used to immunoprecipitate potential ligands from HUVEC lysate. Multiple dishes of freshly cultured HUVEC were lysed in IP lysis buffer. The cell lysate was incubated with Protein A beads coated with hFc ctrl or the hPCDH7 C7-Fc protein, with the DTSSP crosslinker. Proteins bound on beads were further separated by SDS-PAGE. Whole gel fragments were sent for the MS analysis. Black arrows indicate bands of hFc and hPCDH7 C7-Fc proteins used for IP. MS analysis was performed once from a single immunoprecipitation experiment using pooled cells from thirty 15 cm dishes per sample.

Table 4.1 Potential extracellular ligands of the hPCDH7 ECD identified by mass spectrometry.

Protein ID	Protein	MW (kDa)	Peptide	Unique peptide	Location
PDIA1 (P4HB)	Protein disulfide-isomerase	57.1	9	9	Membrane Intracellular
EFEMP1 (FBLN3)	EGF-containing fibulin-like extracellular matrix protein	54.6	3	3	Extracellular

Protein disulphide-isomerase (PDIA1) is an intracellular protein that is externalized by several cell types, including endothelial cells (Araujo *et al.*, 2017). It regulates redox of cell-surface and extracellular proteins (Flaumenhaft *et al.*, 2016). PDIA1 is implicated in vascular remodelling (Tanaka *et al.*, 2016) and integrin-dependent cell adhesion (Lahav *et al.*, 2000).

In contrast, EGF-containing fibulin-like extracellular matrix protein (EFEMP1) is an extracellular glycoprotein. EFEMP1 induces EGFR autophosphorylation thus activating downstream MAPK and Akt pathways (Camaj *et al.*, 2009). It plays a role in chondrocyte and glial cell differentiation (Wakabayashi *et al.*, 2010). It is also involved in the tumour angiogenesis (Seeliger *et al.*, 2009; Song *et al.*, 2011; Chen *et al.*, 2013) and growth, migration and invasion of tumour cells in several types of cancer (Dou *et al.* 2016; Han *et al.* 2017; Hu *et al.* 2009; Zhuo Wang *et al.* 2015; Yin *et al.* 2016).

Due to time and resource limitations, only EFEMP1 was further examined. Although with less peptide hits, EFEMP1 was chosen due to its association with tumour angiogenesis and its clear extracellular location.

4.6 EFEMP1 is expressed in HUVEC and its expression level is not affected upon treatment with the hPCDH7 C5-Fc and hPCDH7 C7-Fc fusion proteins

To study the potential interaction between EFEMP1 and hPCDH7 ECD, anti-human EFEMP1 antibody was first validated. Western blotting was performed using commercially produced HA tagged EFEMP1 recombinant protein dissolved in PBS. As expected, blotting with anti-human EFEMP1 antibody yielded band of around 60 kDa corresponding to the size of EFEMP1 recombinant protein (Figure 4.8). A band of similar size was observed for the staining with anti-HA antibody, thus confirming anti-human EFEMP1 antibody recognizes its purified target.

Next, the expression of EFEMP1 in HUVEC was investigated. An experiment was performed to determine if EFEMP1 expression levels changed upon the treatment of HUVEC with the hPCDH7 C5-Fc and hPCDH7 C7-Fc. As controls, hFc and hPCDH7 C1-Fc were used. HUVEC were cultured for two days in a complete EBM-2 medium containing 1.54 μ M hFc, hPCDH7 C1-Fc, hPCDH7 C5-Fc or hPCDH7 C7-Fc recombinant proteins. Protein lysates were prepared and equal amounts of protein were separated by SDS-PAGE and blotted for EFEMP1 using validated anti-human EFEMP1 primary antibody. This experiment showed that EFEMP1 is expressed in

HUVEC (Figure 4.9) but its expression did not change upon the treatment with the hPCDH7 ECD-Fc fusion proteins when compared to hFc treated cells.

4.7 Human PCDH7 C7-Fc pull down from HUVEC lysate resulted in nonspecific interactions of EFEMP1 and hPCDH7 ECD

The next step was to validate the potential interaction between the hPCDH7 ECD and EFEMP1 identified by mass spectrometry. The pulldown on HUVEC lysate was performed according to the protocol described earlier in this chapter, using hPCDH7 C5-Fc and hPCDH7 C7-Fc coated protein A beads. As a control, hFc and non-functional hPCDH7 C1-Fc coated beads were used. The experiment was repeated several times. Representative data are shown in Figure 4.10. Staining with anti-human Fc antibody confirmed a signal of all Fc fusion proteins eluted from the samples however hPCDH7 C7-Fc was partially degraded (Figure 4.10A). After a mild stripping of the membrane, the blots were incubated with anti-human EFEMP1 antibody (Figure 4.10B). Although the staining revealed the presence of the band corresponding to EFEMP1 protein, this band was observed also for the control hFc sample suggesting nonspecific interactions with hFc fragment of the proteins. Therefore, the potential interaction between the hPCDH7 ECD and EFEMP1 could not be validated.

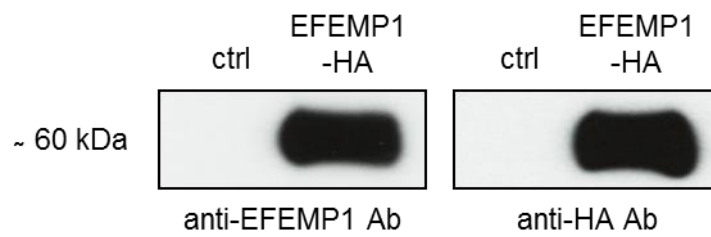


Figure 4.8 Anti-human EFEMP1 antibody recognizes a recombinant EFEMP1-HA protein. Western blot analysis of a purified EFEMP1-HA protein with anti-human EFEMP1 and anti-HA tag antibodies. The experiment was performed once.

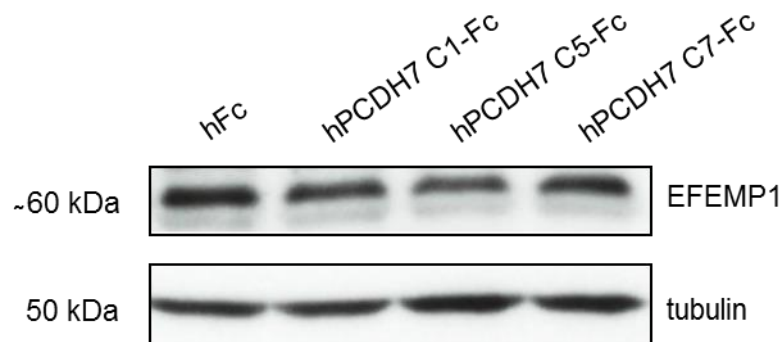


Figure 4.9 EFEMP1 is expressed in HUVEC and its expression does not change upon treatment with hPCDH7 ECD-Fc fusion proteins. HUVEC were cultured with the addition of inhibitory active hPCDH7 C5-Fc and hPCDH7 C7-Fc proteins. As controls, hFc and non-functional hPCDH7 C1-Fc were used. All proteins were added to the culture medium to a final concentration of 1.54 μ M. Protein cell lysates were collected after two days of culture. Western blot analysis of the cell lysates with anti-human EFEMP1 and anti-human tubulin antibodies. The experiment was performed once.

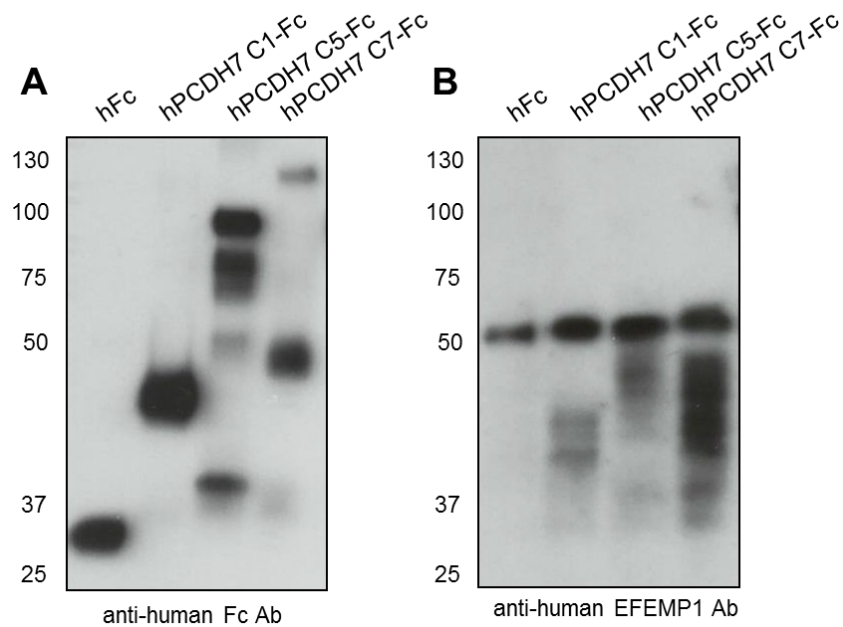


Figure 4.10 Pulldown of EFEMP1 from HUVEC lysate is nonspecific. Multiple dishes of freshly cultured HUVEC were lysed in IP lysis buffer. The cell lysate was incubated with Protein A beads coated with hPCDH7 C5-Fc, hPCDH7 C7-Fc protein and control hFc or non-functional hPCDH7 C1-Fc, with the DTSSP crosslinker. A representative Western blot analysis of beads post IP with A) anti-human Fc and B) anti-human EFEMP1 antibodies. The experiment was performed four times with similar results.

4.8 The interaction between hPCDH7 ECD-Fc fusion proteins and EFEMP1-HA recombinant protein was nonspecific

A potential interaction between the hPCDH7 ECD-Fc and EFEMP1 was also investigated using purified proteins. It was anticipated that this would yield a definitive result without interference from other proteins found in whole HUVEC lysate.

Protein A beads were coated with hFc control, hPCDH7 C1-Fc, hPCDH7 C5-Fc or hPCDH7 C7-Fc proteins. Next, beads were incubated with purified EFEMP1-HA recombinant protein diluted in the IP binding buffer with or without the addition of DTSSP crosslinker according to the same protocol as all previous IP experiments performed on cells. The experiment was performed several times in various conditions. Representative results are shown in Figure 4.11. The control anti-human Fc staining confirmed a successful coating of beads with appropriate Fc-tagged recombinant proteins for all samples (Figure 4.11). Moreover, staining with anti-HA antibody revealed the band corresponding to EFEMP1-HA protein in all samples. Similarly to the pulldown on HUVEC, the EFEMP1 band was observed for the control hFc and it was independent of the presence of the DTSSP crosslinker. The lack of a clear EFEMP1 band for one of hFc controls (Figure 4.11A) was caused by an air bubble during the transfer (visible white spot on the membrane) although a small portion of the band could be still observed. Nevertheless, this blot was presented since the experiment could not be further repeated due to the low availability of the proteins.

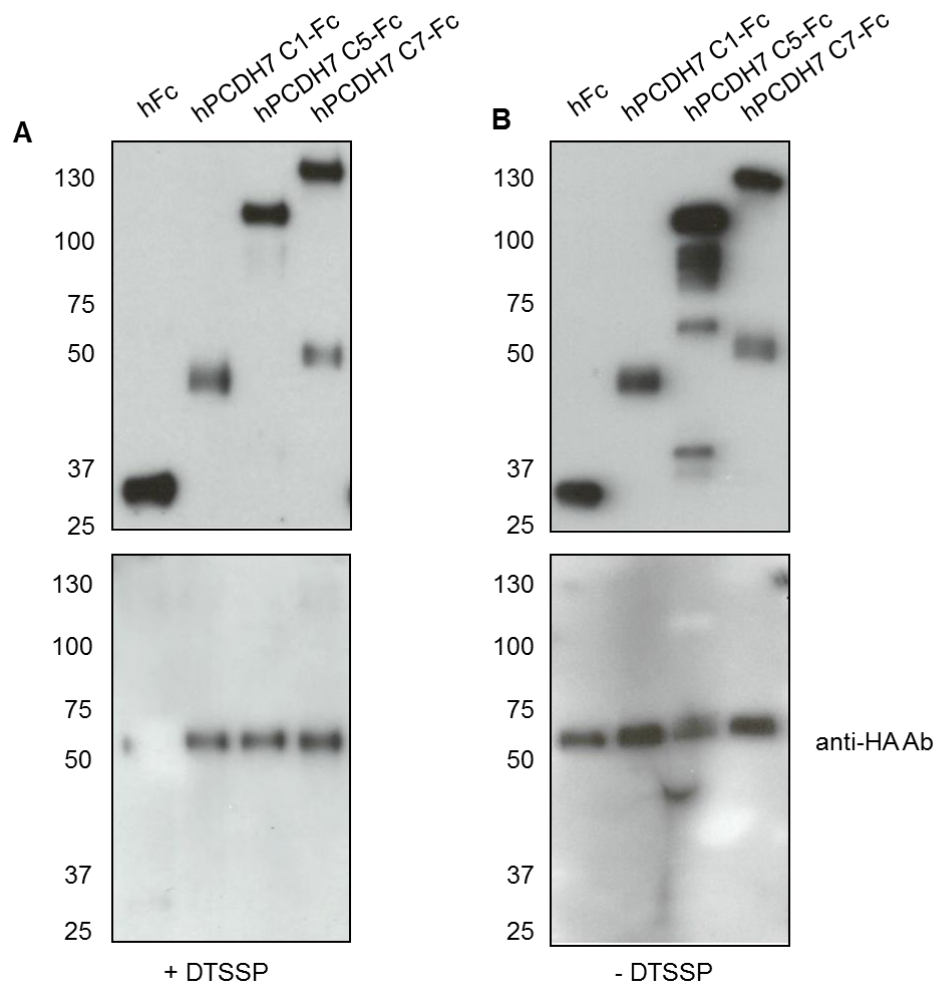


Figure 4.11 The interaction between hPCDH7 ECD-Fc fusion proteins and EFEMP1 is nonspecific. EFEMP1 recombinant protein was incubated with Protein A beads coated with hPCDH7 C5-Fc, hPCDH7 C7-Fc protein and control hFc or non-functional hPCDH7 C1-Fc, with or without the DTSSP crosslinker. The Western blot analysis of post IP beads blotted with anti-human Fc and anti-human EFEMP1 antibodies for samples A) with and B) without the DTSSP crosslinker. The experiment was performed several times in various conditions. The experiment performed under optimized conditions was performed once.

Overall, these data suggest that EFEMP1 interacts with the hFc rather than the hPCDH7 ECD. This corresponds to results obtained for the pulldown on HUVEC.

4.9 PCDH7 is expressed in the 2D HUVEC/PC but not in the 2D HUVEC/HDF *in vitro* endothelial network

As well as investigating extracellular interaction of the hPCDH7 ECD, experiments were performed to determine whether PCDH7 can be detected in formed network in 2D *in vitro* co-culture using immunofluorescent staining. The 2D co-culture assay was chosen because of the simplicity of cell staining. The experiment was also attempted in the 3D co-culture assay but with poor results due to the high background staining of the fibrin matrix.

First, the suitability of anti-human PCDH7 antibody for staining fixed cells was determined. Thus, HEK293T cells were seeded on cover slips and transiently transfected with pWPI-hPCDH7a FL co-expressing GFP. As a control, HEK293T transfected with only GFP were used. Cells were fixed after 48 h and stained with anti-human PCDH7 antibody, followed by a fluorescently labelled secondary antibody. As shown in Figure 4.12, positive PCDH7 staining was observed only in hPCDH7 FL transfected cells but not in the control cells. A strong membrane and partially cytoplasmic PCDH7 expression was present at cell-cell contacts of only PCDH7 positive, neighbouring cells. Exclusively cytoplasmic PCDH7 staining was observed for isolated PCDH7 positive cells or for positive cells that were in contact

with untransfected cells. These data confirm that anti-human PCDH7 antibody can be successfully used for an immunofluorescence staining of fixed cells.

In order to examine PCDH7 expression in endothelial tubules, staining of endothelial specific adhesion protein CD31 was tested. GFP transduced HUVEC were used in the 2D HUVEC/HDF co-culture assay where HDF were cultured on glass cover slips as described in the Materials and Methods. After 6 days cells were fixed and stained with anti-human CD31 antibody with fluorescently labelled secondary antibody and mounted in a DAPI containing solution onto the microscope slides. Images of the network were taken using a fluorescence microscope. As shown in Figure 4.13, anti-human CD31 antibody specifically stained endothelial cell plasma membrane within the network clearly showing that such network is generated by multiple connected cells. DAPI staining distinguished between more flattened elongated nuclei of endothelial cells forming the network and oval nuclei of fibroblasts.

Next, 2D co-culture assay was performed with untransduced HUVEC seeded on top of a monolayer of HDF cultured on cover slips. Fixed cells were stained with anti-human CD31 or anti-human PCDH7 antibodies and mounted in DAPI onto the microscope slides. The staining was repeated several times on samples from three different co-culture experiments with the same results. Representative images are presented in Figure 4.14. Staining with anti-human CD31 revealed a nicely formed endothelial network. In contrast, PCDH7 staining could not be observed in any samples.

Since we have shown that HUVEC form a network also on pericyte monolayer (Figure A.6), the experiment was repeated several times on samples from three different 2D HUVEC/PC co-culture. Representative images are presented in Figure 4.15. The experiment was technically difficult due to the fragility of pericytes resulting in the presence of many dead cells after 6 days of co-culture. This could be observed by DAPI staining (small irregular blue dots). As expected, CD31 staining was successful. Moreover, a weak but visible PCDH7 staining was observed on both endothelial network and pericytes however it was more evident within the cells rather than on the plasma membrane. The PCDH7 signal was generally weak in all the experiments.

Since a signal for PCDH7 was present in pericytes, its expression in this cell type was tested. Thus, equal amounts of HUVEC, HDF and PC protein lysate were separated by SDS-PAGE and blotted with anti-human PCDH7 antibody, using tubulin as a loading control. As shown in Figure 4.16 PCDH7 expression was detected in HUVEC and PC but not HDF. These results support the immunofluorescence staining of PCDH7 in PC and suggest it is expressed in this cell type.

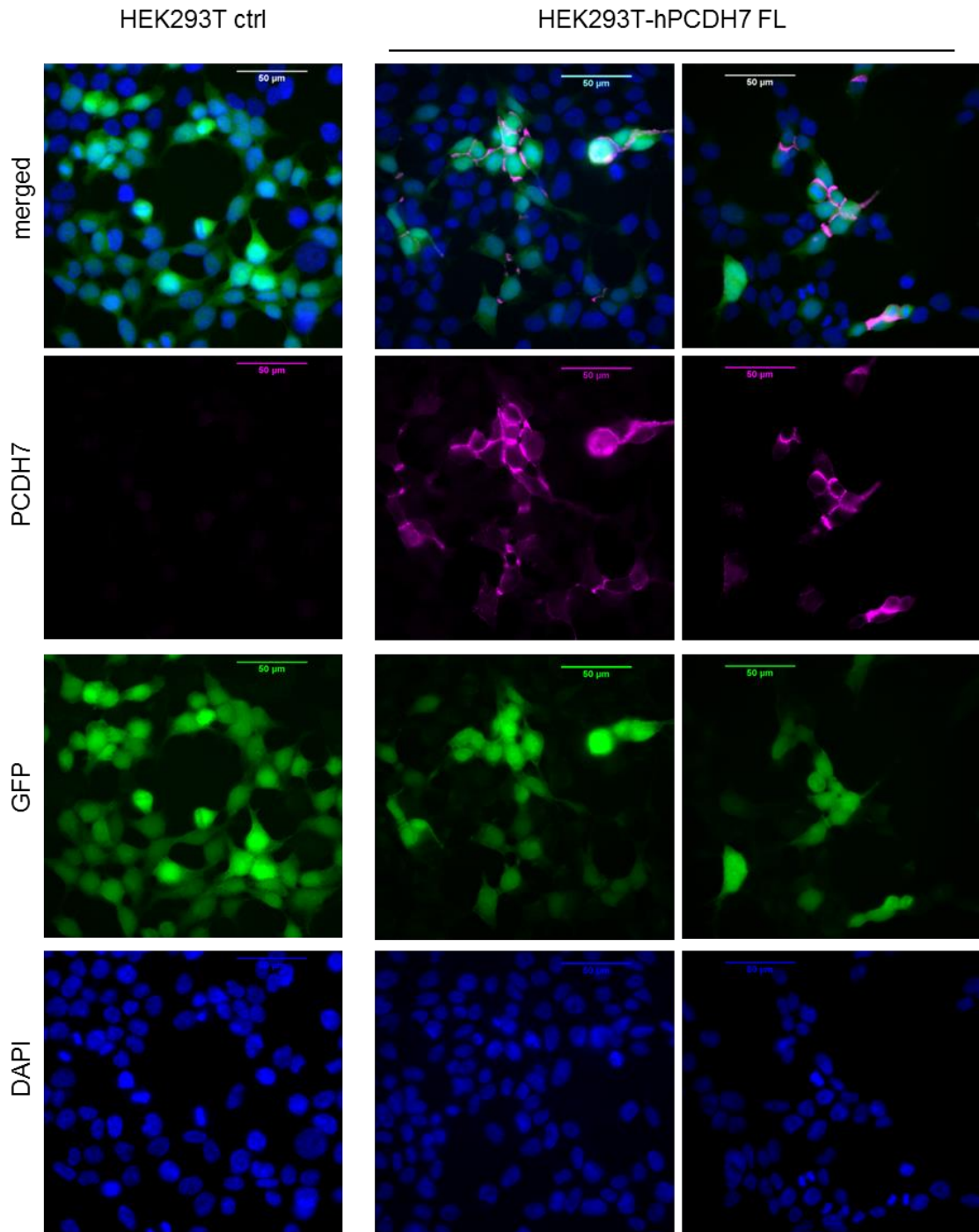


Figure 4.12 Anti-human PCDH7 antibody recognizes hPCDH7 FL localised at cell-cell contacts of PCDH7 positive cells. HEK293T cells were seeded on glass cover slips and transiently transfected with pWPI-hPCDH7 FL plasmid which also encodes GFP. Cells transfected with pWPI encoding GFP were used as a control. After 48 h, the cells were fixed with 4% PFA, stained with anti-human PCDH7 and mounted in DAPI onto the microscope slides. Images were taken using a fluorescence microscope. This antibody validation was performed once.

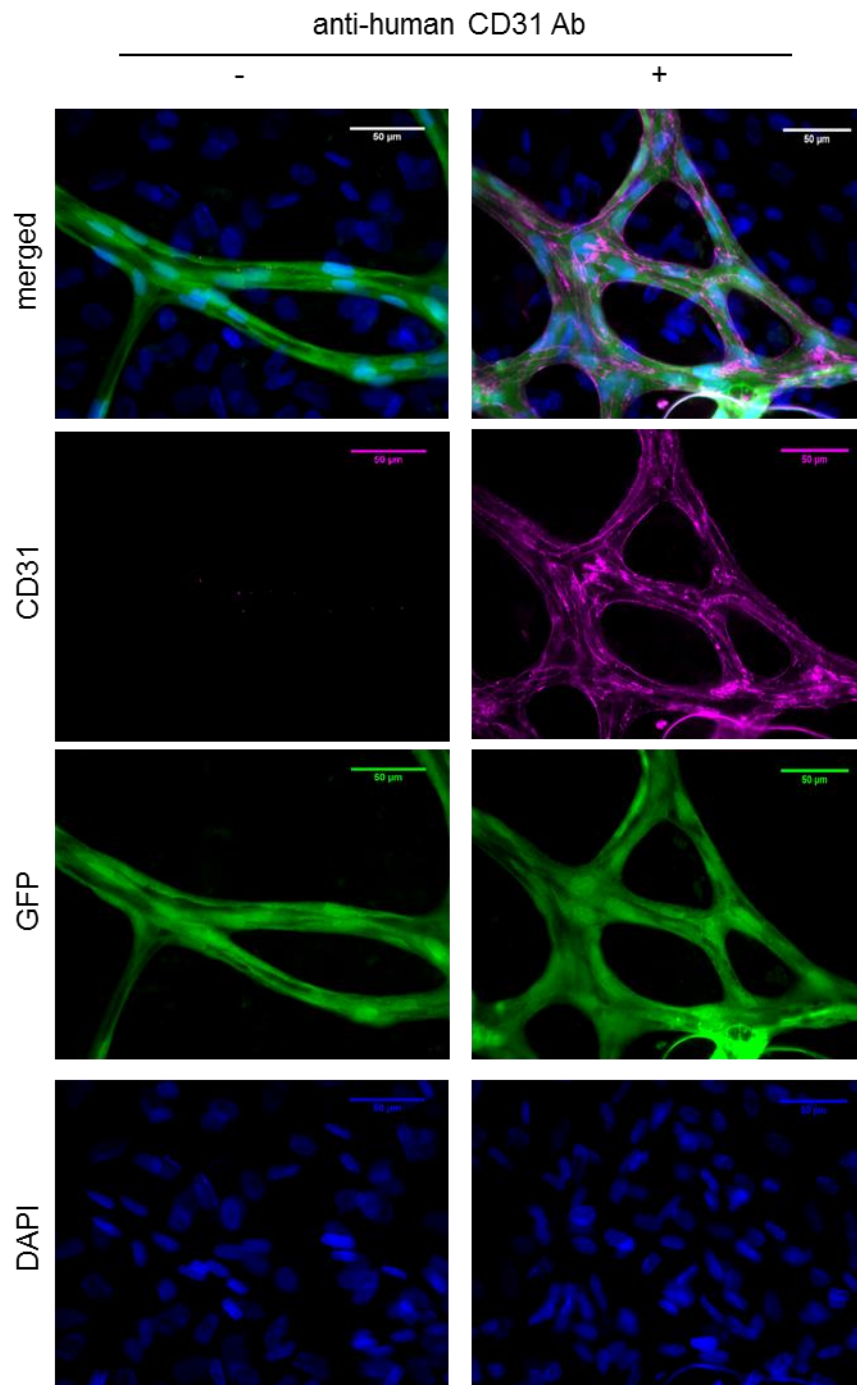


Figure 4.13 Staining with anti-human CD31 antibody enables visualisation of endothelial cell membranes within the network. GFP transduced HUVEC were seeded on top of a monolayer of HDF cultured on glass cover slips and 2D HUVEC/HDF co-culture assay was performed according to a standard protocol. The cells were fixed with 4% PFA at day 6, stained with anti-human CD31 antibody and mounted in DAPI onto the microscope slides. Images were taken using a fluorescence microscope. The experiment was performed once.

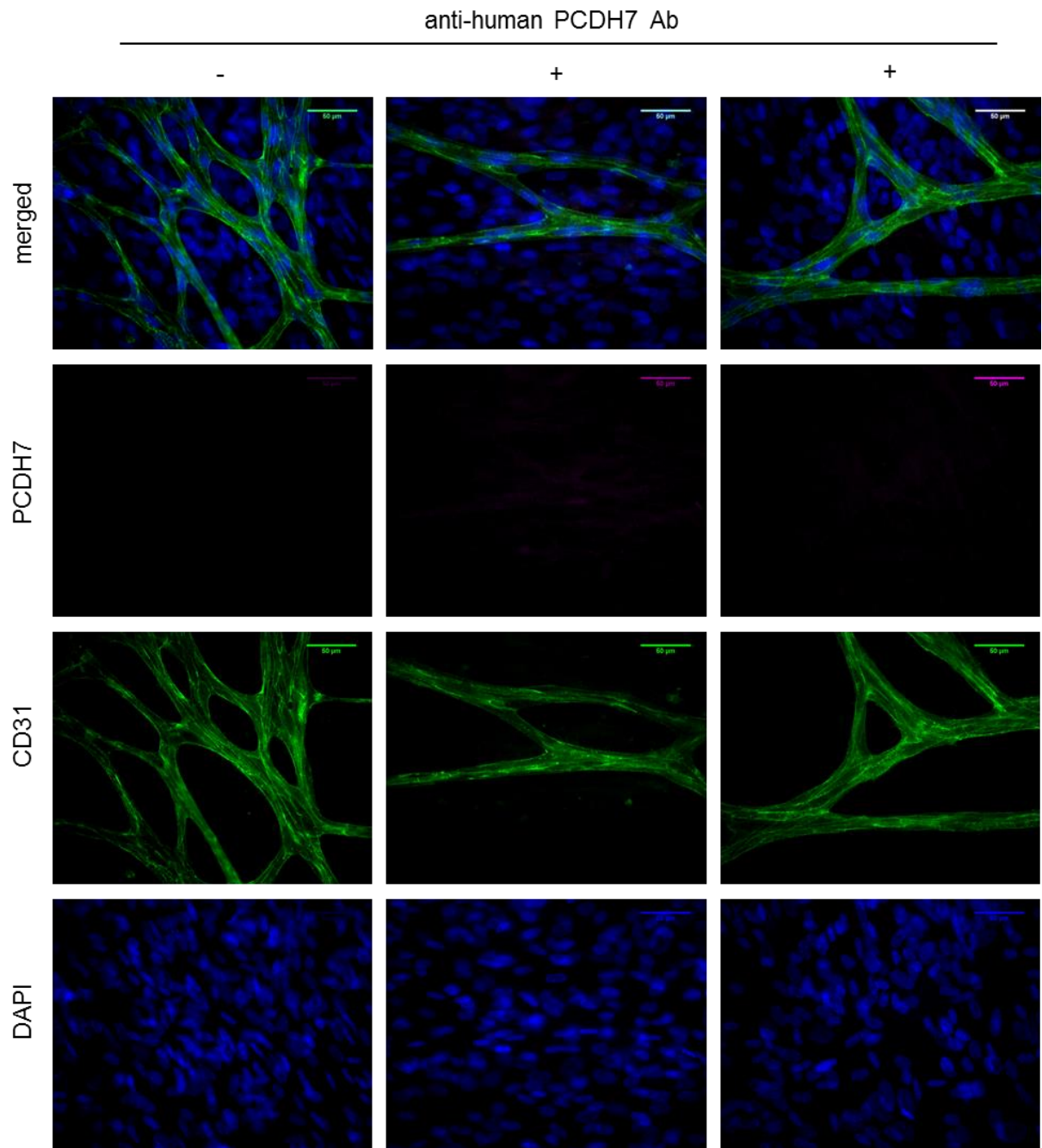


Figure 4.14 PCDH7 is not detected in the 2D HUVEC/HDF co-culture network. HUVEC were seeded on top of a monolayer of HDF cultured on glass cover slips and 2D HUVEC/HDF co-culture assay was performed according to a standard protocol. The cells were fixed with 4% PFA at day 6, stained with both anti-human CD31 and anti-human PCDH7 antibodies and mounted in DAPI onto the microscope slides. Images were taken using a fluorescence microscope. Representative images from one of three experiments.

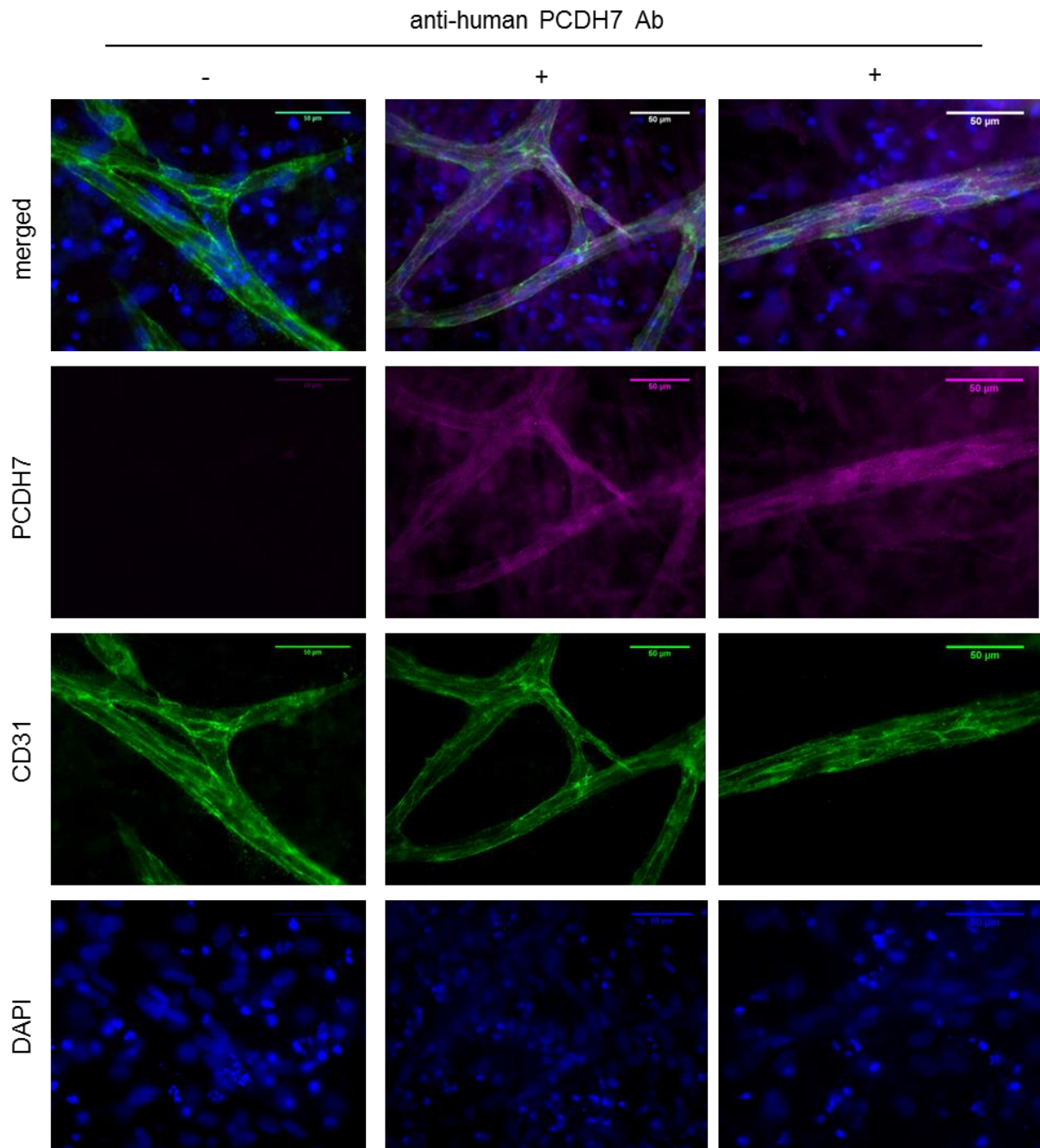


Figure 4.15 PCDH7 is detected in the 2D HUVEC/PC co-culture network. HUVEC were seeded on top of a monolayer of PC cultured on glass cover slips and 2D HUVEC/PC co-culture assay was performed according to a standard protocol. The cells were fixed with 4% PFA at day 6, stained with both anti-human CD31 and anti-human PCDH7 antibodies and mounted in DAPI onto the microscope slides. Images were taken using a fluorescence microscope. Representative images from one of three experiments.

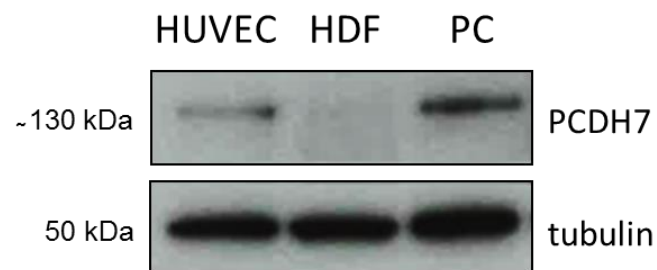


Figure 4.16 PCDH7 is expressed in PC but not in HDF. Western blot analysis of HUVEC, HDF and PC protein lysates with anti-human PCDH7 antibody with tubulin as a loading control. The experiment was performed once.

4.10 Discussion

In this chapter, interactions of the hPCDH7 ECD with endothelial cells were investigated using flow cytometry and immunoprecipitation. Firstly, by flow cytometry it was not possible to show any binding of the hPCDH7 ECD-Fc fusion proteins to either HEK293T overexpressing hPCDH7 FL or HUVEC. Secondly, no homophilic interaction of the hPCDH7 ECD was detectable using a pulldown of HEK293T-hPCDH7 FL-FLAG with hPCDH7 C7-Fc. Also, hPCDH7 ECD-Fc fusion proteins did not increase adherence of HUVEC in an adhesion assay. The mass spectrometry analysis performed in HUVEC pulldown samples revealed two potential ligands of hPCDH7 ECD: PDIA1 and EFEMP1 from which EFEMP1 was further investigated. However, the IP interaction studies between the hPCDH7 ECD-Fc and EFEMP1 were not validated. Finally, PCDH7 expression could be detected in HUVEC tubules when they were co-cultured with pericytes, but not with fibroblasts; pericytes were also found to express PCDH7.

Flow cytometry is a suitable technique to detect stable or strong protein-protein interactions. As no binding to HUVEC and HEK293T-hPCDH7 FL cells was observed, we hypothesize that PCDH7 interactions are rather transient and/or unstable. Such weak interactions have been reported for other non-clustered PCDHs like PCDH8 or PCDH19 (Kim *et al.*, 2011), therefore this scenario seems to be the most likely. Likewise, we could not confirm hPCDH7 ECD homophilic interactions by pulldown from HEK293T expressing epitope tagged PCDH7 using either mass spectrometry or Western blot analysis. Our negative results are consistent with

the data of Blevins *et al.* (2011) who show a lack of homophilic interactions of hPCDH7 ECD in a standard bead aggregation assay. It would have been useful to include a positive control in the immunoprecipitation experiments. For instance, VE-cadherin ECD-Fc pulldown could be performed on HEK293T overexpressing VE-cadherin FL. VE-cadherin exhibits a strong homophilic interaction (Vincent *et al.*, 2004) that should be easy to detect. Interestingly, a strong membrane PCDH7 expression localized on cell-cell contacts was observed using immunofluorescence staining of HEK293T cells overexpressing hPCDH7 FL-FLAG. Given that this only occurred in adjacent cells which both expressed PCDH7, this suggests the presence of homophilic interactions of PCDH7. Similar observations were reported for PCDH1, which was confirmed to be involved in the cell adhesion in epithelial cells (Faura Tellez *et al.* 2016).

Yoshida (2003) reported a positive role of PCDH7 in the cell-cell adhesion of mouse fibroblasts overexpressing PCDH7 in a standard cell aggregation assay. We have tried a similar assay using HEK293T-hPCDH7 FL cells with untransfected HEK293T cells as a control. However, control cells formed spontaneous aggregates making the results unreliable. The findings of Yoshida (2003) were contradicted by Blevins *et al.* (2011) who did not observe any adhesive properties of purified hPCDH7 ECD. These discrepancies might be partially explained by work conducted on *Xenopus* orthologue of PCDH7, NFPC (Rashid *et al.*, 2006). This work showed that NFPC has adhesive activity *in vivo*; however it is lost after inhibition of the interactions of its intracellular domain. This suggests that adhesive properties of PCDH7 might be difficult to confirm without the presence of intracellular domain regulating this

function. Indeed, we were unable to determine adhesive properties of purified PCDH7 ECD using an adhesion assay. However, a strong membrane staining localized on cell-cell contacts of HEK293T overexpressing PCDH7 FL suggested its role in the cell adhesion similarly to PCDH1 mentioned above.

The hPCDH7 ECD-Fc fusion protein inhibits HUVEC proliferation and network formation as presented in Chapter 3. Since PCDH7 expression in HUVEC is very low, it seems likely that hPCDH7 ECD mediates these effects by binding to proteins on the HUVEC surface rather than itself. This is supported by the observation that PCDH7 expression was not detected in HUVEC co-cultured with fibroblasts. Therefore, we have attempted to identify its binding ligands on HUVEC surface using immunoprecipitation. Mass spectrometry analyses on pulldown samples revealed two potential candidates, PDIA1 and EFEMP1, from which only EFEMP1 was further studied. However, since the control hFc protein pulled down EFEMP1 we concluded that there was likely no interaction between the hPCDH7 ECD-Fc and EFEMP1. Since HUVEC lysate was first pre-cleared with protein A beads, it is likely that EFEMP1 bound to hFc fragment of the proteins and suggest false positive data for EFEMP1 detected by mass spectrometry. To reduce the chance of nonspecific interactions, the IP experiment might be conducted with different tag such as GST. Alternatively, other techniques for the identification of ligands could be employed, for example stable isotope labelling with amino acids in cell culture (SILAC) immunoprecipitation combined with mass spectrometry (Emmott *et al.*, 2014). In this method, stably isotope labelled cells are subsequently transfected with plasmid DNA encoding tagged protein of interest or control protein followed by cell lysis and affinity

purification using tag fragment. Equal amounts of purified experimental and control samples are mixed and analysed using mass spectrometry. Statistical analysis of SILAC-labelled peptide ratios discriminates between interacting proteins and nonspecific binding contamination even for low affinity protein-protein interactions.

Although not included in this work, the second ligand candidate protein disulphide-isomerase (PDIA1) would be interesting to study. PDIA1 is externalized in HUVEC (Araujo *et al.*, 2017), therefore interaction with the extracellular domain of PCDH7 is possible.

PCDH7 expression was observed when HUVEC were co-cultured with pericytes but not fibroblasts. This might suggest that the expression of PCDH7 by PC enhance its expression in HUVEC although this was not further investigated at this stage. It would be interesting to transduce HDF with PCDH7 to determine whether this could induce higher expression of PCDH7 on HUVEC.

Some PCDHs were shown to interact with and/or affect the expression of classical cadherins. Specifically, PAPC, a *Xenopus* orthologue of PCDH8, downregulates the adhesive properties of C-cadherin (Chen *et al.*, 2006), PCDH19 forms complexes with N-cadherin in the neural tube in zebrafish (Biswas *et al.*, 2010) and PCDH7 was shown to modulate the expression of E-cadherin in gastric cancer (Chen *et al.*, 2017). Therefore, we have briefly tested whether treatment with the hPCDH7 ECD-Fc fusion proteins would affect the expression of VE-cadherin in HUVEC, however no difference was observed on Western blot (Figure 4.18).

Overall, these data did not identify any binding partners for the extracellular domain of PCDH7. Although the techniques employed in this chapter are widely used, they depend on strong interactions between the proteins and it is likely that interactions between hPCDH7 ECD and its targets are too weak to detect in these assays. For further studies, other approaches might be considered such as label transfer protein interaction analysis. This method involves the transfer of a certain moiety (for example biotin) between two proteins. A successful relocation of a label suggests interactions occurring between two studied proteins. Label transfer kits and protocols are commercially available. A similar concept was presented by Liu *et al.* (2007) however their method could be applied in protein's native environment. Due to time and budget constraints these possibilities were not explored in this project. Although this work has not fully achieved its objectives, it provided initial insight and lays important ground work for further investigations of PCDH7 function in endothelial cells.

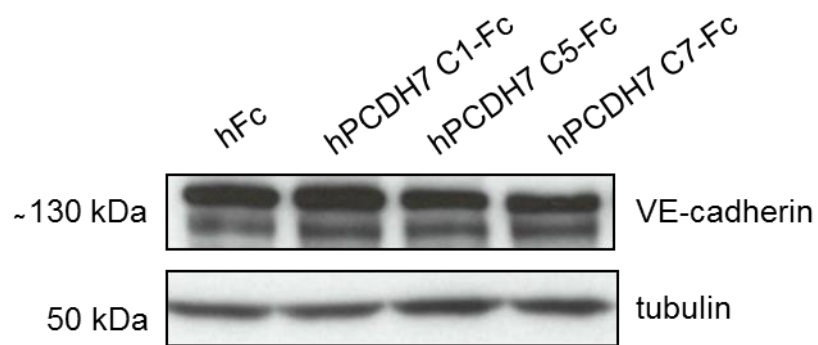


Figure 4.17 The expression of VE-cadherin does not change upon treatment with the hPCDH7 ECD-Fc fusion proteins. HUVEC were cultured with the addition of inhibitory active hPCDH7 C5-Fc and hPCDH7 C7-Fc proteins. As controls, hFc and non-functional hPCDH7 C1-Fc were used. All proteins were added to the culture medium to a final concentration of 1.54 μ M. Protein lysates were collected after two days of culture. Western blot analysis of cell lysates with anti-human VE-cadherin and anti-human tubulin antibodies. The experiment was performed once.

**CHAPTER 5: THE IDENTIFICATION OF POTENTIAL
COLORECTAL CANCER TUMOUR
VASCULATURE MARKERS AND INVESTIGATION
OF GENE FUNCTION IN THE ENDOTHELIAL
CELLS**

CHAPTER 5: THE IDENTIFICATION OF POTENTIAL COLORECTAL CANCER TUMOUR VASCULATURE MARKERS AND INVESTIGATION OF GENE FUNCTION IN THE ENDOTHELIAL CELLS

5.1 Introduction

The need to develop more specific and effective anti-vascular drugs is strongly driving the search for new tumour endothelial markers. Various approaches have been successfully utilized as reviewed in Chapter 1. Dutch biotech company SomantiX B.V. has performed a transcriptomic analysis of tumour and normal endothelial cells isolated from patients diagnosed with colorectal cancer (CRC) by using fluorescence-activated cell sorting as will be described later in this chapter. This method was successfully used to identify Apelin (APLN) as a putative biomarker for bevacizumab response (Zuurbier *et al.*, 2017). In this project, the endothelial gene signature identified by SomantiX was used to select potential vascular markers. This chapter discusses the identification of potential markers in CRC tumour and normal endothelial and epithelial cells using qPCR analysis.

Moreover, this chapter presents an attempt to further study the potential effect of several selected genes on endothelial network formation using shRNA-mediated knockdown in HUVEC. Lentiviral DNA encoding shRNA is known to integrate into the cell genome (Manjunath *et al.*, 2009). Therefore, it was anticipated that shRNA-mediated knockdown should be more stable over time when compared to transient

transfection with siRNA duplexes thus allowing easier detection of potential effects on endothelial network formation.

Based on the results, the four genes *APLN*, *ESM-1*, *MMP12* and *EREG*, will be further validated as TEMs at SomantiX.

5.2 SomantiX B.V. successfully performed a transcriptomic analysis of colorectal (CRC) tumour vs. healthy colon endothelial cells

SomantiX BV has performed a transcriptomic analysis of isolated primary CRC and healthy colon samples, resected from patients of VU University Medical Center (VUMC) in Amsterdam, the Netherlands. Researchers from SomantiX have developed and optimized a method of tissue dissociation and its separation into several cell fractions using fluorescence-activated cell sorting. Fluorescent-labelled anti-CD31, anti-EpCAM and anti-CD45 antibodies enabled endothelial cells to be specifically identified and sorted. The characteristic staining patterns of endothelial cells, epithelial cells and leucocytes are listed in Table 5.1. The introduction of anti-CD45 marker enabled differentiation between CD31+CD45+ leucocytes (e.g. monocytes) and CD31+CD45- endothelial cells therefore reducing the background of unwanted cell types in the endothelial fraction.

Cell sorting was performed on 10 tumour and 5 healthy colon tissues and enriched fractions of endothelial (CD31+CD45-) and epithelial cells (CD31-CD45-EpCAM+) were isolated. An example of flow cytometry analysis is presented in Figure 5.1.

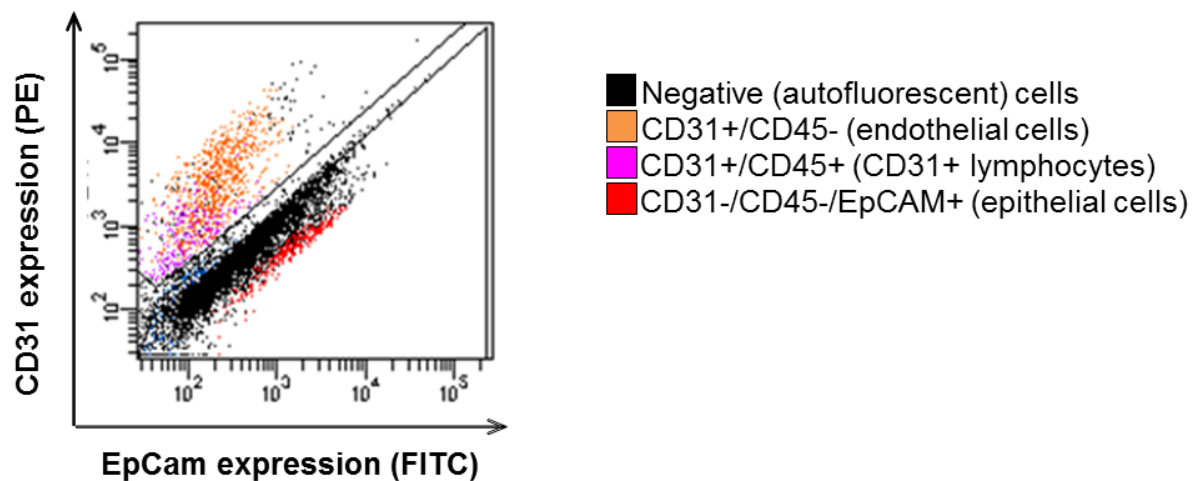


Figure 5.1 Representative example of flow cytometry cell sorting analysis conducted by SomantiX. Y-axis represents CD31-PE signal. X-axis corresponds to EpCAM-FITC expression. Endothelial cells (CD31+CD45-) are labelled in orange. Epithelial cells (CD31-CD45-EpCAM+) are labelled in red. Lymphocytes (CD31+CD45+) are labelled in pink. Black cells correspond to auto fluorescent cells that were negative for all markers. PE – phycoerythrin, FITC – fluorescein. Image copied with permission.

Table 5.1 Antibodies and appropriate fluorescent labels used for the detection and sorting of different cell types. Table adapted from SomantiX. PE – phycoerythrin, APC – allophycocyanin, FITC - fluorescein

Cell fraction	Antibodies		
	Anti-CD31	Anti-CD45	Anti-EpCAM
Endothelial cells	+	-	-
Epithelial cells	-	-	+
CD31+ leucocytes	+	+	-
Fluorescent label	PE	APC	FITC

Endothelial cells were directly used for RNA isolation and a transcriptomic analysis using Agilent expression microarrays. Comparing tumour versus healthy endothelial cells data resulted in a list of around 2500 upregulated genes for the CRC vasculature. The signature contained well-known endothelial and angiogenesis-associated genes and previously described TEMs, thus validating the approach (Table 5.2).

Potential CRC vascular biomarkers were selected based on their function, cellular localisation (cell surface or extracellular) and any published reports linking the gene with angiogenesis and cancer. Genes with the upregulation fold change more than 2 ($\log_{2}FC=1$) were considered.

Table 5.2 Examples of well-known angiogenesis-associated genes and TEMs upregulated in CRC endothelial cells based on the transcriptomic analysis performed by SomantiX B.V. Genes were listed with a descending logFC value. LogFC=log2 fold change

Gene name	Gene abbreviation	logFC	p-value
E-selectin	<i>SELE</i>	4.68	0.01
Matrix metalloproteinase 9	<i>MMP9</i>	4.25	0.005
Ras homolog family member J	<i>RhoJ</i>	2.87	0.04
Melanoma cell adhesion molecule	<i>MCAM</i>	2.56	0.07
Endoglin	<i>ENG</i>	2.55	0.11
Roundabout guidance receptor 4	<i>ROBO4</i>	2.5	0.17
von Willebrand factor	<i>VWF</i>	2.38	0.25
Matrix metalloproteinase 2	<i>MMP2</i>	2.31	0.04
C-type lectin domain containing 14A	<i>CLEC14A</i>	2.3	0.15
Anthrax toxin receptor 1	<i>TEM8</i>	1.97	0.25

5.3 Analysis of the microarray data enables selection of potential CRC vascular markers

Various online tools were used as a first selection to check function and endothelial specificity of genes; these included GeneCards (www.genecards.org), Genevestigator (www.genevestigator.com) and BioGPS (www.biogps.com). Genevestigator contains a collection of public microarrays and RNAseq datasets. It was used to investigate the expression of genes across different tissues and organs. BioGPS and GeneCards contain a complete summary about gene and protein function with references to the literature, their expression profile and links to various gene and protein databases. Based on the above criteria, ten genes were

selected for further qPCR analysis of tumour and healthy endothelial cells samples (Table 5.3).

Table 5.3 List of potential CRC vascular markers based on the microarray data analysis. Information on the gene expression, location and function was collected from www.genecards.org, www.genevestigator.com and www.biogps.com. +++ Highly endothelial specific; ++ Expressed in endothelium and some other tissue types; + Non endothelial specific (based on genevestigator data); logFC= log2 fold change

Gene ID	Gene name	LogFC	p-value	Endothelial specificity	Location
<i>APLN</i>	Apelin	4.0	0.01	+++	Extracelullar
<i>MMP12</i>	Matrix metalloproteinase 12	3.98	0.02	+	Extracelullar
<i>C1orf54</i>	Chromosome 1 open reading frame 54	3.18	0.03	+++	Uncharacterized (potentially extracellular)
<i>ESM-1</i>	Endothelial cell-specific molecule 1	3.06	0.03	+++	Extracelullar
<i>EREG</i>	Epiregulin	2.72	0.14	+	Extracelullar
<i>PROCR</i>	Protein C receptor	2.51	0.06	+++	Transmembrane
<i>HYAL2</i>	Hyaluronoglucosamidase 2	2.34	0.2	++	Cell surface protein
<i>DCHS1</i>	Dachsous Cadherin Related-1 (Protocadherin 16)	2.05	0.09	++	Transmembrane
<i>STAB1</i>	Stabilin 1	1.7	0.43	+++	Transmembrane
<i>FAM174B</i>	Family with sequence similarity 174	1.21	0.45	+	Transmembrane (potential)

5.4 Analysis of endothelial expression and qPCR primer validation for selected genes

The expression of the selected genes was first investigated in endothelial cells. This enabled the validation of gene specific qPCR primers and verified whether the function of potential markers could then be studied in HUVEC. *HPRT1* (hypoxanthine phosphoribosyltransferase 1) and *BGUS* (β -glucuronidase) were selected as housekeeping reference genes. For each gene, several pairs of primers were designed and validated for their specificity. When possible, amplicons spanned exon boundaries which ensured the amplification of cDNA rather than genomic DNA.

The primer specificity and correct product sizes were checked by qPCR using HUVEC cDNA and –RT control (cDNA reaction without reverse transcriptase). To ensure reliable results of the qPCR analyses, primers sets that amplified products from genomic DNA were excluded. This was done using qPCR with human genomic DNA.

The SYBR green qPCR analysis was performed on four different HUVEC RNA isolates as described in the Materials and Methods. The results indicated that most of the selected genes were detected in HUVEC (Figure 5.2A). However, no expression was observed for the *EREG* and *MMP12* genes. The values show the relative expression of mRNA levels of candidate genes compared to the reference genes in HUVEC calculated as described in the Materials and Methods. It is not possible to

compare expression levels between the genes as the relative efficiency of the primer pairs was not equivalent.

To ensure reliable qPCR results, the reaction products were verified on agarose gels after every qPCR run. Figure 6.2B shows representative images of qPCR reaction products from one experiment. Primers amplified genes of interest while not giving a product in –RT control and genomic DNA control. This was confirmed by the analysis of the primers' melting curves (Figure A.9).

The absence of *MMP12* and *EREG* mRNA in HUVEC was investigated as it may be due to faulty primer sets or the fact that these genes were not expressed in HUVEC. Both *MMP12* and *EREG* were present in epithelial cells. Therefore, primers were validated using cancer epithelial MCF7 breast carcinoma cell line cDNA and –RT control using qPCR. Indeed, results showed that both *MMP12* and *EREG* were detected in MCF7 cDNA although their expression was much lower when compared to *HPRT1* and *BGUS* (Figure 5.3, primers' melting curves are shown in Figure A.10). Bands were absent in MCF7 –RT control thus confirming the specificity of the primer sets. Therefore, we concluded that *MMP12* and *EREG* were not expressed in HUVEC.

Overall, these results showed that these primer sets can be successfully used in a SYBR green qPCR analysis on tumour and healthy endothelial cell samples. Additionally, these data suggested that the function of most of these potential tumour vasculature markers could be studied in HUVEC.

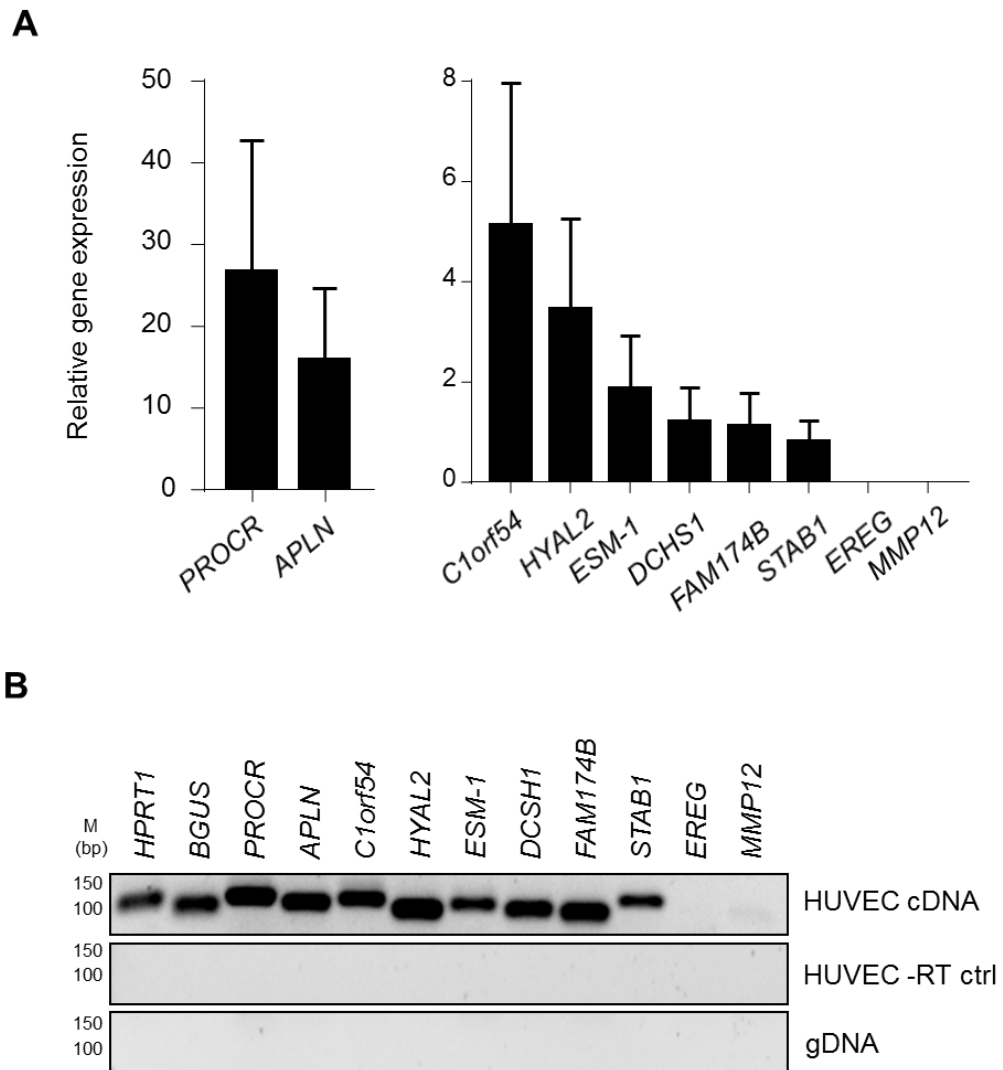


Figure 5.2 Most selected potential markers are expressed in HUVEC and gene specific qPCR primers amplify correctly-sized DNA fragments. A) SYBR green qPCR was performed on HUVEC cDNA synthesized from three independent HUVEC RNA isolates (N=3; n=2) using gene specific qPCR primers listed in the Materials and Methods. Values indicate a relative mRNA expression level of selected genes compared to the reference genes; Error bars represent SD; B) Representative images of qPCR reaction products for cDNA and -RT control samples on agarose gel from one of three experiments. PCR using genomic DNA (gDNA) as a template was used as an extra negative control.

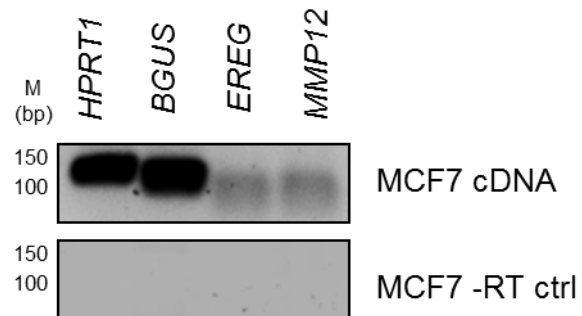


Figure 5.3 *EREG* and *MMP12* specific qPCR primer sets amplify *EREG* and *MMP12* cDNA fragments from MCF7 cells and do not give a background on -RT. MCF7 cDNA and -RT were synthesized from isolated MCF7 RNA. qPCR was performed for the same primer sets as used in HUVEC, in duplicates for each reaction. *HPRT1* and *BGUS* qPCR primers were used as a positive control. qPCR products were verified on agarose gel. The validation of primers was performed twice with similar results. MCF7 - human breast adenocarcinoma.

5.5 Study of selected targets expression in TEC and NEC samples provided by SomantiX revealed several genes enriched in TECs

The next step was to investigate the differences in the expression of selected genes between tumour and normal endothelial cells. Again, qPCR analysis was performed using cDNA provided by SomantiX. Unfortunately, the low efficiency of RNA isolation and its poor quality (Figure A.12) limited the amount of samples that could be used. Only three tumour endothelial cell (TEC) and one normal endothelial cell (NEC) samples were available. Due to these limitations, only a single reaction for each gene was performed. Additionally, tumour (TEpiC) and healthy (NEpiC) epithelial fractions were studied. This revealed more insight into the expression of targets in primary CRC tissue. As a control of the cell separation process conducted by SomantiX, specific markers for endothelial cells, epithelial cells and leucocytes were used: *ANGPT2*, *EpCAM* and *CD45*, respectively. Primers were also validated for their specificity on human endothelial (HUVEC) and epithelial (MFC7) cells using qPCR (Figure 5.4, melting curves are shown in Figure A.11). Unfortunately, leucocytes/lymphocytes cells were not available to validate CD45 primers.

The expression of control markers confirmed that the isolation and sorting of different cell types was performed successfully. As expected, *ANGPT2* gene was expressed only in endothelial but not in epithelial cells (Figure 5.5A). The expression of *CD45* in all samples was on the border of detection (Figure 5.5B) suggesting there is very little leucocyte derived mRNA in separated fractions. As expected, *EpCAM* was strongly present in epithelial cells. Additionally, its expression was enriched in tumour

endothelial samples (Figure 5.5C). The microarray data revealed down-regulation of this gene in analysed TEC samples (logFC = -0.51). Therefore, this indicated a potential contamination of TEC with epithelial-derived mRNA. However, the relative expression value in TECs was unusually high. Such enrichment in *EpCAM* expression in TECs when compared to epithelial fractions may not have been caused by the contamination but rather problems with primers specificity.

The qPCR data revealed the presence of *ESM-1* and *APLN* mRNA exclusively in TEC samples but neither the NEC nor the epithelial cells (Figure 5.6A and 5.6B). *MMP12* and *EREG* were strongly expressed in TEC but not NEC and to a lower extent in the tumour epithelial cells but not normal epithelial cells (Figure 5.6C and 5.6D). *STAB1* was enriched in TEC with low expression in the NEC sample and absent in epithelial fractions (Figure 5.6E). *PROCR* expression was observed in tumour fractions (both endothelial and epithelial) and additionally, in normal endothelial cells (Figure 5.6F). *C1orf54* and *HYAL2* did not show differential expression in TEC versus NEC and were absent in epithelial fractions (Figure 5.6G and 5.6H). Moreover, *FAM174B* gene was present in all fractions (Figure 5.6I). In contrast, *DCHS1* was barely detected in any samples (Figure 5.6J).

Due to their exclusive expression in TEC but not NEC, *APLN* and *ESM-1* were considered as promising markers for CRC vasculature while *EREG* and *MMP12* as markers of the whole CRC tumour. Although they were not validated as TEMs in this project, the work is continued at SomantiX. The function of selected candidates is briefly reviewed below.

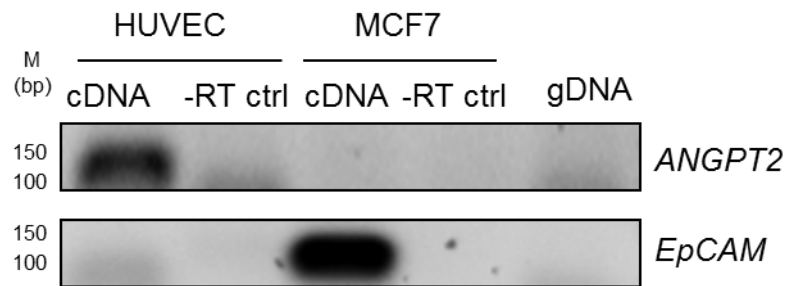


Figure 5.4 *ANGT2* and *EpCAM* qPCR primer validation. cDNA and –RT control were synthesized from isolated HUVEC or MCF7 RNA. qPCR was performed for *ANGPT2* and *EpCAM* specific primers, in duplicates for every reaction. Products were verified on agarose gel. The validation of primers was performed twice with similar results. PCR using genomic DNA (gDNA) as a template was used as an extra negative control.

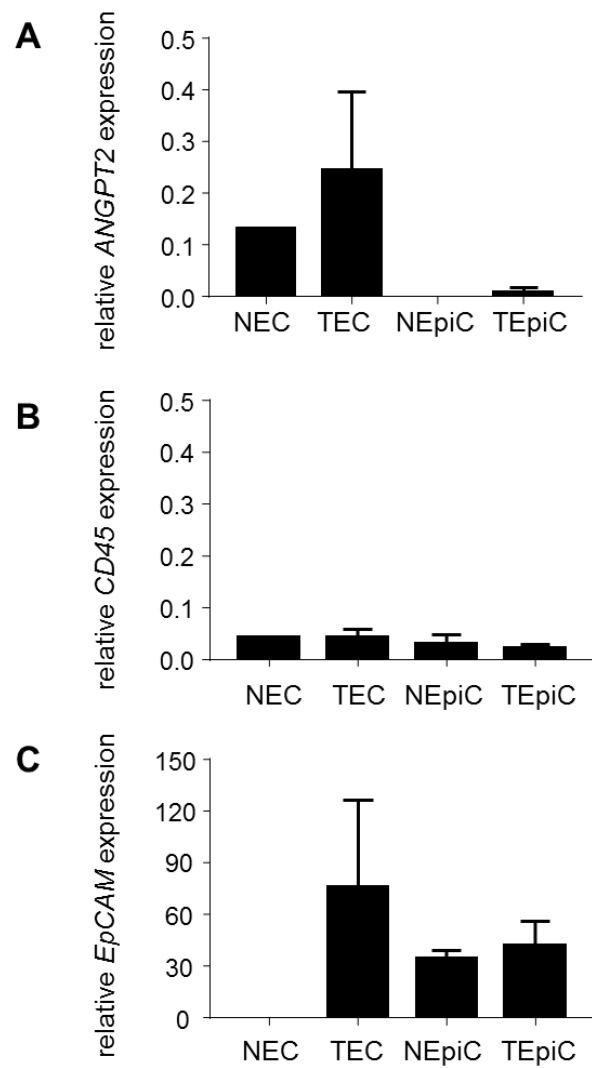


Figure 5.5 The mRNA expression of *ANGPT2*, *CD45* and *EpCAM* markers confirmed a successful separation of different cell fractions for transcriptomic analysis. The graph shows qPCR results for the relative expression of A) *ANGPT2*, B) *CD45* and C) *EpCAM* genes in NEC (N=1), TEC (N=3), NEpiC (N=4) and TEpiC (N=4) samples. Error bars represent SD. NEC- healthy endothelial cells; TEC- tumour endothelial cells; NEpiC – healthy epithelial cells; TEpiC – tumour epithelial cells.

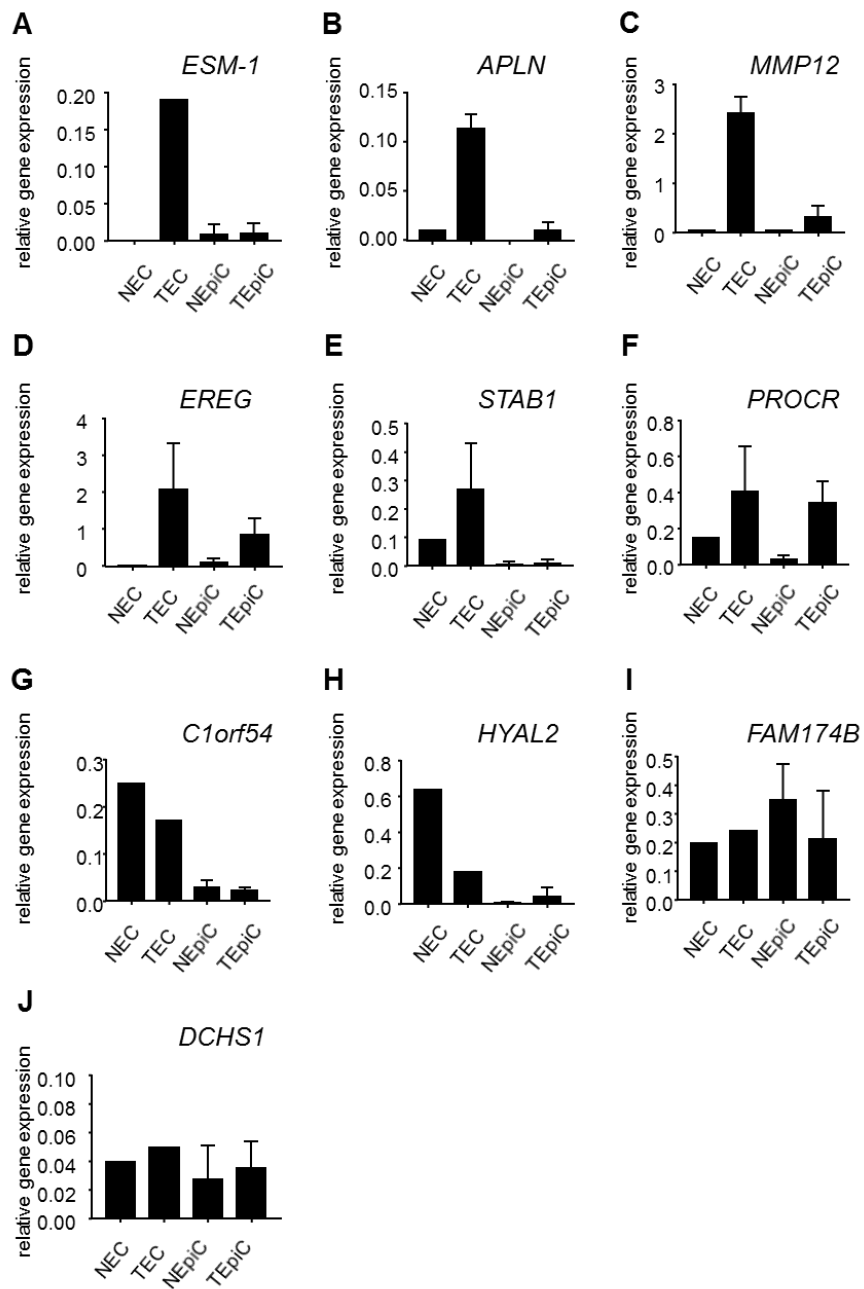


Figure 5.6 qPCR analysis of candidate TEMs. The graph shows results of SYBR green qPCR analysis of A) *ESM-1*, B) *APLN*, C) *MMP12*, D) *EREG*, E) *STAB1*, F) *PROCR*, G) *C1orf54*, H) *HYAL2* and I) *FAM174B* and J) *DCHS1* gene expression in NEC (N=1), TEC (N=3), NEpiC (N=4) and TEpiC (N=4) samples. Error bars represent SD. NEC- healthy endothelial cells; TEC- tumour endothelial cells; NEpiC – healthy epithelial cells; TEpiC – tumour epithelial cells.

APLN and its receptor (APJ) (Tatemoto *et al.*, 1998) are present in many human tissues therefore they seem to play a role in variety of physiological processes including angiogenesis (Back *et al.*, 2011; Yang *et al.*, 2016). APLN expression is upregulated in many types of tumours such as NSCLC, gastroesophageal, prostate and endometrial cancer or colon and hepatocellular adenocarcinoma (Yang *et al.* 2016). It was also shown to play a crucial role in stimulating tumour neovascularization *in vivo* (Sorli *et al.*, 2007). Moreover, APLN was proposed to be involved in tumour vessel maturation (Kidoya *et al.*, 2012). Elevated APLN expression is often associated with tumour progression and invasiveness.

ESM-1 was reported to have no direct effect on the angiogenesis and sprouting of HUVEC (Rennel *et al.*, 2007), although, others implicated a modulating role for ESM-1 in tumour angiogenesis (Chen *et al.*, 2010). Rocha *et al.* (2014) showed that ESM-1 is required for leukocyte extravasation and augmenting VEGF signalling suggesting that ESM-1 can enhance tumour angiogenesis rather than having a direct effect on tumour blood vessels. ESM-1 is very abundant for example in CRC (Zuo *et al.*, 2008), hepatocellular carcinoma (Huang *et al.*, 2009), pancreatic neuroendocrine tumours (Lin *et al.*, 2017), prostate carcinoma (Lai *et al.*, 2017) and oral cancer (Yang *et al.*, 2017) and it is often associated with tumour progression and poor prognosis.

MMP12 is a member of matrix metalloproteinase family. Its role in tumour progression has been reported. MMP12 was also shown to have anti-proliferative activity on endothelial cells *in vitro* (O'Reilly *et al.*, 1994) and anti-angiogenic activity

in vivo in murine colon cancer or melanoma models (Gorrin-Rivas *et al.* 2000; Xu *et al.* 2008) by generating angiostatin from plasminogen. MMP12 was successfully applied in melanoma cell therapy (Laurenzana *et al.*, 2014). On the other hand, high expression of MMP12 has been correlated to invasive character of lung adenocarcinoma (Lv *et al.*, 2015).

REG (epiregulin) is a growth regulating peptide belonging to the epidermal growth factor (EGF) family (Toyoda *et al.*, 1995). As a mitogen, REG plays a role in many physiological processes such as cell proliferation, wound healing and angiogenesis reviewed by Riese *et al.* (2014). On the other hand, deregulated REG expression is associated with bladder cancer progression and invasiveness (Thøgersen *et al.*, 2001; Nicholson *et al.*, 2004). Moreover, its expression is elevated in other tumour types such as colorectal, breast, head, neck or lung (Riese *et al.*, 2014).

As part of this project we have chosen to study three genes enriched in tumour endothelial cells: *PROCR*, *STAB1* and *C1orf54*. Both *STAB1* and *PROCR* were enriched in TEC samples but their proangiogenic potential has not been extensively studied as described below. Therefore, we further investigated their function in endothelial cells. We also chose to determine the function of the uncharacterized gene *C1orf54*. Its expression was not increased in TEC samples but the microarray data suggested its high upregulation (logFC = 3.18).

PROCR is described as a multifunctional receptor for many ligands (Rao *et al.*, 2004). *PROCR* has been reported to promote or limit tumour growth and metastasis

depending on the tumour type. For instance, PROCR can promote breast cancer cell migration (Beaulieu *et al.*, 2007) and metastasis of lung adenocarcinoma (Antón *et al.*, 2012). In contrast, endothelial overexpression of PROCR inhibits B16-F10 melanoma cells lung metastasis (Bezuhly *et al.*, 2009). One of PROCR's ligands, activated protein C (APC) is important in many processes such as blood coagulation and cytoprotection. APC activates the MAPK pathway in HUVEC resulting in increased cell proliferation and angiogenesis *in vitro* (Uchiba *et al.*, 2004). More recently, PROCR expression was shown to be a characteristic marker of vascular endothelial stem cells (V ESCs) (Yu *et al.*, 2016).

STAB1 has been described as a receptor with multiples functions (Kzhyshkowska *et al.*, 2006). In healthy individuals, STAB1 is expressed mostly on tissue macrophages and noncontinuous endothelial cells. STAB1 expressed by macrophages functions as a scavenger receptor and is responsible for the clearance of waste molecules (Goerdts *et al.*, 1993). Endothelial-expressed STAB1 is involved in mediating leukocyte cell adhesion and transmigration through the vasculature (Salmi *et al.*, 2004). It has been reported that STAB1 might control tumour growth and metastasis by immunomodulation of lymphocyte trafficking (Karikoski *et al.*, 2014). Treatment with anti-STAB1 antibody resulted in the reduction of B16 primary and metastatic tumours in wild type mice. Moreover, smaller primary tumours were observed in STAB1 knockout mice. The angiogenic potential of STAB1 *in vitro* was implicated by Adachi *et al.* (2002) who showed that FE-1-1 (anti-human STAB1) monoclonal antibody reduced HUVEC tubule formation in Matrigel tube forming assay.

In contrast, the function of C1ORF54 is unknown. C1ORF54 is a putative extracellular protein. Based on the Ensembl database, there are two annotated transcript variants that differ in the sequence of a last exon.

In order to determine the potential function of these genes on the endothelial network formation *in vitro*, the shRNA-mediated knockdown of *STAB1*, *PROCR* and *C1orf54* was performed in HUVEC and it will be further presented in this chapter.

5.6 Anti-human C1ORF54 and PROCR antibodies recognize their targets

To ensure reliable Western blotting to detect knockdown of the candidate genes, commercial anti-human PROCR and anti-human C1ORF54 antibodies were first validated. To validate anti-human PROCR primary antibody, commercially available *PROCR* cDNA was cloned into pcDNA3.1 expression vector. In contrast, *C1orf54* cDNA was cloned into pSecTag/FRT/V5-His secretion vector containing V5 and His tags. Using pSecTOPO vector enables the production and purification of a recombinant protein if desired for further studies. The cloning protocols and DNA templates are described in the Materials and Methods. The *STAB1* cDNA for cloning was not commercially available so the validation of anti-human STAB1 antibody was not performed.

PROCR negative COS-7 cells were transiently transfected with pcDNA-PROCR plasmid and HEK293FT cells were transiently transfected with pSecC1ORF54-V5-

His plasmid. Untransfected COS-7 cells and HEK293FT cells were used as controls. After 48 h of incubation, cells were lysed in RIPA buffer. Equal amounts of protein were separated by SDS-PAGE and blotted with appropriate antibodies. A band corresponding to PROCR was observed only in pcDNA-PROCR transfected COS-7 cells while being absent in the control cells (Figure 5.7A) confirming anti-human PROCR antibody recognizes PROCR protein. According to UniProt (www.uniprot.org) predictions, C1ORF54 protein should be around 20 kDa. Indeed, staining with a commercial anti-human C1ORF54 antibody revealed a band corresponding to this size when C1ORF54 was overexpressed (Figure 5.7B) and a similar band was observed for anti-V5 antibody, thus confirming the results. These results indicate that both anti-human PROCR and anti-human C1ORF54 antibodies showed reactivity towards their targets when overexpressed in cell lines.

5.7 Validation of shRNA-mediated knockdown was successful for *PROCR* but not for *C1orf54* and *STAB1*

Next, commercial shRNAs targeting *PROCR*, *C1orf54* and *STAB1* were purchased from Sigma and validated. Five shRNAs per gene were initially tested for their knockdown potential on mRNA level (Figure 5.8). HUVEC were transduced with lentivirus encoding appropriate shRNA as described in the Materials and Methods. Two shRNAs showing the highest efficiency were further validated. Again, HUVEC

were transduced and RNA and proteins were isolated 48 h after transduction. The knockdown validation was performed three times with similar results.

Selected *PROCR* targeting shRNAs significantly reduced *PROCR* mRNA expression for around 75% for sh1 and 95% for sh2 (Figure 5.9A). A similar trend was observed on a protein level (Figure 5.9B) thus confirming successful and efficient knockdown of *PROCR* protein in HUVEC. Since mRNA knockdown was accompanied consistently by protein knockdown, qPCR analysis was chosen to confirm knockdown in HUVEC used in the assays described later in the chapter.

In contrast, *C1orf54* specific shRNA-mediated knockdown resulted in 75% and 60% reduction of *C1orf54* gene expression for sh1 and sh2, respectively (Figure 5.10A). Despite promising qPCR data, C1ORF54 protein was not detected in any of HUVEC samples (Figure 5.10B). The experiment was performed independently several times with the same outcome. It is likely that C1ORF54 endogenous expression in HUVEC is too low to be detected by the commercial antibody or *C1orf54* mRNA is present but not translated into protein. Another possibility is that there might be a different splice variant of C1ORF54 that cannot be detected by this particular antibody.

Unfortunately, it was difficult to reliably observe the decrease of *STAB1* expression on Western blot. This could be due to a low to moderate expression of endogenous *STAB1* and/or poor binding of the anti-human *STAB1* antibody. The knockdown of *STAB1* studied at the mRNA level revealed 80% and 60% reduction of the gene expression using sh1 and sh2, respectively (Figure 5.8C). For further studies,

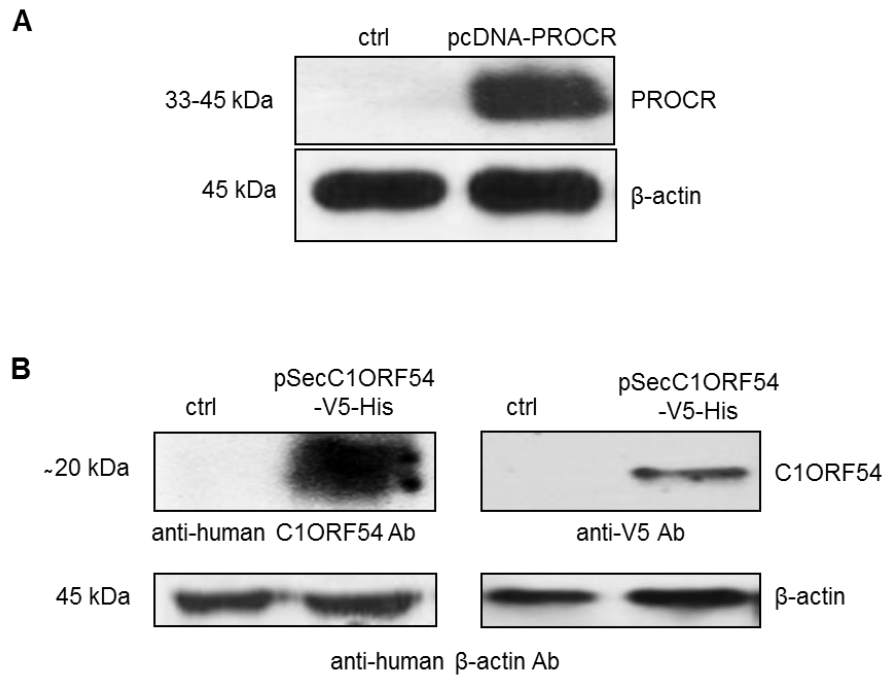


Figure 5.7 Validation of anti-human PROCR and anti-human C1ORF54 antibodies. HEK293T cells were transiently transfected with pcDNA-PROCR or pSec-C1ORF54-V5-His. Untransfected cells were used as a control. Proteins were extracted 48 h post transfection. Western blot analysis of A) anti-human PROCR and B) anti-human C1ORF54 antibodies. Protein extracts were blotted with anti-human β -actin antibody as a loading control. Validation of antibodies was performed once.

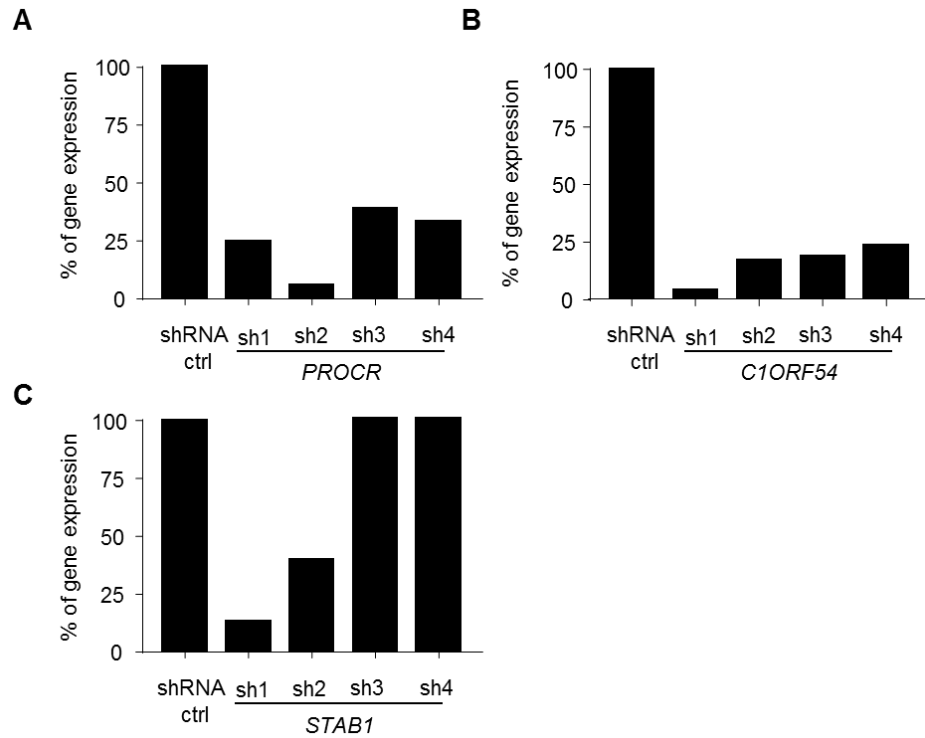


Figure 5.8 ShRNA-mediated knockdown of *PROCR*, *C1orf54* and *STAB1* results in a reduction of mRNA expression. HUVEC were transduced with lentiviruses encoding shRNA. Two days after transduction, RNA was collected and used in SYBR green qPCR analysis. Graphs show the percentage of A) *PROCR*, B) *C1orf54* and C) *STAB1* gene expression after the knockdown in the comparison to the control (100%). The initial validation of shRNAs was performed once.

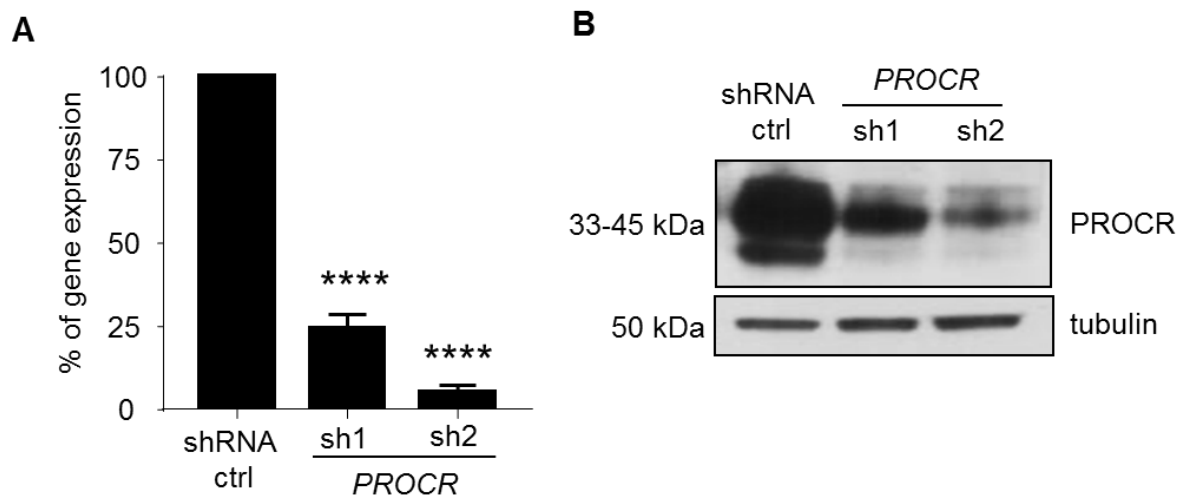


Figure 5.9 PROCR is successfully knocked down by using specific shRNAs. HUVEC were transduced with lentiviruses encoding specific *PROCR* sh1 and sh2. RNA and proteins were collected 48 h post transduction and used for A) qPCR analysis of *PROCR* gene expression, 1-way ANOVA, Tukey test; **** $p < 0.0001$. Error bars represent SD. The experiment was performed three times (N=3) in duplicates (n=2). B) Western blot analysis of *PROCR* expression from one of three experiments using anti-human *PROCR* antibody. Protein extracts were blotted with anti-human tubulin antibody as a loading control.

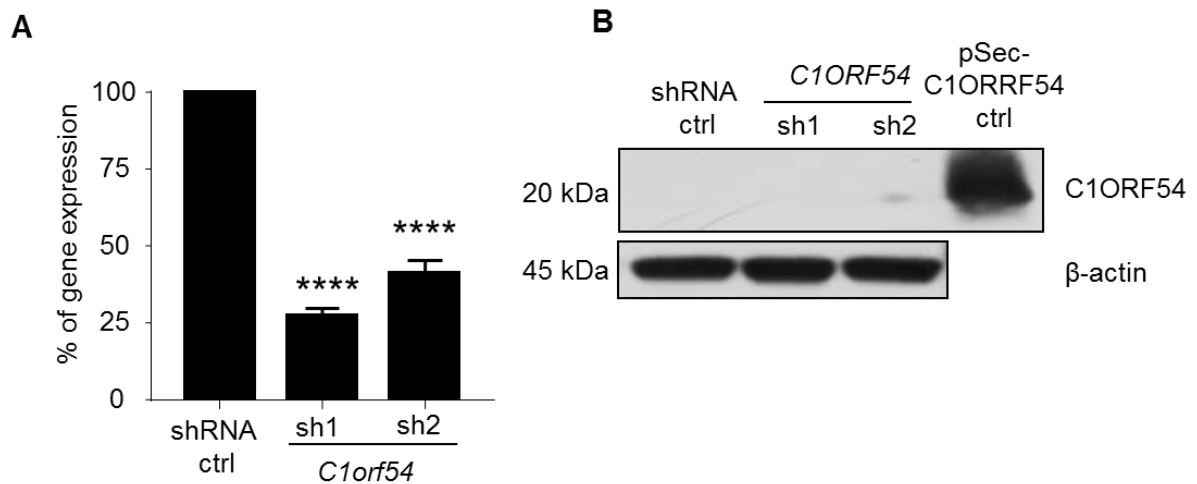


Figure 5.10 Despite a successful knockdown of *C1orf54* on mRNA level, C1ORF54 protein is undetectable in HUVEC. HUVEC were transduced with lentiviruses encoding specific *C1orf54* sh1 and sh2. After 48 h cells were harvested and RNA and protein extracts were prepared. A) qPCR analysis of *C1orf54* gene expression, 1-way ANOVA, Tukey test; **** $p < 0.0001$; Error bars represent SD. The experiment was performed three times (N=3) in duplicates (n=2). B) Western blot analysis of C1ORF54 expression from one of three experiments using anti-human C1ORF54 antibody. Protein extracts were blotted with anti-human β -actin antibody as a loading control. Overexpression HEK293T-C1ORF54 cell protein lysate was used as a positive control of antibody performance.

the knockdown efficiency was measured only on mRNA level. To reduce the chance of false positive or negative knockdown results, a non-functional *STAB1* sh3 (Figure 5.8) was used as an extra control. Since sh3 did not reduce *STAB1* mRNA level it was assumed it should not have any influence on the endothelial network formation.

Because of the difficulties in detecting endogenous C1ORF54 protein and very limited information on its potential function, studies on this protein were not continued in this project.

5.8 Determining the role of *STAB1* and *PROCR* knockdown on endothelial network formation in 3D HUVEC/HDF co-culture assay

The gene knockdown in HUVEC was performed according to the protocol described in the Materials and Methods. It was observed that the antibiotic treatment resulted in a dramatic decrease of HUVEC proliferation and thus was omitted in our assays. The effect of *PROCR* and *STAB1* knockdown was studied using a 3D HUVEC/HDF *in vitro* co-culture assay in fibrin matrix. HUVEC were co-transduced with two lentiviruses, one expressing validated shRNA and other expressing GFP protein. Cells were collected 48 h post transduction and used in the assay as described in the Materials and Methods. To confirm the knockdown, RNA was isolated from the remaining cells.

PROCR loss resulted in a small impairment of the HUVEC network formation after 5 days of the assay (Figure 5.11A). Although the total branching length of

the network was significantly lower only for sh2, a slight decrease could be measured also for sh1 (Figure 5.11B). A similar trend was observed for the number of junctions, though the reductions were not statistically significant. *PROCR* sh2 showed a higher knockdown efficiency than sh1 (Figure 5.11C). Therefore, it was hypothesized that to detect a significant effect of *PROCR* loss, a high knockdown of at least 90% is required.

A non-significant reduction of the network formation was observed for *STAB1* knockdown cells compared with control transduced cells (Figure 5.12A). The network branching length and the number of junctions for both *STAB1* sh1 and sh2 were decreased when compared to the control (Figure 5.12B). Unfortunately, a similar effect was observed for non-functional sh3 control suggesting off-target activity. Moreover, the calculated knockdown efficiencies for sh1 and sh2 (Figure 5.12C) did not correspond to their impact on the network formation. For example, sh1 with 75% knockdown had a weaker effect than sh2 which showed ~ 50% of the knockdown, suggesting non-specific activity of either one or both shRNAs. Altogether, these data suggest there might an inhibition upon *STAB1* loss however due to clear off-target effects of shRNAs no conclusion can be drawn. Therefore, other approaches have to be considered and it is essential to confirm the *STAB1* expression loss at the protein level.

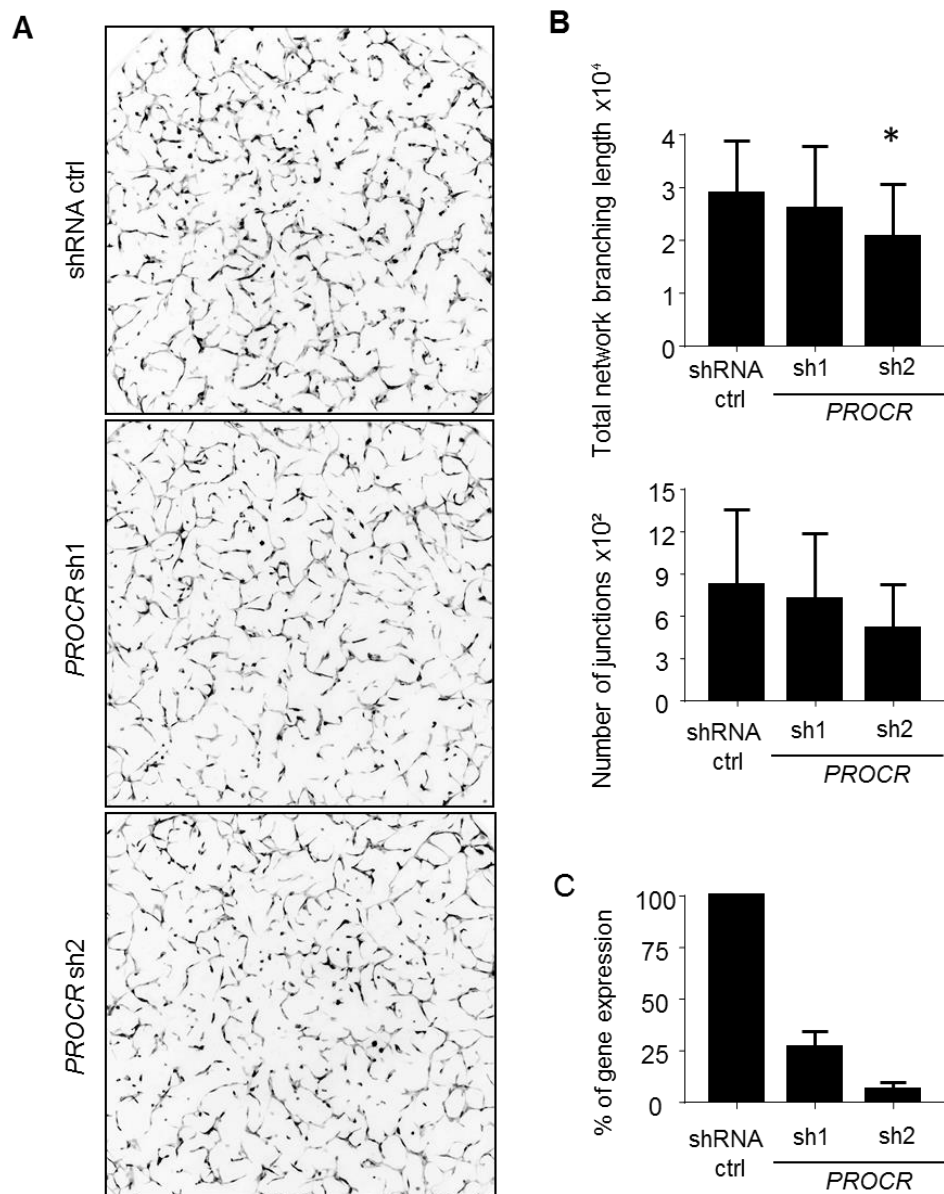


Figure 5.11 shRNA-mediated *PROCR* knockdown in HUVEC results in a decrease of the endothelial network formation. HUVEC were co-transduced with two lentiviruses, one encoding *PROCR* shRNA and second encoding GFP protein. Two days after transduction, cells were used in a 3D *in vitro* HUVEC/HDF co-culture assay; A) Representative images of one of three experiments at day 5. Images were taken using a fluorescence microscope and inverted to a white background for a better visualisation of the network. B) The total network branching length and the number of junctions were determined using ImageJ angiogenesis analyser plug in. C) qPCR analysis of *PROCR* gene expression; 1-way ANOVA, Tukey test; * $p < 0.05$; Error bars represent SD. The experiment was performed three times (N=3) in triplicates (n=3).

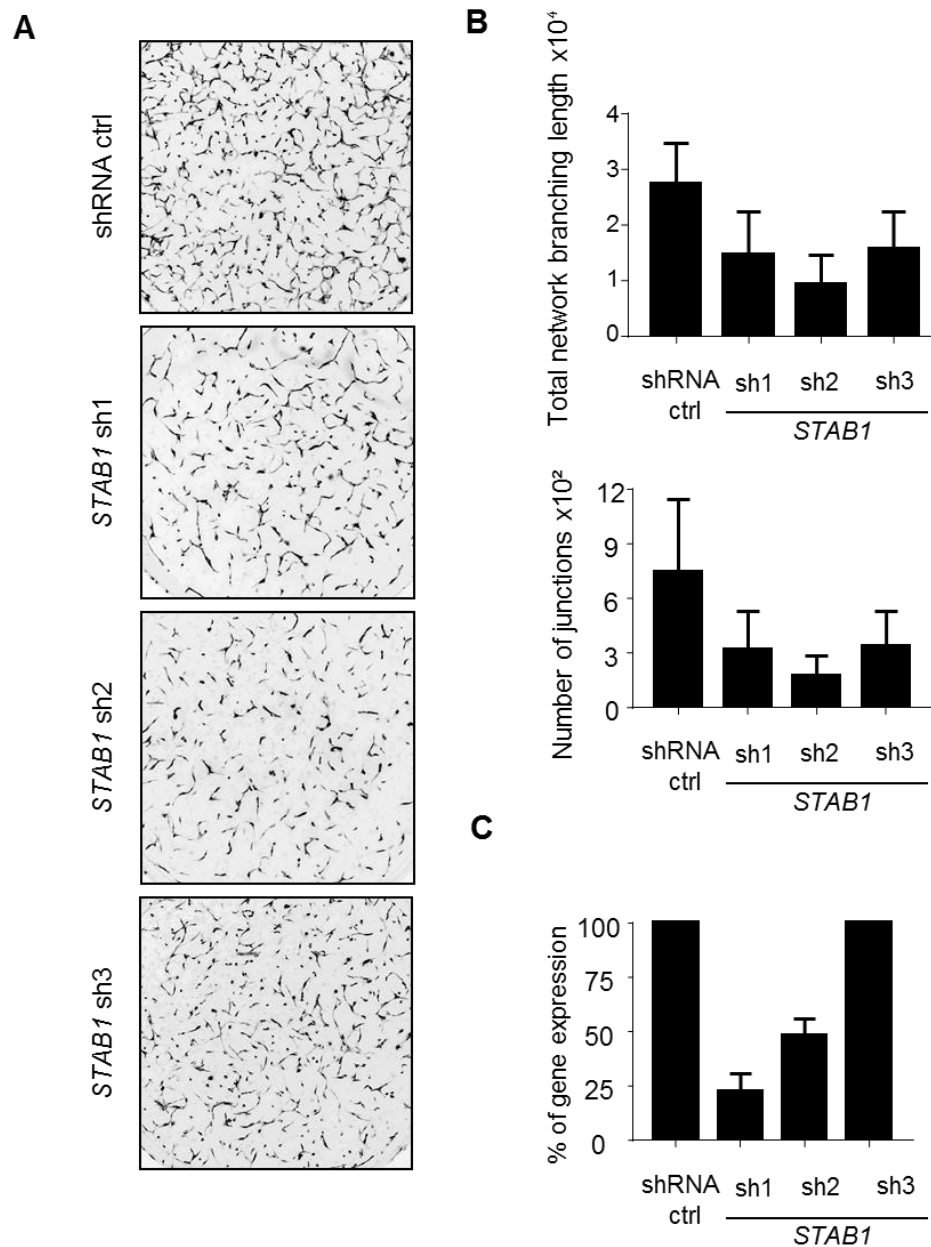


Figure 5.12 The level of shRNA-mediated *STAB1* knockdown in HUVEC does not correlate with the impairment of the endothelial network formation. HUVEC were co-transduced with lentiviruses encoding *STAB1* shRNA and GFP. Two days after transduction, cells were used in a 3D *in vitro* HUVEC/HDF co-culture assay; A) Representative images of the assay at day 5. Images were taken using a fluorescence microscope and inverted to a white background for a better visualisation of the network. B) The total network branching length and the number of junctions were determined using ImageJ angiogenesis analyser plug in. C) qPCR analysis of *STAB1* gene expression; 1-way ANOVA, Tukey test; Error bars represent SD. The experiment was performed three times (N=3) in triplicates (n=3).

5.9 Discussion

In this chapter, several potential TEMs candidates were selected based on qPCR analysis on CRC tumour (TEC) and normal (NEC) endothelial cells provided by SomantiX B.V. Four candidates were chosen for further validation: *APLN*, *ESM-1*, *MMP12* and *EREG* as TEMs. As a second part of this work, the potential angiogenic function of *PROCR*, *STAB1* and the uncharacterized *C1orf54* genes, enriched in TEC samples, was investigated. Gene specific shRNA-mediated knockdown in HUVEC was used in conjunction with 3D HUVEC/HDF co-culture angiogenesis assay. Unfortunately, this approach did not yield adequate data to determine the function of these genes.

The expression of initially selected genes (*APLN*, *MMP12*, *C1orf54*, *ESM-1*, *EREG*, *PROCR*, *HYAL2*, *DCSH1*, *STAB1* and *FAM174B*) from SomantiX CRC signature was also compared with the microarray analysis conducted by Joseph Wragg, a former member of our laboratory (Wragg, 2016). Most of identified genes (except *DCSH1* and *FAM174B*) were also found upregulated in colorectal TEC compared with NEC, validating the finding that these genes were upregulated in the vasculature of colon cancer.

Several potential CRC TEM gene candidates were selected based on qPCR analysis: *APLN*, *ESM-1*, *MMP12* and *EREG* and their angiogenic role has been reported as reviewed earlier in this chapter. Due to the very limited amount of TEC and NEC material used in this study it is necessary to undertake further isolation of

CRC tumour samples to confirm, support and improve the quality of the data described above. This is being pursued by researchers at SomantiX. Because of technical difficulties such as delays in delivery of tissue arrays, further validation of APLN, ESM-1, MMP12 and EREG as TEMs using IHC on colorectal tumour and normal tissue or tissue arrays was not conducted. Again, work will be continued by researchers in the Netherlands. As mentioned in the introduction of this chapter, studies conducted by SomantiX and their collaborators revealed APLN as a novel biomarker for bevacizumab response prediction in CRC (Zuurbier *et al.*, 2017).

As a second part of this work, the potential angiogenic function of *PROCR*, *STAB1* and uncharacterized *C1orf54* genes enriched in TEC samples, was investigated using the 3D HUVEC/HDF *in vitro* angiogenesis assay.

The literature reports that PROCR function is not limited to endothelial cells. PROCR expression in cancer cells has been described but its role is complex as reviewed earlier in this chapter. A significant but small effect upon PROCR knockdown was observed only after a complete loss of the protein expression. This small effect indicates that PROCR-mediated signalling is not crucial for the efficient development of a network of endothelial tubules although PROCR has been shown to be important in VESC differentiation into PC and EC (Yu *et al.*, 2016). The decrease in network formation is most likely caused by disrupting the function of PROCR ligands such as APC, as previously reported by Uchiba *et al.* (2004).

Unfortunately, studies on STAB1 angiogenic function were not successful. ShRNA-mediated knockdown did not give high reduction of *STAB1* mRNA expression and some nonspecific effects were observed. Other approaches such as siRNA-mediated knockdown could be explored. To study the function of STAB1, blocking antibodies including anti-stabilin-1 mAb FE1-1 could be also utilized (Kzhyshkowska *et al.*, 2006). These antibodies bind to different binding sites of STAB1 ligands thus blocking its receptor activity, and this has been patented and developed by Faron Pharmaceuticals (patent ID WO2003057130A2). The role of STAB1 in lymphocyte trafficking during tumour growth (Salmi *et al.*, 2004) might suggest that this is its primary function on the endothelium rather than playing a role in angiogenesis. However, the STAB1 extracellular domain is composed of several different ligand binding sites (Kzhyshkowska *et al.*, 2006) including a SPARC binding domain. SPARC is an extracellular matrix binding protein that is produced and cleaved during angiogenesis (Lane *et al.*, 1994) and one of generated peptides is reported to regulate angiogenesis (Sage *et al.*, 2003). Thus, it would be interesting to further explore this topic and study the effect of SPARC-binding domain itself of endothelial network formation.

Despite promising qPCR results, we were unable to detect C1ORF54 protein in HUVEC. Firstly, C1ORF54 expression might be too low to be detected by Western blot by commercial antibody. Secondly, the protein might be expressed only in certain but currently ill-defined conditions or processes. Due to difficulties in detecting C1ORF54, we were not able to reveal the function of this protein in HUVEC. Alternative approaches could include overexpressing it in HUVEC which might give

an insight into its endothelial cell function. On the other hand, the pro- or anti-angiogenic potential of C1ORF54 recombinant protein (for example Fc fused) could be studied on the endothelial cells alone or in the co-culture with fibroblasts using a similar methodology as is presented for hPCDH7 C7-Fc in Chapter 3. Finally and importantly, the expression of C1ORF54 in tumour and normal tissue samples can be still investigated using IHC or *in situ* hybridization using commercial antibodies or antibodies raised in-house against recombinant C1ORF54-Fc.

Although the aim of this work was not achieved due to technical and time limitations, it was a first step in the identification of novel TEMs in colorectal cancer.

CHAPTER 6: GENERAL DISCUSSION

6.1 General discussion

A market need for novel and more efficient anti-vascular therapies is strongly driving a search for new targets on tumour vasculature. Zhuang *et al.* (2015) has identified PCDH7 in TECs of NSCLC. Although PCDH7 has been reported in many types of cancer with context dependent function, to date work of Zhuang *et al.* (2015) is the only report showing its expression in endothelial cells. While PCDH7 intracellular interactions in cancer cells have been addressed, insight into the function of its extracellular domain is limited. We hypothesized that PCDH7 plays a role in angiogenesis and PCDH7 ECD or its ligand(s) could serve as potential anti-vascular targets in the future. A deeper understanding of the biology of potential targets enables the development of more specific anti-vascular strategies directed towards the target's specific functions. Thus, the first major aim of this thesis was to determine whether PCDH7 regulates endothelial network formation *in vitro* using a soluble recombinant version of PCDH7 extracellular domain fused to Fc. Secondly, we have attempted to identify its ligands on the endothelial cell surface.

In Chapter 3, by applying various *in vitro* angiogenesis assays we have successfully demonstrated that the hPCDH7 ECD-Fc exhibits a significant inhibitory activity on endothelial cell network formation when HUVEC were co-cultured with HDF and negatively affects endothelial cell proliferation and chemotaxis. These data support our hypothesis that PCDH7 plays a role in angiogenesis. We have also determined that this inhibitory activity is located within the first five N-terminal cadherin repeats of PCDH7 ECD. Further to this, we have shown that HDF do not express PCDH7 but

interestingly, PCDH7 is present in PC. Moreover, we could not detect PCDH7 on endothelial network of 2D HUVEC/HDF co-culture while positive staining was observed for 2D HUVEC/PC co-culture. We hypothesize that the expression of endogenous PCDH7 in HUVEC network when co-cultured with PC is induced by PCDH7 expressed by PC. It would be interesting to determine whether HDF engineered to express PCDH7 could induce PCDH7 expression in HUVEC network as is observed for HUVEC/PC co-culture. Indeed, its presence in the tumour endothelium may be influenced by the expression of PCDH7 on tumour cells and/or on other stromal cells in the tumours. A similar dependence was reported for PCDH7 expressing cancer cells and astrocytes in brain metastasis (Chen *et al.*, 2016). Although PC support endothelial network formation in both 3D and 2D HUVEC/PC co-culture assays (Figure A.6), we did not perform *in vitro* assays with pericytes due to their fragility and tendency to detach from the culture plate. However, it would have been interesting to determine whether soluble hPCDH7 ECD-Fc influences the expression of PCDH7 by either PC or HUVEC. This would give insight in how its expression is regulated.

If these promising *in vitro* data are further confirmed in, for example, lung microvascular cells as a better model for NSCLC, the next step would be to conduct *in vivo* studies in mice using the mouse version of PCDH7 ECD (mPCDH7 ECD-Fc). Once produced, mPCDH7 ECD-Fc could be used to confirm its inhibitory activity in mice using *in vivo* angiogenesis assays such as sponge implantation assay. Moreover, to evaluate the effect on mPCDH7 ECD-Fc on tumour vessels it could be tested in mice with subcutaneously implanted tumours.

During this project, we have also attempted to overexpress PCDH7 protein in HUVEC to determine the effect of PCDH7 overexpression on cell adhesion and endothelial network formation. We used a lentiviral transduction approach, but encountered problems with transduction efficiency. Our bicistronic lentiviral vector encoded PCDH7 linked via an IRES system to eGFP to enable the detection of positively transduced HUVEC expressing PCDH7. However, the large plasmid size resulted in inefficient viral packaging. To pursue this approach the lentiviral vector would have to be re-engineered to be smaller. This could be achieved by using a fluorescent protein encoded by shorter DNA. Alternatively, the IRES controlled fluorescent marker could be removed and transduced cells could be isolated by FACS based on their expression of PCDH7 itself using suitable antibodies to its extracellular domain.

The interactions of the extracellular domain of PCDH7 with endothelial cell surface protein(s) are unknown. Thus, we aimed to identify potential ligand(s) of the hPCDH7 ECD on the endothelial cell surface and to determine the nature of these interactions as presented in Chapter 4. We hypothesized that we can successfully identify binding partners of hPCDH7 ECD by applying several commonly used methodologies. This in turn would enhance knowledge about the biological function of PCDH7. The expression of PCDH7 at the membrane and cell-cell junctions in overexpression cell line suggests that it has a role in homophilic cell adhesion. On the other hand, the lack of PCDH7 expression in 3D HUVEC/HDF co-culture assay strengthened our hypothesis that the hPCDH7 ECD must be exerting its effects via heterophilic interactions. Although we have applied several well established methods such as

flow cytometry and immunoprecipitation as presented in Chapter 4, we could not detect adhesive properties or any heterophilic or homophilic interactions of recombinant soluble hPCDH7 ECD-Fc fusion proteins. We cannot exclude that the ECD of PCDH7 interacts both with itself and alternative binding partners depending on the cellular context.

Methodologies used to identify binding partner of hPCDH7 ECD-Fc were not sufficient to detect any interactions suggesting they are weak. Additionally, other factors can influence protein-protein interactions such as conformational changes required to stabilize interactions or the necessity for additional proteins required to stabilize the interactions of the PCDH7 ECD with its ligand(s). These would likely be disrupted during cell lysis and immunoprecipitation. Alternative techniques enabling the detection of low-affinity binding could be applied to enable identification of binding partner(s). For example, avidity-based extracellular interaction screen (AVEXIS) was developed as a protein microarray platform (Sun *et al.*, 2012) enabling high-throughput screening of low-affinity protein interactions. In this method, the extracellular domains of cell surface proteins are recombinantly produced as both biotinylated soluble monomers and β -lactamase-tagged soluble pentamers (Bushell *et al.*, 2008). To allow interactions pentamerized 'prey' proteins are added to the plate coated with monomeric 'bait' proteins. Interactions between 'bait' and 'prey' proteins are detected using β -lactamase-mediated reaction. Others have proposed methods involving *in vivo* crosslinking together with mass spectrometry (Vasilescu *et al.*, 2004) or analysis of extracellular proteome (Lin *et al.*, 2008).

Although not achieved in this work, the identification of the binding partners of the PCDH7 ECD will help to elucidate the mechanism of its blocking activity. This together with further mapping of the region of the ECD involved in its activity may lead to the development of novel strategies to block interactions between PCDH7 and its ligand(s) based on PCDH7 ECD-derived small proteins or peptides. Such approaches have been extensively investigated for tumour vascular targeting, tumour targeting and tumour imaging (Zhao *et al.*, 2018). For example, many RGD-containing peptides have been generated to target $\alpha v \beta 3$ integrin, a TEM that is present on vessels of many types of tumours. One of the peptides, Cilengitide, has completed Phase II clinical trial for the treatment of glioma (www.clinicaltrials.gov; accessed 8 August 2018).

The third aim of the thesis was to identify potential TEMs in colorectal cancer as presented in Chapter 5. This was performed in collaboration with SomantiX B.V. The company has performed a transcriptomic analysis of tumour and normal endothelial cells isolated from patients with colorectal cancer. We hypothesized that this endothelial signature will enable identification of novel TEMs in CRC. While a number of potential targets were identified, the study was compromised by low availability of TEC and NEC samples. This was due both to a limited number of suitable samples collected and technical difficulties in isolating endothelial cells from the tumour mass. A greater number of samples would have facilitated the target validation via qPCR, but ultimately targets require validation *in situ* by techniques such as immunohistochemical staining of tissue arrays. Interestingly one TEM

candidate identified as part of this study, APLN, has been proposed as novel biomarker for bevacizumab response as mentioned before (Zuurbier *et al.*, 2017).

Aside of the main goal of the identification of novel TEMs, we have also studied angiogenic potential of three genes, *PROCR*, *STAB1* and *C1orf54*, upregulated in TEC when compared to NEC. We chose to conduct shRNA-mediated knockdown in HUVEC. We found that *PROCR* knockdown resulted in a minor impairment of endothelial network formation in 3D HUVEC/HDF co-culture assay, and so appears not be essential for this process. ShRNA-mediated knockdown of *STAB1* in HUVEC gave inconsistent results, with defects in network formation not correlating with levels of network formation inhibition. Due to the lack of expression in HUVEC it was not possible to study the uncharacterised protein encoded by *C1orf54*. Overall, we have concluded that our strategy of using shRNAs was not successful and alternative approaches should be used. For example, antibody-mediated blocking of STAB1 function in HUVEC could be useful to better study its function in angiogenesis. Also, C1ORF54 remains an interesting molecule which expression could be further characterised using immunohistochemical staining on a variety of human cancer and normal tissues.

Though it was not possible to comprehensively identify and validate novel TEMs in colorectal cancer as initially hypothesized, many aspects of what is presented are being further pursued and lay a foundation for the future identification of novel targets in this tumour type.

APPENDIX

A

Enter accession, gi, or FASTA sequence (A refseq record is preferred) [Clear](#)

Range

Forward primer From To [Clear](#)

Reverse primer From To

Or, upload FASTA file [Choose File](#) No file chosen

Primer Parameters

Use my own forward primer (5'->3' on plus strand) [Clear](#)

Use my own reverse primer (5'->3' on minus strand) [Clear](#)

PCR product size Min: 80 Max: 150

of primers to return: 10

Primer melting temperatures (T_m) Min: 57.0 Opt: 60.0 Max: 63.0 Max T_m difference: 3

Exon/intron selection

A refseq mRNA sequence as PCR template input is required for options in the section

Exon junction span: Primer must span an exon-exon junction

Exon junction match: Exon at 5' side: 7 Exon at 3' side: 4

Minimal number of bases that must anneal to exons at the 5' or 3' side of the junction

Intron inclusion: Primer pair must be separated by at least one intron on the corresponding genomic DNA

Intron length range: Min: 1000 Max: 1000000

Note: Parameter values that differ from the default are highlighted in yellow

B

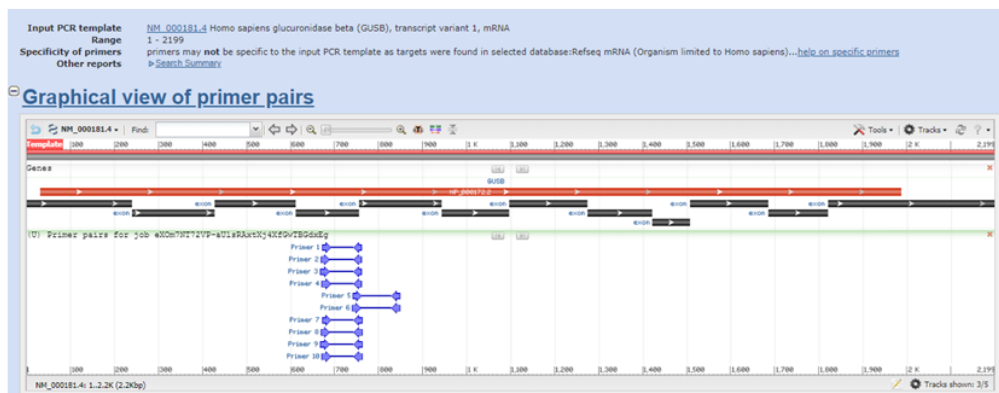


Figure A.1 Example of qPCR primer design using the Primer-BLAST tool. A) A screenshot of the settings for a design of qPCR primers specific to *BGUS* (gene accession number NM_00181). B) A screenshot of the results of the Primer-BLAST run showing ten pairs of primers designed for *BGUS*.

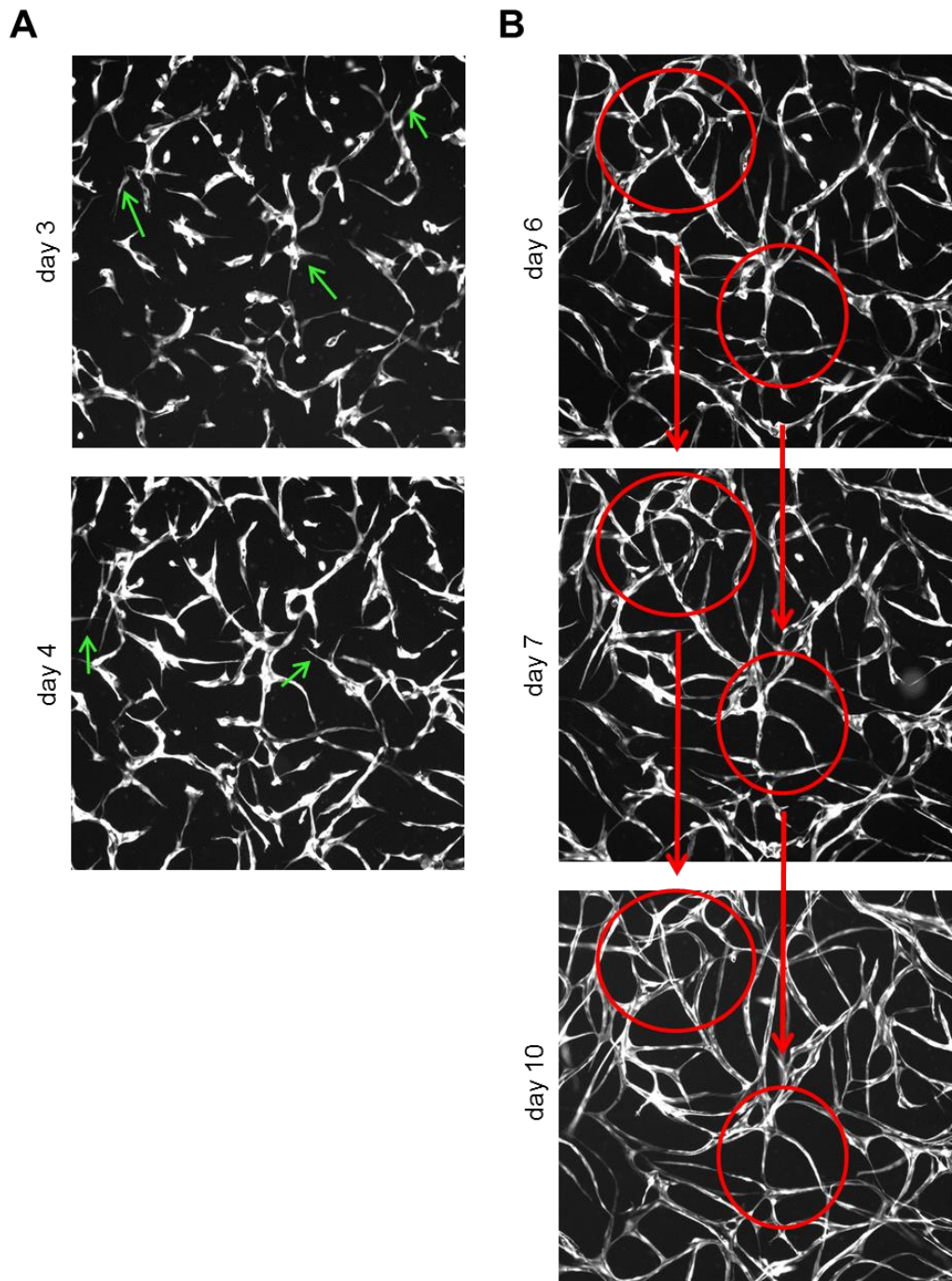


Figure A.2 3D HUVEC/HDF co-culture *in vitro* angiogenesis assay involves different steps of angiogenic process. All images represent the same well at different days during the assay. A) Multiple cell extensions, sprouts and protrusions can be observed (few examples indicated by green arrows) at first days of the assay. B) Fusion of the tubes, network maturation and possibly lumen formation occurs after day 6. Red circles show the same areas of the well during different stages of the network development. Images were taken using a fluorescence microscope (10x magnification).

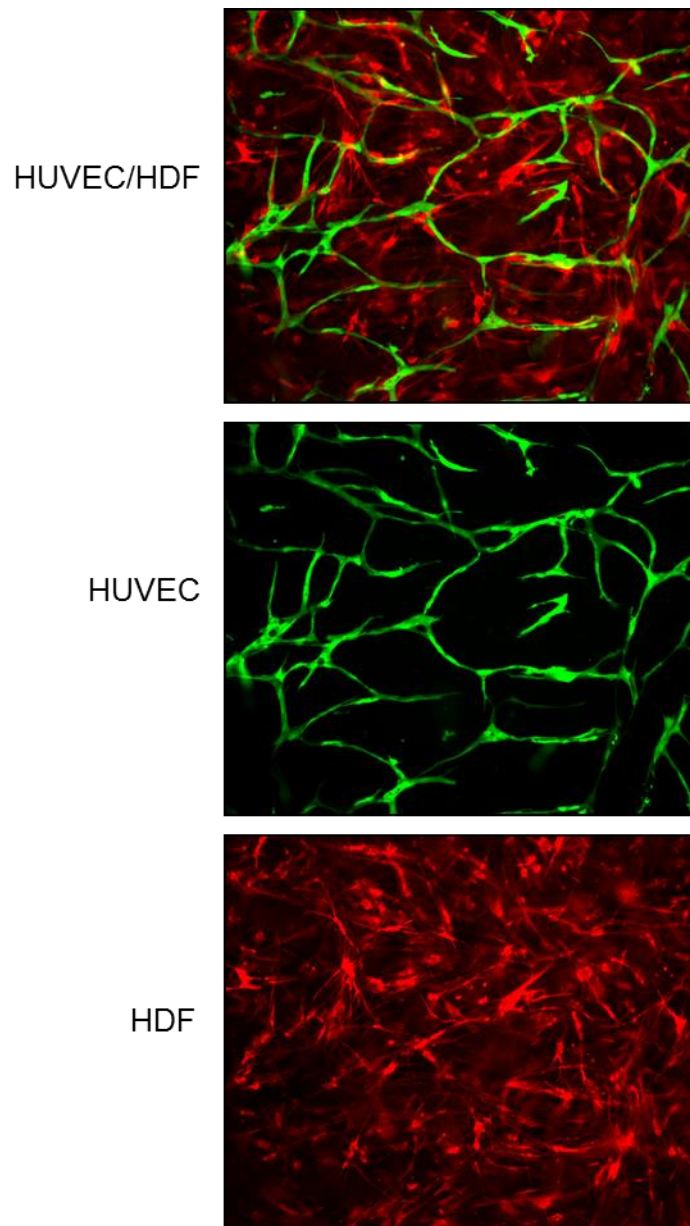


Figure A.3 Human dermal fibroblasts form a scaffold in the fibrin matrix in 3D HUVEC/HDF co-culture assay. GFP transduced HUVEC (green) were mixed with mCherry transduced HDF (red) and embedded in the fibrin matrix. Images were taken using a fluorescence microscope (10x magnification). Representative images from day 8 of co-culture.

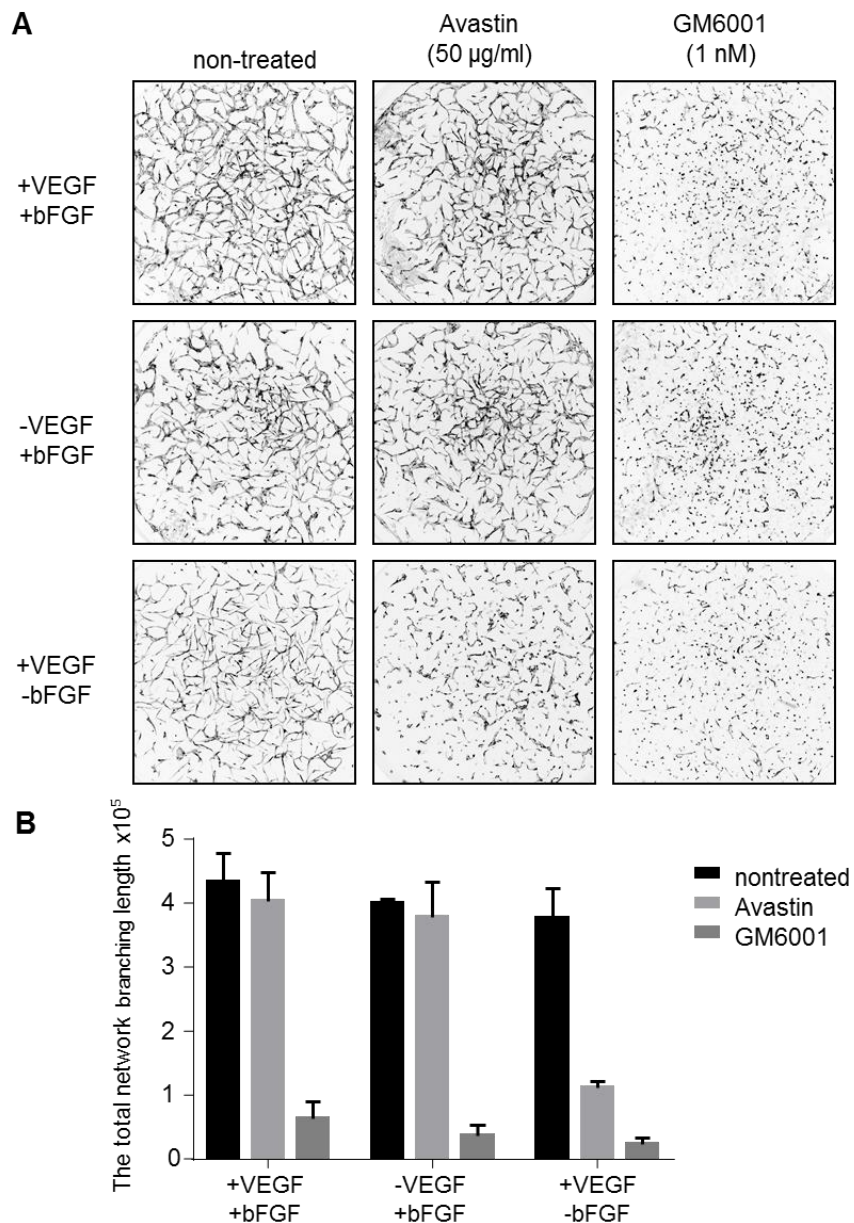


Figure A.4 3D HUVEC/HDF co-culture assay depends on the VEGF/bFGF signalling pathway and MMP-mediated ECM degradation. GFP transduced HUVEC were mixed with fibroblasts and embedded in the fibrin matrix. Cells were cultured in different media (a complete EBM-2 containing both VEGF/bFGF, EBM-2 with VEGF and without bFGF or EBM-2 with bFGF and without VEGF) in the presence of the inhibitors Avastin (VEGF inhibitor) or GM6001 (general MMP inhibitor). Non-treated cells were used as a control. A) Representative images of the network at day 10. Images were taken using a fluorescence microscope (2x magnification) and inverted to a white background for a better visualisation of the network. B) The total network branching length determined for different media conditions. The experiment was performed once in triplicates (N=1; n=3).

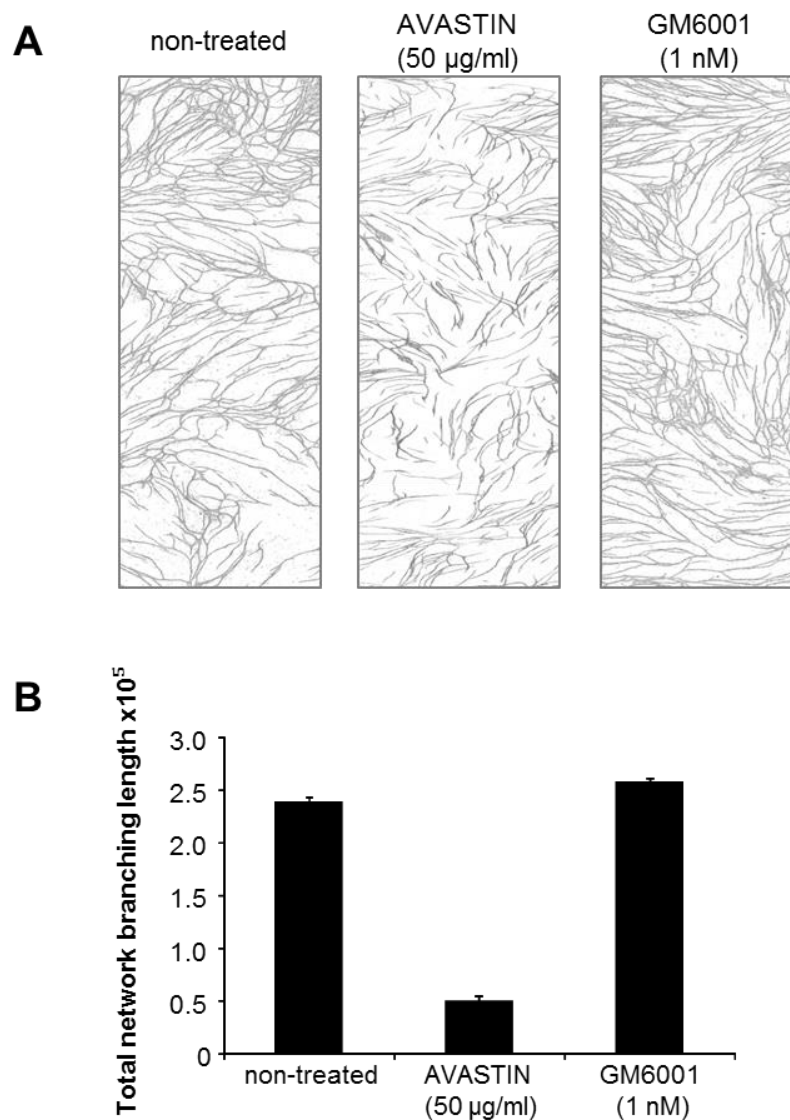


Figure A.5 2D HUVEC/HDF co-culture assay depends on the VEGF signalling pathway but it does not require MMP-mediated ECM degradation. HUVEC were seeded on top of fibroblast monolayer. Cells were cultured in a complete EBM-2 medium containing both VEGF and bFGF in the presence of Avastin (VEGF inhibitor) or GM6001 (general MMP inhibitor) at the concentration of 50 µg/ml and 1 nM, respectively. Non-treated cells were used as a control. A) Representative images (5x magnification) of the network at day 6. Images were taken using a light microscope. B) The total network branching length determined for different conditions. The experiment was performed once in triplicates (N=1; n=3).

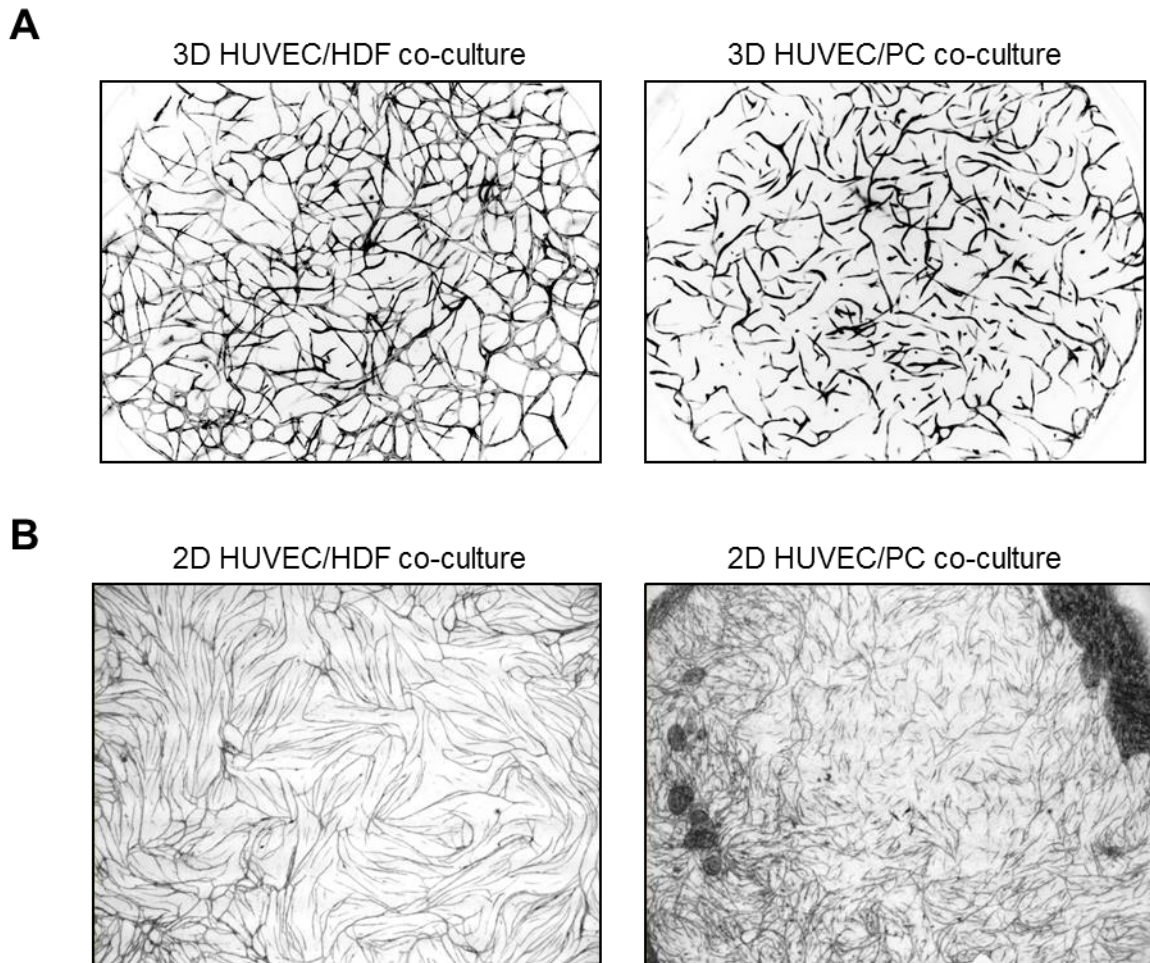


Figure A.6 Human pericytes support HUVEC network formation in both 3D and 2D co-culture assays. A) GFP transduced HUVEC were mixed either with HDF or PC, embedded in the fibrin matrix and cultured in a complete EBM-2 medium. Representative images of the network at day 10. Images were taken using a fluorescence microscope and inverted to a white background for a better visualisation of the network. B) HUVEC were seeded on top of a confluent monolayer of HDF or PC. Representative images of the network at day 6. Images were taken using a light microscope. In all cases, each image represents a whole well. The experiments were performed several times with similar results.

>hPCDH7 FL-FLAG (1077 aa)

MLRMRTAGWARGWCLGCLLLLPLSLSLAAAKQLLRYRLAEEGPADVRIGNVASDLGIVTGSSEVTFSLSESGSEYLKIDNLTGELSTSERRI
DREKLPQCCMIFDENECFLDFEVSVIGPSQSWVDLFEQVIVLDINDNTPTFPSVLTLTVEENRVPVGTLYLLPTATDRDFGRNGIERYELL
QEPGGGGSGGESRRAGAADSAPYPGGGGNGASGGGGSGSKRRLDASEGGGGTNPGRSSVFLQVADTPDGEKQPQLIVKGALDRE
QRDSYELTLRVRDGGDPPRSSQAILRVLITDVNDNSPRFEKSVYEADLAENSAPGTPILQLRAADLDVGVNGQIEYVFGAATESVRRLLRL
DETSGLVSVLHRIDREEVNQLRFTVMARDRGQPPKTDKATVVLNIKDEDNVPSIEIRKIGRIPLKDGVANVAEDVLVDTPIALVQVSDRDQ
GENGVVTCVVGDPVFPKLPASDTEGDQNKKKYFLHTSTPLDYEATREFNVIVAVDVGSPSLSSNNSLIVKVGDTNDNPPMFGQSVVEV
YFPENNIPGERVATVLTADDSGKNAEIAYSLDSSVMGIFAIDPDSGDILVNTVLDREQTDREYEFKVNADKDGIPVLOGSTTVIVQVADKND
NDPKFMQDVFTFYVKENLQPNSPVGMVTVMDADKGRNAEMSLYIEENNNIFSIENTGTIYSTMSFDREHQTTYTRVKAVDGGDPPRSA
TATVSLFVMDENDNAPTTLVLPKNISYTLPPSSNVRTVVATVLTADSDDGINADLNYSIVGGNPFKLFEDPTSGVVSLVGLTKQHYGLHRL
VVQVNDSSGQPSQSTTLVHVFNESVSNATAIDSQIARSLHIPLTQDIAGDPSYEISKQRLS**IVIGVAVAGIMTVILILIVVMARYCRSKNKNGY**
EAGKDHEDFFTPQQHDKSKPKKDKKKNKSKQPLYSSIVTVEASKPNQRYDSVNEKLSDSPSMGRYRSVNGGPGSPDLARHYKSSS
PLPTVQLHPQSPTAGKKHQAVQDLPPANTFVAGAGDNISIGSDHCSEYSCQTNNKYSQMRLHPYITVFGDYKDDDDK

>hPCDH7 C7-Fc (1114 aa)

MLRMRTAGWARGWCLGCLLLLPLSLSLAAAKQLLRYRLAEEGPADVRIGNVASDLGIVTGSSEVTFSLSESGSEYLKIDNLTGELSTSERRI
DREKLPQCCMIFDENECFLDFEVSVIGPSQSWVDLFEQVIVLDINDNTPTFPSVLTLTVEENRVPVGTLYLLPTATDRDFGRNGIERYELL
QEPGGGGSGGESRRAGAADSAPYPGGGGNGASGGGGSGSKRRLDASEGGGGTNPGRSSVFLQVADTPDGEKQPQLIVKGALDRE
QRDSYELTLRVRDGGDPPRSSQAILRVLITDVNDNSPRFEKSVYEADLAENSAPGTPILQLRAADLDVGVNGQIEYVFGAATESVRRLLRL
DETSGLVSVLHRIDREEVNQLRFTVMARDRGQPPKTDKATVVLNIKDEDNVPSIEIRKIGRIPLKDGVANVAEDVLVDTPIALVQVSDRDQ
GENGVVTCVVGDPVFPKLPASDTEGDQNKKKYFLHTSTPLDYEATREFNVIVAVDVGSPSLSSNNSLIVKVGDTNDNPPMFGQSVVEV
YFPENNIPGERVATVLTADDSGKNAEIAYSLDSSVMGIFAIDPDSGDILVNTVLDREQTDREYEFKVNADKDGIPVLOGSTTVIVQVADKND
NDPKFMQDVFTFYVKENLQPNSPVGMVTVMDADKGRNAEMSLYIEENNNIFSIENTGTIYSTMSFDREHQTTYTRVKAVDGGDPPRSA
TATVSLFVMDENDNAPTTLVLPKNISYTLPPSSNVRTVVATVLTADSDDGINADLNYSIVGGNPFKLFEDPTSGVVSLVGLTKQHYGLHRL
VVQVNDSSGQPSQSTTLVHVFNESVSNATAIDSQIARSLHIPLTQDIAGDPSYEISKQR**GSSSSEPKSCDKTHTCPPCPAPELLGGPSVFL**
FPPKPKDTLMISRTPEVTCVVDVSHEDPEVKFNWYVDGVEVHNAKTKPREEQYNSTYR VVSVLTVLHQDWLNGKEYKCKVSNKALPAPI
EKTISKAKGQPREPQVYTLPPSRDELTKNQVSLTCLVKGFYPSDIAVEWESNGQPENNYKTPPVLDSDGSFFLYSKLTVDKSRWQQGNV
FSCVMHEALHNHYTQKSLSPGK

>hPCDH7 C5-Fc (876 aa)

MLRMRTAGWARGWCLGCLLLLPLSLSLAAAKQLLRYRLAEEGPADVRIGNVASDLGIVTGSSEVTFSLSESGSEYLKIDNLTGELSTSERRI
DREKLPQCCMIFDENECFLDFEVSVIGPSQSWVDLFEQVIVLDINDNTPTFPSVLTLTVEENRVPVGTLYLLPTATDRDFGRNGIERYELL
QEPGGGGSGGESRRAGAADSAPYPGGGGNGASGGGGSGSKRRLDASEGGGGTNPGRSSVFLQVADTPDGEKQPQLIVKGALDRE
QRDSYELTLRVRDGGDPPRSSQAILRVLITDVNDNSPRFEKSVYEADLAENSAPGTPILQLRAADLDVGVNGQIEYVFGAATESVRRLLRL
DETSGLVSVLHRIDREEVNQLRFTVMARDRGQPPKTDKATVVLNIKDEDNVPSIEIRKIGRIPLKDGVANVAEDVLVDTPIALVQVSDRDQ
GENGVVTCVVGDPVFPKLPASDTEGDQNKKKYFLHTSTPLDYEATREFNVIVAVDVGSPSLSSNNSLIVKVGDTNDNPPMFGQSVVEV
YFPENNIPGERVATVLTADDSGKNAEIAYSLDSSVMGIFAIDPDSGDILVNTVLDREQTDREYEFKVNADKDGIPVLOGSTTVIVQVADKND
NDPKFG**S**SSSEPKSCDKTHTCPPCPAPELLGGPSVFLFPPKPKDTLMISRTPEVTCVVDVSHEDPEVKFNWYVDGVEVHNAKTKPREE
QYNSTYR VVSVLTVLHQDWLNGKEYKCKVSNKALPAPIEKTISKAKGQPREPQVYTLPPSRDELTKNQVSLTCLVKGFYPSDIAVEWESN
GQPENNYKTPPVLDSDGSFFLYSKLTVDKSRWQQGNV**F**SCVMHEALHNHYTQKSLSPGK

>hPCDH7 C3-Fc (652 aa)

MLRMRTAGWARGWCLGCLLLLPLSLSLAAAKQLLRYRLAEEGPADVRIGNVASDLGIVTGSSEVTFSLSESGSEYLKIDNLTGELSTSERRI
DREKLPQCCMIFDENECFLDFEVSVIGPSQSWVDLFEQVIVLDINDNTPTFPSVLTLTVEENRVPVGTLYLLPTATDRDFGRNGIERYELL
QEPGGGGSGGESRRAGAADSAPYPGGGGNGASGGGGSGSKRRLDASEGGGGTNPGRSSVFLQVADTPDGEKQPQLIVKGALDRE
QRDSYELTLRVRDGGDPPRSSQAILRVLITDVNDNSPRFEKSVYEADLAENSAPGTPILQLRAADLDVGVNGQIEYVFGAATESVRRLLRL
DETSGLVSVLHRIDREEVNQLRFTVMARDRGQPPKTDKATVVLNIKDEDNVPSI**GSSSSEPKSCDKTHTCPPCPAPELLGGPSVFLFPP**
KPKDTLMISRTPEVTCVVDVSHEDPEVKFNWYVDGVEVHNAKTKPREEQYNSTYR VVSVLTVLHQDWLNGKEYKCKVSNKALPAPIEKT
ISKAKGQPREPQVYTLPPSRDELTKNQVSLTCLVKGFYPSDIAVEWESNGQPENNYKTPPVLDSDGSFFLYSKLTVDKSRWQQGNVFS
CSVMHEALHNHYTQKSLSPGK

>hPCDH7 C1-Fc (380 aa)

MLRMRTAGWARGWCLGCLLLLPLSLSLAAAKQLLRYRLAEEGPADVRIGNVASDLGIVTGSSEVTFSLSESGSEYLKIDNLTGELSTSERRI
DREKLPQCCMIFDENECFLDFEVSVIGPSQSWVDLFEQVIVLDINDNTP**F****GSSSSEPKSCDKTHTCPPCPAPELLGGPSVFLFPPKPKD**
TLMISRTPEVTCVVDVSHEDPEVKFNWYVDGVEVHNAKTKPREEQYNSTYR VVSVLTVLHQDWLNGKEYKCKVSNKALPAPIEKTISK
KGQPREPQVYTLPPSRDELTKNQVSLTCLVKGFYPSDIAVEWESNGQPENNYKTPPVLDSDGSFFLYSKLTVDKSRWQQGNVFS
CSVMHEALHNHYTQKSLSPGK

>hFc (237 aa)

GSSSSEPKSCDKTHTCPPCPAPELLGGPSVFLFPPKPKDTLMISRTPEVTCVVDVSHEDPEVKFNWYVDGVEVHNAKTKPREEQYN
YR VVSVLTVLHQDWLNGKEYKCKVSNKALPAPIEKTISKAKGQPREPQVYTLPPSRDELTKNQVSLTCLVKGFYPSDIAVEWESNGQPEN
NYKTPPVLDSDGSFFLYSKLTVDKSRWQQGNVFSCSVMHEALHNHYTQKSLSPGK

Figure A.7 Amino acid sequences of hPCDH7 FL-FLAG and the hPCDH7 ECD-Fc fusion proteins. Different colours of font highlight the signal peptide (green), the ECD fragments (black), the hFc fragment (red), the TM (orange), the ICD (blue) and FLAG (pink).

>mPCDH7 ECD-Fc (1087 aa)

MLRMRTTGWARGWCLGCCLLLPLCFSLAAAKQLLRYRLAEEGPADVRIQNVASDLGIVTGSSEVTFSLSESGSEYKIDNLTGELSTSERRI
DREKLPQCQMIFDENECLDFEVSIGPSQSWVDLFEGRVIVLDINDNTPTFPSPVLTLTVEENRPVGTLYLLPTATDRDFGRNGIERYELL
QEPGGGGGSGEGRRLLGPADSAPYPGGGGNSASGGGGSGGSKRRLDAPEGGGGTSPSGRSSVFELQVADTPDGEKQPQLIVKQALDRE
QRDSYELTLRVRDGGDPPRSSQAILRVLITDVNDNSPRFEKSVYEADLAENSAPGTPILQLRATDLVGVNGQIEYVFGAATESVRRLLRL
DETSWLSVLHRIDREEVQLRFTVMARDRGQPPKTDKATVVLNIKDENDNVPSIEIRKIGRIPLKDGVANVAEDVLVDTPIALVQVSDRD
QGENGVTCTVVGDPFQLKPADTEGDQNKKKYFLHTSAPLDYETTRETNVIVAVDSGSPSLSSNNSLVVKGDTNDNPPVFGQSVV
EYYPENNIPGERVATVLTADSGKNAEIAYSLDSSVMGTFAIDPDSGDILVNTVLDREQTDRYEFKVNADKGIPLVQGSTTVIVQVADK
NDNDPKFMQDVFTFYVKENLQPNPVMGTVMADKGRNAEMSLYIEENSIFSIENDTGTIYSTMSFDREHQTTYFRVKAVDGGDPP
RSATATVSLFVMDENDNAPTIVLPRNISTLLPPSSNVRTVVATVLTADSDGINADLNYSIVGGNPFKLEIDSTSGVSLVGLTKQKHYG
LHRLVVQVNDSGQPSQSTTTLVHVFVNESVSNATVIDSQIVRSLHTPLTQDIAGDPSYEISKQRGGRGSSSEPKSCDKTHTCPPCPAPE
LLGGPSVFLFPPKPKDTLMISRTPEVTCVVVDVSHEDPEVKFNWYVDGVEVHNAKTKPREEQYNSTYRVVSVLTVLHQDWLNGKEYKCK
VSNKALPAPIEKTISKAKGQPREPQVYTLPPSRDELTKNQVSLTCLVKGFYPSDIAVEWESNGQPENNYKTPPVLDSDGSFFLYSKLTVD
KSRWQQGNVFCFSVMHEALHNHYTQKLSLSLSPGK

>mPCDH7 ECD-His (873 aa)

MLRMRTTGWARGWCLGCCLLLPLCFSLAAAKQLLRYRLAEEGPADVRIQNVASDLGIVTGSSEVTFSLSESGSEYKIDNLTGELSTSERRI
DREKLPQCQMIFDENECLDFEVSIGPSQSWVDLFEGRVIVLDINDNTPTFPSPVLTLTVEENRPVGTLYLLPTATDRDFGRNGIERYELL
QEPGGGGGSGEGRRLLGPADSAPYPGGGGNSASGGGGSGGSKRRLDAPEGGGGTSPSGRSSVFELQVADTPDGEKQPQLIVKQALDRE
QRDSYELTLRVRDGGDPPRSSQAILRVLITDVNDNSPRFEKSVYEADLAENSAPGTPILQLRATDLVGVNGQIEYVFGAATESVRRLLRL
DETSWLSVLHRIDREEVQLRFTVMARDRGQPPKTDKATVVLNIKDENDNVPSIEIRKIGRIPLKDGVANVAEDVLVDTPIALVQVSDRD
QGENGVTCTVVGDPFQLKPADTEGDQNKKKYFLHTSAPLDYETTRETNVIVAVDSGSPSLSSNNSLVVKGDTNDNPPVFGQSVV
EYYPENNIPGERVATVLTADSGKNAEIAYSLDSSVMGTFAIDPDSGDILVNTVLDREQTDRYEFKVNADKGIPLVQGSTTVIVQVADK
NDNDPKFMQDVFTFYVKENLQPNPVMGTVMADKGRNAEMSLYIEENSIFSIENDTGTIYSTMSFDREHQTTYFRVKAVDGGDPP
RSATATVSLFVMDENDNAPTIVLPRNISTLLPPSSNVRTVVATVLTADSDGINADLNYSIVGGNPFKLEIDSTSGVSLVGLTKQKHYG
LHRLVVQVNDSGQPSQSTTTLVHVFVNESVSNATVIDSQIVRSLHTPLTQDIAGDPSYEISKQRVSEGGKPIPNLLGLDSTRTGHHHHHH

Figure A.8 Amino acid sequences of the mPCDH7 ECD(C7)-Fc and the mPCDH7 ECD(C7)-His fusion proteins. Different colours of font highlight the signal peptide (green), the ECD (black), the hFc fragment (red), His tag (pink) and linker (blue).

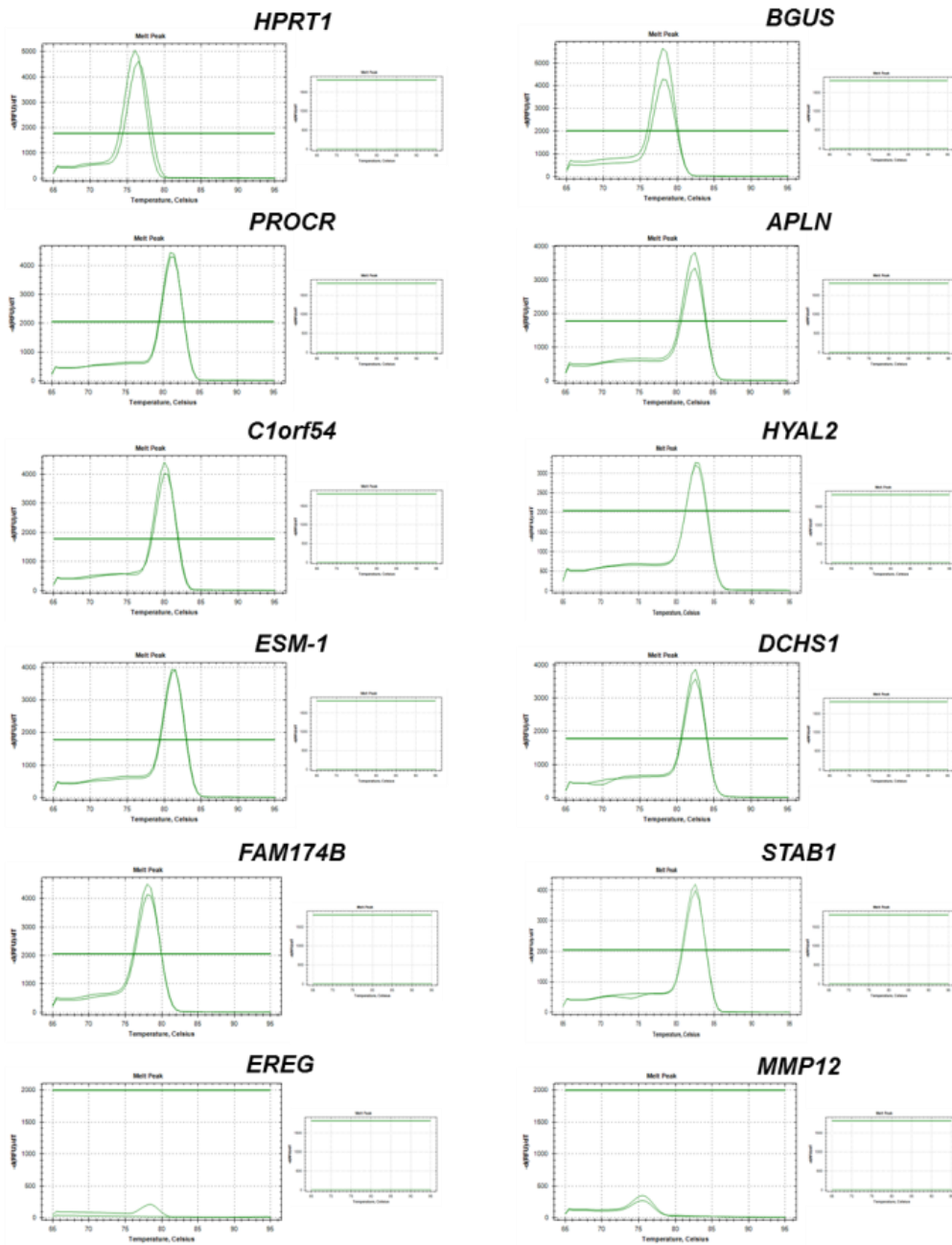
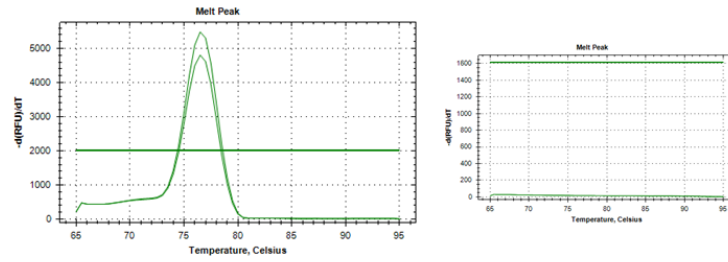
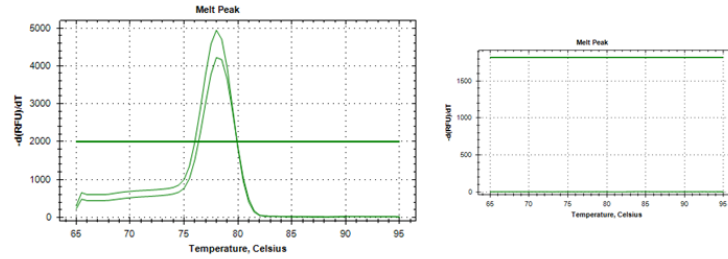


Figure A.9 Melting curves of gene specific qPCR primers. Representative images of melting curves for gene specific qPCR primers. Reactions were performed on HUVEC cDNA (larger images) and HUVEC –RT control (smaller images), in duplicates for every sample.

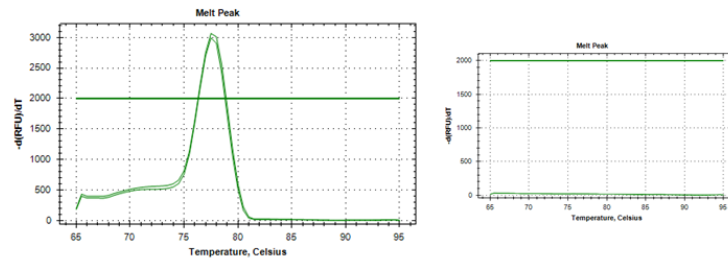
HPRT1



BGUS



EREG



MMP12

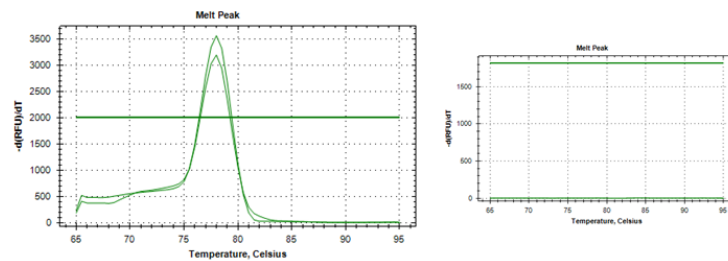
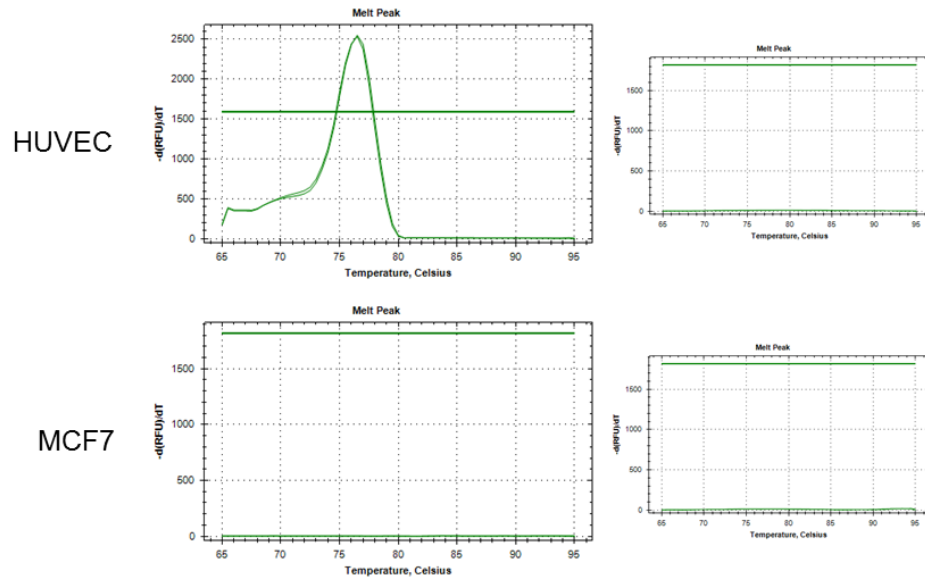


Figure A.10 Melting curves of *EREG* and *MMP12* specific qPCR primers. Representative images of melting curves for *EREG* and *MMP12* specific qPCR primers. Reactions were performed on MCF7 cDNA (larger images) and MCF7 -RT control (smaller images), in duplicates for every sample.

ANGPT2



EpCAM

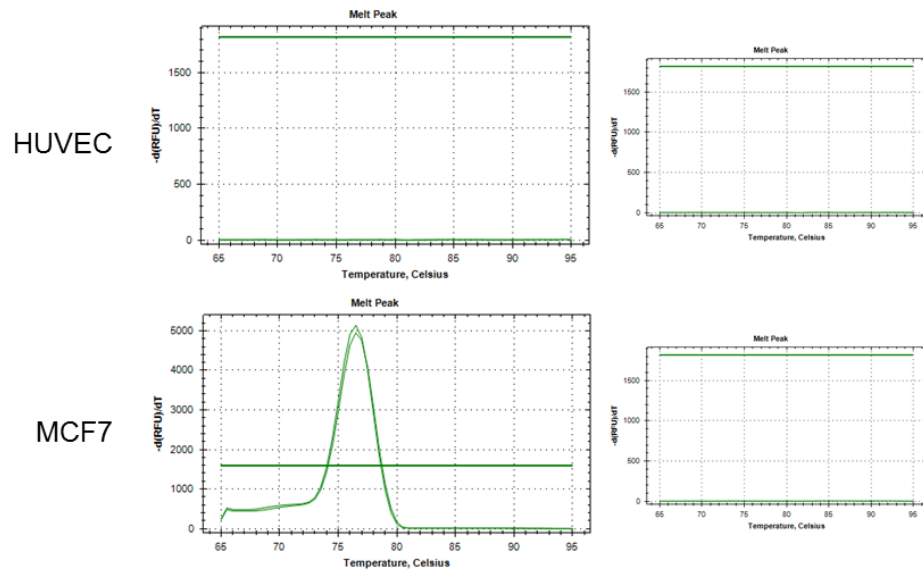


Figure A.11 Melting curves of *ANGPT2* and *EpCAM* specific qPCR primers. Representative images of melting curves for *ANGPT2* and *EpCAM* specific qPCR primers. Reactions were performed on HUVEC and MCF7 cDNA (larger images) and HUVEC and MCF7 –RT control (smaller images), in duplicates for every sample.

Sample normal/tumour		Nanodrop measurements		
		RNA concentration (ng/ μ l)	280/260 ratio	260/230 ratio
NEC	Normal endothelial cells	53	1.77	1.35
TEC1	Tumour endothelial cells – sample 1	30	1.81	0.42
TEC2	Tumour endothelial cells – sample 2	12	1.9	0.02
TEC3	Tumour endothelial cells – sample 3	26	2.01	0.05
NEpiC1	Normal epithelial cells – sample 1	16	2.0	0.19
NEpiC2	Normal epithelial cells – sample 2	126	2.0	1.9
NEpiC3	Normal epithelial cells – sample 3	81	1.7	1.8
NEpiC4	Normal epithelial cells – sample 4	37	2.0	1.2
TEpiC1	Tumour epithelial cells – sample 1	233	1.9	2.0
TEpiC2	Tumour epithelial cells – sample 2	486	2.0	1.8
TEpiC3	Tumour epithelial cells – sample 3	51	1.8	1.0
TEpiC4	Tumour epithelial cells – sample 4	34	1.7	1.3

Figure A.12 Yield and purity of normal and tumour endothelial and epithelial samples provided by SomantiX used for qPCR reaction. NEC – normal endothelial cells; TEC – tumour endothelial cells; NEpiC – normal epithelial cells; TEpiC – tumour epithelial cells.

REFERENCES

Abraham, S., Yeo, M., Montero-Balaguer, M., Paterson, H., Dejana, E., Marshall, C. J., Mavria, G. (2009) 'VE-Cadherin-Mediated Cell-Cell Interaction Suppresses Sprouting via Signaling to MLC2 Phosphorylation', *Current Biology*, 19(8), pp. 668-674 doi: 10.1016/j.cub.2009.02.057.

Adachi, H., Tsujimoto, M. (2002) 'FEEL-1, a novel scavenger receptor with in vitro bacteria-binding and angiogenesis-modulating activities', *Journal of Biological Chemistry*, 277(37), pp. 34264–34270, doi: 10.1074/jbc.M204277200.

Albini, A., Benelli, R., Noonan, D. M., Brigati, C. (2004) 'The "chemoinvasion assay": a tool to study tumor and endothelial cell invasion of basement membranes.', *The International journal of developmental biology*, 48(5-6), pp. 563-571, doi: 10.1387/ijdb.041822aa.

Antón, I., Molina, E., Luis-Ravelo, D., Zanduetta, C., Valencia, K., Ormazabal, C., Martínez-Canarias, S., Peruena, N., Pajares, M. J., Agorreta, J., Montuenga, L. M., Segura, V., Wistuba, I. I., De Las Rivas, J., Hermida, J., Lecanda, F. (2012) 'Receptor of activated protein C promotes metastasis and correlates with clinical outcome in lung adenocarcinoma.', *American journal of respiratory and critical care medicine*, 186(1), pp. 96-105, doi: 10.1164/rccm.201110-1826OC.

Araujo, T. L. S., Zeidler, J. D., Oliveira, P. V. S., Dias, M. H., Armelin, H. A., Laurindo, F. R. M. (2017) 'Protein disulfide isomerase externalization in endothelial cells follows classical and unconventional routes', *Free Radical Biology and Medicine*. 103(2016), pp. 199–208, doi: 10.1016/j.freeradbiomed.2016.12.021.

Auerbach, R., Lewis, R., Shinnars, B., Kubai, L., Akhtar, N. (2003) 'Angiogenesis Assays: A Critical Overview', *Clinical Chemistry*, 40, pp. 32–40, doi: 10.1373/49.1.32.

Back, M., Dahlen, S.-E., Drazen, J. M., Evans, J. F., Serhan, C. N., Shimizu, T., Smitzu, T., Rovati, G. E. (2011) 'International Union of Basic and Clinical Pharmacology. LXXXIV: Leukotriene Receptor Nomenclature, Distribution, and Pathophysiological Functions', *Pharmacological Reviews*, 63(3), pp. 539–584, doi: 10.1124/pr.110.004184.

Bae, Y. H., Park, K., Mrsny, R. J. (2013) *Cancer targeted drug delivery: An elusive dream*, Springer New York, doi: 10.1007/978-1-4614-7876-8.

Beaulieu, L. M., Church, F. C. (2007) 'Activated protein C promotes breast cancer cell migration through interactions with EPCR and PAR-1', *Experimental Cell Research*, 313(4) pp. 677-687 doi: 10.1016/j.yexcr.2006.11.019.

Bergers, G., Benjamin, L. E. (2003) 'Tumorigenesis and the angiogenic switch', *Nature Reviews Cancer*, 3(6), pp. 401–410. doi: 10.1038/nrc1093.

Bezuhyly, M., Cullen, R., Esmon, C. T., Morris, S. F., West, K. a., Johnston, B., Liwski, R. S. (2009) 'Role of activated protein C and its receptor in inhibition of tumor metastasis', *Blood*, 113(14), pp. 3371–3374. doi: 10.1182/blood-2008-05-159434.

Bielenberg, D. R., Zetter, B. R., Program, V. B. (2016) 'The contribution of

angiogenesis to the process of metastasis', *Cancer Journal (US)*, 21(4), pp. 267–273. doi: 10.1097/PPO.000000000000138.The.

Bishop, E. T., Bell, G. T., Bloor, S., Broom, I. J., Hendry, N. F. K., Wheatley, D. N. (1999) 'An in vitro model of angiogenesis: Basic features', *Angiogenesis*, 3(4), pp. 335-344, doi: 10.1023/A:1026546219962.

Biswas, S., Emond, M. R., Jontes, J. D. (2010) 'Protocadherin-19 and N-cadherin interact to control cell movements during anterior neurulation', *Journal of Cell Biology*, 191(5), pp. 1029–1041. doi: 10.1083/jcb.201007008.

Blevins, C. J., Emond, M. R., Biswas, S., Jontes, J. D. (2011) 'Differential expression, alternative splicing, and adhesive properties of the zebrafish $\delta 1$ -protocadherins', *Neuroscience*, 199, pp. 523–534. doi: 10.1016/j.neuroscience.2011.09.061.

Bradley, R. S., Espeseth, A., Kintner, C. (1998) 'NF-protocadherin, a novel member of the cadherin superfamily, is required for *Xenopus* ectodermal differentiation', *Current Biology*, 8(6), pp. 325-334, doi: 10.1016/S0960-9822(98)70132-0.

Brooke, M. A., Nitoiu, D., Kelsell, D. P. (2012) 'Cell-cell connectivity: Desmosomes and disease', *Journal of Pathology*, 226(2), pp. 158–171. doi: 10.1002/path.3027.

Bujko, M., Kober, P., Mikula, M., Ligaj, M., Ostrowski, J., Siedlecki, J. A. (2015) 'Expression changes of cell-cell adhesion-related genes in colorectal tumors', *Oncology Letters*, 9(6), pp. 2463–2470. doi: 10.3892/ol.2015.3107.

Burrows, F. J., Derbyshire, E. J., Tazzari, P. L., Amlot, P., Gazdar, F., King, S. W., Letarte, M., Vitetta, E. S., Thorpe, P. E. (1995) 'Up-regulation of endoglin on vascular endothelial cells in human solid tumors: implications for diagnosis and therapy.', *Clinical cancer research: an official journal of the American Association for Cancer Research*, 1(12), pp. 1623-1634.

Bushell, K. M., Söllner, C., Schuster-Boeckler, B., Bateman, A., Wright, G. J. (2008) 'Large-scale screening for novel low-affinity extracellular protein interactions', *Genome Research*, 18(4), pp. 622-630, doi: 10.1101/gr.7187808.

Camaj, P., Seeliger, H., Ischenko, I., Krebs, S., Blum, H., De Toni, E. N., Faktorova, D., Jauch, K. W., Bruns, C. J. (2009) 'EFEMP1 binds the EGF receptor and activates MAPK and Akt pathways in pancreatic carcinoma cells', *Biological Chemistry*, 390(12), pp. 1293-1302, doi: 10.1515/BC.2009.140.

Carmeliet, P., Jain, R. K. (2011) 'Molecular mechanisms and clinical applications of angiogenesis', *Nature*. doi: 10.1038/nature10144.

Carnemolla, B., Balza, E., Siri, A., Zardi, L., Nicotra, M. R., Bigotti, A., Natali, P. G. (1989) 'A tumor-associated fibronectin isoform generated by alternative splicing of messenger RNA precursors', *Journal of Cell Biology*, 108(3), pp. 1139–1148. doi: 10.1083/jcb.108.3.1139.

Carrizo, M. (2017) 'Loss of E-Cadherin Expression and Epithelial Mesenchymal Transition (EMT) as Key Steps in Tumor Progression', *Journal of Cancer Prevention*

& *Current Research*, 7(3), pp. 1-6, doi: 10.15406/jcpcr.2017.07.00235.

Casanovas, O., Hicklin, D. J., Bergers, G., Hanahan, D. (2005) 'Drug resistance by evasion of antiangiogenic targeting of VEGF signaling in late-stage pancreatic islet tumors', *Cancer Cell*, 8(4), pp. 299-309, doi: 10.1016/j.ccr.2005.09.005.

Chabot, S., Jabrane-Ferrat, N., Bigot, K., Tabiasco, J., Provost, A., Golzio, M., Noman, M. Z., Giustiniani, J., Bellard, E., Brayer, S., Aguerre-Girr, M., Megetto, F., Giuriato, S., Malecaze, F., Galiacy, S., Jais, J-P., Chose, O., Kadouche, J., Chouaib, S., Teissie, J., Abitbol, M., Bensussan, A., Le Bouteiller, P. (2011) 'A novel antiangiogenic and vascular normalization therapy targeted against human CD160 receptor', *The Journal of Experimental Medicine*, 208(5), pp. 973–986. doi: 10.1084/jem.20100810.

Chaudhary, A., Hilton, M. B., Seaman, S., Haines, D. C., Lemotte, P. K., Tschantz, W. R., Zhang, X. M., Fleming, T., St. Croix, B. (2013) 'TEM8/ANTXR1 Blockade Inhibits Pathological Angiogenesis and Potentiates Tumoricidal Responses against Multiple Cancer Types', 21(2), pp. 212–226. doi: 10.1016/j.ccr.2012.01.004.TEM8/ANTXR1.

Chen, H. F., Ma, R. R., He, J. Y., Zhang, H., Liu, X. L., Guo, X. Y., Gao, P. (2017) 'Protocadherin 7 inhibits cell migration and invasion through E-cadherin in gastric cancer', *Tumor Biology*, 39(4), doi: 10.1177/1010428317697551

Chen, J., Wei, D., Zhao, Y., Liu, X., Zhang, J. (2013) 'Overexpression of EFEMP1 correlates with tumor progression and poor prognosis in human ovarian carcinoma', *PLoS One*, 8(11), doi: 10.1371/journal.pone.0078783.

Chen, L. Y., Liu, X., Wang, S. L., Qin, C. Y. (2010) 'Over-expression of the Endocan gene in endothelial cells from hepatocellular carcinoma is associated with angiogenesis and tumour invasion', *Journal of International Medical Research*, 38(2), pp. 498-510, doi: 10.1177/147323001003800213.

Chen, M. W., Vacherot, F., De la Taille, A., Gil-Diez-de-Medina, S., Shen, R., Friedman, Burchardt, M., Chopin, D. K., R. A., Buttyan, R. (2002) 'The emergence of protocadherin-PC expression during the acquisition of apoptosis-resistance by prostate cancer cells', *Oncogene*, 21(51), pp. 7861-7871, doi: 10.1038/sj.onc.1205991.

Chen, Q., Boire, A., Jin, X., Valiente, M., Er, E. E., Lopez-Soto, A., Jacob, L. S., Patwa, R., Shah, H., Xu, K., Cross, J. R., Massague, J. (2016) 'Carcinoma-astrocyte gap junctions promote brain metastasis by cGAMP transfer', *Nature*, 533(7604), pp. 493-498, doi: 10.1038/nature18268.

Chen, X., Gumbiner, B. M. (2006) 'Paraxial protocadherin mediates cell sorting and tissue morphogenesis by regulating C-cadherin adhesion activity', *Journal of Cell Biology*, 174(2), pp. 301–313. doi: 10.1083/jcb.200602062.

Chidgey, M., Garrod, D. (2016) 'Desmosomal Cadherins', in *The Cadherin Superfamily: Key Regulators of Animal Development and Physiology*, Springer Japan, pp.159-193, doi: 10.1007/978-4-431-56033-3_7.

Chung, A. S., Ferrara, N. (2011) 'Developmental and Pathological Angiogenesis', *Annual Review of Cell and Developmental Biology*, 27(1), pp. 563–584. doi: 10.1146/annurev-cellbio-092910-154002.

Clarke, J. D., Zhu, T. (2006) 'Microarray analysis of the transcriptome as a stepping stone towards understanding biological systems: practical considerations and perspectives', *The plant journal: for cell and molecular biology*, 45(4), pp. 630–650. doi: 10.1111/j.1365-313X.2006.02668.x.

Czekierdowski, A., Stachowicz, N., Czekierdowska, S., Lozinski, T., Gurynowicz, G., Kluz, T. (2018) 'Prognostic significance of TEM7 and nestin expression in women with advanced high grade serous ovarian cancer.', *Ginekologia polska*, 89(3), pp. 135–141. doi: <https://dx.doi.org/10.5603/GP.a2018.0023>.

Dou, C. Y., Cao, C. J., Wang, Z., Zhang, R. H., Huang, L. L., Lian, J. Y., Xie, W. L., Wang, L. T. (2016) 'EFEMP1 inhibits migration of hepatocellular carcinoma by regulating MMP2 and MMP9 via ERK1/2 activity', *Oncology Reports*, 35(6), pp. 3489–3495. doi: 10.3892/or.2016.4733.

Eccles, S. A., Court, W., Patterson, L., Sanderson, S. (2009) 'In vitro assays for endothelial cell functions related to angiogenesis: proliferation, motility, tubular differentiation, and proteolysis.', *Methods in molecular biology (Clifton, N.J.)*, 467, pp.159-181, doi: 10.1007/978-1-59745-241-0_9.

Emmott, E., Goodfellow, I. (2014) 'Identification of Protein Interaction Partners in Mammalian Cells Using SILAC-immunoprecipitation Quantitative Proteomics', *Journal of Visualized Experiments*, 89, pp. 1–8. doi: 10.3791/51656.

Emond, M., Biswas, S., Blevins, C., Jontes, J.D. (2011) 'A complex of protocadherin-19 and N-cadherin mediates a novel mechanism of cell adhesion', *Journal of Cell Biology*, 195(7), pp. 1115-1121

Essler, M., Ruoslahti, E. (2002) 'Molecular specialization of breast vasculature: A breast-homing phage-displayed peptide binds to aminopeptidase P in breast vasculature', *Proceedings of the National Academy of Sciences*, 99(4), pp. 2252-2257, doi: 10.1073/pnas.251687998.

Faura Tellez, G., Willemse, B. W. M., Brouwer, U., Nijboer-Brinksma, S., Vandepoele, K., Noordhoek, J. A., Heijink, I., de Vries, M., Smithers, N. P., Postma, D. S., Timens, W., Wiffenm L., van Roy, F., Holloway, J. W., Lackie, P. M., Nawijm, M. C., Koppelman, G. H. (2016) 'Protocadherin-1 Localization and Cell-Adhesion Function in Airway Epithelial Cells in Asthma', *Plos One*, 11(10), p. e0163967. doi: 10.1371/journal.pone.0163967.

Favre, C. J., Mancuso, M., Maas, K., McLean, J. W., Baluk, P., McDonald, D. M. (2003) 'Expression of genes involved in vascular development and angiogenesis in endothelial cells of adult lung', *American Journal of Physiology - Heart and Circulatory Physiology*, 285(5), pp. H1917-H1938, doi: 10.1152/ajpheart.00983.2002.

Flaumenhaft, R., Furie, B. (2016) 'Vascular thiol isomerases', *Blood*, 128(7), pp. 893-901, doi: 10.1182/blood-2016-04-636456.

Ghilardi, C., Chiorino, G., Dossi, R., Nagy, Z., Giavazzi, R., Bani, M. R. (2008) 'Identification of novel vascular markers through gene expression profiling of tumor-derived endothelium', *BMC Genomics*, 9(201), doi: 10.1186/1471-2164-9-201.

Gill, J. H., Loadman, P. M., Shnyder, S. D., Cooper, P., Atkinson, J. M., Ribeiro Morais, G., Patterson, L. H., Falconer, R. A. (2014) 'Tumor-targeted prodrug ICT2588 demonstrates therapeutic activity against solid tumors and reduced potential for cardiovascular toxicity', *Molecular Pharmaceutics*, 11(4), pp. 1294-1300, doi: 10.1021/mp400760b.

Goerdts, S., Bhardwaj, R., Sorg, C. (1993) 'Inducible expression of MS-1 high-molecular-weight protein by endothelial cells of continuous origin and by dendritic cells/macrophages in vivo and in vitro.', *The American journal of pathology*, 142(5), pp. 1409–22.

Gorrin-Rivas, M. J., Arai, S., Furutani, M., Mizumoto, M., Mori, A., Hanaki, K., Maeda, M., Furuyama, H., Kondo, Y., Imamura, M. (2000) 'Mouse macrophage metalloelastase gene transfer into a murine melanoma suppresses primary tumor growth by halting angiogenesis', *Clinical Cancer Research*, 6(5), pp. 1647-1654.

Gumbiner, B. M. (2016) 'Classical Cadherins', in *The Cadherin Superfamily: Key Regulators of Animal Development and Physiology*, Springer Japan, pp. 41-70, doi: 10.1007/978-4-431-56033-3_3.

Guo, Y., Hu, J., Wang, Y., Peng, X., Min, J., Wang, J., Matthaiou, E., Cheng, Y., Sun, K., Tong, X., Fan, Y., Zhang, P. J., Kandalaf, L. E., Inrving, M., Coucos, G., Li, C. (2018) 'Tumour endothelial marker 1/endosialin-mediated targeting of human sarcoma', *European Journal of Cancer*, 90, pp. 111–121. doi: 10.1016/j.ejca.2017.10.035.

Han, A. L., Veeneman, B. A., El-Sawy, L., Day, K. C., Day, M. L., Tomlins, S. A., Keller, E. T. (2017) 'Fibulin-3 promotes muscle-invasive bladder cancer', *Oncogene*, 36(37), pp. 5243–5251. doi: 10.1038/onc.2017.149.

Hanahan, D., Folkman, J. (1996) 'Patterns and emerging mechanisms of the angiogenic switch during tumorigenesis', *Cell*, 86(3), pp. 353-364, doi: 10.1016/S0092-8674(00)80108-7.

Hanahan, D., Weinberg, R. A. (2000) 'The hallmarks of cancer.', *Cell*, 100(1), pp. 57-70, doi: 10.1007/s00262-010-0968-0.

Hayashi, S., Takeichi, M. (2015) 'Emerging roles of protocadherins: from self-avoidance to enhancement of motility', *Journal of Cell Science*, 128(8), pp. 1455–1464. doi: 10.1242/jcs.166306.

Herbert, J. M. J., Stekel, D., Sanderson, S., Heath, V. L., Bicknell, R. (2008) 'A novel method of differential gene expression analysis using multiple cDNA libraries applied to the identification of tumour endothelial genes.', *BMC genomics*, 9(153), doi: 10.1186/1471-2164-9-153.

Hetheridge, C., Mavria, G., Mellor, H. (2011) 'Uses of the *in vitro* endothelial–

fibroblast organotypic co-culture assay in angiogenesis research', *Biochemical Society Transactions*, 39(6), pp. 1597-1600, doi: 10.1042/BST20110738.

Hoeben, A., Landuyt, B., Highley, M. S., Wildiers, H., Van Oosterom, A. T., De Bruijn, E. A. (2004) 'Vascular endothelial growth factor and angiogenesis.', *Pharmacological reviews*, 56(4), pp. 549-580, doi: 10.1124/pr.56.4.3.549.

Hollebecque, A., Massard, C., Soria, J. C. (2012) 'Vascular disrupting agents: A delicate balance between efficacy and side effects', *Current Opinion in Oncology*, 24(3), pp. 305-315, doi: 10.1097/CCO.0b013e32835249de.

Homan, C. C., Pederson, S., To, T. H., Tan, C., Piltz, S., Corbett, M. A., Wolvetang, E., Thomas, P. Q., Jolly, L. A., Gecz, J. (2018) 'PCDH19 regulation of neural progenitor cell differentiation suggests asynchrony of neurogenesis as a mechanism contributing to PCDH19 Girls Clustering Epilepsy', *Neurobiology of Disease*, 116, pp. 106-119, doi: 10.1016/j.nbd.2018.05.004.

Hong, H., Severin, G. W., Yang, Y., Engle, J. W., Zhang, Y., Barnhart, T. E., Liu, G., Leigh, B. R., Nickles, R. J., Cai, W. (2012) 'Positron emission tomography imaging of CD105 expression with 89Zr-Df-TRC105', *European Journal of Nuclear Medicine and Molecular Imaging*, 39(1), 138-148, doi: 10.1007/s00259-011-1930-x.

Hoshina, N., Tanimura, A., Yamasaki, M., Inoue, T., Fukabori, R., Kuroda, T., Yokoyama, K., Tezuka, T., Sagara, H., Hirano, S., Kiyonari, H., Takada, M., Kobayashi, K., Watanabe, M., Kano, M., Nakazawa, T., Yamamoto, T. (2013) 'Protocadherin 17 regulates presynaptic assembly in topographic corticobasal ganglia circuits', *Neuron*, 78(5), pp. 839-854, doi: 10.1016/j.neuron.2013.03.031.

Hu, B., Thirtamara-Rajamani, K. K., Sim, H., Viapiano, M. S. (2009) 'Fibulin-3 is uniquely upregulated in malignant gliomas and promotes tumor cell motility and invasion.', *Molecular cancer research*, 7(11), pp. 1756-1770, doi: 10.1158/1541-7786.MCR-09-0207.

Huang, G.-W., Tao, Y.-M., Ding, X. (2009) 'Endocan expression correlated with poor survival in human hepatocellular carcinoma.', *Digestive diseases and sciences*, 54(2), pp. 389-94, doi: 10.1007/s10620-008-0346-3.

Hulpiau, P., Gul, I. S., Van Roy, F. (2016) 'Evolution of Cadherins and associated catenins', in *The Cadherin Superfamily: Key Regulators of Animal Development and Physiology*, Springer Japan, pp. 13-37, doi: 10.1007/978-4-431-56033-3_2.

Humniecki, L., Gorn, M., Suchting, S., Poulsom, R., Bicknell, R. (2002a) 'Magic roundabout is a new member of the roundabout receptor family that is endothelial specific and expressed at sites of active angiogenesis', *Genomics*, 79(4), pp. 547-552. doi: 10.1006/geno.2002.6745.

Humniecki, L., Bicknell, R. (2000) 'In silico cloning of novel endothelial-specific genes', *Genome Research*, 10(11), pp. 1796-1806, doi: 10.1101/gr.150700.

Hurwitz, H., Fehrenbacher, L., Novotny, W., Cartwright, T., Hainsworth, J., Heim, W., Berlin, J., Baron, A., Griffing, S., Holmgren, E., Ferrara, N., Fyfe, G., Rogers, B.,

Ross, R., Kabbinavar, F. (2004) 'Bevacizumab plus irinotecan, fluorouracil, and leucovorin for metastatic colorectal cancer.', *The New England Journal of Medicine*, 350, pp. 2335-2342, doi: 10.1056/NEJMoa032691.

Jain, R. K. (2005) 'Normalization of tumor vasculature: An emerging concept in antiangiogenic therapy', *Science*, 307(5706), pp. 58-62, doi: 10.1126/science.1104819.

Jontes, J. D. (2016) 'The nonclustered protocadherins', in *The Cadherin Superfamily: Key Regulators of Animal Development and Physiology*, Springer Japan, pp. 223-250, doi: 10.1007/978-4-431-56033-3_9.

Junghans, D., Heidenreich, M., Hack, I., Taylor, V., Frotscher, M., Kemler, R. (2008) 'Postsynaptic and differential localization to neuronal subtypes of protocadherin beta16 in the mammalian central nervous system.', *The European journal of neuroscience*, 27(3), pp. 557-571, doi: 10.1111/j.1460-9568.2008.06052.x.

Karikoski, M., Marttila-Ichihara, F., Elima, K., Rantakari, P., Hollmén, M., Kelkka, T., Gerke, H., Huovinen, V., Irjala, H., Holmdahl, R., Salmi, M., Jalkanen, S. (2014) 'Clever-1/stabilin-1 controls cancer growth and metastasis', *Clinical Cancer Research*, 20(24), pp. 6452–6464. doi: 10.1158/1078-0432.CCR-14-1236.

Khan, K. A., Naylor, A. J., Khan, A., Noy, P. J., Mambretti, M., Lodhia, P., Athwal, J., Korzystka, A., Buckley, C. D., Wilcox, B. E., Mohammed, F., Bicknell, R. (2017) 'Multimerin-2 is a ligand for group 14 family C-type lectins CLEC14A, CD93 and CD248 spanning the endothelial pericyte interface', *Oncogene*, 36(44), pp. 6097-6108, doi: 10.1038/onc.2017.214.

Kidoya, H., Kunii, N., Naito, H., Muramatsu, F., Okamoto, Y., Nakayama, T., Takakura, N. (2012) 'The apelin/APJ system induces maturation of the tumor vasculature and improves the efficiency of immune therapy', *Oncogene*, 31(27), pp. 3254–3264. doi: 10.1038/onc.2011.489.

Kim, S. Y., Yasuda, S., Tanaka, H., Yamagata, K., Kim, H. (2011) 'Non-clustered protocadherin', *Cell Adhesion and Migration*, 5(2), pp. 97-105, doi: 10.4161/cam.5.2.14374.

Kong, D. H., Kim, M. R., Jang, J. H., Na, H. J., Lee, S. (2017) 'A review of anti-angiogenic targets for monoclonal antibody cancer therapy', *International Journal of Molecular Sciences*, 18(8), pp. 1–25. doi: 10.3390/ijms18081786.

Kraft, B., Berger, C. D., Wallkamm, V., Steinbeisser, H., Wedlich, D. (2012) 'Wnt-11 and Fz7 reduce cell adhesion in convergent extension by sequestration of PAPC and C-cadherin', *Journal of Cell Biology*, 198(4), pp. 695-709, doi: 10.1083/jcb.201110076.

Kuo, F., Histed, S., Xu, B., Bhadrasetty, V., Szajek, L. P., Williams, M. R., Wong, K., Wu, H., Lane, K., Coble, V., Vasalaty, O., Griffiths, G. L., Paik, C. H., Elbuluk, O., Szot, C., Chaudhary, A., St. Croix, B., Choyke, P., Jagoda, E. M. (2014) 'Immuno-PET imaging of tumor endothelial Marker 8 (TEM8)', *Molecular Pharmaceutics*, 11(11), pp. 3996–4006. doi: 10.1021/mp500056d.

- Kzhyskowska, J., Gratchev, A., Goerdts, S. (2006) 'Stabilin-1, a homeostatic scavenger receptor with multiple functions', *Journal of Cellular and Molecular Medicine*, 10(3), pp. 635–649. doi: 10.1111/j.1582-4934.2006.tb00425.x.
- Lafleur, M. A., Handsley, M. M., Knäuper, V., Murphy, G., Edwards, D. R. (2002) 'Endothelial tubulogenesis within fibrin gels specifically requires the activity of membrane-type-matrix metalloproteinases (MT-MMPs).', *Journal of cell science*, 115(17), pp. 3427–38. doi: 10.1038/35036374.
- Lahav, J., Gofer-Dadosh, N., Luboshitz, J., Hess, O., Shaklai, M. (2000) 'Protein disulfide isomerase mediates integrin-dependent adhesion', *FEBS Letters*, 475(2), pp. 89-92, doi: 10.1016/S0014-5793(00)01630-6.
- Lai, C.-Y., Chen, C.-M., Hsu, W.-H., Hsieh, Y.-H., Liu, C.-J. (2017) 'Overexpression of Endothelial Cell-Specific Molecule 1 Correlates with Gleason Score and Expression of Androgen Receptor in Prostate Carcinoma', *International Journal of Medical Sciences*, 14(12), pp. 1263–1267. doi: 10.7150/ijms.21023.
- Lane, T. F., Iruela-Arispe, M. L., Johnson, R. S., Sage, E. H. (1994) 'SPARC is a source of copper-binding peptides that stimulate angiogenesis', *Journal of Cell Biology*, 125(4), pp. 929-943, doi: 10.1083/jcb.125.4.929.
- Laurenzana, A., Biagioni, A., D'Alessio, S., Bianchini, F., Chillà, A., Margheri, F., Luciani, C., Mazzanti, B., Pimpinelli, N., Torre, E., Danese, S., Calorini, L., Del Rosso, M., Fibbi, G. (2014) 'Melanoma cell therapy: Endothelial progenitor cells as shuttle of the MMP12 uPAR-degrading enzyme.', *Oncotarget*, 5(11), pp. 3711-3727, doi: 10.18632/oncotarget.1987.
- Lefebvre, J. L. (2017) 'Neuronal territory formation by the atypical cadherins and clustered protocadherins', *Seminars in Cell and Developmental Biology*, 69, pp. 111–121. doi: 10.1016/j.semcdb.2017.07.040.
- Li, A.-M., Tian, A.-X., Zhang, R.-X., Ge, J., Sun, X., Cao, X.-C. (2013) 'Protocadherin-7 induces bone metastasis of breast cancer', *Biochemical and Biophysical Research Communications*, 436(3), pp. 486-490, doi: 10.1016/j.bbrc.2013.05.131.
- Lin, H., Lee, E., Hestir, K., Leo, C., Huang, M., Bosch, E., Halenbeck, R., Wu, G., Zhou, A., Behrens, D., Hollenbaugh, D., Linnemann, T., Qin, M., Wong, J., Chu, K., Doberstein, S. K., Williams, L. T. (2008) 'Discovery of a cytokine and its receptor by functional screening of the extracellular proteome', *Science*, 32(5877), pp. 807-811, doi: 10.1126/science.1154370.
- Lin, L.-Y., Yeh, Y.-C., Chu, C.-H., Won, J. G. S., Shyr, Y.-M., Chao, Y., Li, C.-P., Wang, S.-E., Chen, M.-H. (2017) 'Endocan expression is correlated with poor progression-free survival in patients with pancreatic neuroendocrine tumors', *Medicine*, 96(41), p. e8262. doi: 10.1097/MD.00000000000008262.
- Lin, Y.-L., Wang, Y.-L., Fu, X.-L., Li, W.-P., Wang, Y.-H., Ma, J.-G. (2016) 'Low expression of protocadherin7 (PCDH7) is a potential prognostic biomarker for primary non-muscle invasive bladder cancer', *Oncotarget*, 7(19), pp. 28384–28392. doi:

10.18632/oncotarget.8635.

Liu, B., Archer, C. T., Burdine, L., Gillette, T. G., Kodadek, T. (2007) 'Label transfer chemistry for the characterization of protein-protein interactions', *Journal of the American Chemical Society*, 129(41), pp. 12348-12349, doi: 10.1021/ja072904r.

Lv, F.-Z., Wang, J.-L., Wu, Y., Chen, H.-F., Shen, X.-Y. (2015) 'Knockdown of MMP12 inhibits the growth and invasion of lung adenocarcinoma cells.', *International journal of immunopathology and pharmacology*, 28(1), pp. 77–84. doi: 10.1177/0394632015572557.

Lyden, D., Hattori, K., Dias, S., Costa, C., Blaikie, P., Butros, L., Chadburn, A., Heissig, B., Marks, W., Witte, L., Wu, Y., Hicklin, D., Zhu, Z., Hackett, N. R., Crystal, R. G., Moore, M. A. S., Hajjar, K. A., Manova, K., Benezra, R., Rafii, S. (2001) 'Impaired recruitment of bone-marrow-derived endothelial and hematopoietic precursor cells blocks tumor angiogenesis and growth', *Nature Medicine*, 7(11), pp. 1194-1201, doi: 10.1038/nm1101-1194.

Lyons, S., Marnane, M., Reavey, E., Williams, N., Costello, D. (2017) 'PCDH19-related epilepsy: A rare but recognisable clinical syndrome in females', *Practical Neurology*, 17(4), pp. 314-317, doi: 10.1136/practneurol-2016-001521.

Mah, K. M., Weiner, J. A. (2016) 'Clustered protocadherins', in *The Cadherin Superfamily: Key Regulators of Animal Development and Physiology*, Springer Japan, pp.195-222, doi: 10.1007/978-4-431-56033-3_8.

Manjunath, N., Wu, H., Subramanya, S., Shankar, P. (2009) 'Lentiviral delivery of short hairpin RNAs', *Advanced Drug Delivery Reviews*, 61(9), pp. 732-745, doi: 10.1016/j.addr.2009.03.004.

Masiero, M., Simões, F. C., Han, H. D., Snell, C., Peterkin, T., Bridges, E., Mangala, L. S., Wu, S. Y. Y., Pradeep, S., Li, D., Han, C., Dalton, H., Lopez-Berestein, G., Tuynman, J. B., Mortensen, N., Li, J. L., Patient, R., Sood, A. K., Banham, A. H., Harris, A. L., Buffa, F. M. (2013) 'A core human primary tumor angiogenesis signature identifies the endothelial orphan receptor ELTD1 as a key regulator of angiogenesis', *Cancer Cell*, 24(2), pp. 229-241, doi: 10.1016/j.ccr.2013.06.004.

Mavria, G., Vercoulen, Y., Yeo, M., Paterson, H., Karasarides, M., Marais, R., Bird, D., Marshall, C. J. (2006) 'ERK-MAPK signaling opposes Rho-kinase to promote endothelial cell survival and sprouting during angiogenesis', *Cancer Cell*, 9(1), pp. 33–44. doi: 10.1016/j.ccr.2005.12.021.

Mayer, R. J. (2004) 'Two steps forward in the treatment of colorectal cancer.', *The New England journal of medicine*, 350(23), pp. 2406-2408, doi: 10.1056/NEJMe048098.

Mentzer, S. J., Konerding, M. A. (2014) 'Intussusceptive angiogenesis: Expansion and remodeling of microvascular networks', *Angiogenesis*, 17(3), pp. 499-509, doi: 10.1007/s10456-014-9428-3.

Mita, M. M., Sargsyan, L., Mita, A. C., Spear, M. (2013) 'Vascular-disrupting agents in

oncology', *Expert Opinion on Investigational Drugs*, 22(3), pp. 317–328. doi: 10.1517/13543784.2013.759557.

Mura, M., Swain, R. K., Zhuang, X., Vorschmitt, H., Reynolds, G., Durant, S., Beesley, J. F. J., Herbet, J. M. J., Sheldon, H., Andre, M., Sanderson, S., Glen, K., Luu, N. T., McGettrick, H. M., Antczak, P., Falciani, F., Nash, G. B., Nagy Z. S., Bicknell, R. (2012) 'Identification and angiogenic role of the novel tumor endothelial marker CLEC14A', *Oncogene*, 31(3), pp. 293-305, doi: 10.1038/onc.2011.233.

Nagy, J. A., Chang, S. H., Dvorak, A. M., Dvorak, H. F. (2009) 'Why are tumour blood vessels abnormal and why is it important to know?', *British Journal of Cancer*, 100(6), pp. 865-869, doi: 10.1038/sj.bjc.6604929.

Nicholson, B. E., Frierson, H. F., Conaway, M. R., Seraj, J. M., Harding, M. A., Hampton, G. M., Theodorescu, D. (2004) 'Profiling the evolution of human metastatic bladder cancer', *Cancer Research*, 64(21), pp. 7812-7821, doi: 10.1158/0008-5472.CAN-04-0826.

Noy, P. J., Lodhia, P., Khan, K., Zhuang, X., Ward, D. G., Verissimo, A. R., Bacon, A., Bicknell, R. (2015) 'Blocking CLEC14A-MMRN2 binding inhibits sprouting angiogenesis and tumour growth', *Oncogene*, 34(47), pp. 5821-5831, doi: 10.1038/onc.2015.34.

O'Reilly, M. S., Holmgren, L., Shing, Y., Chen, C., Rosenthal, R. A., Moses, M., Lane, W., S., Cao, Y., Sage, E. H., Folkman, J. (1994) 'Angiostatin: A novel angiogenesis inhibitor that mediates the suppression of metastases by a lewis lung carcinoma', *Cell*, 79(2), pp. 315-328, doi: 10.1016/0092-8674(94)90200-3.

Oh, P., Li, Y., Yu, J., Durr, E., Krasinska, K. M., Carver, L. A., Testa, J. E., Schnitzer, J. E. (2004) 'Subtractive proteomic mapping of the endothelial surface in lung and solid tumours for tissue-specific therapy', *Nature*, 429(6992), pp. 629–635. doi: 10.1038/nature02580.

Özlü, N., Qureshi, M. H., Toyoda, Y., Renard, B. Y., Mollaoglu, G., Özkan, N. E., Bulbul, S., Poser, I., Timm, W., Hyman, A. A., Mitchison, T. J., Steen, J. A. (2015) 'Quantitative comparison of a human cancer cell surface proteome between interphase and mitosis.', *The EMBO journal*, 34(2), pp. 251-265, doi: 10.15252/embj.201385162.

De Palma, M., Biziato, D., Petrova, T. V. (2017) 'Microenvironmental regulation of tumour angiogenesis', *Nature Reviews Cancer*, 17(8), pp. 457–474. doi: 10.1038/nrc.2017.51.

Piper, M., Dwivedy, A., Leung, L., Bradley, R. S., Holt, C. E. (2008) 'NF-protocadherin and TAF1 regulate retinal axon initiation and elongation in vivo.', *The Journal of neuroscience: the official journal of the Society for Neuroscience*, 28(1), pp. 100–5. doi: 10.1523/JNEUROSCI.4490-07.2008.

Poduri, A. (2015) 'Meta-analysis revives genome-wide association studies in epilepsy', *Epilepsy Currents*, 15(3), pp. 122-123, doi: 10.5698/1535-7597-15.3.122.

- Potente, M., Gerhardt, H., Carmeliet, P. (2011) 'Basic and therapeutic aspects of angiogenesis', *Cell*, 146(6), pp. 873–887. doi: 10.1016/j.cell.2011.08.039.
- Rao, L. V. M., Esmon, C. T., Pendurthi, U. R. (2014) 'Endothelial cell protein C receptor: A multiliganded and multifunctional receptor', *Blood*, 124(10), pp. 1553-1562, doi: 10.1182/blood-2014-05-578328.
- Rapisarda, A., Melillo, G. (2009) 'Role of the hypoxic tumor microenvironment in the resistance to anti-angiogenic therapies', *Drug Resistance Updates*, 12(3), pp. 74-80, doi: 10.1016/j.drug.2009.03.002.
- Rashid, D., Newell, K., Shama, L., Bradley, R. (2006) 'A requirement for NF-protocadherin and TAF1/Set in cell adhesion and neural tube formation', *Developmental Biology*, 291(1), pp. 170–181. doi: 10.1016/j.ydbio.2005.12.027.
- Redies, C., Vanhalst, K., Van Roy, F. (2005) 'δ-Protocadherins: Unique structures and functions', *Cellular and Molecular Life Sciences*, 62(23), pp. 2840-2852, doi: 10.1007/s00018-005-5320-z.
- Ren, D., Zhu, X., Kong, R., Zhao, Z., Sheng, J., Wang, J., Xu, X., Liu, J., Cui, K., Zhang, X. H. F., Zhao, H., Wong, S. T. C. (2018) 'Targeting brain-adaptive cancer stem cells prohibits brain metastatic colonization of triple-negative breast cancer', *Cancer Research*, 78(8), pp. 2052–2064. doi: 10.1158/0008-5472.CAN-17-2994.
- Rennel, E., Mellberg, S., Dimberg, A., Petersson, L., Botling, J., Ameer, A., Westholm, J. O., Komorowski, J., Lassaile, P., Cross, M. J., Gerwins, P. (2007) 'Endocan is a VEGF-A and PI3K regulated gene with increased expression in human renal cancer', *Experimental Cell Research*, 313(7), pp. 1285-1294, doi: 10.1016/j.yexcr.2007.01.021.
- Rettig, W. J., Garin-Chesa, P., Healey, J. H., Su, S. L., Jaffe, E. A., Old, L. J. (1992) 'Identification of endosialin, a cell surface glycoprotein of vascular endothelial cells in human cancer.', *Proceedings of the National Academy of Sciences of the United States of America*, 89(22), pp. 10832-10836.
- Ribatti, D., Crivellato, E. (2012) "Sprouting angiogenesis", a reappraisal', *Developmental Biology*. Elsevier, 372(2), pp. 157–165. doi: 10.1016/j.ydbio.2012.09.018.
- Riese, D. J., Cullum, R. L. (2014) 'Epiregulin: Roles in normal physiology and cancer', *Seminars in Cell and Developmental Biology*, 28, pp. 49-56, doi: 10.1016/j.semcd.2014.03.005.
- Rocha, S. F., Schiller, M., Jing, D., Li, H., Butz, S., Vestweber, D., Biljes, D., Drexler, H. C. A., Nieminen-Kelha, M., Vajkoczy, P., Adams, R. H. (2014) 'Esm1 modulates endothelial tip cell behavior and vascular permeability by enhancing VEGF bioavailability', *Circulation Research*, 115(6), pp. 581-590, doi: 10.1161/CIRCRESAHA.115.304718.
- Rubinstein, R., Thu, C. A., Goodman, K. M., Wolcott, H. N., Bahna, F., Manneppalli, S., Ahlsen, G., Chevee, M., Halim, A., Clausen, H., Maniatis, T., Shapiro, L., Honig,

B. (2015) 'Molecular Logic of Neuronal Self-Recognition through Protocadherin Domain Interactions', *Cell*, 163(3), pp. 629-642, doi: 10.1016/j.cell.2015.09.026.

Sage, E. H., Reed, M., Funk, S. E., Truong, T., Steadele, M., Puolakkainen, P., Maurice, D. H., Bassuk, J. A. (2003) 'Cleavage of the matricellular protein SPARC by matrix metalloproteinase 3 produces polypeptides that influence angiogenesis', *Journal of Biological Chemistry*, 278(39), pp. 37849-37857, doi: 10.1074/jbc.M302946200.

Saito, M., Tucker, D. K., Kohlhorst, D., Niessen, C. M., Kowalczyk, A. P. (2012) 'Classical and desmosomal cadherins at a glance', *Journal of Cell Science*, 125(11), pp. 2547–2552. doi: 10.1242/jcs.066654.

Salmi, M., Koskinen, K., Henttinen, T., Elima, K., Jalkanen, S. (2004) 'CLEVER-1 mediates lymphocyte transmigration through vascular and lymphatic endothelium', *Blood*, 104(13), pp. 3849–3857. doi: 10.1182/blood-2004-01-0222.

Schliemann, C., Neri, D. (2007) 'Antibody-based targeting of the tumor vasculature.', *Biochimica et biophysica acta*, 1776(2), pp. 175-192, doi: 10.1016/j.bbcan.2007.08.002.

Schreiner, D., Weiner, J. A. (2010) 'Combinatorial homophilic interaction between - protocadherin multimers greatly expands the molecular diversity of cell adhesion', *Proceedings of the National Academy of Sciences*, 1078, pp. 14893-14898, doi: 10.1073/pnas.1004526107.

Seeliger, H., Camaj, P., Ischenko, I., Kleespies, A., De Toni, E. N., Thieme, S. E., Blum, H., Assmann, G., Jauch, K.-W., Bruns, C. J. (2009) 'EFEMP1 Expression Promotes In vivo Tumor Growth in Human Pancreatic Adenocarcinoma', *Molecular Cancer Research*, 7(2), pp. 189–198. doi: 10.1158/1541-7786.MCR-08-0132.

Shapiro, L., Weis, W. I. (2009) 'Structure and biochemistry of cadherins and catenins.', *Cold Spring Harbor perspectives in biology*, 1(3), doi: 10.1101/cshperspect.a003053.

Shojaei, F. (2012) 'Anti-angiogenesis therapy in cancer: Current challenges and future perspectives', *Cancer Letters*. Elsevier Ireland Ltd, 320(2), pp. 130–137. doi: 10.1016/j.canlet.2012.03.008.

Siemann, D. W. (2004) 'Therapeutic strategies that selectively target and disrupt established tumor vasculature', *Hematology/Oncology Clinics of North America*, 100(12), pp. 2491-2499, doi: 10.1016/j.hoc.2004.06.012.

Siemann, D. W. (2011) 'The unique characteristics of tumor vasculature and preclinical evidence for its selective disruption by Tumor-Vascular Disrupting Agents', *Cancer Treatment Reviews*, 37(1), pp. 63-74, doi: 10.1016/j.ctrv.2010.05.001.

Siemann, D. W., Chaplin, D. J., Horsman, M. R. (2004) 'Vascular-targeting therapies for treatment of malignant disease', *Cancer*, 100(12), pp. 2491–2499. doi: 10.1002/cncr.20299.

- Siemann, D. W., Chaplin, D. J., Horsman, M. R. (2017) 'Realizing the Potential of Vascular Targeted Therapy: The Rationale for Combining Vascular Disrupting Agents and Anti-Angiogenic Agents to Treat Cancer', *Cancer Investigation*, 35(8), pp. 519–534. doi: 10.1080/07357907.2017.1364745.
- Song, E. L., Hou, Y. P., Yu, S. P., Chen, S. G., Huang, J. T., Luo, T., Kong, L. P., Xu, J., Wang, H. Q. (2011) 'EFEMP1 expression promotes angiogenesis and accelerates the growth of cervical cancer in vivo', *Gynecologic Oncology*, 121(1), pp. 174-180, doi: 10.1016/j.ygyno.2010.11.004.
- Sorli, S. C., Le Gonidec, S., Knibiehler, B., Audigier, Y. (2007) 'Apelin is a potent activator of tumour neoangiogenesis', *Oncogene*, 26(55), pp. 7692-7699, doi: 10.1038/sj.onc.1210573.
- Staton, C.A., Lewis, C., Bicknell, R. (2006) *Angiogenesis Assays: A Critical Appraisal of Current Techniques*, John Wiley & Sons.
- St. Croix, B. (2000) 'Genes Expressed in Human Tumor Endothelium', *Science*, 289(5482), pp. 1197-1202, doi: 10.1126/science.289.5482.1197.
- Subbiah, I. M., Lenihan, D. J., Tsimberidou, A. M. (2011) 'Cardiovascular Toxicity Profiles of Vascular-Disrupting Agents', *The Oncologist*, 16(8), pp. 1120-1130, doi: 10.1634/theoncologist.2010-0432.
- Sun, X.-T., Ding, Y.-T., Yan, X.-G., Wu, L.-Y., Li, Q., Cheng, N., Qiu, Y.-D., Zhang, M.-Y. (2004) 'Angiogenic synergistic effect of basic fibroblast growth factor and vascular endothelial growth factor in an in vitro quantitative microcarrier-based three-dimensional fibrin angiogenesis system.', *World Journal of Gastroenterology*, 10(17), pp. 2524–2528. doi: 10.3748/WJG.V10.I17.2524.
- Sun, Y., Gallagher-Jones, M., Barker, C., Wright, G. J. (2012) 'A benchmarked protein microarray-based platform for the identification of novel low-affinity extracellular protein interactions', *Analytical Biochemistry*, 424(1), pp. 45-53, doi: 10.1016/j.ab.2012.01.034.
- Talorete, T. P. N., Bouaziz, M., Sayadi, S., Isoda, H. (2006) 'Influence of medium type and serum on MTT reduction by flavonoids in the absence of cells', *Cytotechnology*, 52(3), pp. 189-198, doi: 10.1007/s10616-007-9057-4.
- Tanaka, L. Y., Araújo, H. A., Hironaka, G. K., Araujo, T. L. S., Takimura, C. K., Rodriguez, A. I., Casagrande, A. S., Gutierrez, P. S., Lemos-Neto, P. A., Laurindo, F. R. M. (2016) 'Peri/Epicellular Protein Disulfide Isomerase Sustains Vascular Lumen Caliber Through an Anticonstrictive Remodeling Effect', *Hypertension*, 67(3), pp. 613–622. doi: 10.1161/HYPERTENSIONAHA.115.06177.
- Tao, L., Huang, G., Song, H., Chen, Y., Chen, L. (2017) 'Cancer associated fibroblasts: An essential role in the tumor microenvironment (review)', *Oncology Letters*, 14(3), pp. 2611-2620, doi: 10.3892/ol.2017.6497.
- Tatemoto, K., Hosoya, M., Habata, Y., Fujii, R., Kakegawa, T., Zou, M. X., Kawamata, Y., Fukusumi, S., Hinuma, S., Kitada, C., Kurokawa, T., Onda, H., Fujino,

M. (1998) 'Isolation and characterization of a novel endogenous peptide ligand for the human APJ receptor', *Biochemical and Biophysical Research Communications*, 251(2), pp. 471-476, doi: 10.1006/bbrc.1998.9489.

Thøgersen, V. B., Sørensen, B. S., Poulsen, S. S., Ørntoft, T. F., Wolf, H., Nexø, E. (2001) 'A subclass of HER1 ligands is a prognostic marker for survival in bladder cancer patients', *Cancer Research*, 61(16), pp. 6227-6233, doi: 10.1158/0008-5472.can-04-0925.

Thorpe, P. E. (2004) 'Vascular Targeting Agents As Cancer Therapeutics', *Clinical Cancer Research*, 10(2), pp. 415-427, doi: 10.1158/1078-0432.CCR-0642-03.

Van Tonder, A., Joubert, A. M., Cromarty, A. D. (2015) 'Limitations of the 3-(4,5-dimethylthiazol-2-yl)-2,5-diphenyl-2H-tetrazolium bromide (MTT) assay when compared to three commonly used cell enumeration assays', *BMC Research Notes*, 8(1), pp. 1–10. doi: 10.1186/s13104-015-1000-8.

Toyoda, H., Komurasaki, T., Uchida, D., Takayama, Y., Isobe, T., Okuyama, T., Hanada, K. (1995) 'Epiregulin. A novel epidermal growth factor with mitogenic activity for rat primary hepatocytes.', *The Journal of biological chemistry*, 270(3), pp. 7495-7500.

Tozer, G. M., Kanthou, C., Baguley, B. C. (2005) 'Disrupting tumour blood vessels', *Nature Reviews Cancer*, 5(6), pp. 423-435, doi: 10.1038/nrc1628.

Trepel, M., Arap, W., Pasqualini, R. (2002) 'In vivo phage display and vascular heterogeneity: Implications for targeted medicine', *Current Opinion in Chemical Biology*, 6(3), pp. 399–404. doi: 10.1016/S1367-5931(02)00336-8.

Uchiba, M., Okajima, K., Oike, Y., Ito, Y., Fukudome, K., Isobe, H., Suda, T. (2004) 'Activated protein C induces endothelial cell proliferation by mitogen-activated protein kinase activation in vitro and angiogenesis in vivo', *Circulation Research*, 95(1), pp. 35-41, doi: 10.1161/01.RES.0000133680.87668.FA.

Vanhalst, K., Kools, P., Staes, K., Van Roy, F., Redies, C. (2005) 'δ-Protocadherins: A gene family expressed differentially in the mouse brain', *Cellular and Molecular Life Sciences*, 62(11), pp. 1247–1259. doi: 10.1007/s00018-005-5021-7.

Vasilatos, S. N., Katz, T. A., Oesterreich, S., Wan, Y., Davidson, N. E., Huang, Y. (2013) 'Crosstalk between lysine-specific demethylase 1 (LSD1) and histone deacetylases mediates antineoplastic efficacy of HDAC inhibitors in human breast cancer cells', *Carcinogenesis*, 34(6), pp. 1196-12017, doi: 10.1093/carcin/bgt033.

Vasilescu, J., Guo, X., Kast, J. (2004) 'Identification of protein-protein interactions using in vivo cross-linking and mass spectrometry', *Proteomics*, 4(12), pp. 3845-3854, doi: 10.1002/pmic.200400856.

Vester-Christensen, M. B., Halim, A., Joshi, H. J., Steentoft, C., Bennett, E. P., Lavery, S. B., Vakhrushev, S. Y., Clausen, H. (2013) 'Mining the O-mannose glycoproteome reveals cadherins as major O-mannosylated glycoproteins', *Proceedings of the National Academy of Sciences*, 110(52), pp. 21018-21023, doi:

10.1073/pnas.1313446110.

Vestweber, D. (2008) 'VE-cadherin: The major endothelial adhesion molecule controlling cellular junctions and blood vessel formation', *Arteriosclerosis, Thrombosis, and Vascular Biology*, 28(2), pp. 223–232. doi: 10.1161/ATVBAHA.107.158014.

Viallard, C., Larrivé, B. (2017) 'Tumor angiogenesis and vascular normalization: alternative therapeutic targets', *Angiogenesis*, 20(4), pp. 409-426, doi: 10.1007/s10456-017-9562-9.

Vincent, P. A., Xiao, K., Buckley, K. M., Kowalczyk, A. P. (2004) 'VE-cadherin: adhesion at arm's length.', *American journal of physiology. Cell physiology*, 286(5), pp. 987-997, doi: 10.1152/ajpcell.00522.2003.

Wakabayashi, T., Matsumine, A., Nakazora, S., Hasegawa, M., Iino, T., Ota, H., Sonoda, H., Sudo, A., Uchida, A. (2010) 'Fibulin-3 negatively regulates chondrocyte differentiation', *Biochemical and Biophysical Research Communications*. Elsevier Inc., 391(1), pp. 1116–1121. doi: 10.1016/j.bbrc.2009.12.034.

Wang, Z., Cao, C.-J., Huang, L.-L., Ke, Z.-F., Luo, C.-J., Lin, Z.-W., Wang, F., Zhang, Y.-Q., Wang, L.-T. (2015) 'EFEMP1 promotes the migration and invasion of osteosarcoma via MMP-2 with induction by AEG-1 via NF-κB signaling pathway.', *Oncotarget*, 6(16), pp. 14191–14208. doi: 10.18632/oncotarget.3691.

Wang, Z., Gerstein, M., Snyder, M. (2009) 'RNA-Seq: A revolutionary tool for transcriptomics', *Nature Reviews Genetics*, 10(1), pp. 57-63, doi: 10.1038/nrg2484.

Weiner, J. A., Jontes, J. D. (2013) 'Protocadherins, not prototypical: a complex tale of their interactions, expression, and functions', *Frontiers in Molecular Neuroscience*, 6(March), pp. 1–10. doi: 10.3389/fnmol.2013.00004.

Weis, S. M., Cheresh, D. A. (2005) 'Pathophysiological consequences of VEGF-induced vascular permeability', *Nature*, 437(7058), pp. 497-504, doi: 10.1038/nature03987.

Wragg, J. (2016) 'Transcriptomic analysis of the tumour vasculature and its clinical relevance', available at: <http://etheses.bham.ac.uk/6544/>

Wragg, J., Finnity, J. P., Anderson, J. A., Ferguson, H. J. M., Porfiri, E., Bhatt, R. I., Murray, P. G., Heath, V. L., Bicknell, R. (2016) 'MCAM and LAMA4 are highly enriched in tumor blood vessels of renal cell carcinoma and predict patient outcome', *Cancer Research*, 76(8), pp. 2314-2326, doi: 10.1158/0008-5472.CAN-15-1364.

Xu, Z., Shi, H., Li, Q., Mei, Q., Bao, J., Shen, Y., Xu, J. (2008) 'Mouse macrophage metalloelastase generates angiostatin from plasminogen and suppresses tumor angiogenesis in murine colon cancer', *Oncology Reports*, 20(1), pp. 81-88.

Yamamoto, M., Wakatsuki, T., Hada, A., Ryo, A. (2001) 'Use of serial analysis of gene expression (SAGE) technology', *Journal of Immunological Methods*, 250(1-2), pp. 46-66, doi: 10.1016/S0022-1759(01)00305-2.

- Yang, W. E., Hsieh, M. J., Lin, C. W., Kuo, C. Y., Yang, S. F., Chuang, C. Y., Chen, M. K. (2017) 'Plasma levels of endothelial cell-specific molecule-1 as a potential biomarker of oral cancer progression', *International Journal of Medical Sciences*, 14(11), pp. 1094–1100. doi: 10.7150/ijms.20414.
- Yang, Y., Lv, S. Y., Ye, W., Zhang, L. (2016) 'Apelin/APJ system and cancer', *Clinica Chimica Acta*. Elsevier B.V., 457, pp. 112–116. doi: 10.1016/j.cca.2016.04.001.
- Yasuda, S., Tanaka, H., Sugiura, H., Okamura, K., Sakaguchi, T., Tran, U., Takemiya, T., Mizoguchi, A., Yagita, Y., Sakurai, T., De Robertis, E. M., Yamagata, K. (2007) 'Activity-Induced Protocadherin Arcadlin Regulates Dendritic Spine Number by Triggering N-Cadherin Endocytosis via TAO2 β and p38 MAP Kinases', *Neuron*, 56(3), pp. 456-471, doi: 10.1016/j.neuron.2007.08.020.
- Yin, X., Fang, S., Wang, M., Wang, Q., Fang, R., Chen, J. (2016) 'EFEMP1 promotes ovarian cancer cell growth, invasion and metastasis via activated the AKT pathway', 7(30). doi: 10.18632/oncotarget.10296.
- Yoshida, K., Yoshitomo-Nakagawa, K., Seki, N., Sasaki, M., Sugano, S. (1998) 'Cloning, expression analysis, and chromosomal localization of BH-protocadherin (PCDH7), a novel member of the cadherin superfamily', *Genomics*, 49(3), pp. 458–461. doi: 10.1006/geno.1998.5271.
- Yoshida, K., Watanabe, M., Kato, H., Dutta, A., Sugano, S. (1999) 'BH-protocadherin-c, a member of the cadherin superfamily, interacts with protein phosphatase 1 alpha through its intracellular domain', *FEBS Letters*, 460(1), pp. 93-98, doi: 10.1016/S0014-5793(99)01309-5.
- Yoshida, K. (2003) 'Fibroblast cell shape and adhesion in vitro is altered by overexpression of the 7a and 7b isoforms of protocadherin 7, but not the 7c isoform', *Cell Mol Biol Lett*, 8(3), pp. 735-741.
- Yu, Q. C., Song, W., Wang, D., Zeng, Y. A. (2016) 'Identification of blood vascular endothelial stem cells by the expression of protein C receptor', *Cell Research*. Nature Publishing Group, 26(10), pp. 1079–1098. doi: 10.1038/cr.2016.85.
- Zhao, N., Qin, Y., Liu, H., Cheng, Z. (2018) 'Tumor-Targeting Peptides: Ligands for Molecular Imaging and Therapy', *Anti-Cancer Agents in Medicinal Chemistry*, 18(1), pp. 74–86. doi: 10.2174/1871520617666170419143459.
- Zhou, X., Updegraff, B. L., Guo, Y., Peyton, M., Girard, L., Larsen, J. E., Xie, X. J., Zhou, Y., Hwang, T. H., Xie, Y., Rodriguez-Canales, J., Vilalobos, P., Behrens, C., Wistuba, I. I., Minna, J. D., O'Donnell, K. A. (2017) 'PROTODADHERIN 7 acts through SET and PP2A to potentiate MAPK signaling by EGFR and KRAS during lung tumorigenesis', *Cancer Research*, 77(1), pp. 187-197, doi: 10.1158/0008-5472.CAN-16-1267-T.
- Zhuang, X., Herbert, J. M. J., Lodhia, P., Bradford, J., Turner, A. M., Newby, P. M., Thickett, D., Naidu, U., Blakey, D., Barry, S., Cross, D.A.E., Bicknell, R. (2015) 'Identification of novel vascular targets in lung cancer', *British Journal of Cancer*, 112(3), pp. 485-94, doi: 10.1038/bjc.2014.626.

Ziegler, J., Pody, R., De Souza, P. C., Evans, B., Saunders, D., Smith, N., Mallory, S., Njoku, C., Dong, Y., Chen, H, Dong, J., Lerner, M., Mian, O., Tummala, S., Battiste, J., Fung, K.M., Wren, J.D., Towner, R. A. (2017) 'ELTD1, an effective anti-angiogenic target for gliomas: Preclinical assessment in mouse GL261 and human G55 xenograft glioma models', *Neuro-Oncology*, 19(2), pp. 175-185, doi: 10.1093/neuonc/now147.

Zuo, L., Zhang, S.-M., Hu, R.-L., Zhu, H.-Q., Zhou, Q., Gui, S.-Y., Wu, Q., Wang, Y. (2008) 'Correlation between expression and differentiation of endocan in colorectal cancer.', *World journal of gastroenterology*, 14(28), pp. 4562-4568, doi: 10.3748/wjg.14.4562.

Zuurbier, L., Rahman, A., Cordes, M., Scheick, J., Wong, T. J., Rustenburg, F., Joseph, J. C., Dynoodt, P., Casey, R., Drillenbur, P., Gerhards, M., Barat, A., Klinger, R., Fender, B., O'Connor, D.P., Betge, J., Ebert, M.P., Gaiser, T., Prehn, J.H.M., Griffioen, A., von Grieken, N., Ylstra, B., Byrne, A.T., van der Flier, L.G., Gallagher, W.M., Postel, R. (2017) 'Apelin: A putative novel predictive biomarker for bevacizumab response in colorectal cancer', *Oncotarget*, 8(26), pp. 42949-42961, doi: 10.18632/oncotarget.17306.

LIST OF ABSTRACTS AND DETAILS OF MEETINGS WHERE WORK CONTAINED IN THIS THESIS WAS PRESENTED

Tumour Microenvironment – Basic Science to Novel Therapies (Including 3D models workshop) Conference

14-16 June 2017 - Nottingham Conference Centre, Nottingham, United Kingdom

Abstract: Extracellular domain of protocadherin 7 (PCDH7)-Fc fusion protein reduces an endothelial network formation *in vitro*

Aleksandra Korzystka, Victoria Heath and Roy Bicknell, Institute of Cardiovascular Sciences, Institute of Biomedical Research, College of Medical and Dental Sciences, University of Birmingham, B15 2TT Birmingham, UK

Vascular targeting is an attractive approach to cancer treatment. Our recently identified lung cancer vascular target, PCDH7 belongs to the cadherin superfamily. Although PCDH7 is present in many types of tumours, its exact function is not fully defined. It was shown to have a role in lung tumourigenesis and promoting brain metastasis. However, its function in the tumour vasculature has not been previously reported. We have shown that PCDH7 siRNA-mediated knockdown in the endothelial cells resulted in reduced network assembly on Matrigel. To further probe the function of PCDH7, the extracellular domain of PCDH7 (PCDH7 ECD) expressed as a fusion protein to Fc was used in a range of *in vitro* assays modelling aspects of angiogenesis. It was anticipated that this soluble protein would interfere with PCDH7 binding its natural ligand(s) and so help determine the role of its interactions. Full length PCDH7 ECD-Fc inhibited endothelial network formation and strongly reduced the number of nodes in an endothelial-fibroblast *in vitro* angiogenesis assay, inhibited cell proliferation but did not influence endothelial cell migration. One of shorter fragments of PCDH7 ECD did exhibit an inhibitory effect suggesting that the full ECD is not necessary for disrupting PCDH7 function in tube formation. To further investigate its putative role in the vasculature we are attempting to identify binding partners of PCDH7 on endothelial cells.

Gordon Research Conference on Angiogenesis

06-11 August 2017 - Salve Regina University, Newport, RI, United States.

Abstract: Extracellular domain of protocadherin 7 (PCDH7)-Fc fusion protein reduces an endothelial network formation *in vitro*;

Aleksandra Korzystka, Victoria Heath and Roy Bicknell, Institute of Cardiovascular Sciences, Institute of Biomedical Research, College of Medical and Dental Sciences, University of Birmingham, B15 2TT Birmingham, UK

Vascular targeting is an attractive approach to cancer treatment. Our recently identified lung cancer tumour vascular target (TEM), PCDH7 belongs to the cadherin superfamily. It is a single transmembrane protein consisting of a long extracellular domain (ECD) of seven cadherin repeats, short transmembrane domain (TMD) and intracellular domain (ICD) that differs between PCDH7 isoforms. Although PCDH7 is present in many types of tumours, its exact function is not defined. It was shown to have a role in lung tumourigenesis and promoting brain metastasis. PCDH7 was also implicated as a prognostic marker in bladder cancer and it was shown to inhibit migration of gastric cancer cells. However, its function in the tumour vasculature has not been previously reported. It was anticipated that that a soluble extracellular fragment of PCDH7 would interfere with binding to its natural ligands on the endothelial cells and so help elucidate its function. Accordingly, a full length PCDH7 ECD and its truncated fragments fused to human Fc were produced and examined in variety of *in vitro* assays. Full length PCDH7 ECD-Fc inhibited endothelial network formation and strongly reduced the number of nodes in an endothelial-fibroblast *in vitro* angiogenesis assay, inhibited cell proliferation but did not influence endothelial cell migration. One of shorter fragments of PCDH7 ECD did exhibit an inhibitory effect suggesting that the full ECD is not necessary for disrupting PCDH7 function in tube formation. To further investigate its putative role in the vasculature we are attempting to identify binding partners of PCDH7 on endothelial cells.